# Hy4Heat

demonstrating
hydrogen for heat

Department for
Business, Energy
& Industrial Strategy

**WORK PACKAGE 7**

# Safety Assessment:
## Consequence Modelling Assessment

# WP7 SAFETY ASSESSMENT

The Hy4Heat Safety Assessment has focused on assessing the safe use of hydrogen gas in certain types of domestic properties and buildings. The evidence collected is presented in the reports listed below, all of which have been reviewed by the HSE.

The summary reports (the Precis and the Safety Assessment Conclusions Report) bring together all the findings of the work and should be looked to for context by all readers. The technical reports should be read in conjunction with the summary reports. While the summary reports are made as accessible as possible for general readers, the technical reports may be most accessible for readers with a degree of technical subject matter understanding.

**Safety Assessment:**
## Precis
An overview of the Safety Assessment work undertaken as part of the Hy4Heat programme.

**Safety Assessment:**
## Conclusions Report
### (incorporating Quantitative Risk Assessment)

A comparative risk assessment of natural gas versus hydrogen gas, including a quantitative risk assessment; and identification of control measures to reduce risk and manage hydrogen gas safety for a community demonstration.

**Safety Assessment:**
## Consequence Modelling Assessment
A comparative modelling assessment of the consequences in the event of a gas leak and ignition event for natural gas and hydrogen gas.

**Safety Assessment:**
## Gas Ignition and Explosion Data Analysis
A review of experimental data focusing on natural gas and hydrogen gas ignition behaviour and a comparison of observed methane and hydrogen deflagrations.

**Safety Assessment:**
## Gas Dispersion Modelling Assessment
A modelling assessment of how natural gas and hydrogen gas disperses and accumulates within an enclosure (e.g. in the event of a gas leak in a building).

**Safety Assessment:**
## Gas Dispersion Data Analysis
A review of experimental data focusing on how natural gas and hydrogen gas disperses and accumulates within an enclosure (e.g. in the event of a gas leak in a building).

**Safety Assessment:**
## Gas Escape Frequency and Magnitude Assessment
An assessment of the different causes of existing natural gas leaks and the frequency of such events; and a review of the relevance of this to a hydrogen gas network.

**Safety Assessment:**
## Experimental Testing - Domestic Pipework Leakage
Comparison of leak rates for hydrogen and methane gas from various domestic gas joints and fittings seen in typical domestic gas installations

# WP7 SAFETY ASSESSMENT

**Safety Assessment:**

## Experimental Testing – Commercial Pipework Leakage

Comparison of hydrogen and methane leak rates on a commercial gas pipework system, specifically the gas meter and equipment contained within the Plant Room of a MOD site.

**Safety Assessment:**

## Experimental Testing - Cupboard Level Leakage and Accumulation

Comparison of the movement and accumulation of leaked hydrogen vs. methane gas within cupboard spaces in a typical domestic property.

**Safety Assessment:**

## Experimental Testing - Property Level Leakage and Accumulation

Comparison of the movement and accumulation of leaked hydrogen vs. methane gas within a typical domestic property.
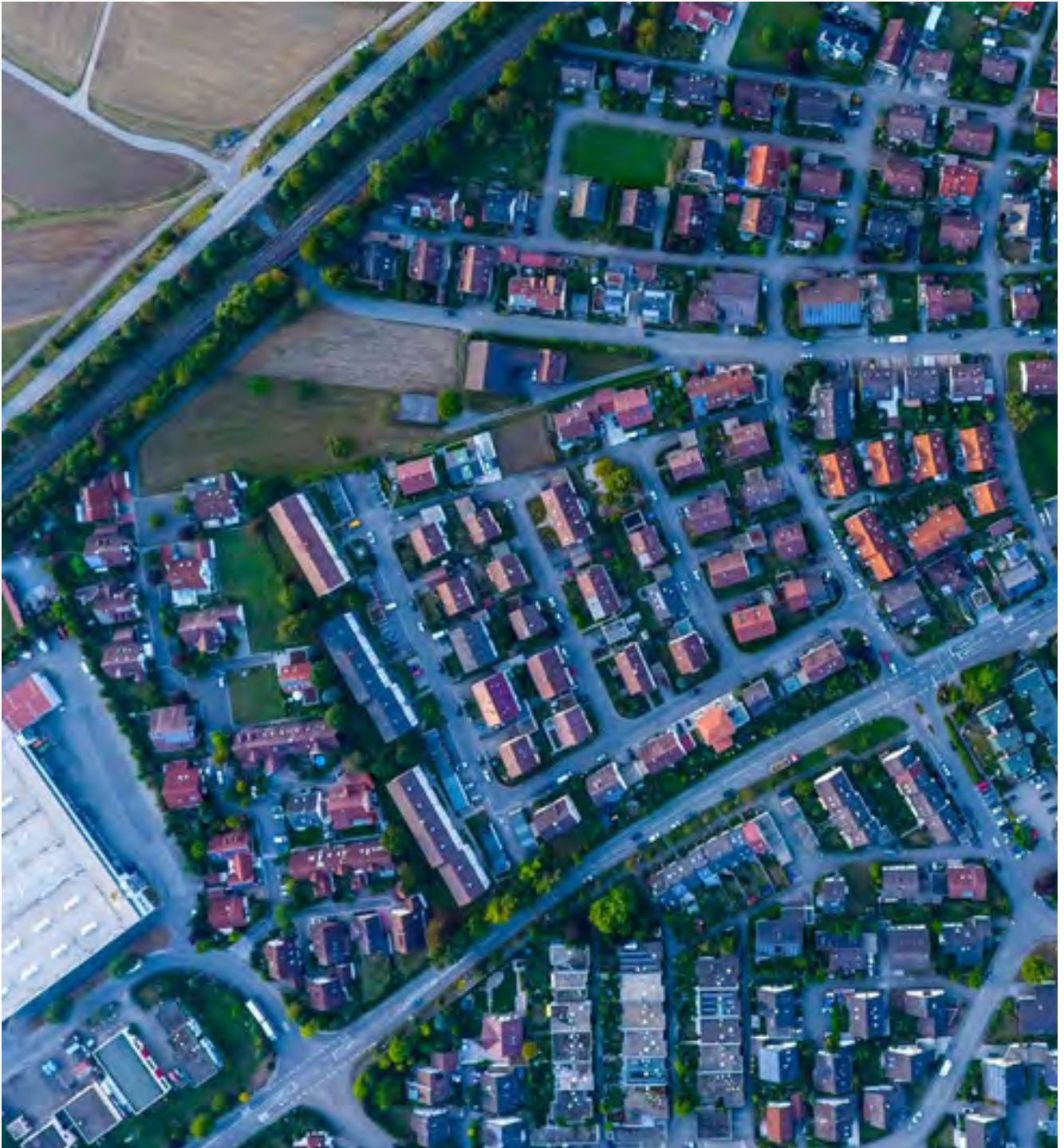
**Safety Assessment:**

## Experimental Testing - Ignition Potential

Investigation of the ignition potential of hydrogen-air mixtures by household electrical items and a comparison with the ignition potential of methane-air mixtures.

# ARUP

<span style="color:red">Hy4Heat</span>

# Consequence Modelling Report

1.0 | 1 May 2021



<span style="color:red">Hy4Heat</span>

ARUP

<span style="color:red">**Department for Business, Energy & Industrial Strategy**</span>

Hy4Heat

Consequence Modelling
Report

ARP-WP7-GEN-REP-0003

1.0 | 1 May 2021

This report takes into account the particular
instructions and requirements of our client.
It is not intended for and should not be relied
upon by any third party and no responsibility
is undertaken to any third party.

# ARUP

# Document verification

| Role | Name | Company |
|------|------|---------|
| Prepared by | Sam Greg | Arup |
| Checked by | Seda Dogruel | Arup |
| Approved by | David Cormie | Arup |
| Programme Technical Review | Mark Crowther | Kiwa Gastec |
| Programme Management Review | Heidi Genoni | Arup |
| Approval to publish | David Cormie | Arup |

**Contact:**

Sam Greg
Senior Consultant

t:  020 7755 3982
e:  Sam.Greg@arup.com
Ove Arup & Partners Ltd
8 Fitzroy Street
London
W1T 4BQ
United Kingdom

arup.com

# Contents

## Tables

## Figures

# Executive Summary

The aim of the Hy4Heat programme is to establish if it is technically possible, safe and convenient to replace natural gas with hydrogen in residential and commercial buildings. This will enable the government to determine whether to proceed to community trials.

The safety assessment covers leaks occurring downstream of the emergency control valve (ECV). The assessment is valid for masonry-built terraced, semi-detached, or detached properties that are up to two storeys but may include, for example, a basement/cellar and/or a loft conversion. This includes homes and 'light' commercial premises such as corner-shops and fish and chip takeaways. This covers the majority of domestic settings in Great Britain and is believed to be sufficient for a broad range of potential community trials. Blocks of flats, houses in multiple occupation (HMOs)[1], those with mechanical (forced) ventilation, prefabricated and high-rise residential buildings are excluded from the assessment and so should not be considered as subjects for hydrogen trials, until further work is undertaken.

To support the safety assessment in determining whether it is technically safe to replace natural gas with hydrogen within residential and commercial buildings, the safety risks arising from gas leaks within buildings, downstream of the ECV, were assessed and evaluated.

In the absence of an industry standard for conveying hydrogen gas through the existing gas network, a detailed risk assessment has been carried out to assess the specific safety risks. A comparative safety risk assessment has been conducted to compare the risks from fire and explosion resulting from a gas leak within a building, for both hydrogen and natural gas.

The comparative safety risk assessment included:

a) Data collection and experimental testing.
b) Experimental data analysis (including analysis of leak integrity test data, dispersion experimental data and deflagration experimental data).
c) Dispersion modelling.
d) Consequence modelling.
e) Quantitative risk assessment (QRA) to obtain numerical estimates of the safety risks for each gas.

This consequence modelling report assesses the consequences of an ignition event occurring within the home environment following a leak and dispersion event. It is part of a suite of several related reports, which consider the event probabilities and the mechanisms of a gas leak and gas dispersion to form the overall safety assessment.

---

[1] Houses in multiple occupation are defined by 'The Licensing and Management of Houses in Multiple Occupation and Other Houses (Miscellaneous Provisions) (England) Regulations 2006' as properties where at least 3 tenants reside, forming more than 1 household and where toilet, bathroom or kitchen facilities are shared with other tenants.

# Technical Report Summary

Leak, dispersion and ignition events for both methane (representing natural gas) and hydrogen have been modelled and the consequences of such events are quantitatively assessed in this report. Two scenarios have been considered in this assessment:

- A leak, dispersion and ignition event occurring within a kitchen of a terraced house
- A leak, dispersion and ignition event occurring within the downstairs of an open plan terraced house.

A terraced house property has been selected because it is considered to be one of the most susceptible forms of construction in relation to gas explosion risks in domestic properties, and it also comprises the single largest proportion of houses in the domestic housing stock in Great Britain.

To quantitatively measure the consequences, the number of people injured, internal and external to a dwelling, following a leak, dispersion and ignition event have been measured using the following criteria:
- Number of people injured from primary injury
- Number of people injured due to secondary injury (e.g. glass throw)
- Number of people injured due to tertiary injury (e.g. injury due to falls)
- Number of people injured due to structural collapse of the dwelling they are occupying
- Number of people injured due to second degree burns.

Although the number of people injured is assessed for each of the criteria above separately, when quantitatively estimating the total number of people injured following a leak, dispersion and ignition event, overlap between the number of people injured by each of the criteria are considered. For example, a person external to the dwelling when an ignition event occurs in the dwelling may receive secondary injuries, tertiary injuries and injuries due to second degree burns. In this assessment this would be counted as one person being injured, not three.

To quantitatively estimate the consequences, vented flammable explosion overpressures arising from internal leak, dispersion and ignition events have been estimated using a semi empirical "simplified" model developed by the Warwick FIRE group at the University of Warwick. It is recognised that this model is highly conservative in the prediction of overpressure at concentrations above approximately 24% hydrogen by volume in air.

Stratification of confined methane and hydrogen clouds in enclosures have been considered in the assessment. The results often compare peak concentration of a stratified confined flammable vapour clouds with number of people injured so that the results can be used in conjunction with the dispersion and probability assessments undertaken in separate parts of the Hy4Heat WP7 work that also forms part of the overall QRA.

The results show for both hydrogen and methane that structural collapse is the largest cause of injuries to building occupants, where the consequences are sufficient to cause collapse of the dwelling. For leak scenarios that do not result in structural collapse of the dwelling, injury due to burns dominates the number of injuries internal to a dwelling. Injuries due to glass throw (also representing debris

throw), following a gas explosion within a dwelling dominate injuries to people outside the dwelling (e.g. in the street) for both methane and hydrogen.

The results of the assessment show that the level of injuries due to leak scenarios where the peak concentration of hydrogen ranges from 5% to 15%, is similar to leak scenarios where the peak concentration of methane ranges from 5% to 8%.

The results also suggest the level of injury due to a leak, dispersion, and ignition event in a domestic setting where the peak concentration range of *hydrogen* is between 15% and 21%, is similar to a leak dispersion, and ignition event in a domestic setting where the peak *methane* concentration range is between 7% to 12% for the downstairs of an open plan terraced house, and between 9% and 10.5% for a closed kitchen.

Between a peak concentration range of 23% to 45% hydrogen, the degree of structural damage and internal injuries is considerably greater than the worst case for methane.

Department for Business, Energy & Industrial Strategy | Hy4Heat
ARP-WP7-GEN-REP-0003 | Issue 01 | 1 May 2021 | Consequence Modelling Report

Page 3

# 1.    Introduction

The Hy4Heat Work Package 7 (WP7), part of the Hy4Heat project, has produced a quantitative risk assessment (QRA) that assesses hydrogen as a potential replacement for natural gas in the domestic environment. The QRA compares the accidental consequences of a dispersion event followed by an ignition event for both natural gas and hydrogen in the domestic environment. An example consequence could be an ignition of a flammable vapour cloud of leaked gas that leads to an explosion event.

Natural gas is widely used in the domestic environment for various forms of heating and an understanding and acceptance by the public of its potential hazards is already well established. By undertaking a QRA for both natural gas and hydrogen, a comparison can be made to determine how the hazards and consequences of hydrogen compare to the hazards and consequences of natural gas. The aim of the assessment is to determine whether hydrogen can be used as an alternative fuel in the domestic environment for heating.

This report looks at the following consequences that could occur in a domestic environment following a leak dispersion and ignition event;

–   Explosion event (deflagration or detonation)

–   Fire

The above two consequences could result in the following human injury or fatality due to one or a combination of:

–   exposure to significant overpressures and impulses from an explosion

–   structural collapse following an explosion causing injury

–   exposure to high velocity projectiles such as shattered glass following an explosion

–   smoke inhalation (poisoning by carbon monoxide or carbon dioxide)

–   third degree or serious burns

If there is a leak and a dispersion, but no ignition then asphyxiation due to displacement of oxygen in an enclosure from fuel gas could also occur.

Throughout the report, a comparison of hydrogen and methane will be continuously made to emphasise that the purpose of the QRA is to demonstrate the differences in potential consequence a dispersion event followed by an ignition event could have in the domestic environment.

Use has been made of the "simplified" model [1] developed by the Warwick FIRE group at the University of Warwick to determine overpressures for the modelling work undertaken in this assessment. It should be stressed that above approximately 24% hydrogen concentration (by volume in air), the "simplified" model is highly conservative in predicting overpressure so prediction of consequences at these high concentrations of hydrogen is also conservative. Consequentially, modelling of ignition events for high concentrations of hydrogen predict overpressure considerably greater that the structural strength of any UK's domestic or commercial buildings. The "simplified" model from [1] is similar to many vented flammable explosion models by modelling a single room containing a homogeneous flammable vapour cloud ignited at one end of the enclosure. Venting of the unburnt gases is assumed to take place through a single vent at the opposite end to the ignition

point and assumes that the volume of the enclosure and the vent area remain constant throughout the combustion process. This does not reflect the reality of many domestic gas explosions where, in practice, a window will fail, then a door, then perhaps another a window, then the ceiling, and then the walls in a domestic dwelling. This "partial venting" effect (i.e. increasing vent area as the combustion of the hydrogen cloud occurs) is not considered in the modelling and means that the results for high concentrations of hydrogen are conservative.

Finally, detail on the assumptions and areas of conservatism used throughout the assessment can be found in Appendix B at the end of the report.

# 2.   Technical background

## 2.1   Comparison of methane and natural gas

In the past there have been extensive studies on the properties and behaviour of *methane* as a flammable gas. *Natural gas* usually contains between 70-90% methane, therefore when describing the characteristics for natural gas; the characteristics can be assumed to be like that of methane. This is reasonable for this study given that when compared with hydrogen, the behaviour of natural gas is similar to methane.

The other main components of natural gas are ethane, propane and butane (Table 1) all of which are classified as having a 'medium' reactivity [2] where methane is classified as having a 'low' reactivity (see Section 2.5). This would suggest that natural gas is slightly more reactive than pure methane. A study that makes a 'safety' comparison between *methane* and *hydrogen* as an 'equivalent' study of *natural gas* and *hydrogen*, will be slightly bias towards natural gas and this is worth noting.

Table 1: Typical composition of Natural Gas (extract from [3]). Percentages are by volume

| Typical Composition of Natural Gas | | |
|---|---|---|
| Methane | $CH_4$ | 70-90% |
| Ethane | $C_2H_6$ | |
| Propane | $C_3H_8$ | 0-20% |
| Butane | $C_4H_{10}$ | |
| Carbon Dioxide | $CO_2$ | 0-8% |
| Oxygen | $O_2$ | 0-0.2% |
| Nitrogen | $N_2$ | 0-5% |
| Hydrogen sulphide | $H_2S$ | 0-5% |
| Rare gases | A, He, Ne, Xe | trace |

## 2.2   Comparison of methane and hydrogen

The hazards associated with the use of natural gas in the domestic environment are well understood and generally accepted by the public. There is also a great deal of "lessons learnt" from past events such as gas explosions and fires in the domestic environment and this in turn has shaped current regulations and gas safety guidance.

Pure hydrogen[2] is not (yet) used in the domestic environment so there is little case study material that can be used from past accidents involving hydrogen in the home. Although both are flammable gases, there are some considerable differences between hydrogen and methane. Table 2 lists in a tabulated form some of the properties of both methane and hydrogen in a comparative format.

---

[2] See other Hy4Heat project material such as [28] regarding comparisons with Towns Gas

Table 2: Comparison of methane and hydrogen properties

| Property | Methane | Hydrogen | Relevance |
|---|---|---|---|
| Density | $0.668 \text{kg/m}^3$ at 20°C. Lighter than air and will fill an enclosure with a more even distribution than Hydrogen | Considerably lighter than air at $0.090 \text{kg/m}^3$. A leak of hydrogen from a leaking pipe will generally start to fill an enclosure from the top down. In a room, this would result in a higher concentration of hydrogen nearer the ceiling. | The relative buoyancy of natural gas or hydrogen to air affects the rate and degree of stratification in an enclosure such as a room in a dwelling. This is further influenced by the geometry and ventilation of that enclosure, plus the injection rate from the gas leak. |
| Flammability (% volume) | Lower Flammability Limit (LFL) of 5.0%<br><br>Stoichiometric concentration of 9.5%<br><br>Upper Flammability Limit (UFL) of 15.0%<br><br>Total range: 10% volume<br><br>The ignitable concentration range (5.0% to 15.0%) of a methane vapour cloud is comparatively small when compared to hydrogen | Lower Flammability Limit (LFL) of 4.0%<br><br>Stoichiometric concentration of 29.5%<br><br>Upper Flammability Limit (UFL) of 75.6%<br><br>Total range: 71.6% volume<br><br>The ignitable concentration range (4.0% to 75.6%) of a hydrogen vapour cloud is large and there is a much higher probability of ignition followed by combustion for a hydrogen vapour cloud when compared to methane. | Flammability range is the range in percentage volume i.e. concentration, at which a flammable vapour cloud can undergo combustion following ignition. Below the LFL the concentration of gas in the cloud is not enough to support combustion. The stoichiometric concentration is the concentration that will support combustion most efficiently. A flammable vapour cloud with a concentration near stoichiometric often results in the largest explosion. Above the Upper Flammability Limit (UFL) the concentration of gas in the cloud is too great such that there is not enough oxygen in the cloud to support combustion. However, a flammable vapour cloud above the stoichiometric concentration can entrain air and subsequently more oxygen as it undergoes combustion, bringing the concentration of the cloud closer to the stoichiometric concentration which increases the efficiency of the reaction process[3]. |
| Heat of combustion $H_C$ | Has a heat of combustion of between 50 and 55 MJ/kg at 25°C [4]. This is equivalent to approximately 33 to 36 | Has a heat of combustion of LHV 119.9 and HHV 141.8 MJ/kg at 25°C [4]. This is equivalent to approximately 10.8 to 12.8 | Although the energy density of methane is higher than the energy density of hydrogen, it is important to also consider the |

3 Terms such as "Fraction of stoichiometric" or "equivalence ratio" are sometimes used to describe the concentration of flammable vapour clouds. For example, a flammable vapour cloud at stoichiometric concentration (9.5% for methane, 29.5% for hydrogen) would have an equivalence ratio of 1.0 and a flammable vapour cloud at twice the stoichiometric concentration (19% methane, 59% hydrogen) would have an equivalence ratio of 2.0

| Property | Methane | Hydrogen | Relevance |
|---|---|---|---|
| | $MJ/m^3$ at ambient conditions (room temperature and atmospheric pressure) for 100% methane | $MJ/m^3$ at ambient conditions for 100% hydrogen. | reactivity of the two gases when making a comparison between them |
| Ignition energy | At 25°C, methane requires a minimum ignition energy of $7.5 \times 10^{-4}$ J [5] at the stoichiometric concentration of around 9.5% vol. This is the typical ignition energy from an ungrounded conductor or a mechanical spark [6]. However, at LFL, the minimum ignition energy for methane is around $10 \times 10^{-3}$ J which is the ignition energy of a bulking brush discharge[4] . | At 25°C, hydrogen requires a minimum ignition energy of $0.28 \times 10^{-4}$ J [5] at the stoichiometric concentration of around 29.5% vol. This is the typical ignition energy from a discharge from clothing [6]. However, at LFL, the minimum ignition energy for methane is similar in magnitude to methane at around $20 \times 10^{-3}$ J | Although the focus of this report is on the *consequences* which feed into the QRA, minimum ignition energy is an important parameter when considering *likelihood* or probability. The lower the minimum ignition energy, the greater the *likelihood* of an ignition of a flammable vapour cloud occurring. |
| Reactivity | Low reactivity. Laminar burning velocity is comparatively slow compared to hydrogen | High Reactivity. Hydrogen has a laminar burning velocity approximately 10 times that of methane. | Reactivity is a qualitative parameter that is generally used to categorize a fuel's propensity to accelerate to high flame speeds. This is discussed further in Section 2.5. |
| Radiative emissive power | Methane has a radiative fraction between 0.15 and 0.34 [4] depending on the efficiency of the combustion process and concentration (such as a fireball following ignition). | Hydrogen burns with a very clean flame and has a relatively low radiative power with a radiative fraction between 0.17 and 0.2 (Table 66.14 [7]). For flames occurring directly at the leak source, this fraction decreases | The combustion of a solid or gas producing a flame/fire has an output power (measured in kW) that is part convective, part radiative. The radiative fraction is the fraction of total fire output that is emitted from the fire via radiation. Both hydrogen and methane have a low radiative fraction, especially for the combustion of a mixture at, or below the stoichiometric concentration. Given that the stoichiometric concentration of methane is considerably lower, it is more likely that a methane cloud will emit a greater radiative power than a hydrogen cloud when undergoing combustion for concentrations above 10% volume. For a confined flammable vapour cloud undergoing combustion in a domestic setting, it likely that some dust or cellulosic material would become entrained. If this were to |

---

[4] A bulking brush discharge is created during the bulking of flammable powders in containers.

| Property | Methane | Hydrogen | Relevance |
|---|---|---|---|
| | | | happen, the increase in radiative energy would be proportionally similar for both confined methane and hydrogen clouds of similar flammable loads with the same mass of dust being entrained. This is a reasonable assumption because the increase in radiative fraction would occur due to the combustion of the dust. |
| Autoignition temperature | Methane has an autoignition temperature ranging from 540°C [8] to 595°C (Table 3.1 [2]) | Hydrogen has an autoignition temperature of approximately 560°C (Table 3.1 [2]). | The autoignition temperature is the temperature at which a flammable gas will initiate combustion and it varies with pressure. In the context of an unburnt flammable vapour cloud at atmospheric pressure in a domestic setting, the cloud would start to undergo combustion if the edge, or any part of the cloud contacted a surface that was hotter than the autoignition temperature of the gas. The autoignition temperature is also relevant when considering a deflagration to detonation transition. This is discussed further in Section 2.9. |
| Ability to detonate? | Requires an ignition source of approximately 93,000kJ [2] to initiate a detonation of a methane vapour cloud. The detonation cell size or width for methane is around 28cm. The likelihood of methane undergoing a deflagration to detonation transition (DTT) is considerably less than for hydrogen under similar environmental conditions. | Requires an ignition source of approximately 5kJ [2] to initiate a detonation of a hydrogen vapour cloud. The detonation cell size or width for hydrogen is around 1.5cm. This results in the combustion of a hydrogen vapour cloud having a greater probability of undergoing a deflagration to detonation transition (DDT) than methane. The lower autoignition temperature also contributes to the higher likelihood of hydrogen detonating when compared to methane | Detonation for flammable gases such as hydrogen and methane are a complicated phenomenon. In short, the smaller the detonation cell size the greater the likelihood of detonation occurring when comparing different flammable gases in the same environment. A detonation blast wave is a shockwave that travels above the speed of sound in the mixture in ambient conditions . Deflagration to detonation transition is discussed in Section 2.9. |

## 2.3    Ignition and flame propagation

Ignition of a flammable vapour cloud can lead to either two modes of combustion and flame propagation; deflagration or detonation. Given the considerably lower energy required to initiate deflagration, the flame propagation mode in most cases will be deflagration. Detonation and DDT of a flammable vapour cloud is covered in Section 2.9. Deflagration "can best be described as a combustion mode in which the propagation rate is dominated by both molecular and turbulent transport processes" [2]. The propagating chemical reaction of the flammable vapour cloud in a deflagration is where the flame front[5] advances into the unreacted substance (i.e. the unburnt part of the flammable vapour cloud) rapidly but at less than the speed of sound (sonic velocity). This advancement of the flame front generates pressures above the ambient atmospheric pressure (usually called overpressure). This is discussed further in Section 2.6
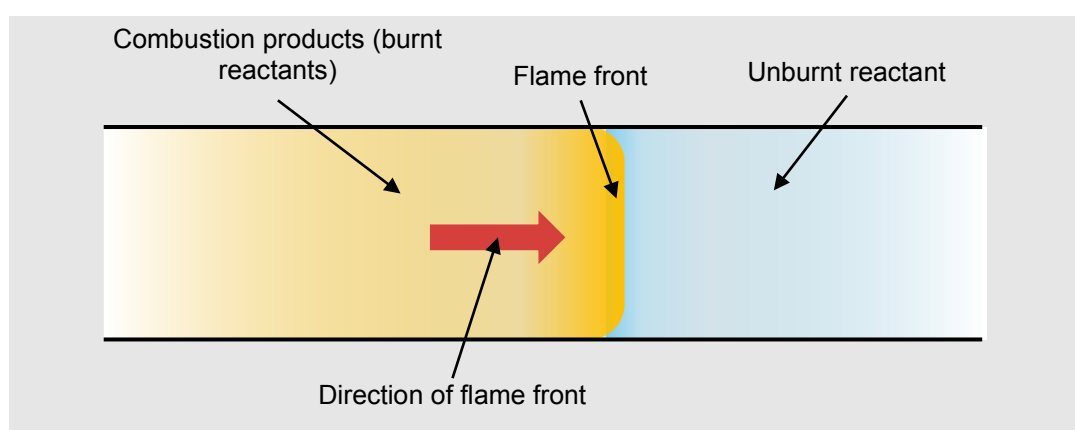


Figure 1: Flame front in a flammable vapour cloud ignition (confined flame front in one direction)

Ignition sources can be divided into "soft" or "hard" ignition sources. Ignition of a flammable vapour cloud to initiate deflagration requires an ignition energy of approximately $10^4$ Joules [2] near the stoichiometric concentration. This is the typical level of energy a spark from a light switch or an open flame from a gas hob in the domestic environment and is classed as a "soft" ignition source. As the % volume concentration decreases, the minimum energy required to initiate an ignition of a flammable vapour cloud increases.

By contrast, direct initiation of detonation of a flammable vapour cloud requires an initiation energy of approximately $10^6$ joules [4] which is comparable to a high-explosive charge, i.e. a "hard" ignition charge. Given that most domestic environments do not contain high explosive charges, it is assumed that direct ignition of detonation of flammable vapour clouds in the domestic environment are highly unlikely to occur.

The location of ignition within a flammable vapour cloud affects the characteristics of the explosion. "An ignition location in the centre of the flammable vapour cloud may lead to higher pressures within the combustion zone because the expansion of the combustion products creates greater confinement

---

[5] The 'flame front' is often referred to as the 'reaction front' in literature.

of the flow than an end ignition. Conversely, an end ignition may be the worst-case scenario in the far-field (beyond the combustion zone) because the length over which turbulent acceleration of the flame front can occur is maximised, putting greater energy into the pressure wave that is propagated into the far field" [9], i.e. when the blast waves passes through a penetration like in Figure 2. This suggests that an ignition in the centre of the flammable vapour cloud would generate higher overpressures on the roof and floor of an enclosure than an ignition at the end of the cloud. Conversely an end ignition would be more onerous for glass throw than an ignition in the centre of a flammable vapour cloud. However, an end ignition would allow the flame front to accelerate to a higher velocity over the length of the enclosure and would result in a higher internal overpressure for a vented explosion (see Section 2.6.2)
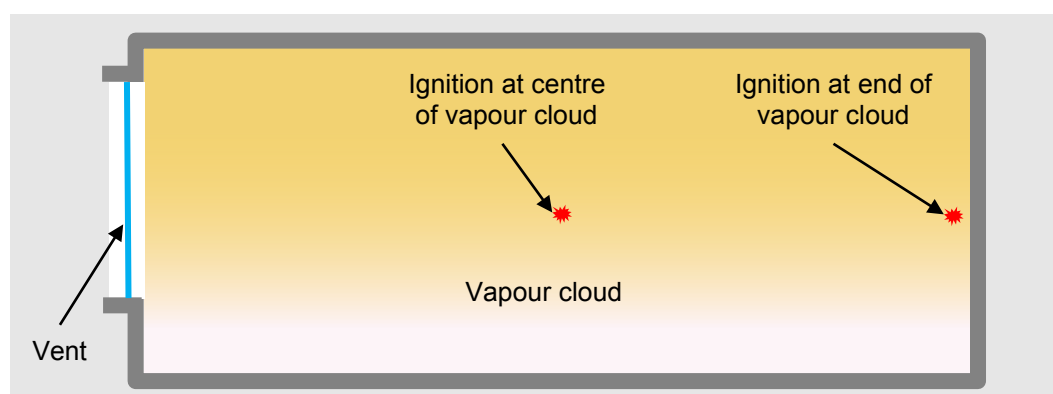


Figure 2: Ignition locations in a confined flammable vapour cloud

## 2.4 Congestion and confinement

Turbulence is what causes vapour clouds undergoing combustion to explode in a deflagrative manner thereby generating significant overpressures and impulses that can cause structural damage and either direct or indirect injury to humans. Turbulence increases the interface between the reactants (fuel and oxygen) and the flame front significantly enhancing the combustion rate of a flammable vapour cloud. The process by which turbulence occurs creates a feedback coupling that further increases the combustion rate (see Figure 4)

Turbulence is created by the following:

- The release of flammable gas itself prior to ignition. If the release of hydrogen or methane into a space is at a high velocity, for example from a small leak in a domestic supply pipe in a dwelling, then the vapour cloud is likely to contain an area of turbulent mixing.

- Turbulence produced in unburned gases expanding ahead of a flame propagating through a congested space (Figure 3). Areas of piping or objects in a confined space but with gaps and spaces between the objects could be classified as a congested space. In a domestic environment, areas of congestion are less common than say an industrial facility associated with the process or oil and gas industry, but local congestion within a cupboard, a cluttered domestic property or even household furnishings could still generate turbulence ahead of the flame front in a flammable vapour cloud explosion

– By external mechanical flow devices such as fans, air conditioning units or mechanical ventilation.
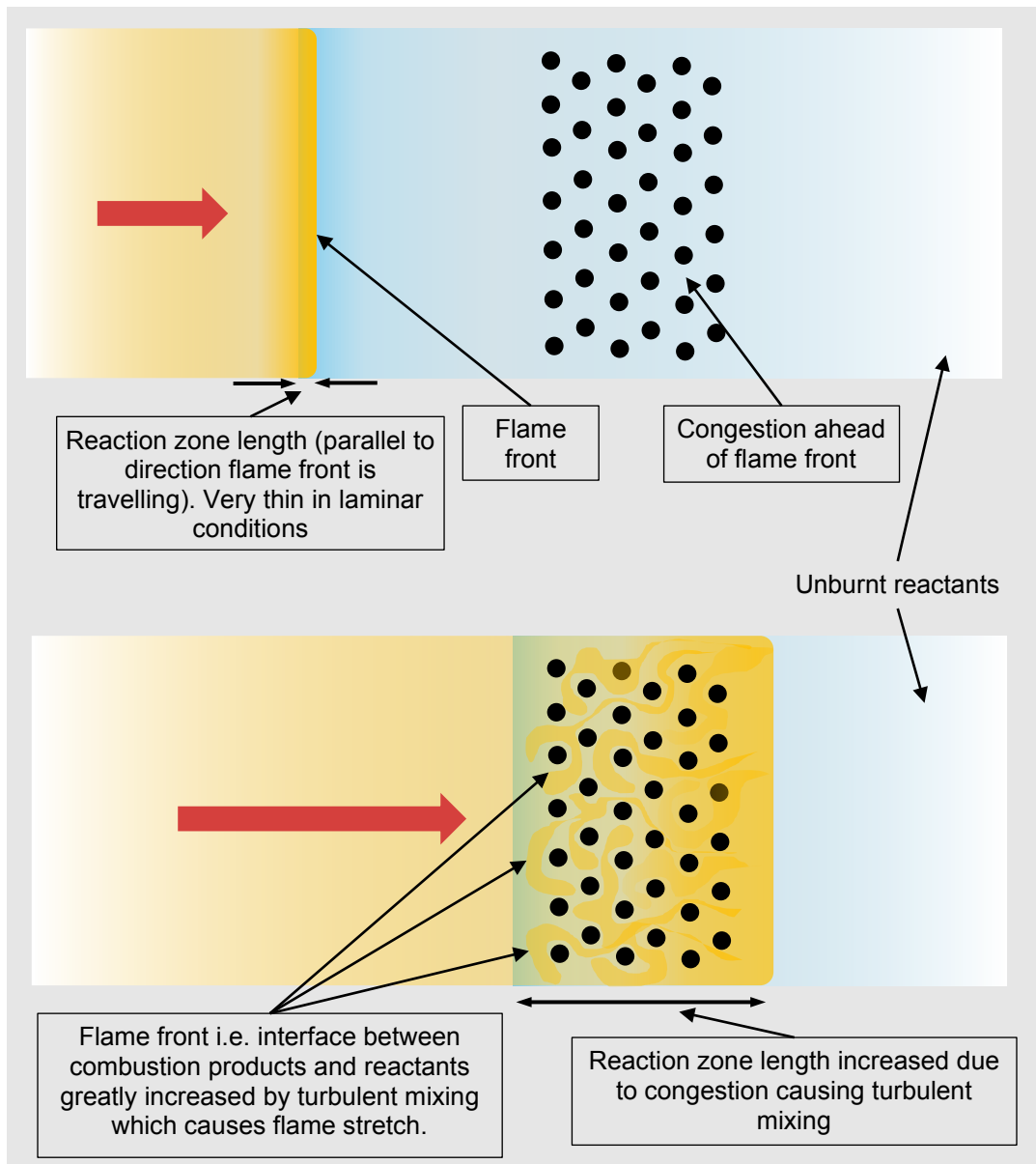


Figure 3: Turbulence created by congestion in an advancing flame front
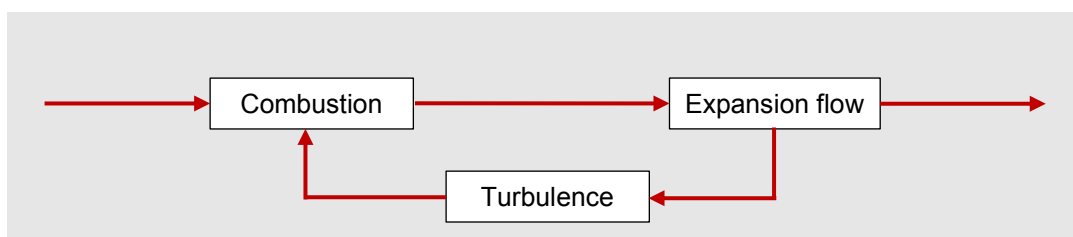


Figure 4: Positive feedback mechanism of a vapour cloud explosion [2]

When the combustion process in a vapour cloud is confined or partially confined the development of the vapour cloud explosion will be affected due to:

    – A pressure build-up in the exploding vapour cloud caused by the interaction of expansion and combustion.

    – Hampering of the expansion allowing the introduction of a combustion enhancing flow structure. i.e. expansion flow

Confinement in a domestic environment would usually occur due to the sides of the enclosure, for example, the walls, floor and ceiling of kitchen in which a hydrogen or methane vapour cloud ignition takes place. The walls, floor and ceiling of a room in a dwelling (prior to their collapse) would likely confine a flammable vapour cloud during combustion such that the expanding gases would be restricted to either two or even one dimension, eventually venting through an opening such as a window, or a door into other enclosures within the dwelling.

## 2.5    Reactivity

Flames speed is the speed at which a reaction zone travels through a flammable mixture of gas and air and is measured relative to a fixed observer i.e. the sum of the burning translational velocities of the unburned gases [2].

Burning velocity is the velocity of the propagation of a flame through flammable gas-air mixture and is relative to the unburned gases immediately ahead of the flame front. Laminar burning velocity is a fundamental property of a gas-air mixture, whereas flame speed depends on a combination of the laminar burning velocity, expansion ratio, confinement, congestion and other turbulence generating effects [2] which accelerate the combustion process and thereby accelerate the velocity of the reaction zone (and the flame speed). A deflagration which does not produce any significant blast overpressures is often referred to as a "flash fire"

Reactivity is a qualitative parameter that is generally used to categorize a fuel's propensity to accelerate to high flame speeds. Van Wigerden and Zeeuwen [10] showed that laminar burning velocity can be used as a scaling parameter for reactivity. Hydrogen is considered to have a high reactivity whilst methane is considered to have low reactivity [2].

When comparing the explosive behaviour of methane and hydrogen in a volume with a certain level of congestion and confinement, the difference in reactivity will govern the difference in flame speed of the combustion for each medium. Flame speed is of great significance because this often governs the explosion strength of the exploding vapour cloud.

## 2.6 Blast waves, confined and vented explosions

### 2.6.1 Blast or pressure waves

The strength of a vapour cloud explosion (or indeed any explosion) is measured quantitatively by calculating the peak overpressure and impulse of the explosion.

A vapour cloud explosion is different from a condensed phase explosion (such as TNT) because the fuel vapour (methane or hydrogen) is dispersed through an oxidant (such as air) and is ignited from a point source (such as a spark from a light switch). The-fuel oxidant mixture is progressively combusted in a chemical reaction and the expansion of the combustion products creates a pressure wave that further accelerates the chemical reaction.

For two observers with infinitesimally small surface areas, at different standoff[6] distances from the centre of an *unconfined* explosion, the idealised incident pressure profile of what the observers may experience is shown in Figure 5. The idealised incident pressure profile indicated in blue is representative of an observer standing close to the edge of a vapour cloud where the rise time is rapid and the incident overpressure higher than for an observer represented by the red profile who is further away.
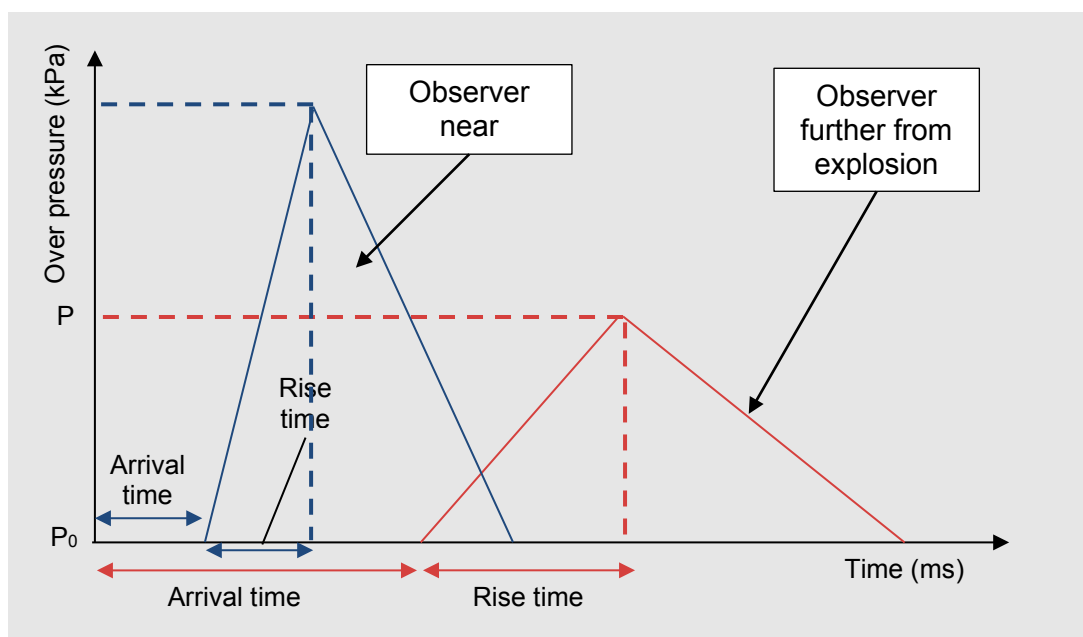


Figure 5: Typical overpressure profiles of a vapour cloud explosion

When a pressure wave from a flammable vapour cloud explosion interacts with a solid surface such as a wall or the surface area of a body, the blast or pressure wave will be reflected with energy being transferred from the blast wave to the wall. For a blast or pressure wave impinging normally upon the

---

[6] Standoff is the distance between the source of the explosion and the location of an observer (such as a person) or target (such as a wall). For a conventional explosive this is relatively easy to define. For a flammable vapour cloud, this can be challenging especially if the observer or target is relatively close to the cloud relative to the cloud size.

wall, the wave is reflected producing a region of compression of the air local to the wall [9]. "On a molecular level, the surface applies an external force to each air molecule which is sufficient to give it equal momentum in the opposite direction. By Newton's third law, the air applies the same external force to the surface. It is due to this change of momentum that the pressure is locally increased above the incident pressure which would occur at the same location. This is termed the reflected pressure." [9]. Figure 6 represents this in a graphical form. The reflected pressure is calculated using the Rankine and Hugoniot method using equation 3.15 from [9].

The impulse from the blast is the integral of the overpressure with time, i.e. the area under the graph in both Figure 5 and Figure 6. This is referred to the incident and reflected impulse respectfully. As well as the overpressure, impulse is also as important to predict because it determines the dynamic response of the structure to which blast overpressures are being applied to.
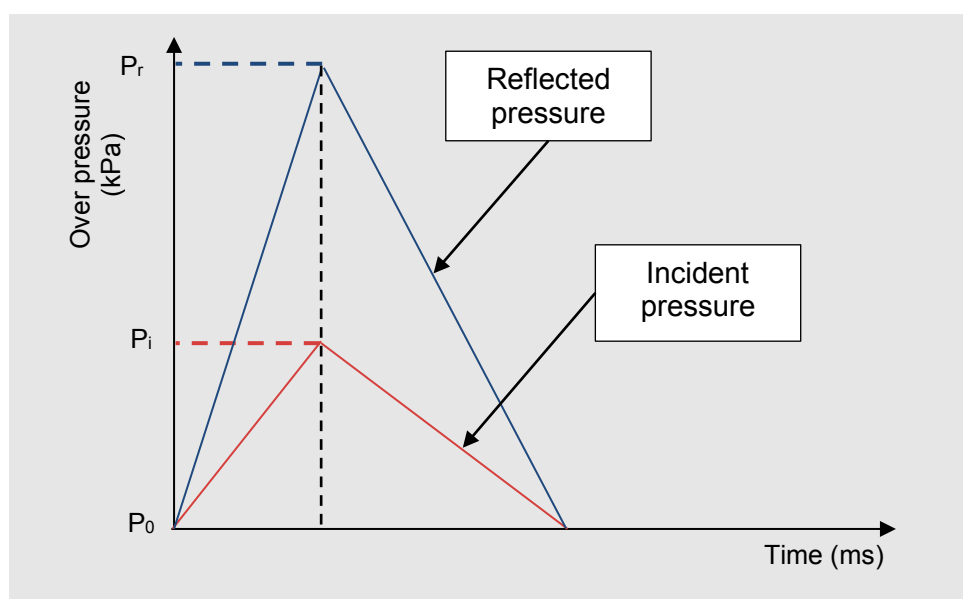


Figure 6: Idealised comparison of incident and reflected pressure on a solid object

### 2.6.2    *Confinement and explosions in vented structures*

Confinement has a significant role in the consequences of a flammable vapour cloud explosion. As well as confinement increasing the flame speed and thereby the strength of the explosion [11], when an explosion occurs within a structure it may be described as either 'unvented' or 'vented' (Figure 7). An unvented structure or enclosure would need to be stronger to resist an explosion than a vented structure where some form of pressure relief would be activated (e.g. by breaking of windows) [9]. The combustion of a flammable vapour cloud in an unvented enclosure is referred to as a "closed vessel deflagration" [7].

Department for Business, Energy & Industrial Strategy                    Hy4Heat
ARP-WP7-GEN-REP-0003 | Issue 01 | 1 May 2021                          Consequence Modelling Report

Page 15
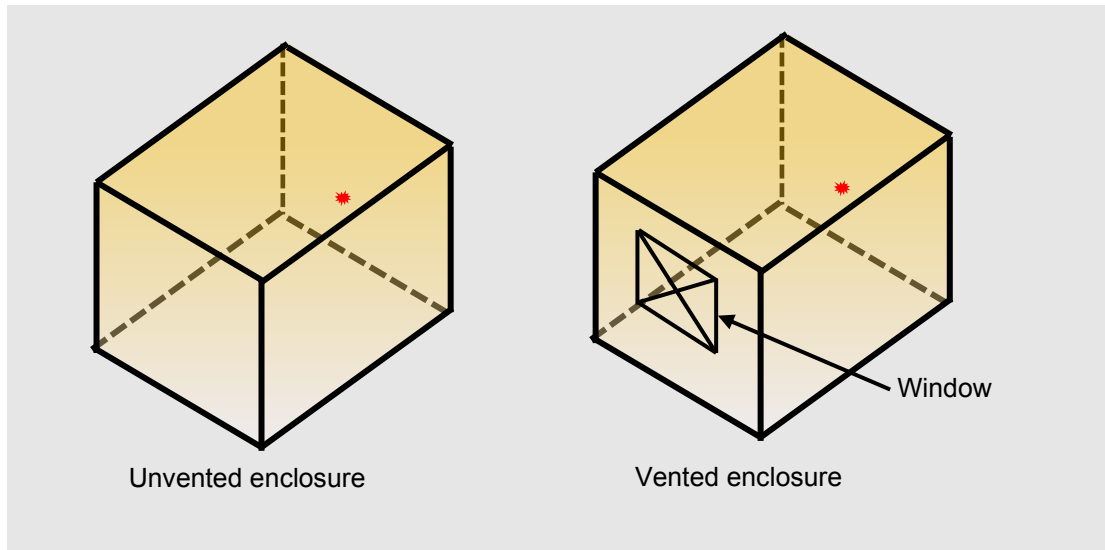
Figure 7: Idealised unvented and vented enclosure

Given that nearly all rooms in a dwelling where a gas leak and vapour cloud formation could occur would have a window or door in it, most vapour cloud explosions in a dwelling would start off initially as a "closed vessel deflagration" and when the internal overpressure causes the windows or doors of the compartment to fail, the explosion transitions to a vented flammable vapour cloud explosion.

This process is depicted in Figure 8 and described below. The numbering refers to the numbering in Figure 8.

1. Initially an enclosure is entirely filled with a confined (unburnt) flammable vapour cloud and is ignited at the opposite end to the vent, which is initially covered (for example a closed door or window).

2. The flame or flame front expands out radially from the point of ignition through the unburnt flammable gas with unburnt gas in front of the flame front and burnt combustion products behind the flame front. Ignoring energy losses to the enclosure boundaries the pressure in the burnt combustion products would adiabatically increase with the rise in temperature due to the combustion process occurring within the 'sealed' enclosure and would increase the internal pressure within the enclosure i.e. the process of a "closed vessel deflagration".

3. The increasing internal enclosure pressure causes the vent a covering such as windows and doors to fail or open.

4. The expanding flame front pushes the unburnt part of the confined flammable vapour cloud out through the open vent where they form a cloud external to the enclosure vent. This cloud is assumed be formed of approximately 90% unburnt flammable gas and 10% burnt combustion products [12][7].

5. The flame front has now reached the vent opening(s) and the enclosure contains only burnt combustion products.

6. The advancing flame front initiates ignition of the external flammable vapour cloud.

7. Explosion of the external cloud occurs and generates a 'back pressure' into the enclosure which interacts with the already increased internal pressure pulse from the expanding flame front in stages 3, 4 and 5 above.

Figure 9 shows a typical internal overpressure profile for the enclosure for the stages described above. If the vent area is small in relation to the volume of the enclosure, the peak internal overpressure will occur after the external explosion has occurred and have an internal overpressure profile like that shown in Figure 10. The ratio of the total vent area to volume of the enclosure is a very important parameter in determining the internal explosion overpressure and internal pressure pulse shape for a vented flammable explosion. It is often quantitatively measured in literature as the vent area divided by the volume of the enclosure to the power of two thirds ($A_v/V^{2/3}$) and referred to as the $K_v$ value, which is dimensionless. Figures 6 and 7 in [13] show the relationship between the value of $K_v$, the peak overpressure, the shape of the internal overpressure pulse and the time that the explosion of the external flammable vapour cloud occurs.

---

[7] In practice, the ratio of unburnt combustible gas to burnt reactants will vary with initial concentration of the flammable vapour cloud mixture in the enclosure prior to ignition, along with other variables such as vent dimensions and degree of stratification.

Note that considerations such as stratification in the enclosure and the presence of obstacles are addressed in Section 3.
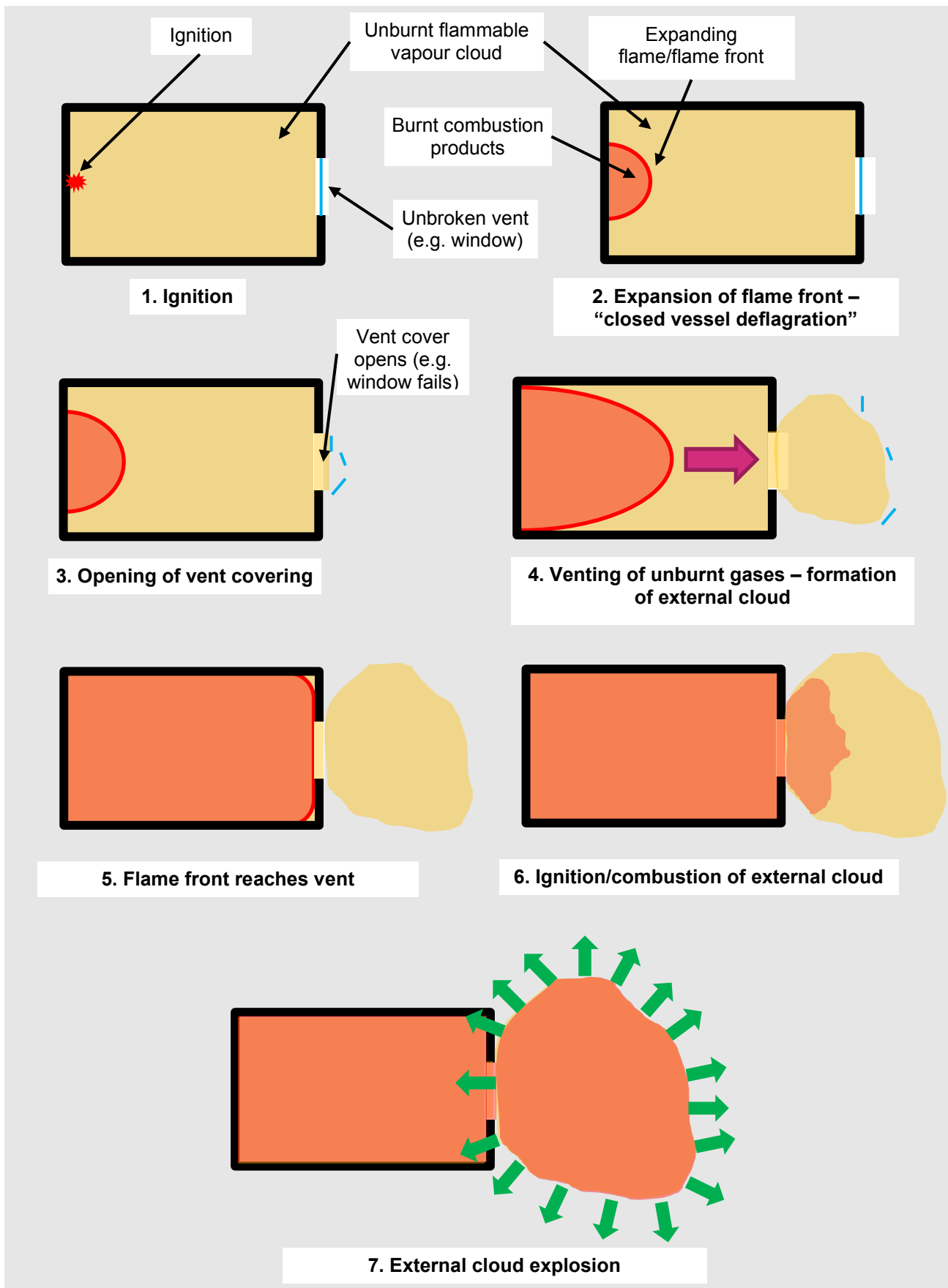
Figure 8: Unvented to vented gas explosion
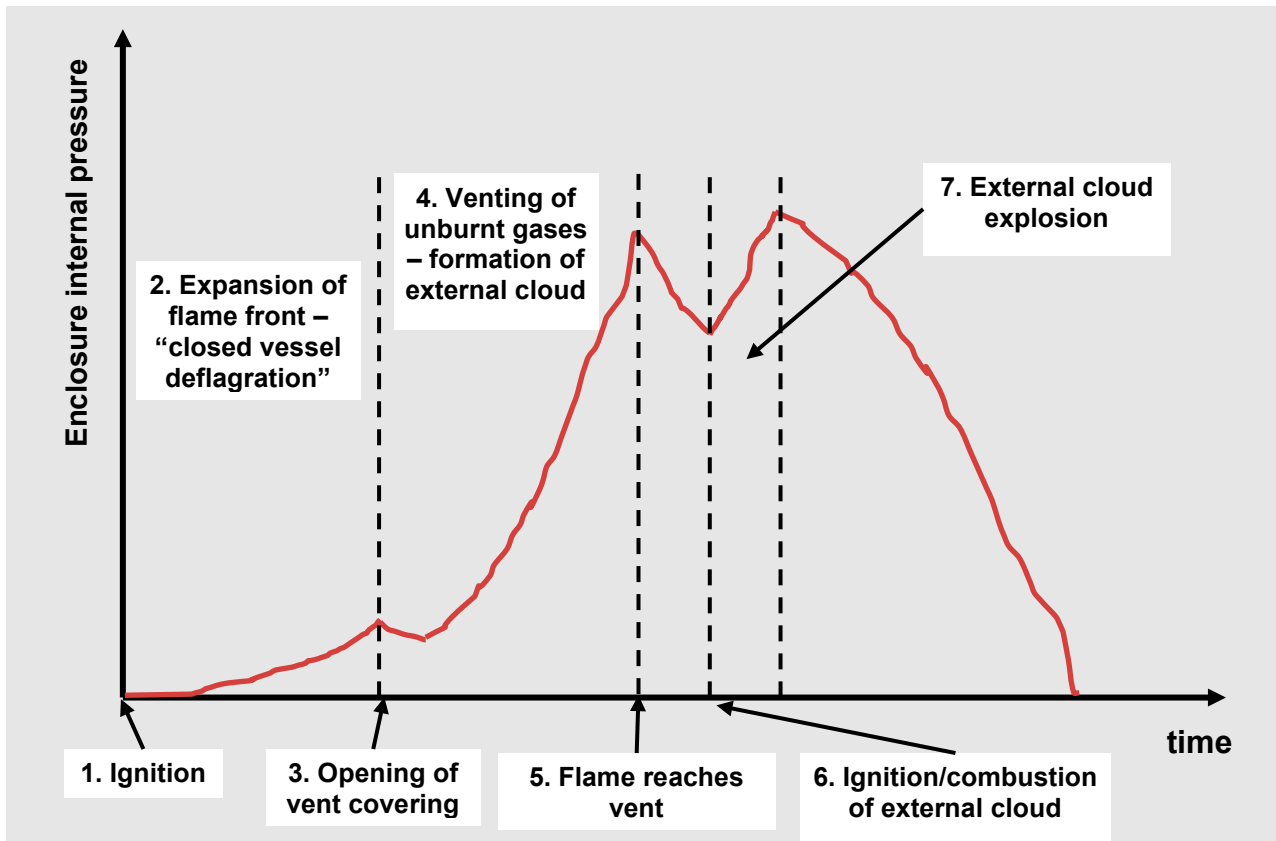
Figure 9: Typical internal pressure profile for a "closed vessel deflagration" transitioning to a vented explosion. See Figure 8 for stages of explosion process
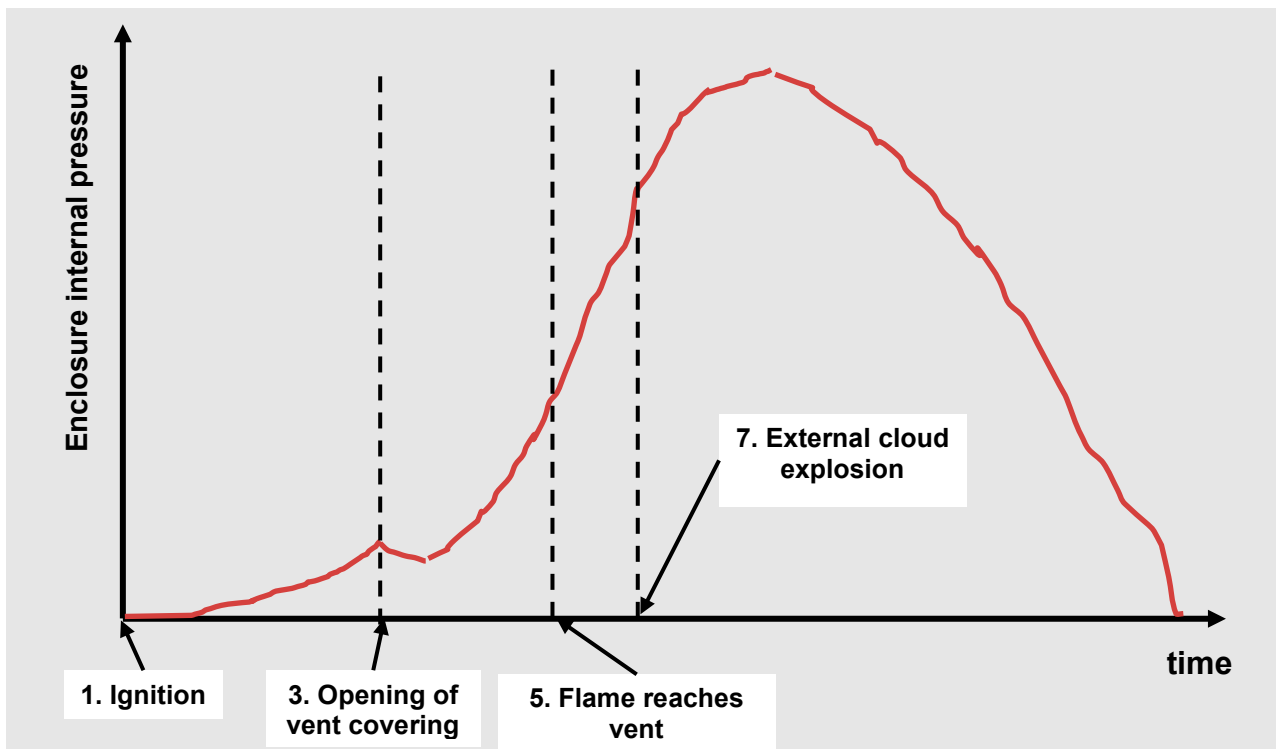


Figure 10: Typical internal pressure profile for a "closed vessel deflagration" transitioning to a vented explosion for an enclosure with a small value of $K_v$

## 2.7 Structural response of masonry to blast loading

The structure or at least the cladding, dividing walls, internal and external walls of the great majority of residential property in the UK is constructed from unreinforced masonry.

Unreinforced masonry such as clay brick walls or breeze block formed walls perform relatively poorly when compared to reinforced concrete walls and exhibits virtually no plastic behaviour. However, masonry walls have some additional lateral load resistance and a significant amount of additional strain energy (i.e. area under the resistance-deflection curve - Figure 12) after brittle flexural failure from axial load arching caused by the wall self-weight and any supported axial load such as floor and wall loads from storeys above [14] (Figure 11).

The ultimate flexural resistance, $r_u$ (sharp spike in Figure 12), of a masonry wall will be a function of the wall deflection, the dynamic rupture strength of the cement or brick (whichever is weaker), and the rigidity of the supports [9]. For the assessment undertaken in this study a dynamic rupture strength for cement of 1.38MPa has been taken in line with guidance from UFC 3-340-2 [14].
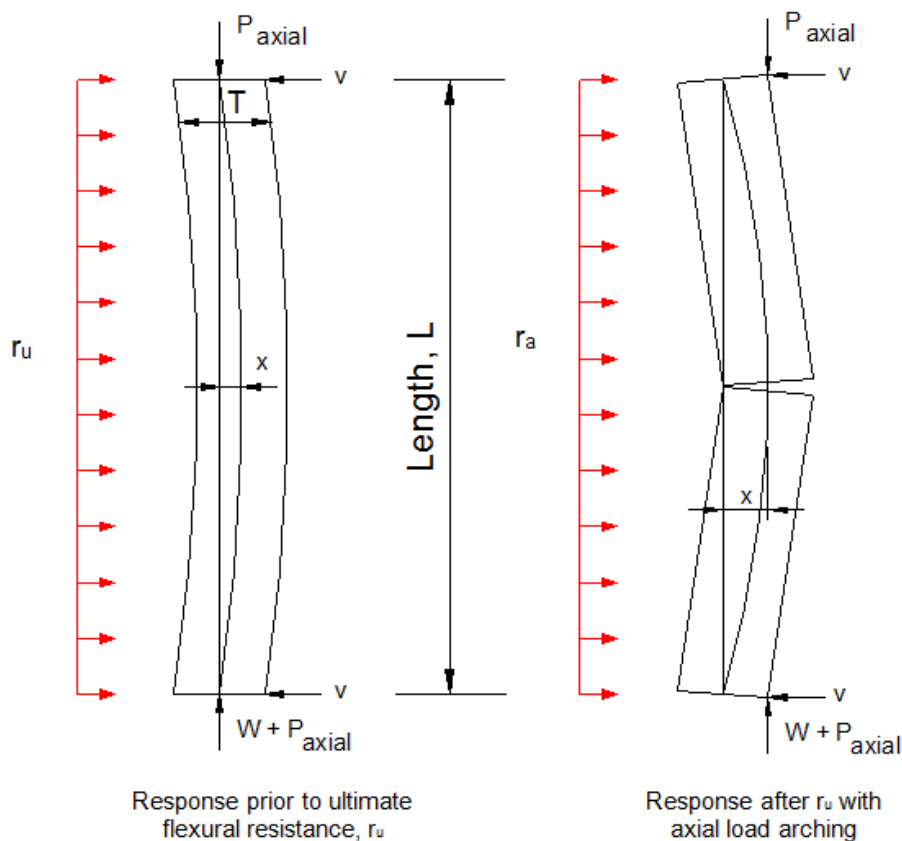


Figure 11: Axial load arching in unreinforced masonry walls (extract from Figure 6-12 in [14])
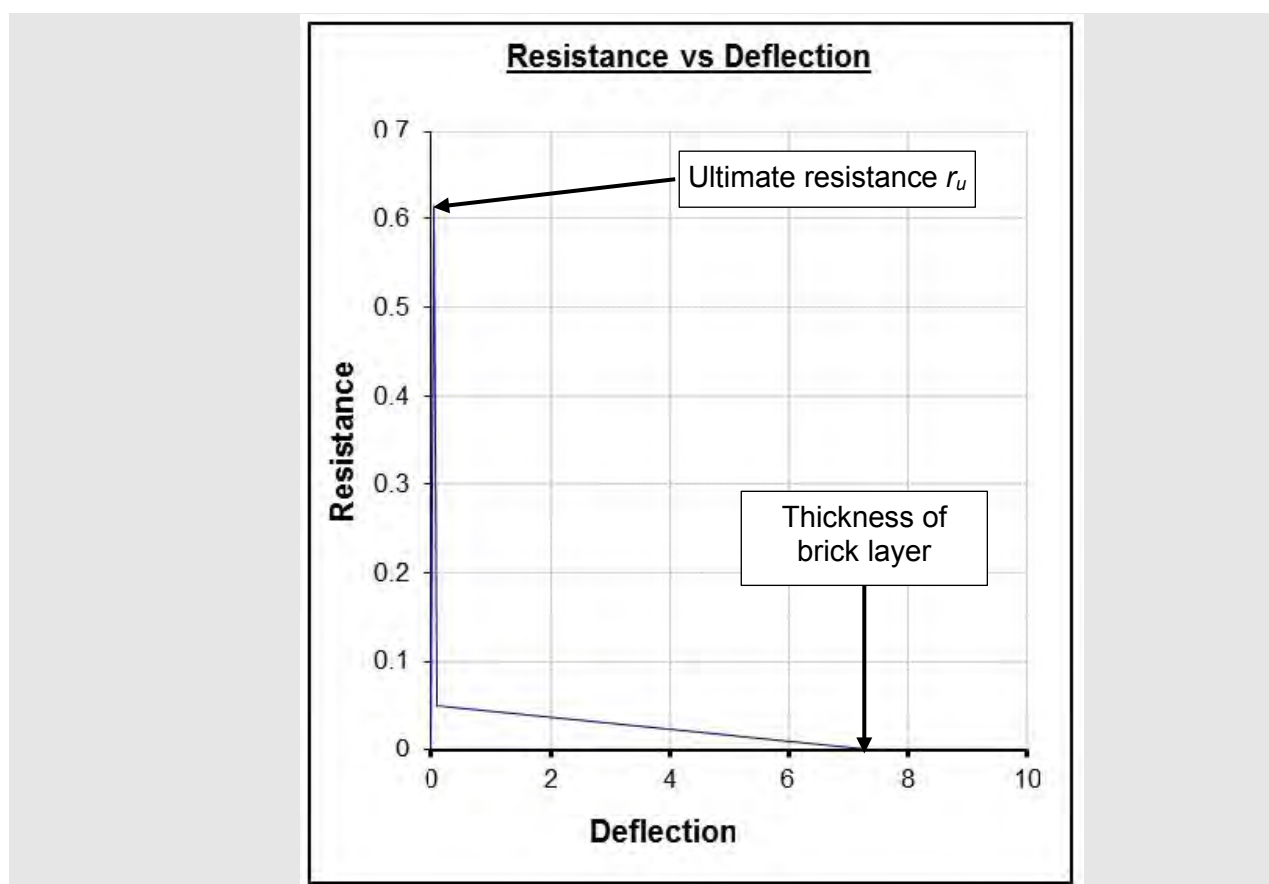
Figure 12: Typical resistance-deflection curve for unreinforced masonry wall with axial load arching (extract from Figure 6-11 in [14])

The resistance to deflection of an unreinforced masonry wall will reduce immediately after the wall resistance reaches the ultimate flexural resistance due to the brittle nature of the tensile bond between the mortar and masonry in the maximum moment regions. The wall will then develop axial load arching, which is characterized by a much lower resistance than initial flexural response, but a much larger deflection to failure[8]. This provides a significant increase in the strain energy before failure and the blast load capacity of unreinforced masonry walls. The axial load ($P_{axial}$ in Figure 11) is significant in determining the maximum strain energy before failure. This means that a wall supporting the dead load of several storeys above (like the ground floor in a block of flats) will have a greater maximum strain energy before failure than a wall only axially supporting a roof loading (such as in a bungalow). However, the wall is still a weak component against blast loading when compared to reinforced masonry or reinforced concrete [14].

The behaviour of a cavity masonry wall under blast load is slightly more complicated to model. A cavity wall is formed by an inner skin and an outer skin of masonry. Approximately 70% of the homes in the UK have cavity wall insulation [15][9]. The use of metal ties to connect the two skins became more common towards the beginning of the 20th century [16] (like those shown in Figure 13). Since

---

[8] Failure is defined as being the point at which the deflection is the same as the thickness of the brick. At this point, the wall no longer has any axial capacity

[9] This is based on a survey in 2013 of the 27.1 million homes in Great Britain.

the mid-1980s, homes have been increasingly built with pre-insulated cavity walls [15] which partially or fully fills the cavity between the outer and inner wall.

For the purpose of the modelling in this report it is assumed that any cavity fill in a wall does not contribute to the resistance function or mass of the cavity masonry wall. The total resistance of a cavity wall is the resistances of the outer and inner wall superimposed (not a wall of 2 times the brick thickness). This is assuming the cavity between the outer and inner wall behaves as an incompressible but non-structural medium. In practice this would not occur, but the total resistance of the wall to blast loading would be similar. The method in UFC-3-340-02 [14] has been used to determine the resistance function and structural response for a typical cavity brick wall to blast loading from an internal flammable explosion.
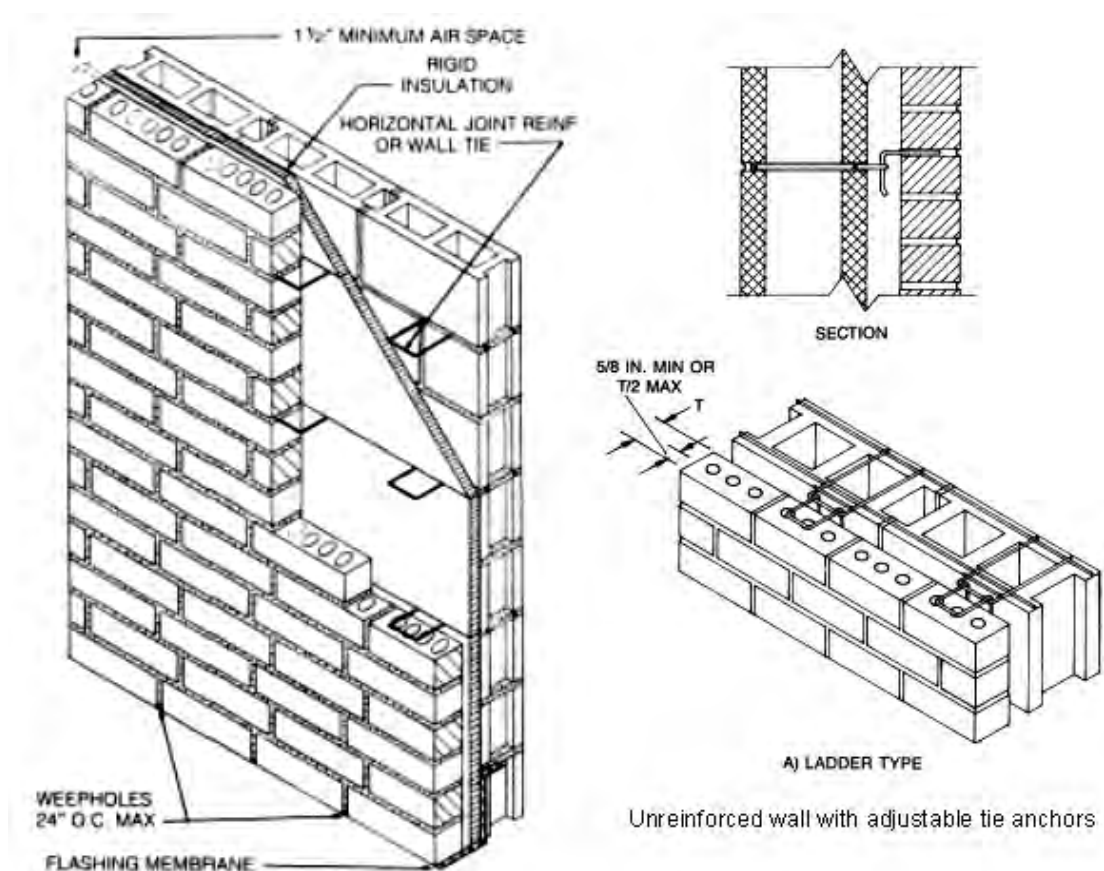


Figure 13: Section of a typical cavity wall from post 1980s with further insulated inner blockwork (extract from

## 2.8 Behaviour of glazing under blast load

The potential hazards from glazing subjected to blast overpressures and impulses are intuitively known to be severe. Monolithic glass is a brittle material that fails suddenly and fragments. The fragments of glass are projected at high velocity causing serious injury to anyone struck by them. This is discussed further in Section 2.10.2 which covers secondary injury.

Nearly all glazing in domestic properties is annealed or float glass. It exhibits brittle fracture due to microscopic randomly distributed surface flaws and scratches across its surface [9]. Annealed glass breaks into angular, jagged and irregular fragments.

Glazing in domestic properties is usually either single or double glazing and is two-way spanning where the glazing pane generates its greatest strength due to the stress system set up in the glass comprising in-plane hoop compression stresses balanced by radial tensile stresses and flexural bending stresses prior to cracking [9].

A dynamic breaking strength[10] for non-heat treated or toughened monolithic glass in the UK can be taken to be 80 N/mm$^2$ [9]. Once the maximum principal tensile stress in the pane reaches the dynamic breaking strength of the glass, brittle fracture is assumed to occur [9]. For a window in a dwelling, this would be the point that the window shatters. The shape of a typical resistance function for a monolithic glass panel is shown in Figure 14
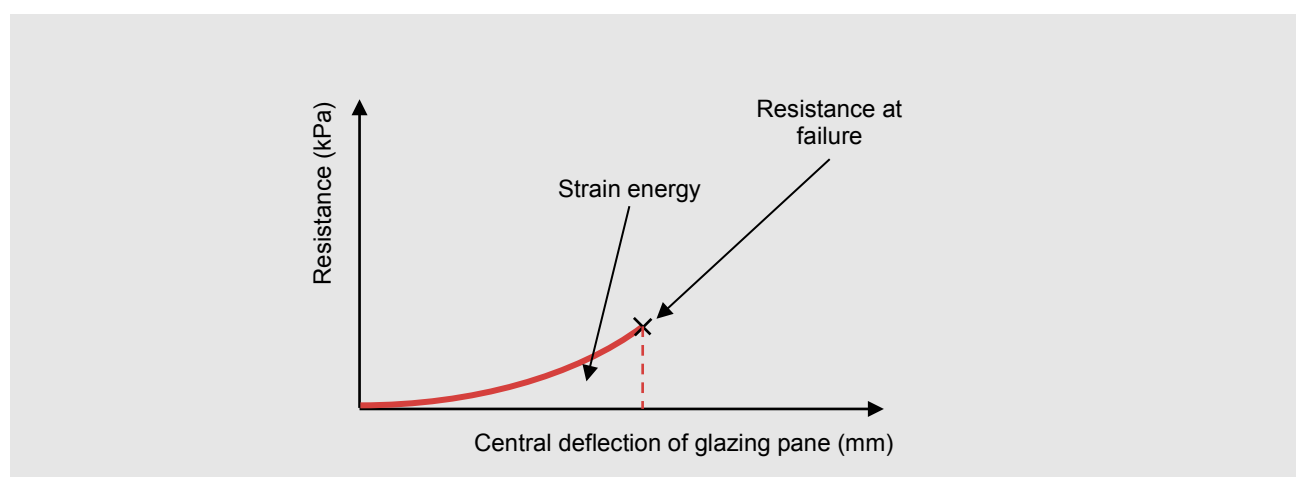


Figure 14: Typical resistance function for a monolithic glass panel

---

[10] Dynamic breaking strength is the breaking strength for a material where the load is applied very rapidly such as under blast loading. It usually differs to the breaking strength of the same material under non-rapid loading associated with static or quasi-static loads.

## 2.9    Deflagration to Detonation (DDT)

The previous sub sections in Section 2 have addressed ignition and flame propagation of a vapour cloud, the significance of congestion and confinement, reactivity, and how a blast wave following ignition of a vapour cloud forms. "The thermodynamic state of a reactive mixture prior to combustion at the flame front (see Figure 1) is determined by adiabatic compression and by turbulent mixing with combustion products" [2] The unburnt mixture in front of the [flame] front is preconditioned for combustion by this compression and turbulent mixing. "If the turbulent mixing becomes too intense, the combustion reaction may quench[11] locally, resulting in a hot and highly reactive mixture of reactants and combustion products. If, at the same time, the autoignition temperature[12] [of the reactants] is exceeded [due to the localised] compression, the mixture ignites again" [2] resulting in a localised constant volume sub-explosion. If the surrounding mixture is sufficiently close to autoignition (because of the compression from a sub-explosion) a detonation wave is formed engulfing the entire flame propagation. This process of local DDT is depicted conceptually in Figure 15.

The principle differences between a detonation and a deflagration [17] is that the flame speed and overpressures are higher in a detonation (often measured in Mach numbers greater than 1.0). For deflagration, flame speed and overpressure have a wide range of values that are highly dependent on the geometrical boundary conditions such as a congestion and confinement in which the flame front is advancing. Once a deflagration has transitioned to a detonation, the flame speed and overpressure are dependent on the mixture (hydrogen-air or methane-air) and no longer on the geometrical boundary conditions (confinement and congestion).

The resulting overpressure-time profile experienced by an observer in the path of a blast wave resulting from a deflagration and a detonation is depicted in Figure 16. A blast wave from a detonation has a very rapid 'rise time' which represents the shock front formed in front of the reaction front.

As mentioned in Table 2, the probability of hydrogen undergoing a deflagration to detonation transition is greater than the probability for methane. A common cause of DDT for hydrogen and other high reactivity gases is when an already highly turbulent flame front passes a series of repeated obstacles. The definition of repeated obstacles is somewhat subjective, and scenarios would require assessment on a case by case basis[13]. For hydrogen the detonation limit[14] for perfect conditions is

---

[11] The term "quenching" is usually associated with the application of water on a fire to quench the flames. The definition of quenching is the rapid transfer of heat energy. When throwing water on a fire, the heat energy of the fire is transferred to the water usually resulting in a billow of steam as the water evaporates and (ideally) the fire going out. In the case of a vapour cloud explosion and DDT, the local quenching of the combustion reaction is highly rapid heat energy transfer from the reactants in the flame front to the unburnt combustion products resulting in a hot and highly reactive mixture of reactants and combustion products.

[12] "If the temperature of a flammable vapour-air mixture is increased sufficiently, it can ignite spontaneously without the introduction of a source of ignition—a "pilot"—such as a flame or spark." [8]

[13] The type of repeated obstacles such as congested pipe racks that have been observed to initiate a DDT are not expected to be present in a domestic setting, especially towards the ceiling where the highest concentration of hydrogen is likely to be. For this reason, DDT in a domestic setting is considered highly unlikely.

[14] The "detonation limit" is the lowest concentration at which DDT of hydrogen is feasible. Below the detonation limit concentration, the steady self-sustained propagation of a detonation wave cannot be supported

Department for Business, Energy & Industrial Strategy          Hy4Heat
ARP-WP7-GEN-REP-0003 | Issue 01 | 1 May 2021          Consequence Modelling Report

Page 25

15% and approximately 18.5% for realistic conditions [18]. Below this concentration, DDT (initiating locally) of hydrogen cannot occur or be sustained.
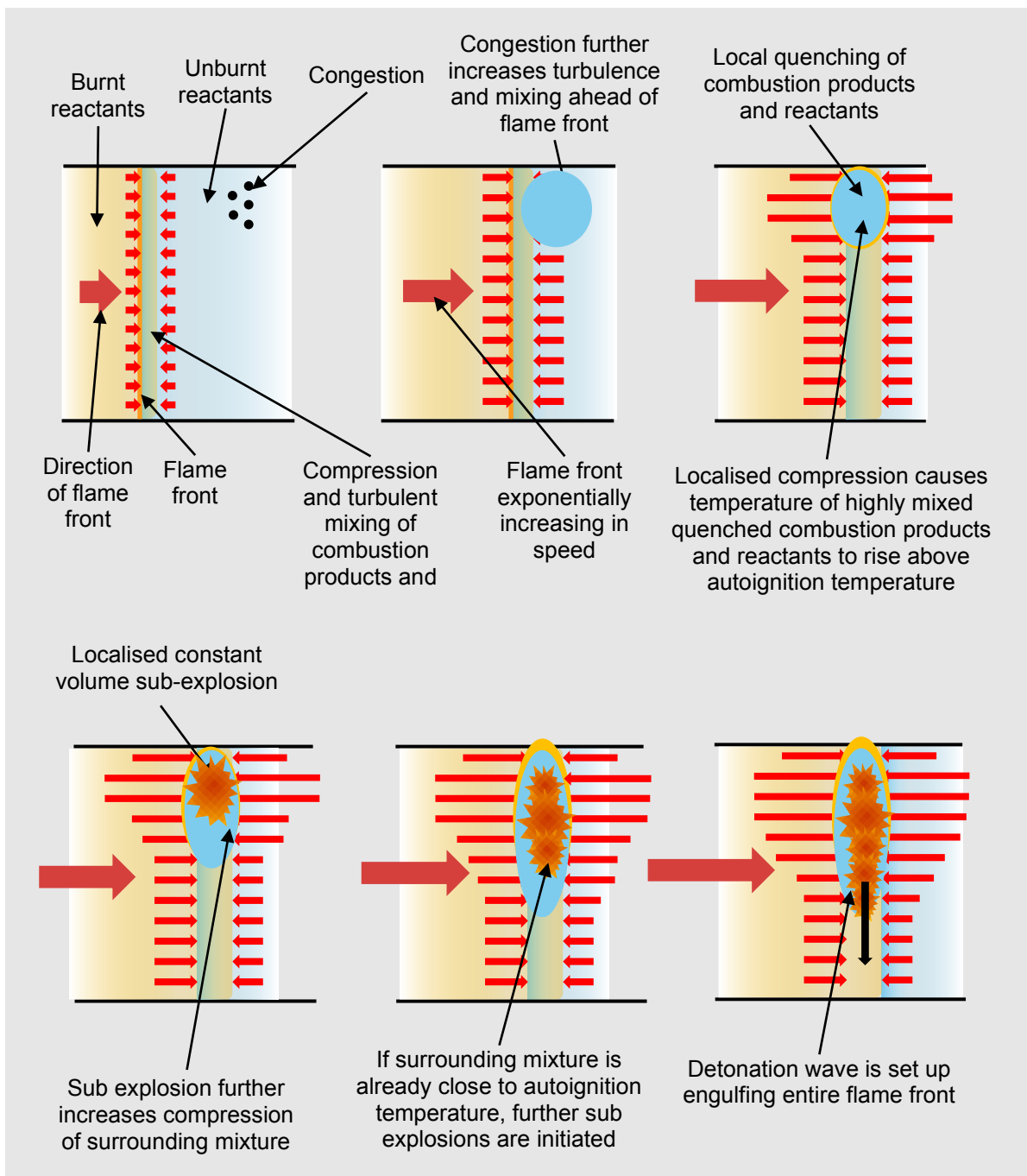


Figure 15: Deflagration Detonation Transition (DDT) in 1 direction (turbulent effects of boundary fluid interaction are not shown)
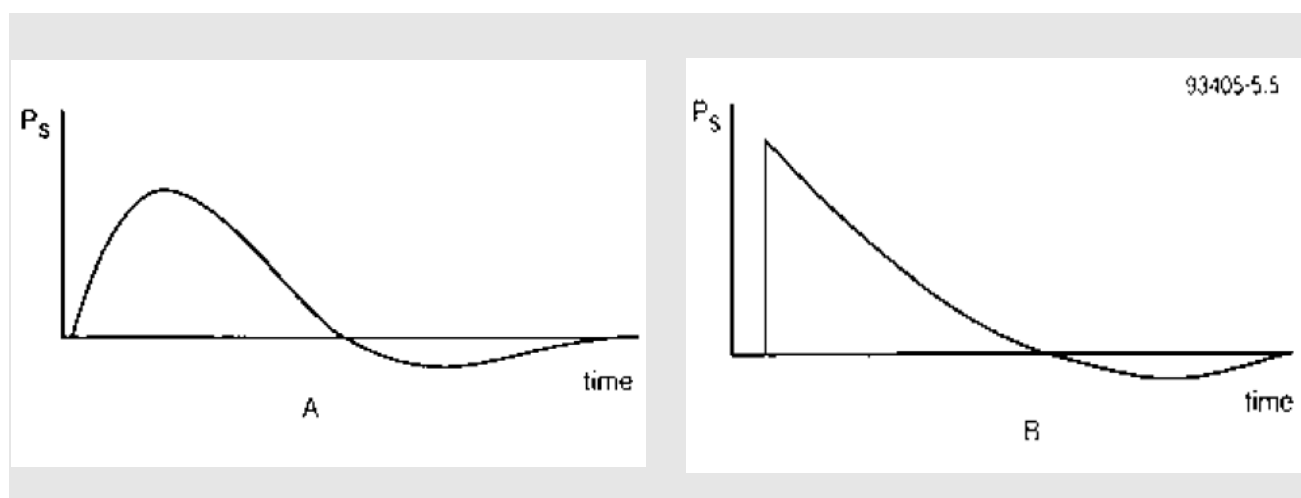
Figure 16: Typical overpressure profile for a deflagration (left) and a detonation or shock wave (right). Extract of Figure 5.5 from [17]

## 2.10 Effects of blast on people

Blast-induced injury are usually defined in three categories:

- Primary injury is damage to the human body due to direct exposure to the blast or pressure wave overpressure and its duration. The location of severe injuries are usually the lungs, ears, larynx, trachea and anywhere where the density difference between adjacent body tissues is greatest.

- Secondary injury is damage to the body due to impact of missiles such as glass fragments that are projected at high velocities because of an explosion and blast or pressure wave. Injuries are usually lacerations, penetration and blunt trauma.

- Tertiary injury is due to the displacement of the entire body due to the accelerative force of a blast or pressure wave followed by the high decelerative impact loading when the body hits a hard object

For a vapour cloud explosion all three of the above injuries could occur individually or in combination.

### 2.10.1 Primary injury

Human tolerance to the blast overpressures is relatively high [19] although it is worth noting that following shock tube and explosive tests, the pressure tolerance for short duration blast loads are higher than for long-duration blast loads. This is relevant because vapour cloud explosions have considerably longer duration blast waves when compared to conventional explosives (such as TNT).

Several factors mean that there is a variation in the degree of 'measurable' damage:

- The orientation of the person relative to the front of the blast wave is a significant factor in determining the amount of injury sustained. For example, a person sitting side on to the blast front will sustain a different level of injury to a person standing face on to the blast front.

- The shape of the pressure front (fast or slow rise, step loading) [19]

- The size, weight and age of the person subject to blast overpressures. Survival is very much dependent on the mass of the human. Figure 17 is from [19] and shows these differences in relation to lung damage. For example, the threshold for 99% chance of survival for a baby weighing 12lbs (5.4kg) exposed to an impulse of 50psi-ms (345kPa-ms) would be a blast overpressure of approximately 50psi (345 kPa). The threshold for 99% chance of survival for man weighing 150lbs (68kg) exposed to an impulse of 50psi-ms would be a blast overpressure of approximately 400psi (2760 kPa).

- The duration of the blast wave. As the duration of the blast wave increases, the maximum overpressure that the average human can tolerate decreases. The threshold for severe lung-haemorrhage pressures are 30 to 40 psi (200 to 275kPa) [19], with lethality due to lung damage being approximately 100 to 120psi (690 to 830kPa). The threshold pressure level for petechial haemorrhage resulting from long-duration loads may be as low as 10 to 15 psi, or approximately one-third that for short duration blast loads.

Figure 1-2 Survival Curves for Lung Damage, Wh = Weight of human being (lbs)
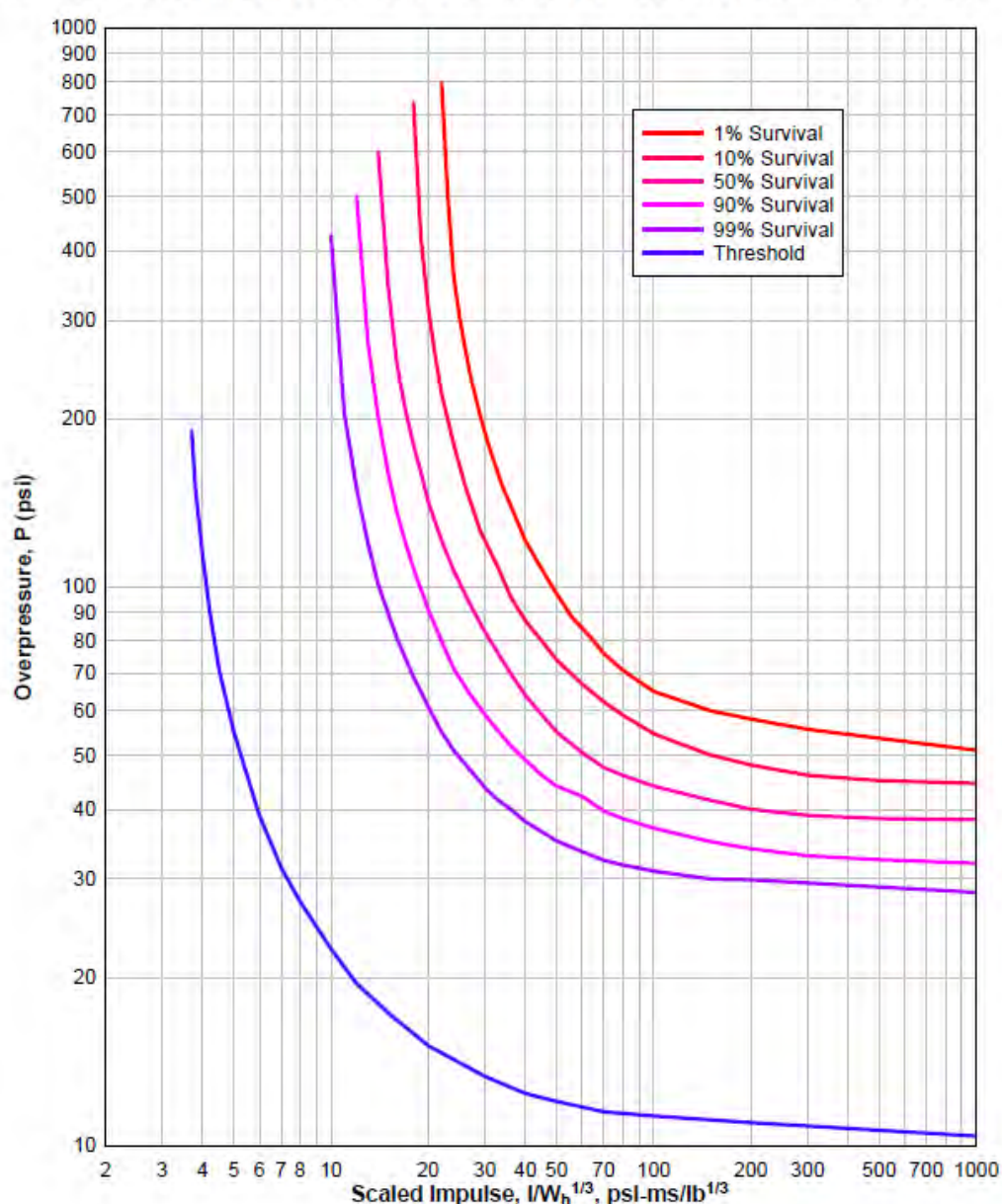
Figure 17: Survival curves for lung damage (Figure 1-2 from [19]).

To quantify the level of primary injury, the iso-damage curves in Figure 17 can be mapped onto relevant geometry related to a domestic or residential setting. An example of this is shown in Figure 18 which is a plan of a street with terraced housing on. Here an explosion within a property generates a blast wave that escapes through an opening such as a window. For a human of a certain weight. the larger radius represents the threshold for lung damage from Figure 17 and the purple radius the threshold for 99% survivability. **In practice, the area subtended by contours in Figure 17 would be very small, if any size at all for domestic gas explosions with the main contribution to injury being secondary, tertiary or burn injuries.**
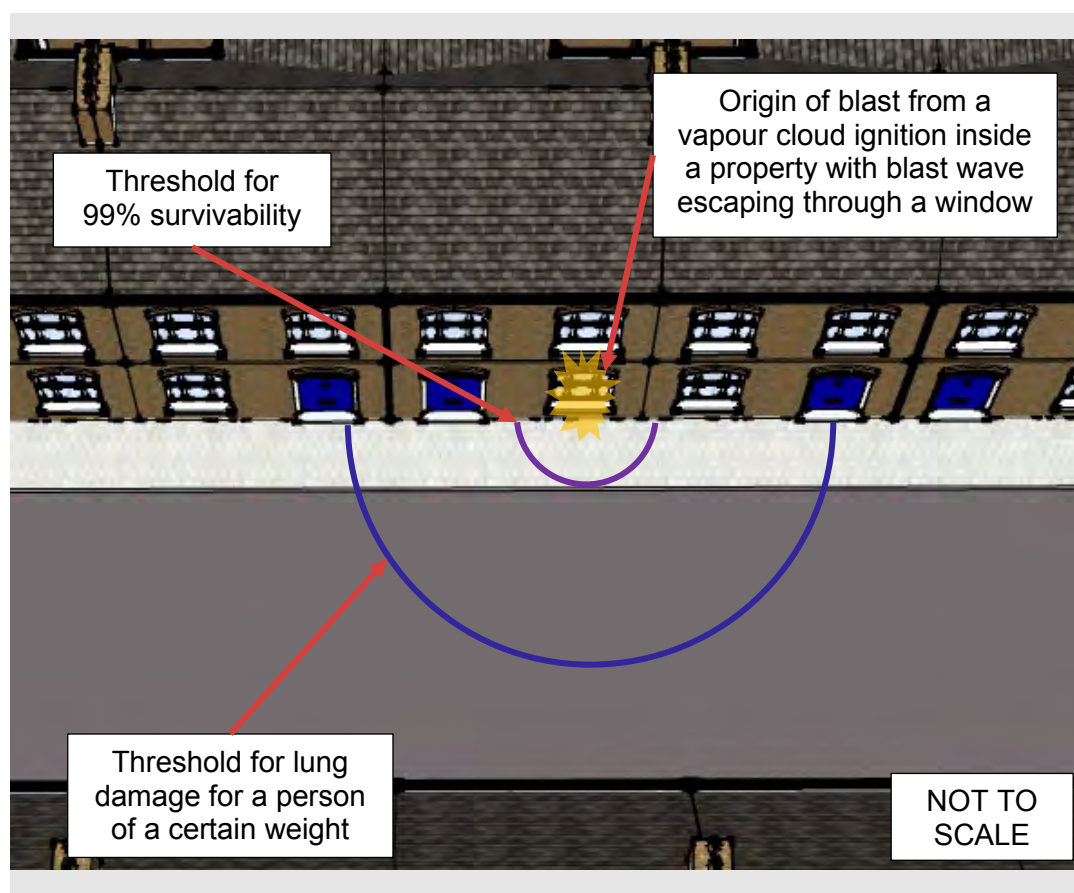
Figure 18: Example of iso-damage curves from Figure 17 mapped onto geometry.

### 2.10.2    *Secondary injury*

In general, human tolerance to fragment impact is very low [19]. Fragments from a vapour cloud explosion can be classified based on their size, velocity, material etc but are usually generated from the breakup of parts of a domestic structure such as windows, walls, or from the displacement of furniture, household items.

Fragments with large mass will also cause serious injuries at relatively low velocities when compared to small fragments (approximately equal or less than 15g) at high velocity. The impact of a relatively large mass with a velocity less than 3m/s against a human can result in serious bodily injury.

When considering secondary effects, distinguishing between cutting and non-cutting fragments is necessary [2]. Cutting fragments penetrate the skin, whereas injuries from noncutting fragments result from contact pressure at impact. A fragment is generally considered to be dangerous if it has a kinetic energy of at least 79 J. But values of 40 to 60 J were found to cause serious wounds [2].

### 2.10.3    Tertiary injury

When a subject is thrown off balance due to bodily interaction with a blast wave, the subject is usually thrown bodily against other persons, furniture, walls and other hard surfaces. Studies have indicated that a probable safe impact tolerance velocity is 3m/s [19]. At a velocity of 5.5m/s there is a 50% probability of skull fracture and at 7 m/s, the probability is nearly 100 percent [19]. This applies to impact with hard, flat surfaces in various body postures.

However, if the line of thrust for head impact with a hard surface is directly along the longitudinal axis of the body (a subject falling head first), the above velocity tolerance does not apply since the head would receive the total kinetic energy of the entire body mass [19].

An investigation of data concerning sudden stops in automobiles and passenger trains indicates that personnel can sustain horizontal accelerations less than 0.44g without being thrown off balance. These accelerations have durations of several seconds; hence, the accelerations from a vapour cloud explosion required to throw a subject off balance are probably greater because of their shorter durations. The tolerable horizontal acceleration of 0.50g required to provide protection against ground-shock effects resulting from nuclear detonations can be conservatively taken as a safe tolerance for tertiary injury for non-restrained personnel (standing, sitting, or reclining)

Quantifying tertiary injury due to a vapour explosion in a domestic property is difficult. However, if assumptions are made such as a person being face on to the propagating blast wave, then with an estimation of the frontal area of a body and a predicted impulse profile from the blast wave, an approximate acceleration exerted on a person can be made.

Ignition of a flammable vapour cloud within the property destroys window and pressure wave escapes house

Reflected overpressure exerted over surface area of a body imposing an acceleration on the persons mass

Acceleration due to the reflected pressure exceeds 0.5g and causes person to lose balance injure them in a fall
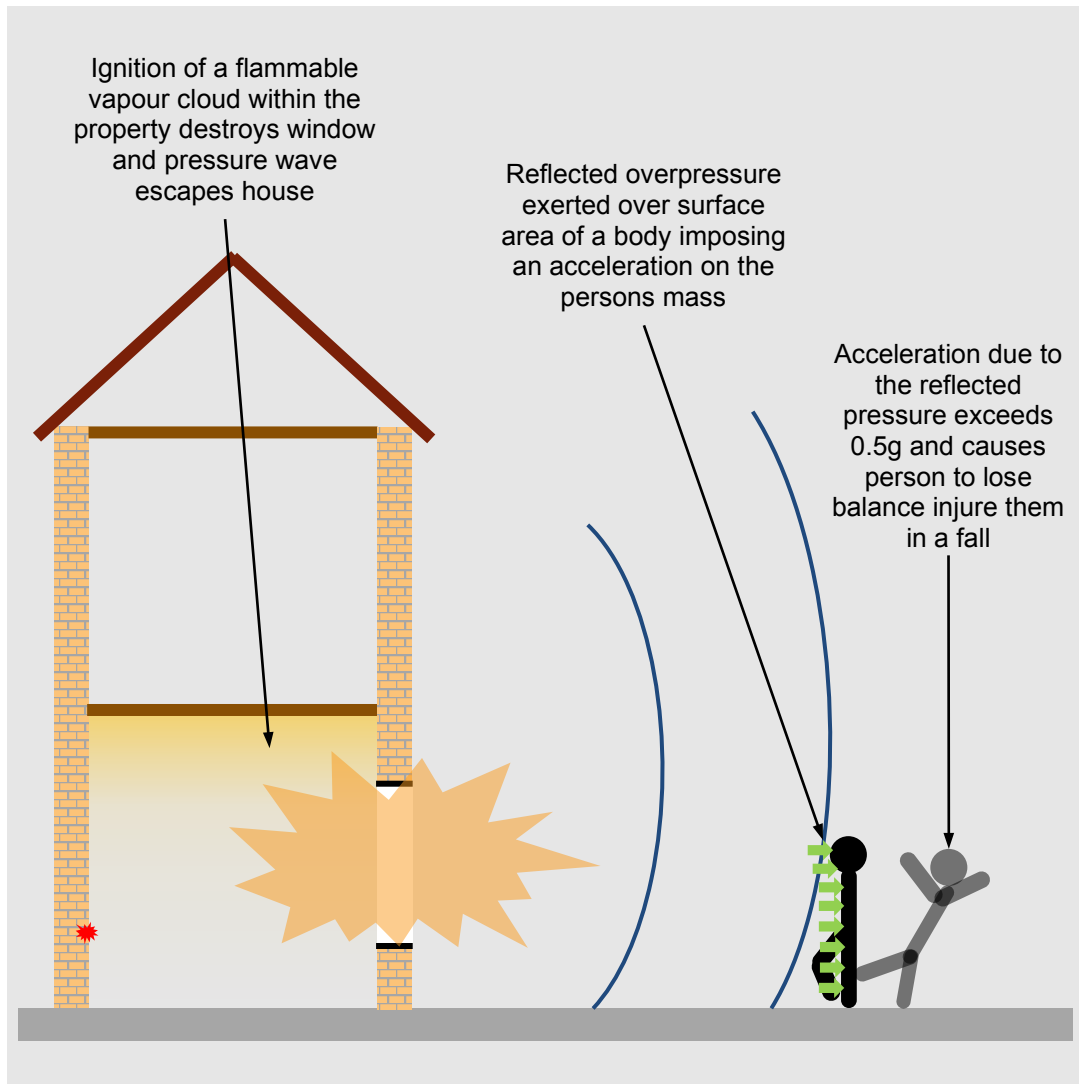
Figure 19: Tertiary injury due to a vapour cloud explosion in a domestic property

## 2.11    Effects of fire on people

A fire in a domestic environment is rarely fuelled by a gas leak alone. A fire in a domestic environment may have been *started* due to a gas leak which is then ignited. Following ignition of a gas leak, the abundance of combustibles within a home would quickly become the dominant source of fuel contributing to the size and power of a fire. This would result in the fire becoming no different to any other fire started by other means such as an electrical fault, an oven etc. Where a gas leak leads to a flammable vapour cloud forming in the domestic environment, the ignition of the flammable vapour cloud could produce a flash fire with severe radiant heat for a very short time scale ($\sim$<1 second).

There are three basic ways in which exposure of fire to a victim can lead to injury, incapacitation or death [8]. These are:

– Heat stroke (or hyperthermia)

– Body surface burns

– Respiratory tract burns

– Asphyxiation

Heat Stroke (or hypothermia) occurs when a subject is exposed to a hot environment and their core body temperature increases above 38-40°C. When the core body temperature reaches 42.5°C death is almost certain unless the subject is treated within minutes [4]. The time to heat stroke occurring depends mainly on the heat flux to which the subject is exposed and is affected by the type of clothing worn, health state of the subject, and level of activity.

Body surface burns can occur due the heat transfer to bare human skin via any of the three main heat transfer methods:

– Conduction where skin comes into contact with a hot surface such as a metal surface.

– Convection where heat transfer to the skin is via hot gases such as smoke passing over the surface of the skin

– Radiant heat where the heat is transferred via infrared radiation from the fire to the skin. An example would be a flash fire or fire ball where despite a victim not being engulfed within the fire, they could be exposed to significant heat flux via radiation from the surface of the flame.

Respiratory tract burns occur when hot gases are inhaled and cause severe damage to the larynx, trachea and lungs. Burns to respiratory tract never occur in the absence of burns to the skin [8].

For a flash fire occurring due to the ignition of a confined flammable vapour cloud within an enclosure such as a kitchen, an occupant of the enclosure would be engulfed in the combusting vapour cloud and subjected to heat transfer to bare skin via convection and radiant heat transfer forms. This would result in injury via body surface burns and respiratory tract burns.

Asphyxiation occurs when a subject is exposed to toxic gases such as carbon monoxide, carbon dioxide and reduced oxygen concentration. Additionally, smoke deposits may physically clog airways.

Measuring injury from the effects of fire is complicated given the number of factors to consider:

- Exposure time

- Health of person

- Different types of heat transfer to body which are usually in a combination of all three

- Toxicity of the smoke which is due to the composition of the combustible loads in the fire

- The environment such as geometry of an enclosure or room where the fire is occurring

- Behaviour of the subject

- Clothing worn and surface area of skin exposed.

A flash fire from the ignition of a vapour cloud (whether explosive or low deflagration) will principally expose a victim to either radiant and/or convective heat transfer. Figure 20 from [7] is a plot of time taken for skin to develop superficial second-degree burns against thermal irradiance in $kW/m^2$. The required exposure time to develop superficial second-degree burns reduces with increasing thermal radiation exposure. Thermal radiative heat transfer on a surface is proportional to the square of the distance from the source. i.e. a person standing at twice the distance from a radiative heat source than the person in front of them will experience a fourfold decrease in thermal radiative heat transfer to their skin.
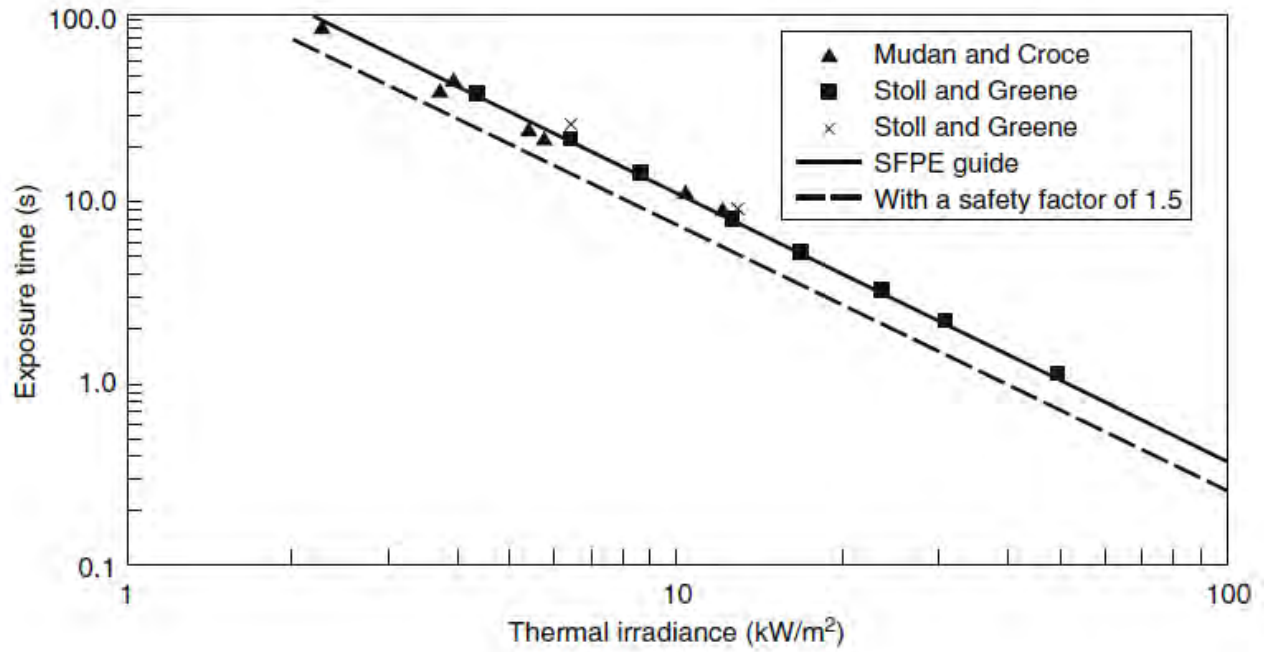
Figure 20: Figure 66.60 from [7]: Time for superficial second-degree burn on a plot of exposure time versus thermal irradiance. fits to data are shown as dashed lines.

# 3.  Methodology

## 3.1  Type of residential dwelling

There are many different housing topologies within the UK so undertaking a consequence assessment that covers a 'typical' residential dwelling in the UK is challenging. A terraced house represents a reasonable choice of a residential dwelling on which to base several assumptions. The following are arguments for basing the consequence modelling assessment on a terraced house:

– Terraced houses have party walls separating each house from the neighbouring houses. This wall is a nearly always a structural wall, the collapse or damage of which would likely cause partial structural collapse to the neighbouring properties to the property in which say a gas explosion occurred. This would indicate that the severity of a gas explosion within a terraced house is greater than when compared to a detached house or semidetached house. Figure 23 and Figure 24 show the damage following a gas explosion in a terraced house and a detached house respectively. Although there is some damage to the exterior of the house in Figure 24, the neighbouring houses to the house where the gas explosion occurred remain structurally intact. The same cannot be said for the neighbouring terraced houses in Figure 23.

– Terraced houses have similar layout configurations throughout when compared to detached or semidetached houses which generally have a greater variety in layout. Terraced houses built in the early 20th century (sometimes referred to as 'two up-two down'), which have not been converted to flats or apartments, often have a kitchen on the ground floor at the back of the house, two reception rooms on the ground floor and two to three bedrooms on the first floor.

– Many terraced houses have been converted to flats with a ground floor flat that has a kitchen at the back of the property, and a first floor flat with a kitchen at either the front or back of the property. However, the consequences of a gas leak related event are the same if not similar as to if the terraced house was one dwelling. However, occupancy levels could differ slightly between a terraced house that has been converted to two flats, and a terraced house that is one dwelling.

As a basis for a "typical" residential property and residential setting to undertake a consequence assessment, a terraced house in a row of terraced housing such as shown in Figure 21 has been taken. Some assumed dimensions for the house and surrounding setting have been made and are shown in Figure 22.

Figure 21: A typical terraced housing street (Extract of Sketchup image from [20])



Figure 22: Some estimated dimensions used to model a residential property in a typical setting (Extract of Sketchup image from [20])

Figure 23: Damage to terraced housing following a domestic gas explosion in Salford – Greater Manchester in November 2010 (image from [21])



Figure 24: Damage to detached housing following a domestic gas explosion in Haxby – Yorkshire in February 2016 (image from [22])

## 3.2 Scenario for comparison

### 3.2.1 Sequence of events

As part of the modelling of the consequences in this report. the event tree below demonstrates the possible sequence of events that could take place taking into consideration the injury criteria described in Sections 2.10 and 2.11. Quantitatively measuring the injury is discussed in Section 3.3.
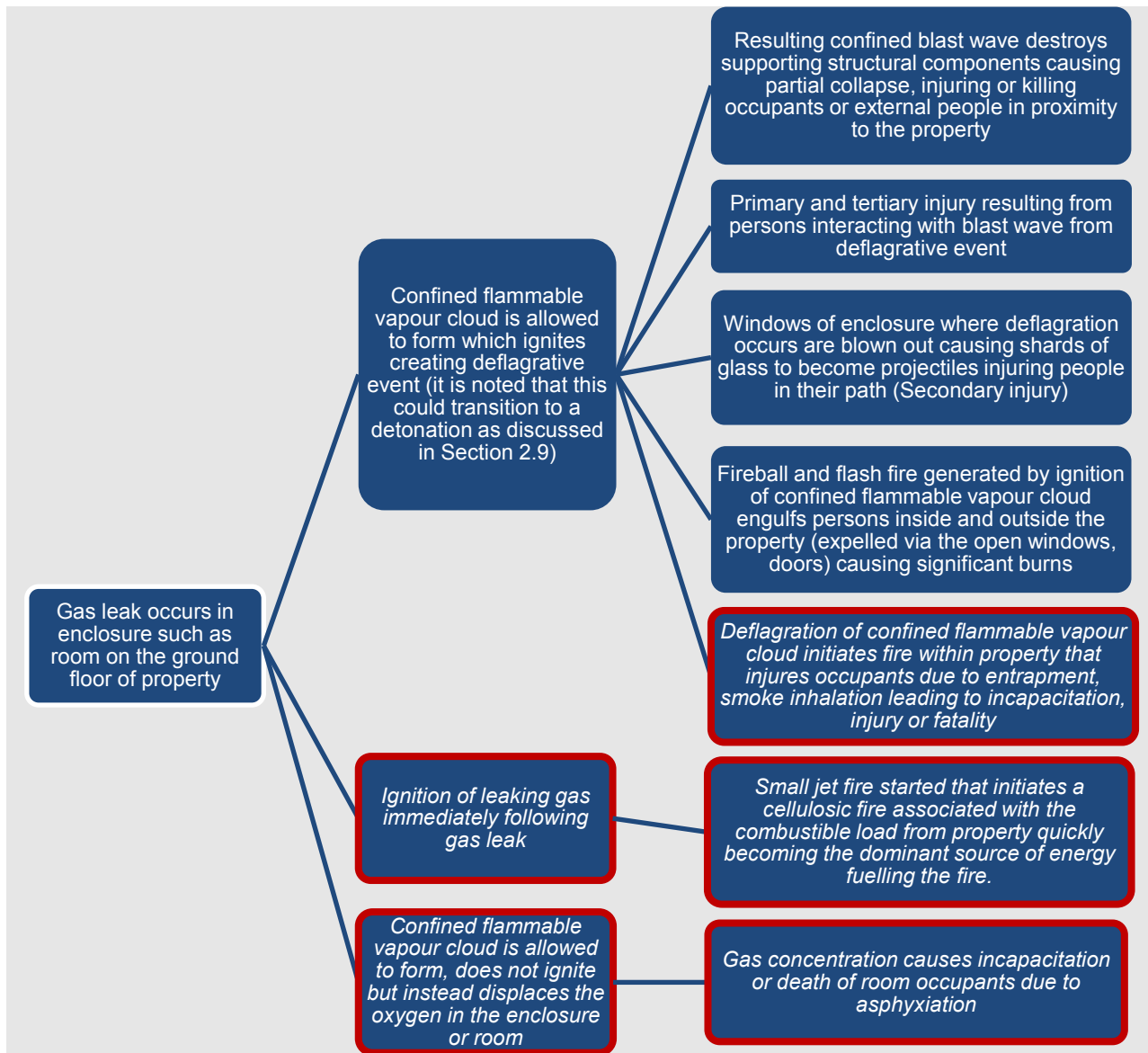


The events in *italics* highlighted with a **red** border in the above event tree *are not considered* in this consequence assessment. As mentioned in Section 2.11, if an ignition of leaking gas immediately following a gas leak were to occur that then further initiates a cellulosic fire associated with the combustible load of the interior of a property, the abundance of combustibles within a home would quickly become the dominant source of fuel contributing to the size and power of a fire. Although the *probability* of this occurring may be different for natural gas and hydrogen, the *consequences* would be the same for both gases given their negligible contribution to the overall heat release rate of a partially or fully developed compartment fire within a domestic setting by the leaking gas. This would

also be the same for the deflagration of a confined flammable vapour cloud in a room in the dwelling that then initiates a compartment fire within the property that injures occupants due to entrapment and smoke inhalation leading to incapacitation, injury or fatality.

Likewise, the *probability* of asphyxiation of the dwelling's occupants due to a confined flammable vapour cloud forming but not igniting may be different, but the *consequences* for both natural gas and hydrogen are very similar.

To expand on the sequence of events discussed in Section 3.2.1, Figure 25 summarises the consequences considered in this report for a scenario where an enclosure within a terraced house is filled with a confined flammable vapour cloud following a leak and dispersion event.

Department for Business, Energy & Industrial Strategy  Hy4Heat
ARP-WP7-GEN-REP-0003 | Issue 01 | 1 May 2021  Consequence Modelling Report

Page 40

Combustion (deflagration) of confined flammable vapour cloud can engulf occupants of dwelling and cause injury external to the dwelling as unburnt gas is expelled through openings and combusts externally

Blast wave (or pressure wave) can cause primary and tertiary injury

Failure of window projecting glazing fragments into street or area in front (and/or behind) dwelling

Ignition of confined flammable vapour cloud following gas leak and dispersion within property creating confined flammable vapour cloud(s)

Collapse of structural walls injuring occupants on all stories of the dwelling

Door blown open or off hinges/fixings with venting of expanding internal gases to outside

Figure 25: Summary of consequences and injuries

### 3.2.2 *Gas leak inside the property*

Two scenarios were considered for this assessment:

– A ground floor kitchen with the dimensions and vents shown in Figure 26. Initially the internal door and window is closed allowing a build-up of gas within the room prior to ignition of the confined flammable vapour cloud.

– The downstairs of an open plan terraced house with the dimensions and vents shown in Figure 27. Initially, the internal door and windows are closed and any opening to the upstairs is assumed to be separate allowing a build-up of gas within the room prior to ignition of the confined flammable vapour cloud.

The above scenarios were considered for both methane and hydrogen with the enclosure dimensions in line with the enclosure dimensions considered in the Hy4Heat dispersion modelling report [23]. The kitchen scenario covers a more traditional layout found in terraced housing (i.e. kitchen and living areas separated) where flame propagation has a short distance to accelerate over in the event of a back-wall ignition. The open plan downstairs of a terraced house scenario represents an open plan layout or a downstairs layout where the back of the house has been extended and where flame propagation from a back-wall ignition would have the depth of the house to accelerate through.
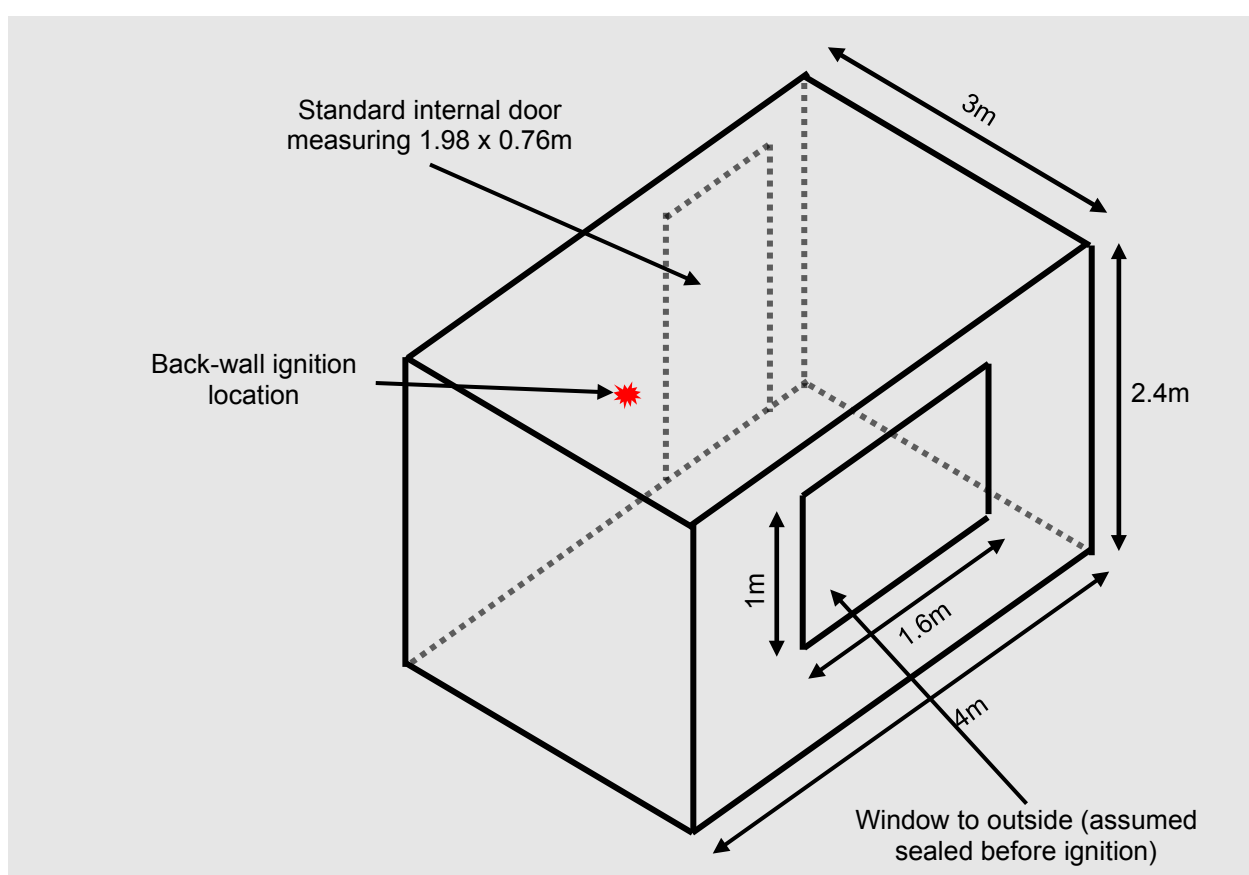


Figure 26: Kitchen used in consequence modelling assessment
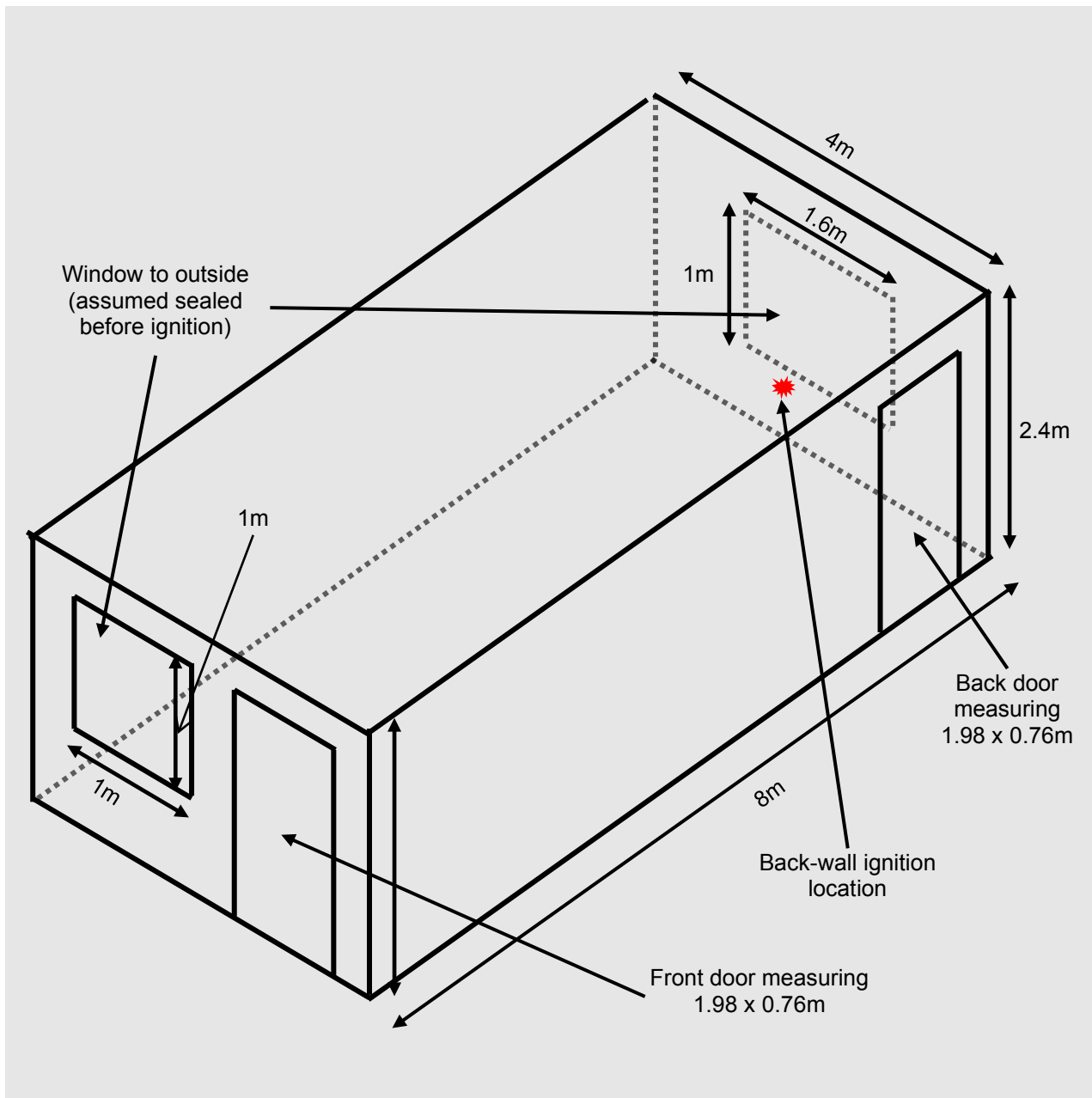
Figure 27: Downstairs of a terraced house used for the consequence modelling

The consequences of a confined flammable vapour cloud ignition were assessed for several concentrations within the flammable range for both methane and hydrogen for each scenario. A back-wall ignition location is considered which is representative of an ignition source such as a light switch on a wall or an electrical appliance at the edge of the room.

### 3.2.3    Stratification

When undertaking a vented explosion assessment for design purposes, the guidance in [1] recommends taking the peak concentration of hydrogen (and methane), which is usually near the top, as the concentration throughout the enclosure. Being less dense than air, both hydrogen and methane stratify within an enclosure when left to reach a steady state, so assuming the entire enclosure has a uniform concentration based on the peak concentration at the top of the enclosure is highly conservative because it is overestimating the combustible inventory when compared to what happens in practice.

Experiments undertaken by DNV GL [24] were analysed to gauge an understanding of the stratification that occurs within a confined flammable vapour cloud in an enclosure of a typical terraced house (such as a kitchen or living room) following a gas leak. The experiments undertaken by DNV GL measured concentration over the height of the room at approximately floor level, one half the height of the enclosure/room, and at ceiling level. This was done for a variety of scenarios and leak locations throughout the house.

A selection of experiments where the leak location was in the basement below the kitchen and living area were chosen as the base cases to produce a regime by which to model stratification[15]. The results from this selection showed that, with the doors closed, for hydrogen dispersion in the kitchen, the mid-height concentration measurements of the enclosure were of similar concentration with the measurement at ceiling level being the highest or peak concentration. This was observed for steady state scenarios (i.e. when the leak rate of gas into the enclosure became equal to the leak rate of gas out of the enclosure)[16]. The mid-height measurement often recorded a concentration within 90 to 95% of the peak concentration. The bottom measurement was often approximately one tenth of the peak concentration near the top of the room and nearly always below the lower flammability concentration for hydrogen (~5% volume). These measurements, although coarse, give some confidence that the stratification of hydrogen in a domestic enclosure can be represented as shown in Figure 28. Here the top third of the kitchen is assumed to have the peak concentration, the middle third approximately 90 to 95% of the peak concentration at the top of the enclosure and the bottom third having a concentration of one tenth of the peak concentration[17].

For methane the stratification within the kitchen enclosure for the DNV GL experiments [24] was less severe with the peak concentration being at ceiling level, the concentration at mid-height being approximately 80-85% of the peak concentration, and the concentration at floor level being approximately three fifths of the peak concentration. These measurements suggest that the stratification of methane in a domestic enclosure such as a kitchen can be represented as shown in Figure 29.

---

[15] See Appendix B for further discussion regarding sensitivity studies.

[16] "A steady state concentration was reached where the concentration increase [from] the previous hour was less than 10 %." [24]

[17] There were several experiments where the observed concentration at ceiling level for hydrogen and methane was very high (+45%) but the concentration at mid height and floor level was at or below the lower flammability limit. This is discussed further under the assumptions in Appendix B.
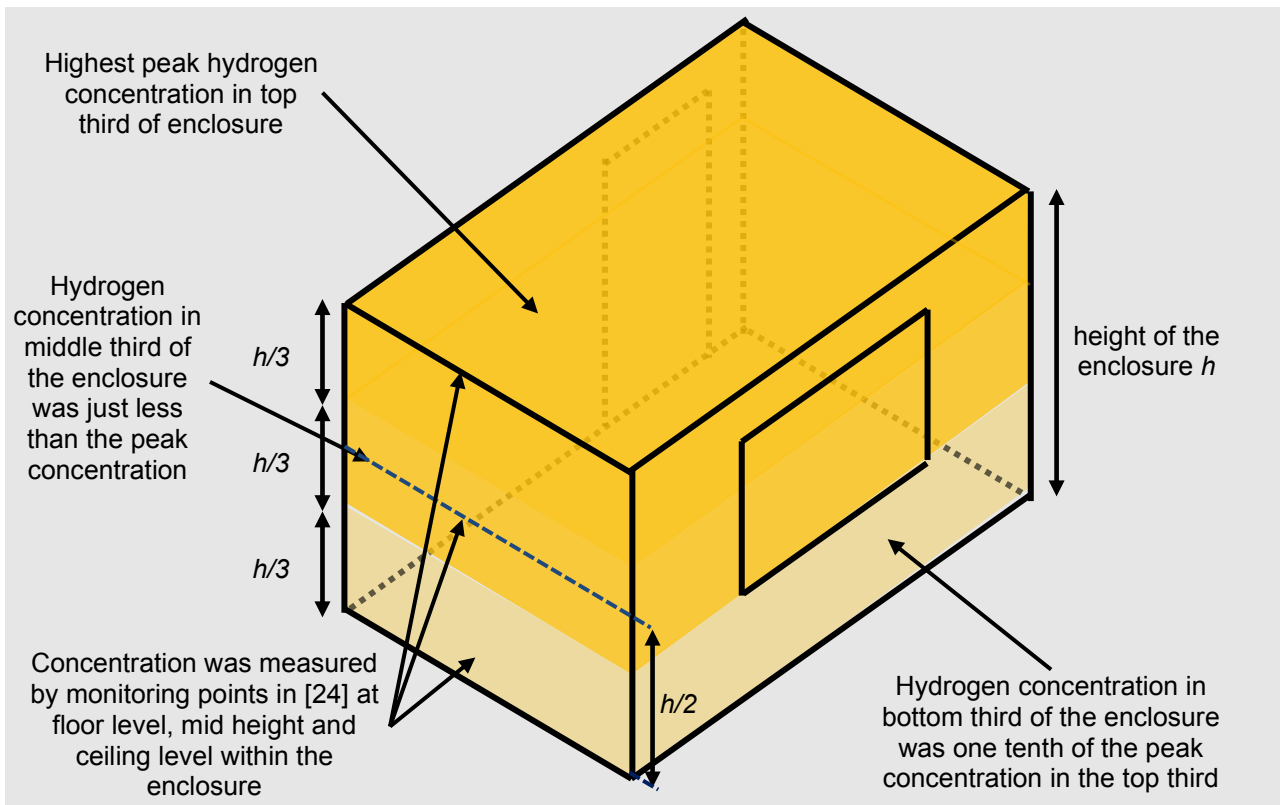
Figure 28: Approximate stratification of *hydrogen* within a domestic enclosure
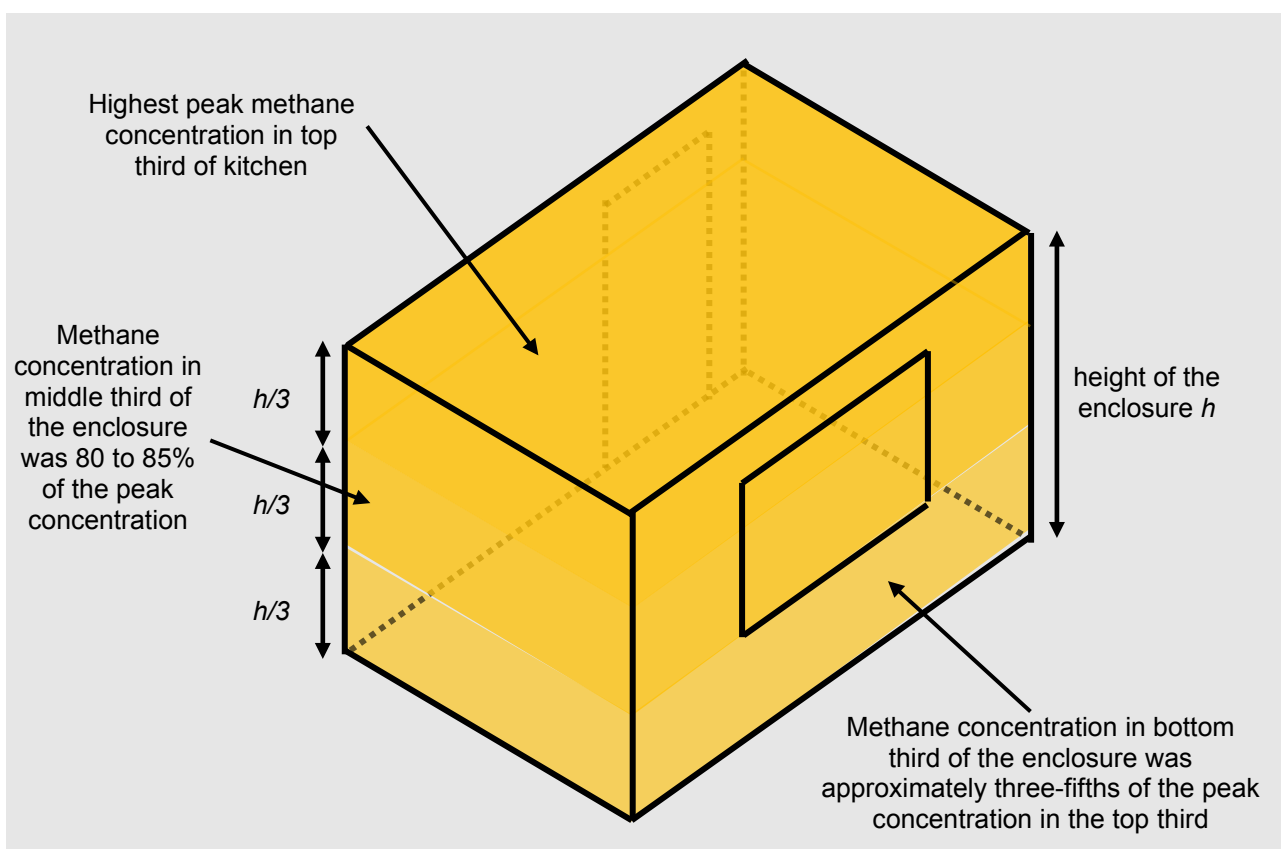


Figure 29: Approximate stratification of *methane* within a domestic enclosure

For the consequence modelling undertaken in this report, the stratification of hydrogen has been considered by assuming the "equivalent volume" of hydrogen contributing to the confined flammable vapour cloud explosion is *two thirds the volume* of the enclosure volume at the peak concentration (Figure 30). The "simplified" model (see Section 3.4.1) used to estimate peak internal overpressures and impulses is based on a homogenous concentration. As mention on page 44, assuming the entire enclosure has a uniform concentration based on the peak concentration at the top of the enclosure is highly conservative. Using an "equivalent volume" approach ensures that all the combustible inventory (in MJ) in the confined hydrogen cloud is considered in the modelling but is more representative of a realistic scenario in a domestic enclosure.
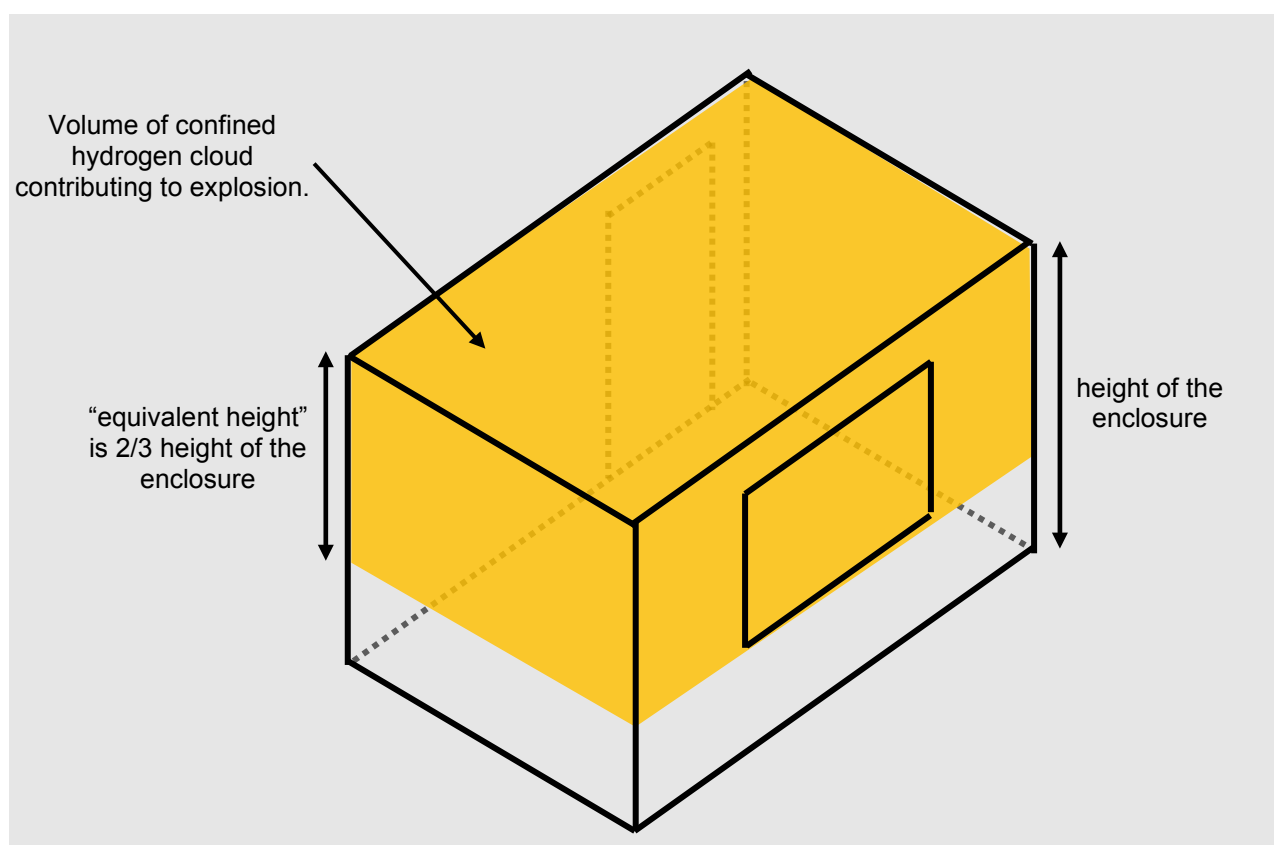


Figure 30: "Equivalent Volume" of a hydrogen vapour cloud at peak concentration in a domestic enclosure

The assumed "equivalent volume" of methane contributing to the confined flammable vapour cloud explosion is *four fifths the volume* of the enclosure volume at the peak concentration (Figure 31).

Further clarity, including examples to explain the approach to considering stratification is provided in Appendix A.
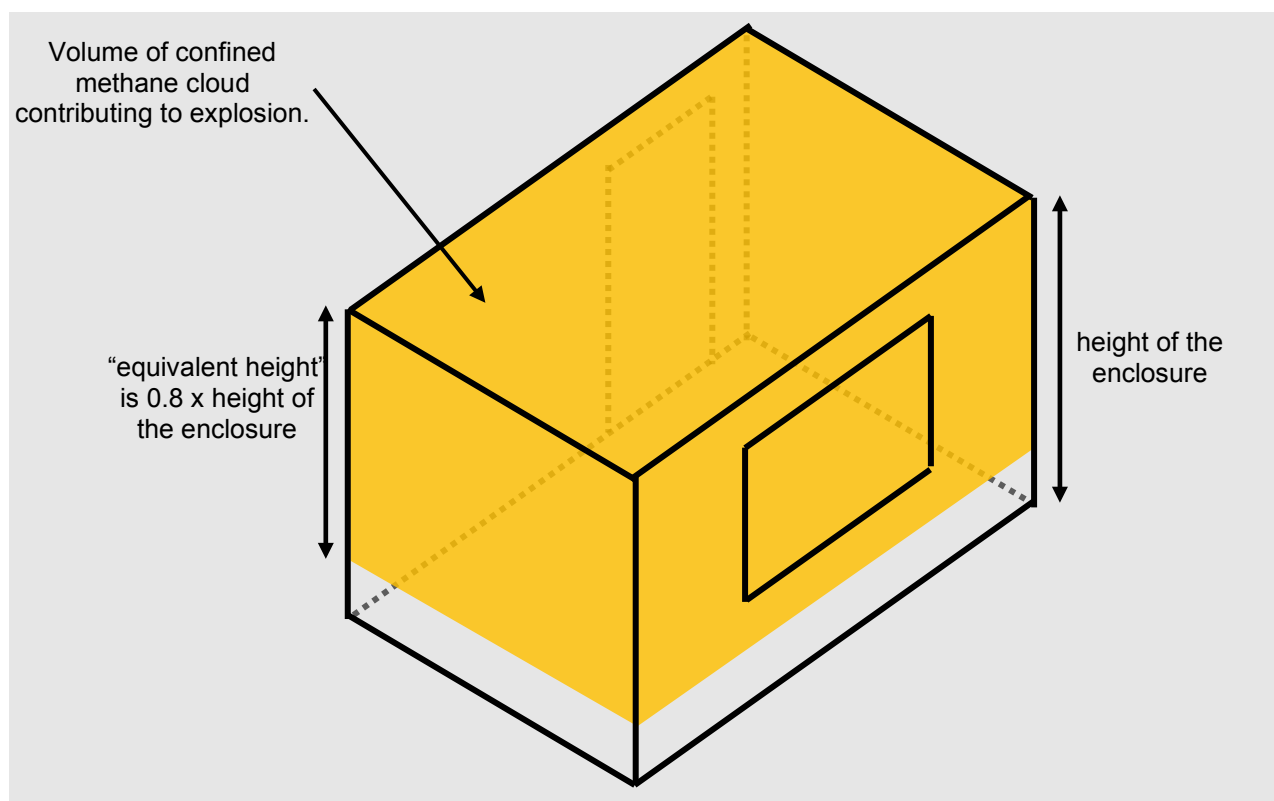
Figure 31: "Equivalent Volume" of a methane vapour cloud at peak concentration in a domestic enclosure

For cases in the Dispersion modelling report [23] where the peak concentration is *above* the UFL of *methane*, the modelling assumes that ignition does not occur when modelling methane. This will likely lead to an underestimate in consequences for methane because even if the peak concentration of a stratified methane cloud is above the UFL, there will still be a region of the cloud that is within the flammable range.

For cases in the Dispersion modelling report [23] where the peak concentration in the enclosure is *above* stoichiometric but below the UFL for *methane*, the "equivalent height" in the modelling is assumed to remain the same (0.8 for methane). In this instance, the stratified confined flammable vapour cloud is modelled as a homogenous confined flammable vapour cloud with a concentration at the peak concentration. Again, this could lead to an underestimate in the consequences for methane because in practice there will a region of the confined stratified methane cloud that will be at or near the stoichiometric concentration.

Modelling above the UFL for *hydrogen* has not been undertaken in this assessment because the peak concentrations observed in nearly all the DNV GL hydrogen dispersion experiments [24] were within the flammable range for hydrogen.

For cases were the peak concentration is *above* stoichiometric but below the UFL for *hydrogen,* the "equivalent volume" is determined by adjusting the peak concentration at the top of the enclosure to match the stoichiometric concentration, and then calculating the "equivalent height" to ensure the

total combustible inventory in the compartment is considered in the modelling (see Appendix A and Figure 80 on page 111 for further clarity). This approach means that the modelled consequences in this assessment (such as vented explosion strength following ignition) conservatively continue to increase in severity with increasing concentration above stoichiometric for hydrogen.

A sensitivity study has been undertaken in Appendix A.2 to compare the "equivalent volume" method in this assessment with the Q9 approach to estimating "equivalent volume" from "A Review of the Q9 Equivalent Cloud Method for Explosion Modelling" chapter in [25]. The results of this sensitivity study showed that the approach to estimating "equivalent volume" in this assessment slightly overestimates the "equivalent volume" by the same degree for both gases when compared to estimating the "equivalent volume" using the Q9 method. It is recognised that further work on modelling stratification is required and that there are several variations of the "equivalent volume" method that should be explored in further detail as per the guidance in [25].

## 3.3 Quantitatively measuring injury

### 3.3.1 Introduction

Injury due to structural collapse, along with primary injury, secondary injury, tertiary injury, and injury due to burns have been quantitatively assessed in the following sub-sections using the criteria in Sections 2.10 and 2.11. A summary of the different ways in which injuries are considered to occur is summarised in Figure 25 on page 41 in Section 3.2.1.

The term 'injury' in this assessment includes fatality and the 'number of people injured' (whether fatally or not) is the value that is measured to provide some means to quantitatively compare hydrogen with methane. It is difficult to quantitatively measure injury given the large number of variables involved. For example, a person in front of a dwelling (in the street) who is standing 2 metres from a window that fails under a vented explosion within the dwelling and projects glass fragments 40 metres horizontally, will almost certainly incur a higher level of injury than a person who is standing 38 metres from the window. However, the consequence modelling in this assessment would categorise both the individuals in this example as "persons injured". The assessment does not go into further levels of graduality in quantitatively measuring consequence, for example, by weighting the different levels of injury.

### 3.3.2 Measuring injury due to structural collapse

Following ignition of the flammable vapour cloud within a ground floor room or enclosure, a confined vapour cloud explosion starting as a "closed vessel deflagration" and transitioning to a vented explosion as described in Section 2.6.2 will exert an overpressure and pulse on the enclosure boundaries (walls, floor and ceiling) as described in Section 2.6. As discussed in Section 2.7, masonry structures, of which most residential properties are, fail in a brittle manner. In most instances the critical structural components of a masonry building are those which are load bearing. Vertical load bearing components tend to be walls and these usually support horizontal load bearing components such as joists and beams, which in turn usually support a floor (on which an occupant might be). The

failure of a load bearing wall will tend to result in further collapse of vertical load bearing components (taking axial load) such as load bearing walls from above, and horizontal load bearing components such as a roof or ceiling/floor.

Determining the resistance and therefore the response of a wall due to overpressures and impulses acting on the wall is described in Section 2.7. This methodology will be used to determine whether a wall has failed under blast load following the ignition of a confined flammable vapour cloud within an enclosure within the ground floor of a house.

Quantitatively measuring the level of structural collapse is a case of determining whether a vertical load bearing component taking axial load has failed. For the scenario of an explosion occurring in a room such as a kitchen on the ground floor of a terraced house that generates overpressures and impulses beyond the capacity of the load bearing walls of the room, it is reasonable to assume that any horizontal structural component (such as a floor) that loses its vertical load bearing support on one side also undergoes collapse. This is visually described in Figure 32 where the loss of the structural element in blue would lead to the loss of the structural elements in red but not to those in black.
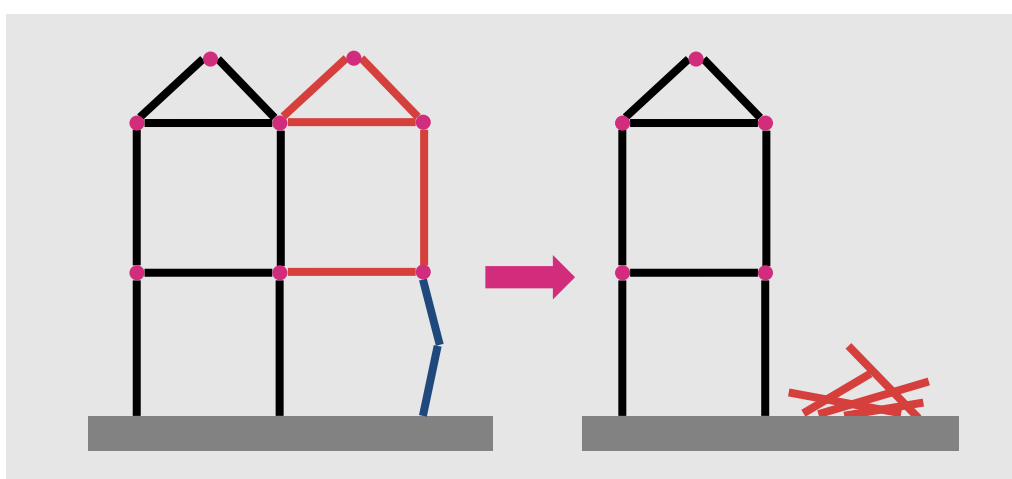


Figure 32: Loss of critical structural components

It is common for floors to be one way spanning in houses with joists usually spanning the shortest span and then floorboards spanning perpendicular to these joists. In a terraced house the joists tend to be across the width of the house. The example scenario in Figure 33 could lead to structural collapse of the house and partial or full collapse of the neighbouring house shaded in Figure 34. The extent of damage in Figure 34 would result in the occupants on the first floor being involved in a fall due to a collapsing floor beneath them and occupants on the ground floor being injured due to structural elements falling on them for both the house where the explosion occurs as well as the neighbouring house.

Technically, injury to dwelling occupants occurring due to structural collapse could be a combination of secondary and tertiary injury. If a person is struck by an element or elements of the structure collapsing on top of them then this could be classed as secondary injury through blunt trauma if the element or elements are heavy and blunt, or penetrations and lacerations if the element or elements are sharp. Likewise, if a person is on the first floor and the floor on which they are standing collapses below them and they injury themselves through falling from height then this could be classed as tertiary injury. For this assessment, occupants internal to the dwellings who are injured due to structural collapse are assessed separately to persons being injured externally through secondary or tertiary injury in the public realm (street).
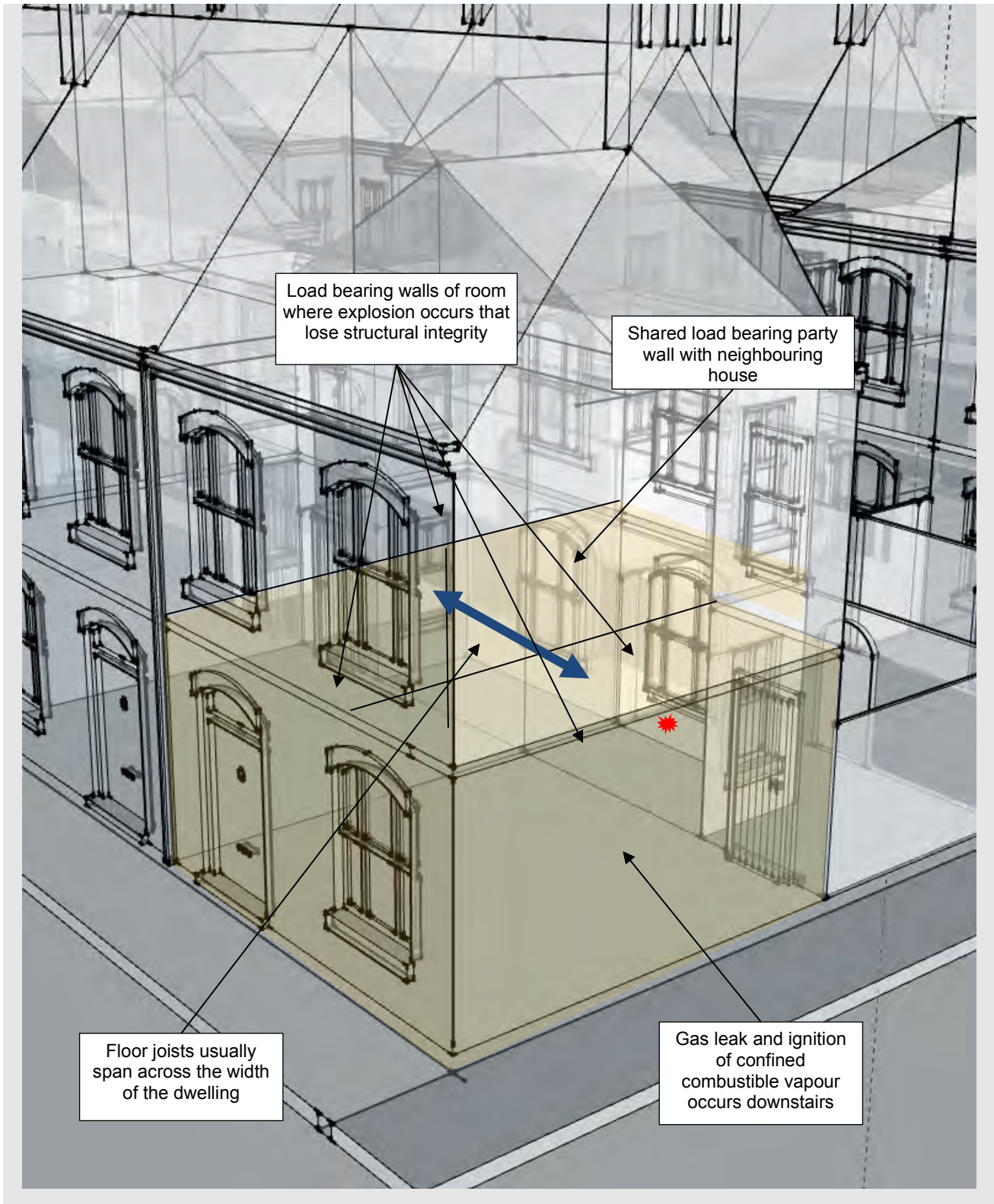
Figure 33: Location of load bearing walls and a possible confined flammable vapour cloud for the downstairs scenario assessed (extract taken from [20]).
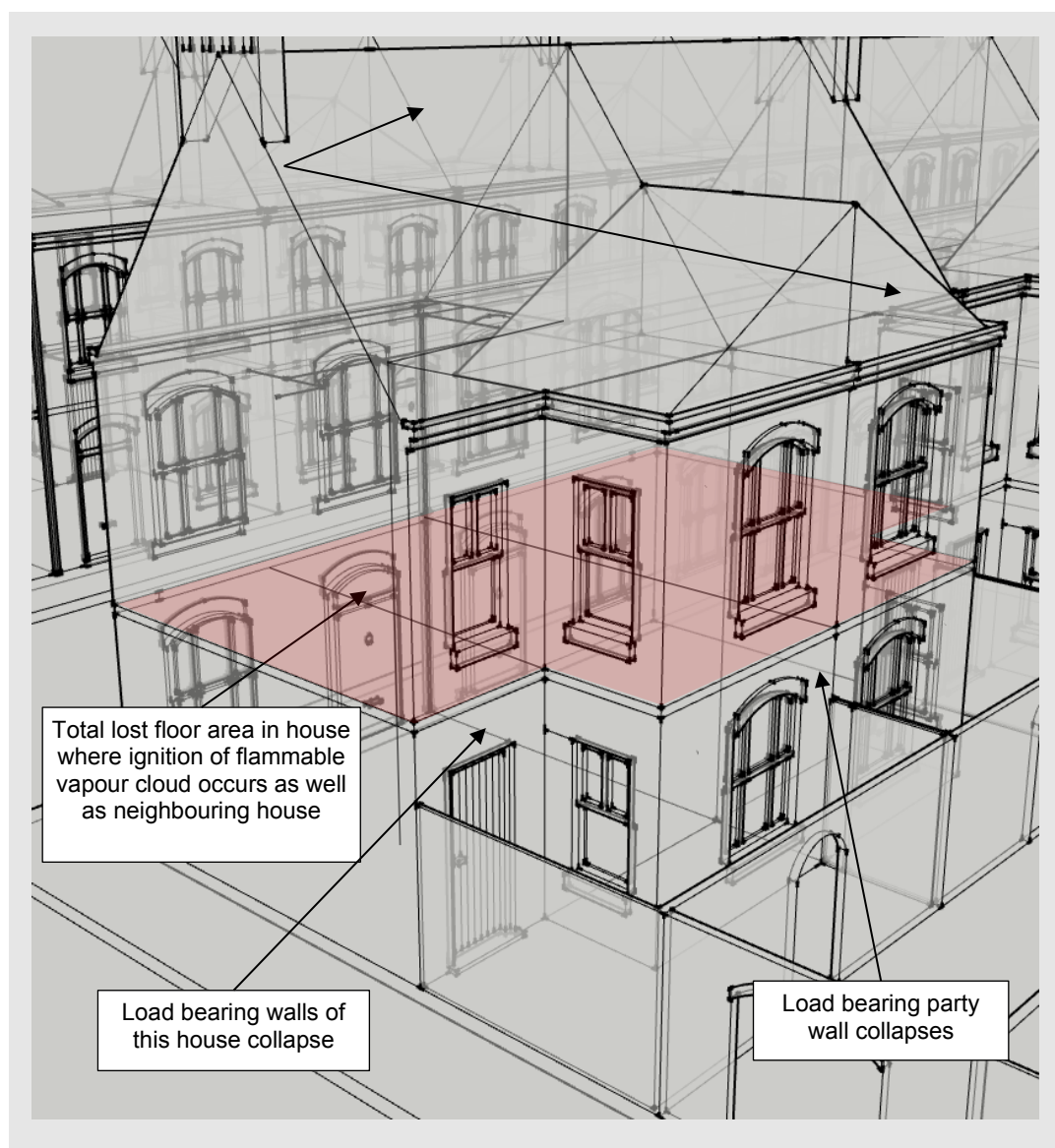
Figure 34: Possible extent of structural collapse following gas leak and ignition of combined flammable vapour cloud in Figure 33 (extract taken from [20])

If the gas explosion is severe, the number of structural elements damaged directly due to the blast overpressure could be more than just the enclosure walls that are confining the flammable vapour cloud prior to ignition. If this is the case, then the level of structural collapse and number of occupants injured will be determined using the same approach. i.e. number of occupants involved in a fall due to a collapsing floor beneath them or being injured due to structural elements falling on them. This is illustrated in Figure 35.
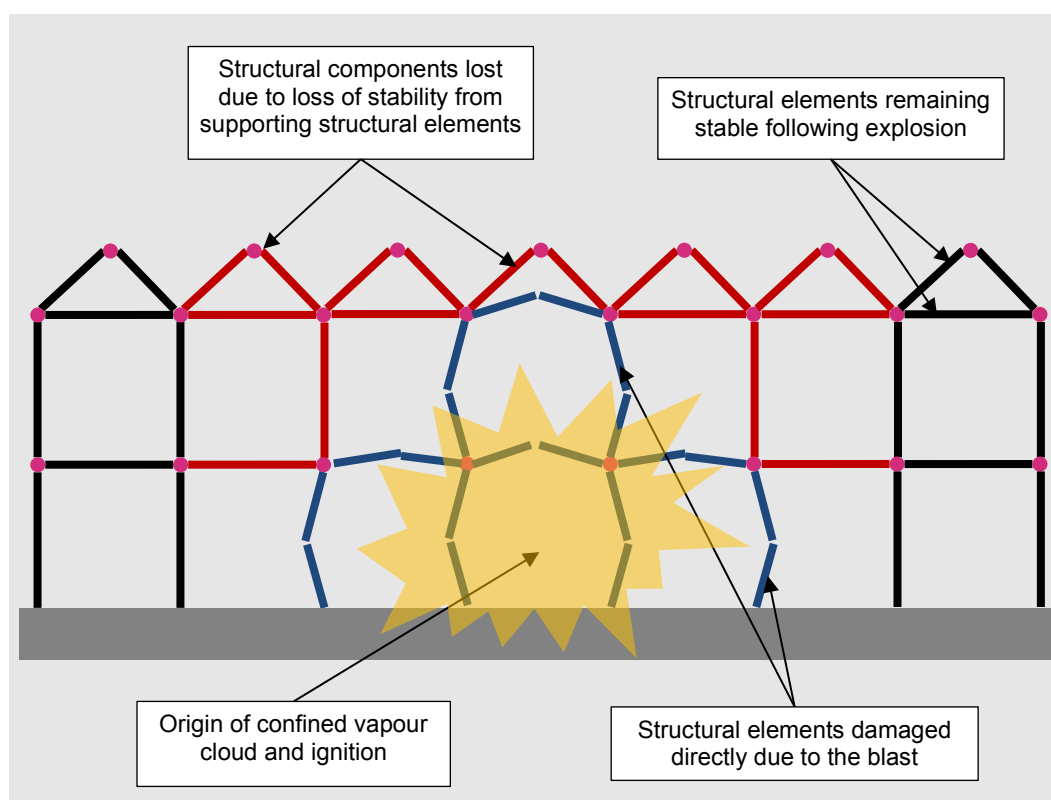
Figure 35: Loss of critical structural components following a severe explosion. In this case up to 5 properties have collapse

Quantifying the level of injury to occupants requires an estimate as to the number of people within the property or around it that could be injured by structural components falling on them.

Setting parameters for occupancy levels for a residential dwelling is difficult given that occupancy in a dwelling is dependent on the time of day, the demographic of people in the dwelling (e.g. elderly, young professionals with no children, a family etc) as well as a range of other highly varying factors. However, for the scenario of a terraced house considered in this assessment, **an occupancy of 1.79 people per dwelling has been used.** This is based on an average occupancy level of 2.4 persons per dwelling from the Office for National Statistics 2017 household assessment [26], along with some adjustment factors to take account an estimate in the variance in occupancy levels throughout a day and working week. Further explanation of this can be found in Appendix C.

### 3.3.3 Measuring primary injury

To quantitatively measure primary injury, the number of people affected external to the property will be the output that is assessed for comparison using the methodology in Section 2.10.1, and the survival curves for lung damage from Figure 17.

Some assumptions are to be made with regards to the weight of persons affected. For this assessment the weight of a person is taken to be 70kg. This is below the average for a man in the UK in 2010, similar to the weight of the average women in the UK in 2010 and greater than the average weight of a child in 2010 [27].

An assumption with regards to the density of people within the public realm following the ignition of a flammable vapour cloud from a gas leak is also required if a quantitative assessment as to the level of injury via primary injury is to be made. It is assumed that any persons inside the property are already injured due structural collapse or injury relating to fire and burns.



Figure 36: Example of quantifying primary injury due to gas cloud explosion (plan view of an example street - extract taken from [20])

For this assessment, a density of people per area in an urban realm is set **at 0.116 x 10<sup>-3</sup> persons per m²** (1 person per 8630m²). This figure is based on some assumptions regarding the frequency that occupants of the dwellings in a street of terraced houses (such as Figure 21) leave their house throughout the day and week, spent time walking down the street, plus some assumptions around the frequency that non-residents to a street (such as the one in Figure 21) walk along it. Further explanation of this can be found in Appendix D.

To obtain a quantitative prediction as to the level of injury, the area external to the property within each threshold contour can be multiplied by $0.116 \times 10^{-3}$ persons per m². For example, in Figure 36, if the area indicated in pink was approximately 30m² the number of people injured due to primary injury (blast overpressure and impulse alone) would be 30m² x [$0.116 \times 10^{-3}$ persons/m²], so 0.00348 persons. A similar method for quantitatively measuring injury has been used for the following subheadings of Section 3.3.

### 3.3.4     *Measuring secondary injury (glass throw)*

To quantitatively measure secondary injury, the number of people affected external to the property will be the output that is assessed for comparison between a methane and hydrogen explosion from the scenarios described in Section 3.2.2. This is reasonable given that the main source of injury to occupants within the property in which a flammable vapour cloud explosion occurs will be injury due to structural collapse as discussed in Section 3.3.1, or injury relating to fire and burns. The main source of secondary injury external to a property where a gas explosion occurs is glass throw following failure of the windows under internal blast loading.

Quantitatively assessing the level of injury due to glass throw can be undertaken using a similar approach as to measuring injury from primary injury as described in Section 3.3.3. Firstly, determining whether glazing has failed (broken) under the blast load is required using the methodology in Section 2.8. If it is determined that the glazing in the window of the room or enclosure where the gas explosion occurs has failed, then determination of the level of glass throw is required. The results using this method show a good correlation to the observed glass throw from experimental work undertaken by Kiwa using their Fire Investigation Box (FIB) [28].

An estimate of the glass throw distance due to an internal gas explosion can be made using an estimate of the overpressure and impulse acting upon a window, the loading at which the window breaks, the mass of the window (the total mass of the glass), the use of kinematic equations, drag force calculation and the use of projectile theory.

To estimate the distance that a piece of glass is thrown, calculation of the force from the blast wave is required. This can be used to determine a horizontal acceleration which the glass experiences. This varies with time, so numerical integration is used to estimate the distance the glass travels during the time it is being accelerated by the blast wave (Figure 38). Projectile theory and kinematic equations can be then used to estimate the total distance the glass travels before it hits the floor (Figure 37).
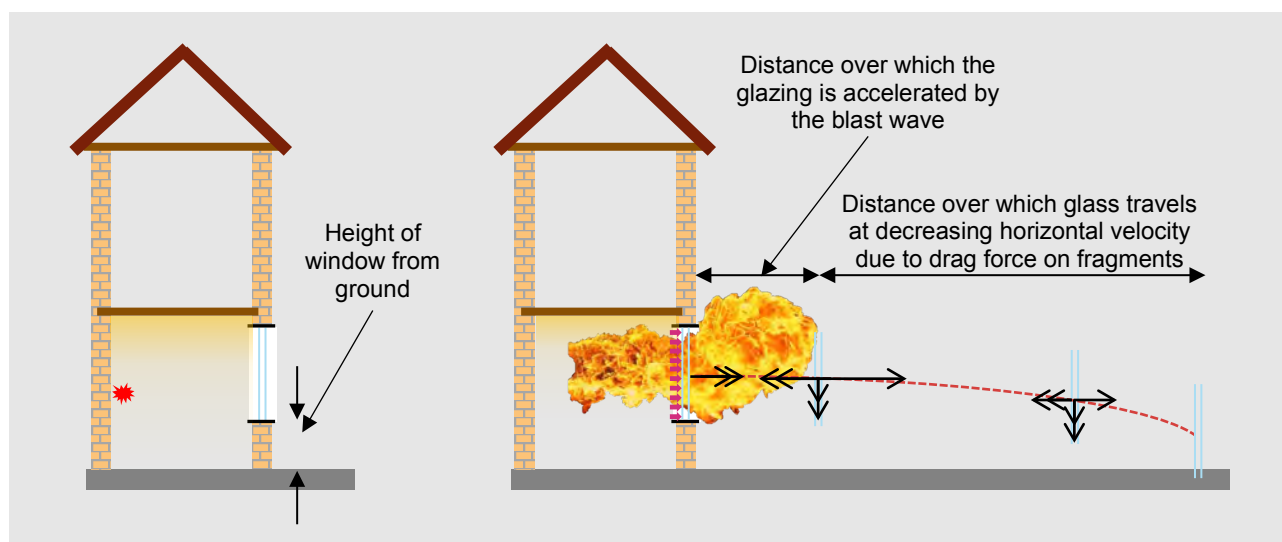
Figure 37: Calculating glass throw distance

Figure 37 seems to show the glass throw distance being calculated as if the glazing panel remains in one piece. In practice, the window will shatter, but the total surface area over which the blast wave pressures act upon the window are conservatively assumed to be the same whether the window remains in one piece or is in many pieces. Likewise, the total mass of the individual window fragments is equal to the total mass of the window in one piece. The thickness determines the mass per unit area of the window, and is the parameter that affects the distance over which the glazing is accelerated by the blast wave (along with the surface area, peak overpressure and impulse)

The drag force on the accelerated window (or fragments) is calculated assuming the fragments are rotating about an axis perpendicular to the horizontal direction that they are travelling in once the initial accelerating overpressure has gone to zero at the end of the initial internal pressure pulse (Figure 38)

To quantitatively measure injury from glass throw, an estimation as to the density of people in the area in proximity to the window which has failed is required (i.e. in the street in front of the dwelling). The same density from Section 3.3.3 of $0.116 \times 10^{-3}$ persons per $m^2$ is taken to undertake a comparative assessment of glass throw between methane and hydrogen. Like the methodology used in Section 3.3.3, an area over which the glass throw occurs is calculated assuming the angle of projection is 45° from the normal to the face of the window (see Figure 39) and the distance the glass is thrown prior to hitting the ground. The assessment was undertaken for an annealed single-glazed window with a 4mm thickness.
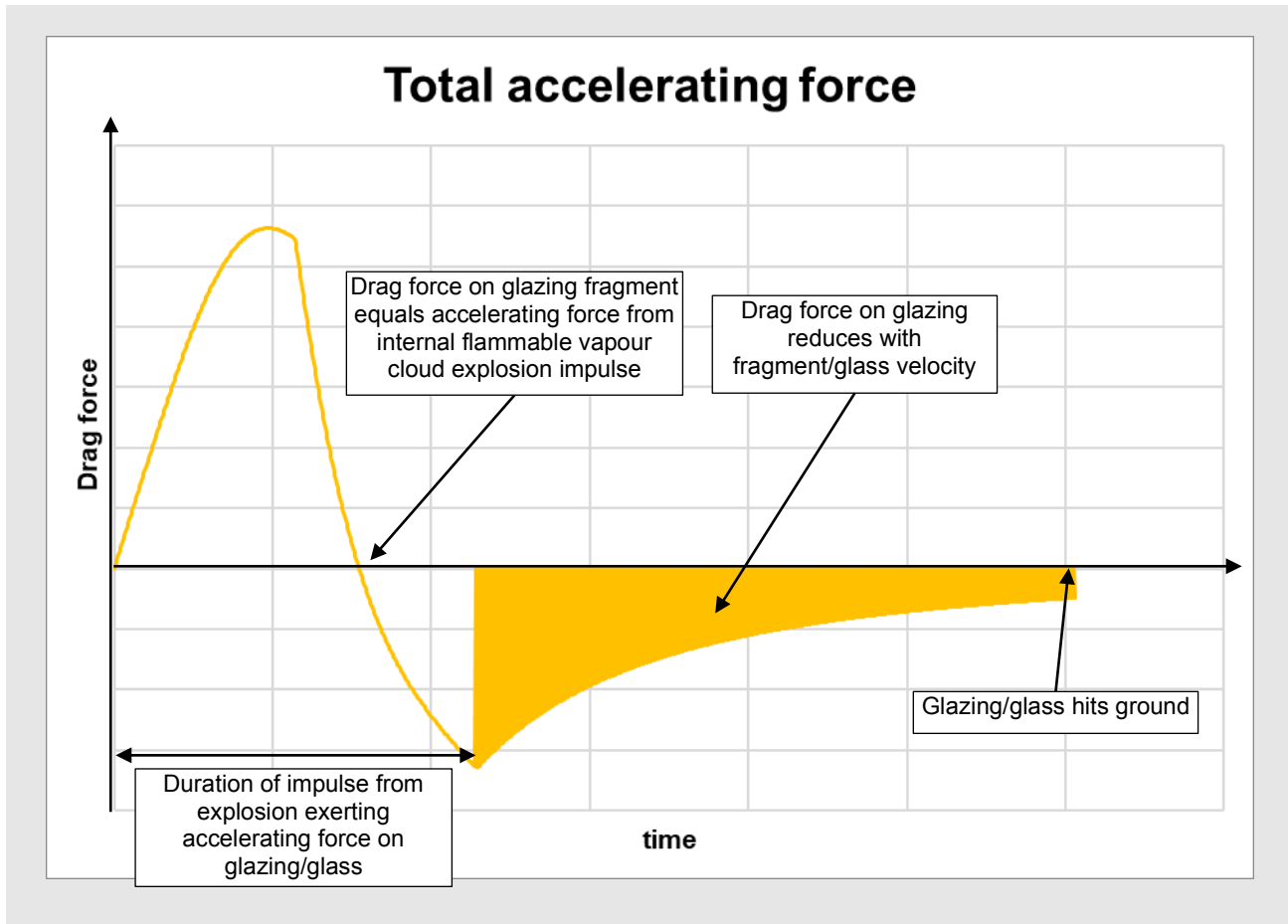
Figure 38: Example profile of total force exerted on glazing / glazing fragments during glass throw
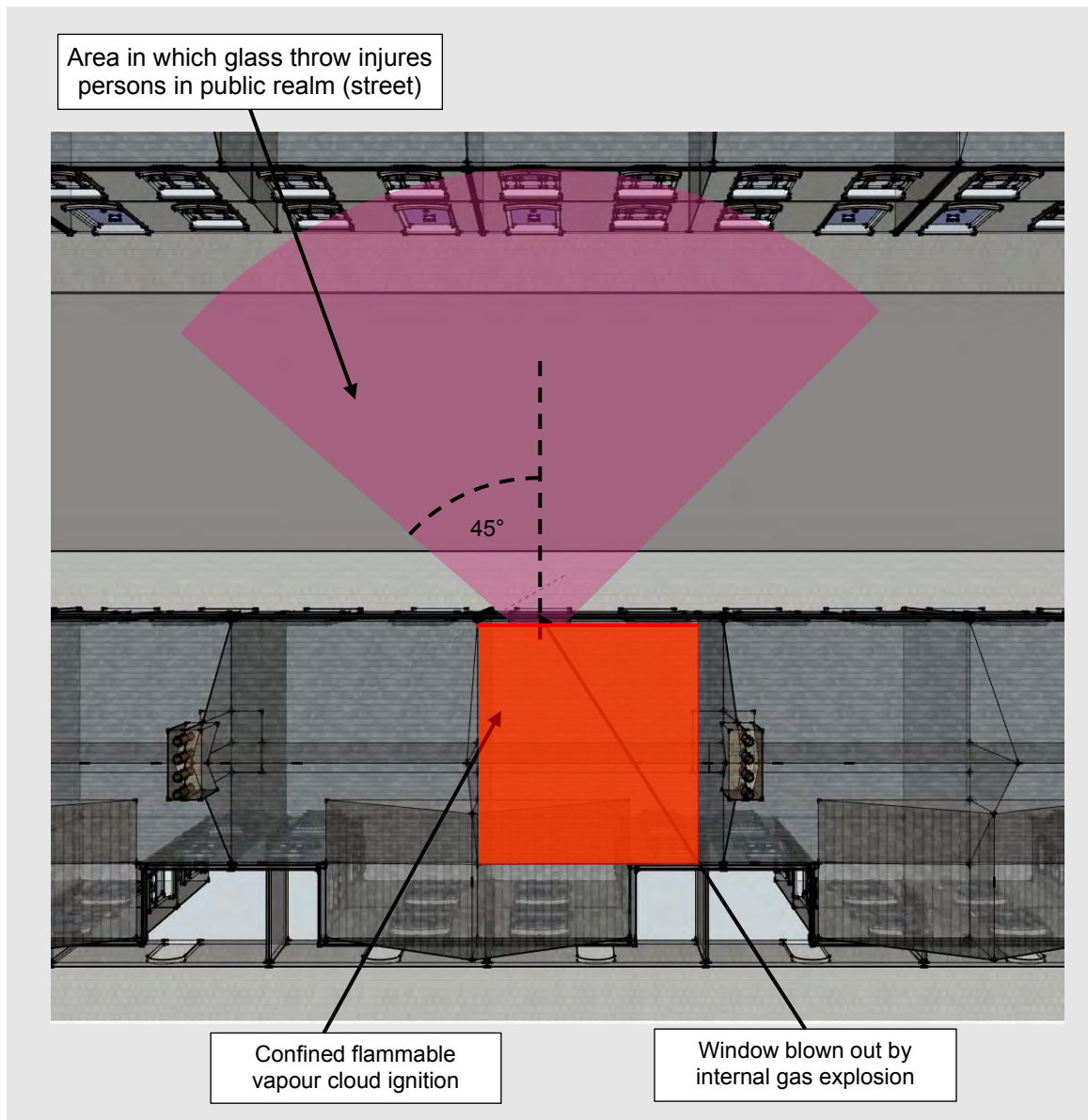
Figure 39: Quantifying secondary injury due to gas cloud explosion (plan view of an example street - extract taken from [20])

### 3.3.5    *Measuring tertiary injury*

To quantitatively measure primary injury, the number of people affected external to the property will be the output that is assessed for comparison using the methodology in Section 2.10.3. This is reasonable given that the main source of injury to occupants within the property in which a flammable vapour cloud explosion occurs will be injury due to structural collapse as discussed in Section 3.3.1, or injury relating to fire and burns.

To calculate whether the overpressure from the ignition of a flammable vapour cloud ignition in a room in the dwelling causes persons external to the property to overbalance and injure themselves, a mass and surface area of a person subjected to the reflected overpressure must be assumed. For this study, the parameters in Table 3 have been assumed for calculating tertiary injury. It is assumed that the persons torso and legs are initially normal to the pressure wave generated by the ignition of the flammable vapour cloud.

Table 3: Assumed parameters for calculating tertiary injury.

| Parameter | Value | Reference |
|---|---|---|
| Mass of person | 70 kg | [27] |
| Height of person | 1.65m | Average height of a female in the UK is 1.64m according to [29]. This is taking into account men, women and children. |
| Height of head | 23.6cm | Assumed to be a seventh of a person's height [30]. This gives an average frontal surface area of a head as $0.122m^2$. |
| Width of and average torso | 41cm | Assumed to be 2.5 times the width of a head. |
| **Total area of an average body** | **0.527 m²** | N/A |

A standoff at which the overpressure and impulse become too low to impose an acceleration of 0.5g or more on a person with the parameters in Table 3 is determined (see Figure 40) and this is used to calculate an area over which the acceleration on person is 0.5g or greater. To quantitatively measure tertiary injury, an estimation as to the density of people in the area in proximity to the house where the ignition of the flammable vapour cloud is required. The same density from Section 3.3.3 of 0.116 x $10^{-3}$ persons per $m^2$ is taken to undertake a comparative assessment of tertiary injury between natural gas and hydrogen.
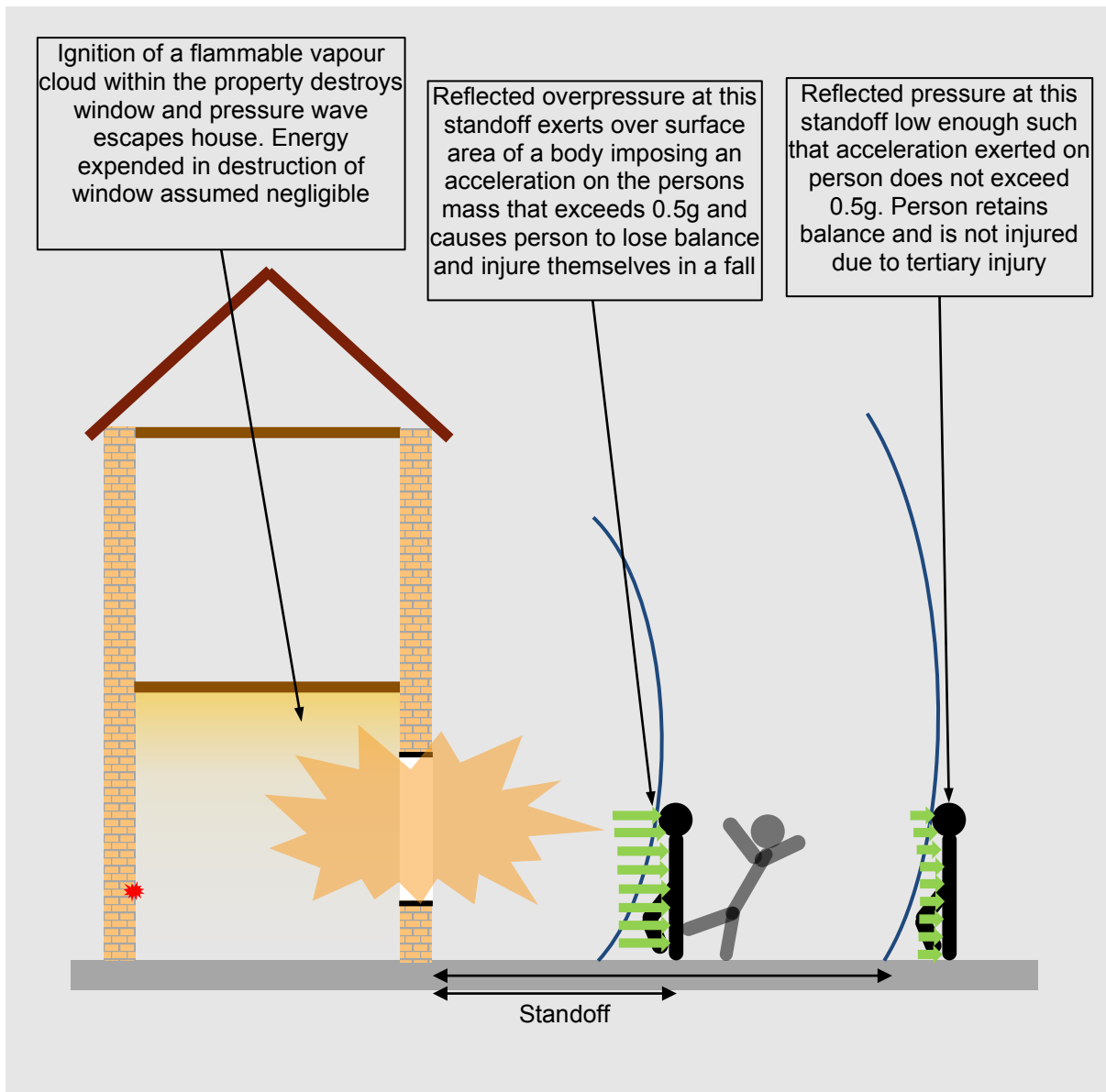
Figure 40: Tertiary injury due to a vapour cloud explosion in a domestic property

Area in which any persons are subjected to an acceleration exceeding 0.5g.

Confined flammable vapour cloud ignition
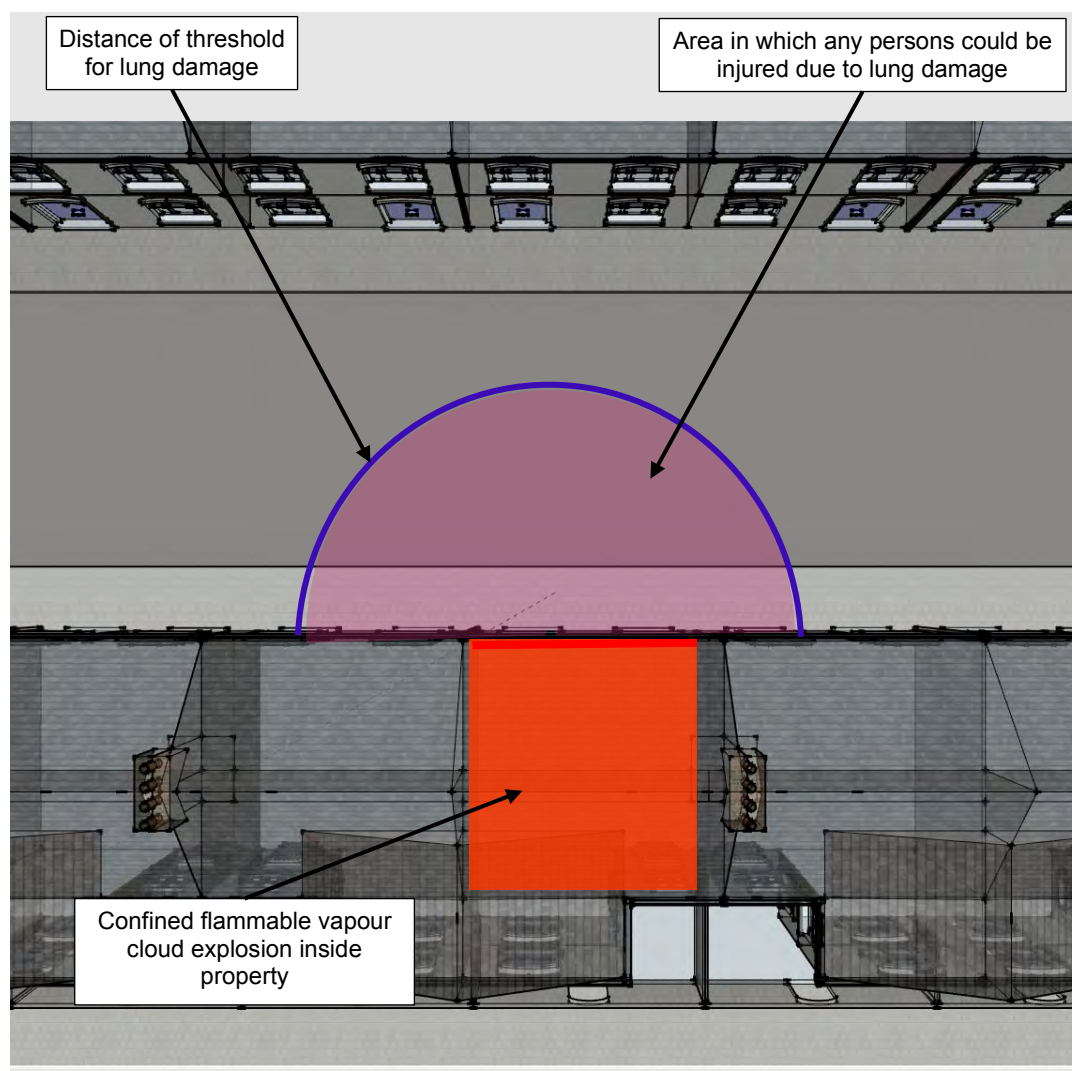
Energy expended in destruction of window ignored
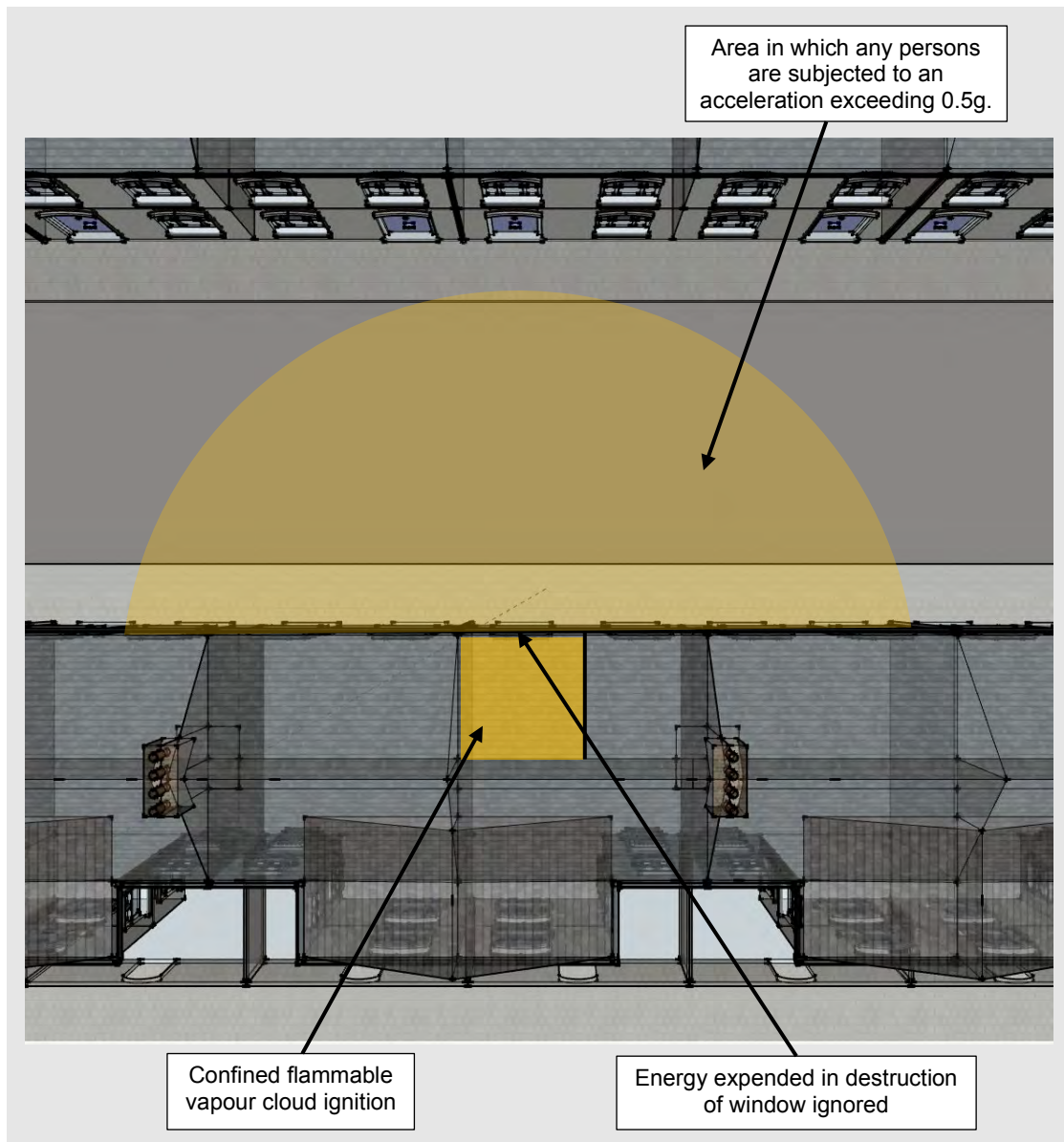
Figure 41: Example of quantifying tertiary injury due to gas cloud explosion (plan view of an example street - extract taken from [20])

### 3.3.6 *Measuring of injuries from burns*

It is difficult to quantitatively measure injury from burns for both methane and hydrogen flash fires/deflagrations, especially when impingement is considered where a combination of heat transfer to the skin occurs via radiation and convection. Empirical and engineering models for fireballs being expelled through a vent to the outside of a building are based on hydrocarbon experimental data and are not currently validated for hydrogen.

To quantitatively measure injury due to burns, the number of people affected internally and external to the property will be the output that is assessed for comparison. If the confined flammable vapour cloud explosion within the enclosure when ignition takes place is strong enough to fail the load bearing walls of the enclosure, the main source of injury to occupants within the property in which a flammable vapour cloud explosion occurs will be injury due to structural collapse as discussed in Section 3.3.1. If the explosion is not strong enough to fail the load bearing walls forming the enclosure boundaries where the gas leak and ignition occurs, then there is still the possibility the occupants of the enclosure are injured by the flash fire.

For determining the number of injuries due to burns for the occupants of the enclosure where the confined flammable vapour cloud undergoes ignition, **it is assumed that any occupant of the enclosure impinged (engulfed) in the flammable vapour cloud as it undergoes combustion, is injured with second-degree burns**. This is assumed to be due to direct radiative or convective heat transfer to bare skin, and/or burns from clothing that has ignited. Although this methodology is in line with methods used to calculate the quantity of injury in the process industry, it is highly conservative to assume second-degree burn injuries occur for a person impinged in a combusting confined vapour cloud regardless of the concentration and radiative fraction of the gas (methane or hydrogen) undergoing combustion in a domestic setting. In practice, low concentrations of methane and especially hydrogen, close to the lower flammability limit are unlikely to produce a level of heat transfer to bare skin via radiation and convection that induce second-degree burn injuries for a person impinged in a burning cloud. Work undertaken by Kiwa during their FIB tests for the H100 project (similar in volume to the kitchen scenario in this assessment), showed that second degree burns did not occur for concentrations of hydrogen up to 30% [28] for skin impinged within the combusting confined hydrogen cloud.

If the confined flammable vapour cloud explosion within the enclosure when ignition takes place is strong enough to fail the vents of the enclosure (windows, doors), then a 'fireball' will be produced by the venting of burnt and unburnt gases through the vents into the rest of the rooms of the dwelling on the same floor, and/or external to the property into the street or public realm. The size of the fireball produced due to venting will be dependent on how momentum driven it is. For the low concentrations of methane and hydrogen, the fireball will have a low momentum if it escapes the enclosure at all. For higher concentrations, the fireball will be momentum driven. "The NFPA 68 standard provides an empirical correlation to predict the maximum size of a fireball produced during venting of a deflagration" [7]. The axial extent, *D,* of the hazard area from the vent location can be calculated using

$$D = 3.1 \left(\frac{V}{n}\right)^{0.402}$$

Where $V$ is the volume of the compartment and $n$ is the number of vents, which, for the scenarios looked at in this assessment is a minimum of 2.
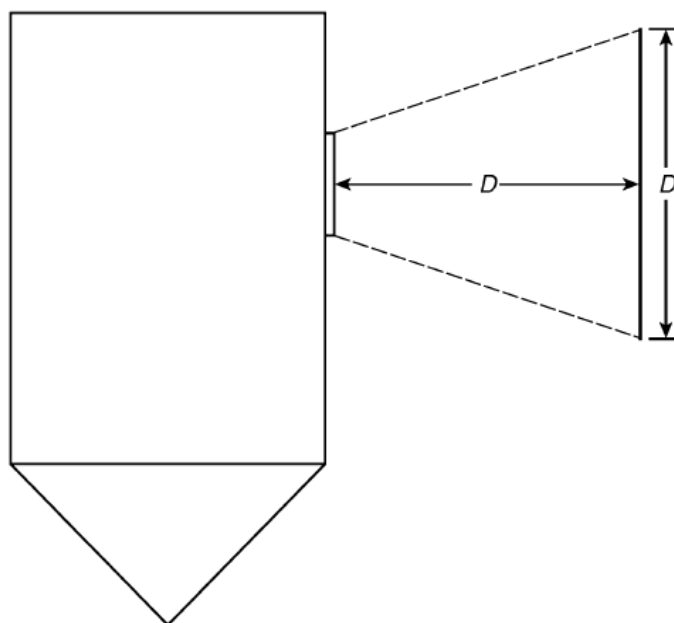


Figure 42 Axial extent of a fireball (Figure 71.10 from [7])

The NFPA method is used to determine the area in the public realm or street that would be impinged by the fireball produced from a vented deflagration from an enclosure within a dwelling following failure of the vents such as the windows and doors. An estimation as to the mass and combustible load (in MJ) of unburnt gas ejected as a cloud has been made using equation (5) from [1] to determine the volume of the external cloud (based on the enclosure volume), along with the density and heat of combustion of both methane and hydrogen (see Table 2). It is assumed that the vented gases are composed 90% of burnt gases and 10% of unburnt gases [12].

Estimating the duration that the vented fireball burns for has been estimated using equation 66.72 from [7] which is the "burning duration for momentum dominated fireballs":

$$t_d = 0.45m^{1/3}$$

Where $m$ is the mass of the gas in the external cloud calculated using equation (5) from [1].

An average heat release rate (HRR) for the fireball is estimated by dividing the combustible load by the fireball duration. A radiative fraction of 0.23 is taken for methane [4] and 0.17 for hydrogen [7], along with the estimate of the average HRR to make an estimate of the heat release rate per unit area (HRRPUA) at the edges of the fireball. The configuration factors in Appendix A of [7] and the graph in Figure 20 are used to estimate the area external to the vents and enclosure (in the street) that isn't impinged by the fireball(s) from the vented deflagration, *but* is within the boundaries of where second-degree burns would occur due to *radiative heat transfer* (Figure 44).

To quantitatively measure injury from second-degree burns external to the dwelling, an estimation as to the density of people in the area in proximity to the house where the ignition of the flammable vapour cloud is required. The same density from Section 3.3.3 of $0.116 \times 10^{-3}$ persons per $m^2$ is taken to undertake a comparative assessment of injury from second-degree burns between natural gas and hydrogen.
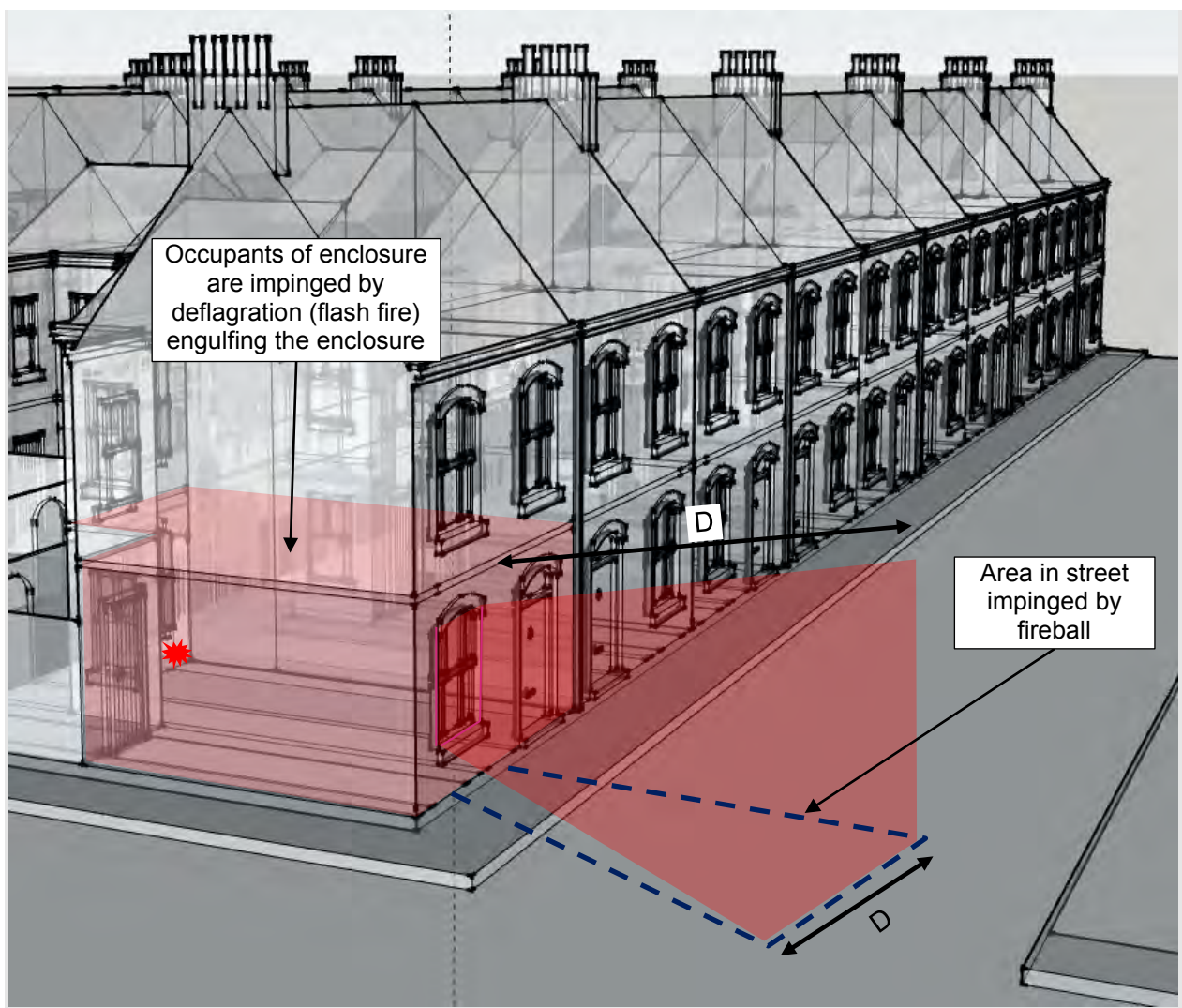


Figure 43: Dimensions of a fireball in the street following a vented deflagration within an enclosure in a terraced house dwelling (extract taken from [20])

It is recognised that this empirical method has been developed for hydrocarbons and has not been tested for hydrogen deflagrations. However, as discussed in Section 3.3.7, **in nearly all circumstances, the area in the public realm (i.e. the street) enveloped by the approximated fireball with the dimensions calculated using the NFPA 68 method, is already within the glass throw hazard area i.e. injuries due to glass throw will dominate the quantity of injuries in the public realm area.**

Finally, a sensitivity study has been undertaken using methods from Chapter 36 of [7] to determine whether the dominant mechanism for body surface burns is likely to be clothing catching fire rather than radiative heat transfer to exposed skin for persons *not engulfed* within the extent of the fireball. The sensitivity study showed that although there is a 'boundary' *outside* the estimated dimensions of the fireball where the radiative heat flux to clothing would cause ignition of the clothing to occur, this 'boundary' is always within the area in the street not impinged by the vented fireball where second-degree burns would occur due to radiative heat transfer to the skin (see Figure 44).
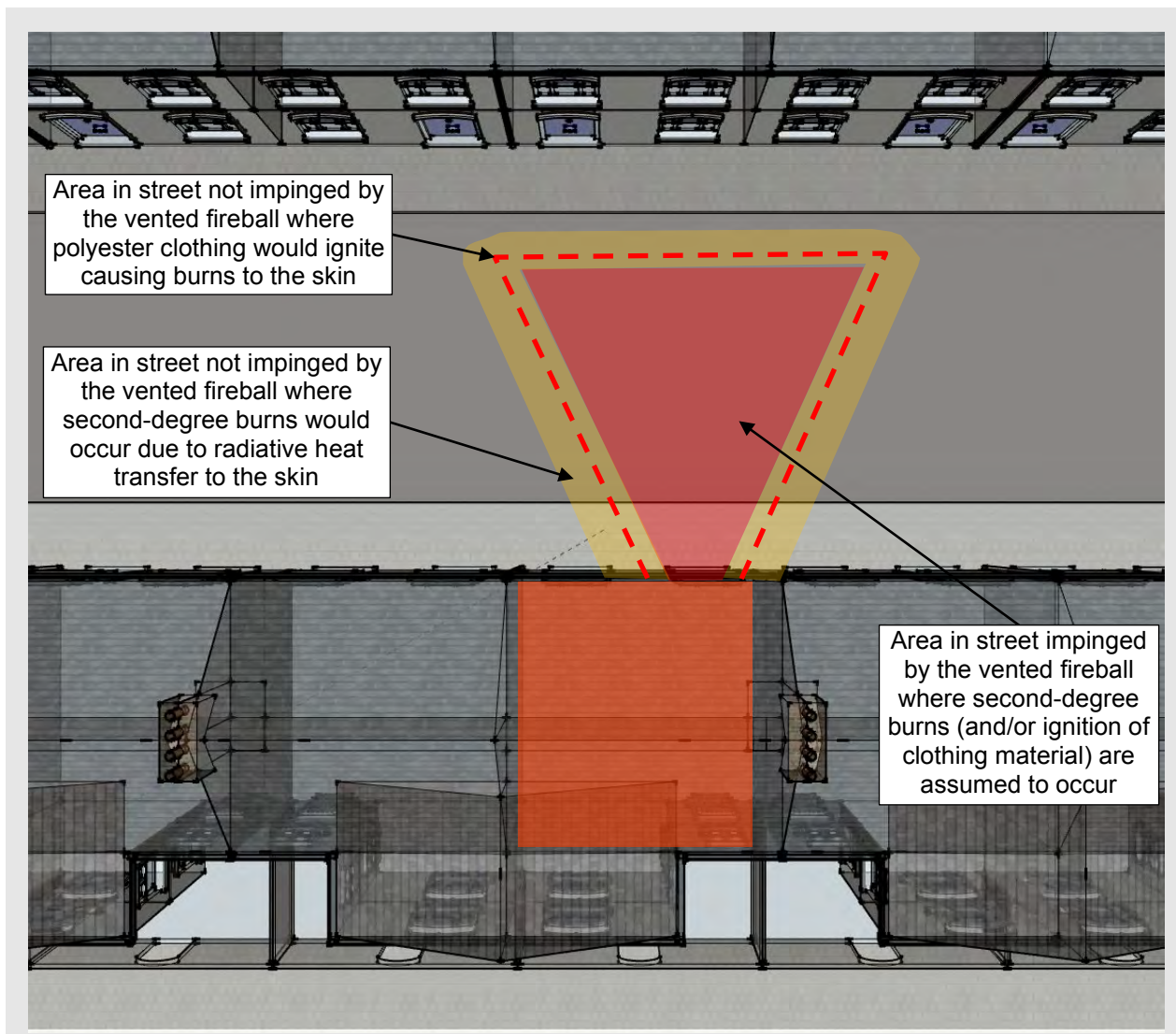


Figure 44: Area of impingement and total area where second-degree burns would occur from vented deflagration fireball (extract taken from [20]).

### 3.3.7    *Overlap in quantitatively measuring injury*

The different injuries being quantitatively measured using the methods described in Sections 3.3.1 to 3.3.6 will overlap meaning that individually measuring the injury level for each type of injury and then summing them together to determine the total number of persons injured will result in some element of 'double counting' for the same initiating event (i.e. ignition leading to explosion). For example, the area estimated over which people will be injured due to high velocity glazing fragments being projected will cover the area impinged by a fireball from the vented deflagration, and some of the area where tertiary injury would occur (see Figure 45 for an example). The results in Section 4 evaluate the level to which this occurs to reduce the element of 'double counting' when totalling the number of people injured due to an initiating event.
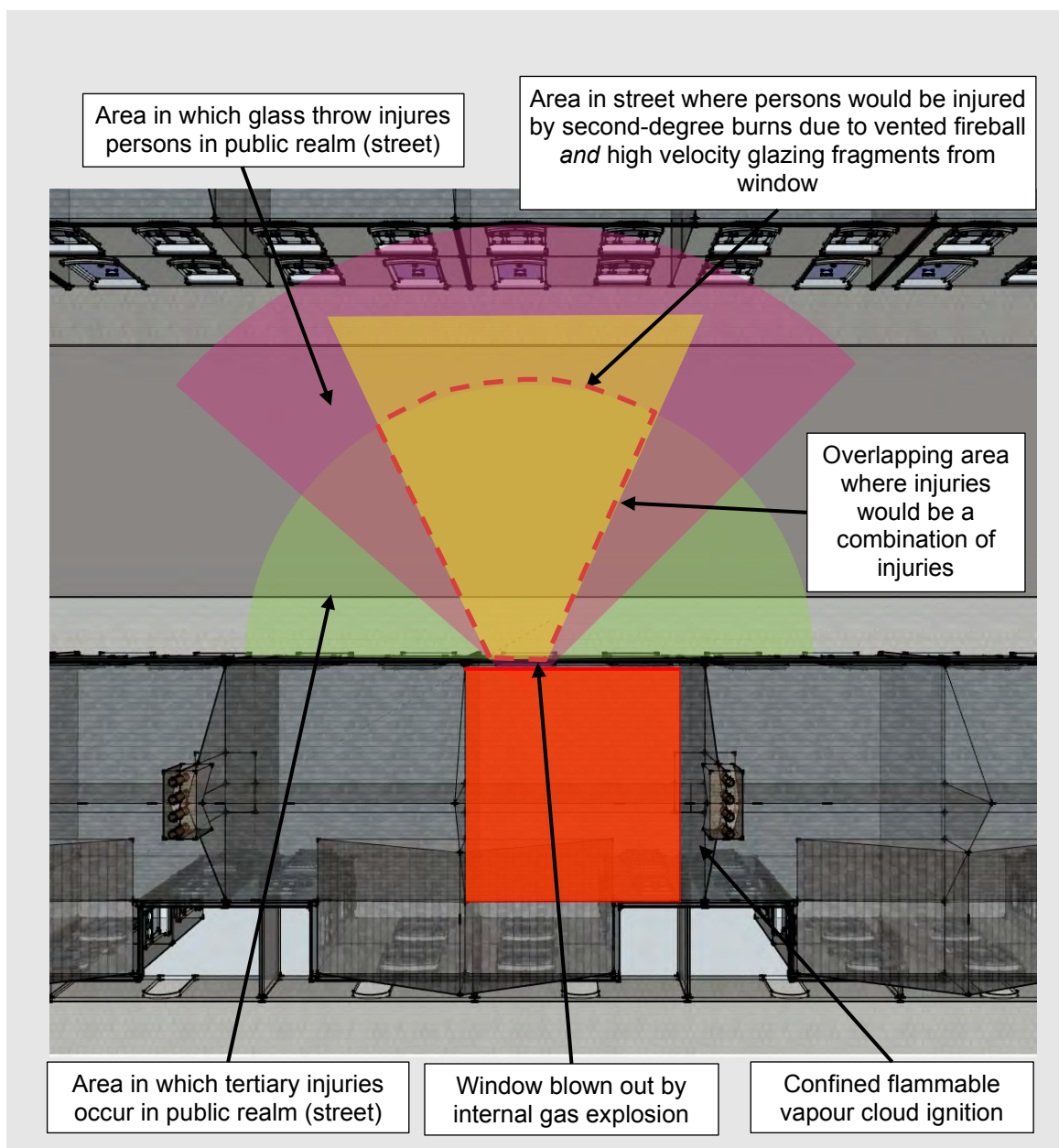


Figure 45: Example of overlapping injuries – secondary injury and injury from second-degree burns (extract taken from [20])

## 3.4 Input parameters

### 3.4.1 Determining overpressures and impulses

To quantitatively measure the level of injury due to an ignition of a confined flammable vapour cloud within an enclosure, the internal overpressure and impulse needs to be estimated based on the following input parameters (see Section 2 for technical background):

– Concentration of the flammable gas (hydrogen or methane in this case) in the enclosure

– The volume of the enclosure

– The total vent area and the location of the vents

– The location of the ignition source

– The location of obstacles and the extent of congestion and confinement that will increase the turbulent flow ahead of the flame front as it expands

– The extent of stratification of the gas in the enclosure where the initiating event occurs.

The phenomena of a "closed vessel deflagration" transitioning to a vented explosion is described in Section 2.6.2. There has been extensive research in modelling these phenomena separately but less so for the two processes ("closed vessel deflagration" and vented explosions) in combination given the complexities involved.

A.Sinha and J.Wen from the University of Warwick FIRE research group have published two papers that detail a "New Engineering" method to determine the peak internal overpressures from a vented enclosure hydrogen explosions ( [12], [1]) The method can also be used to calculate the internal overpressure from a vented methane explosion. The first paper ( [12]) undertakes an evaluation of the existing vented explosion models; EN-14994 model [31], NFPA-68 model [32], the FM global model [33] and the Molkov & Bragin 2015 model [34]. It also compares the existing vented explosion models to all published experimental data for vented hydrogen and hydrocarbon explosions. The second paper [1] expands on the work in the first paper and presents a "simplified" model to estimate internal overpressures for vented hydrogen and methane explosions considering the input parameters listed above, along with validation of the model against existing experimental data.

The "simplified" model does not calculate impulse. Following advice provided through personal meetings and correspondence with both J.Wen and A.Sinha, and using further work published in [35] and [13], the "simplified" model in [1] has been expanded upon to estimate the length of the internal pulse and subsequently the impulse. Validation of this modification (and further validation of the overpressure estimate) has been undertaken with comparison made to experimental data, some of which comes from the current UK hydrogen research programmes (Hy4Heat, H100, etc) and some of which is from published global data. The validation exercise indicated that the modified methodology provides a conservative estimate of the impulse when compared to experimental data. However, it is noted by the authors that although the "simplified" model is a refinement of the previously developed semi-empirical models mentioned, the range of experimental data is still very limited especially for high concentrations of hydrogen.

Predicting overpressures and impulses from vented flammable vapour cloud explosions is difficult given the complex combustion processes involved. Whilst the "simplified" model is the most suitable for both hydrogen and hydrocarbon explosions compared to other empirically based models mentioned on the previous page, the validation in [1] and validation of the model undertaken on this project showed that the "simplified" model still tends to overestimate the internal overpressure resulting from a vented flammable vapour cloud explosion for both methane and hydrogen

Accounting for stratification has already been discussed in Section 3.2.3 and as mentioned in Section 2.6.2, the $K_V$ value (ratio of vent area to enclosure volume) has a significant effect on the peak internal overpressure and impulse from a vented flammable vapour cloud explosion. Although the "equivalent volume" (see Section 3.2.3) of the confined flammable vapour cloud at the peak concentration is used in the "simplified" model [1], the total actual vent area of the enclosure is used. This is conservative because in practice, the vent area (windows and doors) will not decrease and no consideration is made for the "partial" vent area provided by the difference between the actual enclosure volume and the "equivalent volume" which will have some effect in reducing the overpressure.

### 3.4.2    *Consideration of household objects and furniture*

The "simplified" model from [1] includes a methodology to consider the presence of obstacles that are cylindrical or cuboid in shape such as piping in the case of process machinery, or household furniture and items in the case of a domestic setting. The model approximates the surface area of the flame front for an empty enclosure as half the internal surface area of the enclosure for an end ignition and a quarter of the flame surface area for a central ignition. The flame front surface area is an important input because it determines the flame speed and therefore the peak internal overpressure of the vented explosion. "Obstacle can be treated as a bluff body in flame path. Flow past an obstacle creates a recirculation wake region in the downstream direction. This recirculation region has high shear at its boundary, and it impedes flame moving towards the obstacle in the downstream direction." [1]. In the case of vented explosions, the additional flame wrapped around an obstacle or obstacles increases the flame front surface area and results in an increase in internal overpressure. The "simplified" model takes this into account by including the additional flame surface area due to the flame wrap around and recirculation effect from the presence of obstacles.
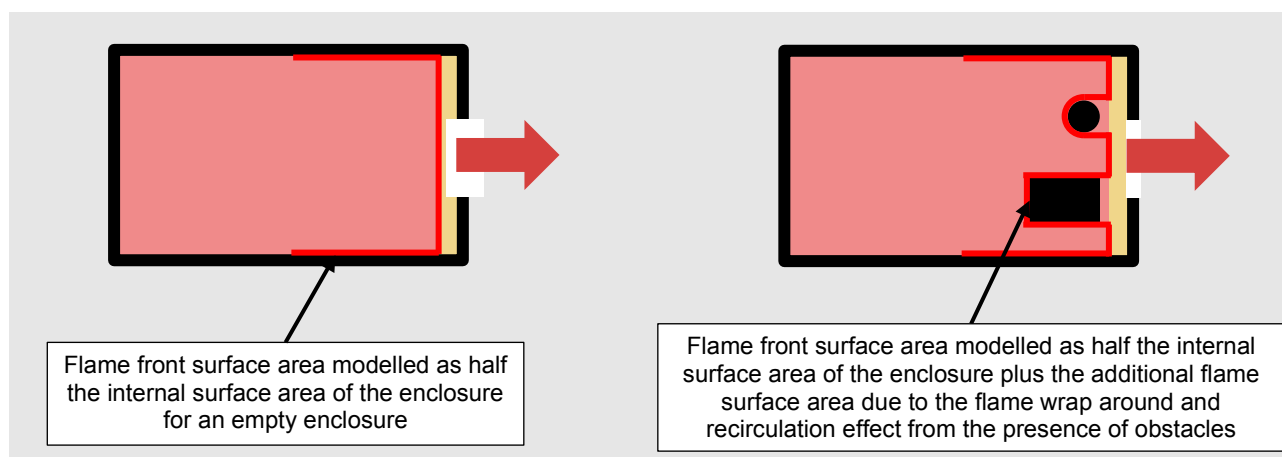
Figure 46: Consideration of obstacles in the "simplified" model

Although the enclosure in the kitchen scenario is assumed to have furniture such as cabinetry and appliances (see example in Figure 47), it is not realistic to model the furniture on the edges of the enclosure as objects that increase the flame surface area. In practice the flame cannot "wrap around" these obstacles as the reaction front expands if they are in the corners and edges of such a small enclosure against the wall. The kitchen scenario is therefore modelled without any internal furniture using the simplified method as shown in Figure 48 i.e. an enclosure with no internal obstacles.

However, for the downstairs of an open plan terraced house scenario, modelling has been undertaken by considering the internal furniture in Table 4 (for dimensions of the modelled kitchen and downstairs of an open plan terraced house scenarios, see Figure 26 and Figure 27 respectively).
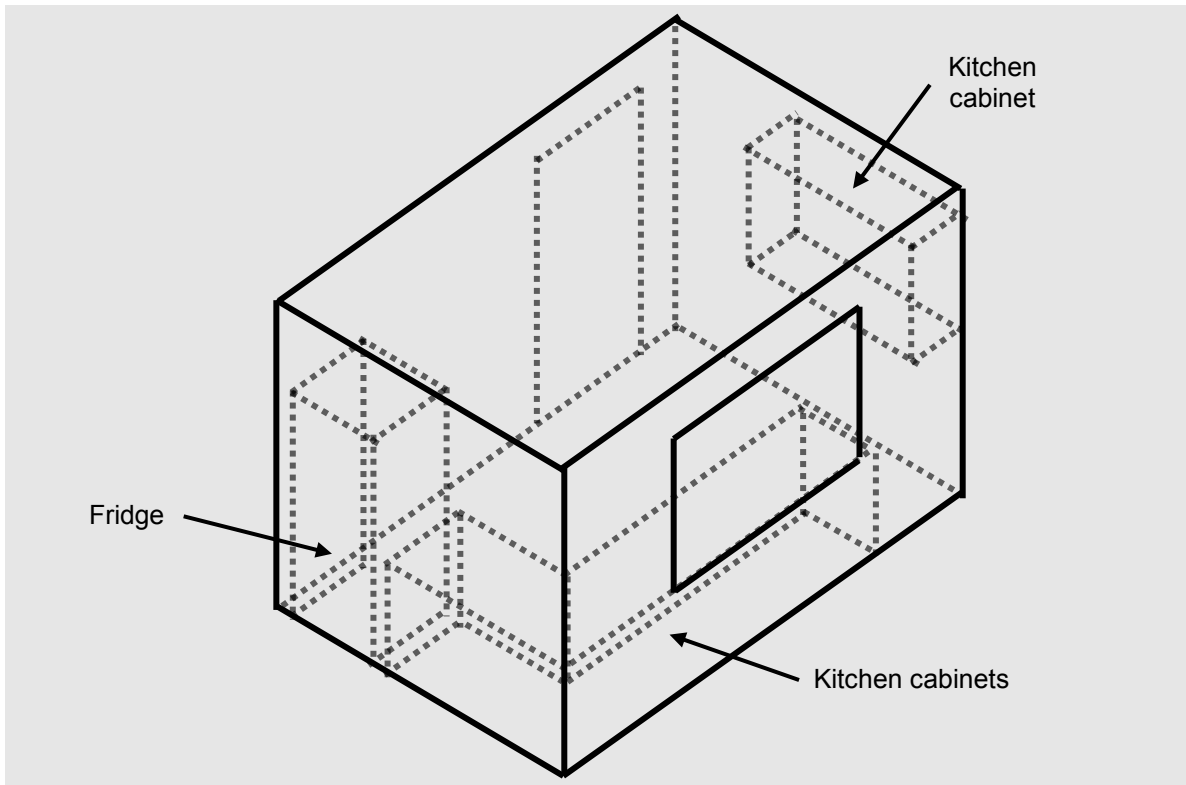
Figure 47: Example realistic geometry in a small kitchen
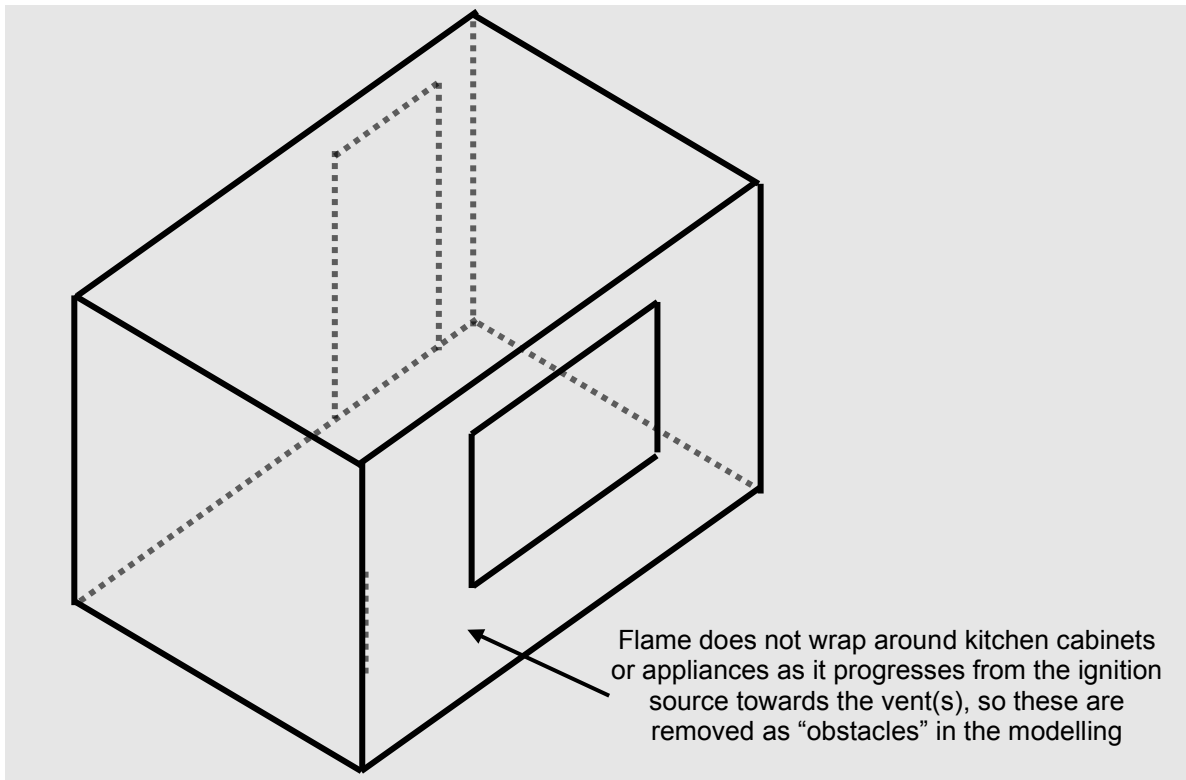


Figure 48: Kitchen scenario is modelled without internal furniture.

Table 4: Furniture included in the modelled downstairs of an open plan terraced house scenario

| Obstacle or object | Shape | Diameter / edge length orthogonal to vent if cuboid (m) | Second edge length parallel to vent if cuboid (m) | Height of obstacle or object (m) |
|---|---|---|---|---|
| Kitchen table | Cuboid | 2 | 0.8 | 0.8 |
| Chair for kitchen table | Cylinder | 0.4 | - | 0.8 |
| Chair for kitchen table | Cylinder | 0.4 | - | 0.8 |
| Chair for kitchen table | Cylinder | 0.4 | - | 0.8 |
| Chair for kitchen table | Cylinder | 0.4 | - | 0.8 |
| Sofa parallel to the front wall vent(s) – simplified to a cuboid | Cuboid | 0.6 | 1.5 | 0.8 |
| Sofa perpendicular to front wall vent(s) – simplified to a cuboid | Cuboid | 1.5 | 0.6 | 0.8 |
| Coffee table | Cuboid | 0.6 | 0.4 | 0.4 |
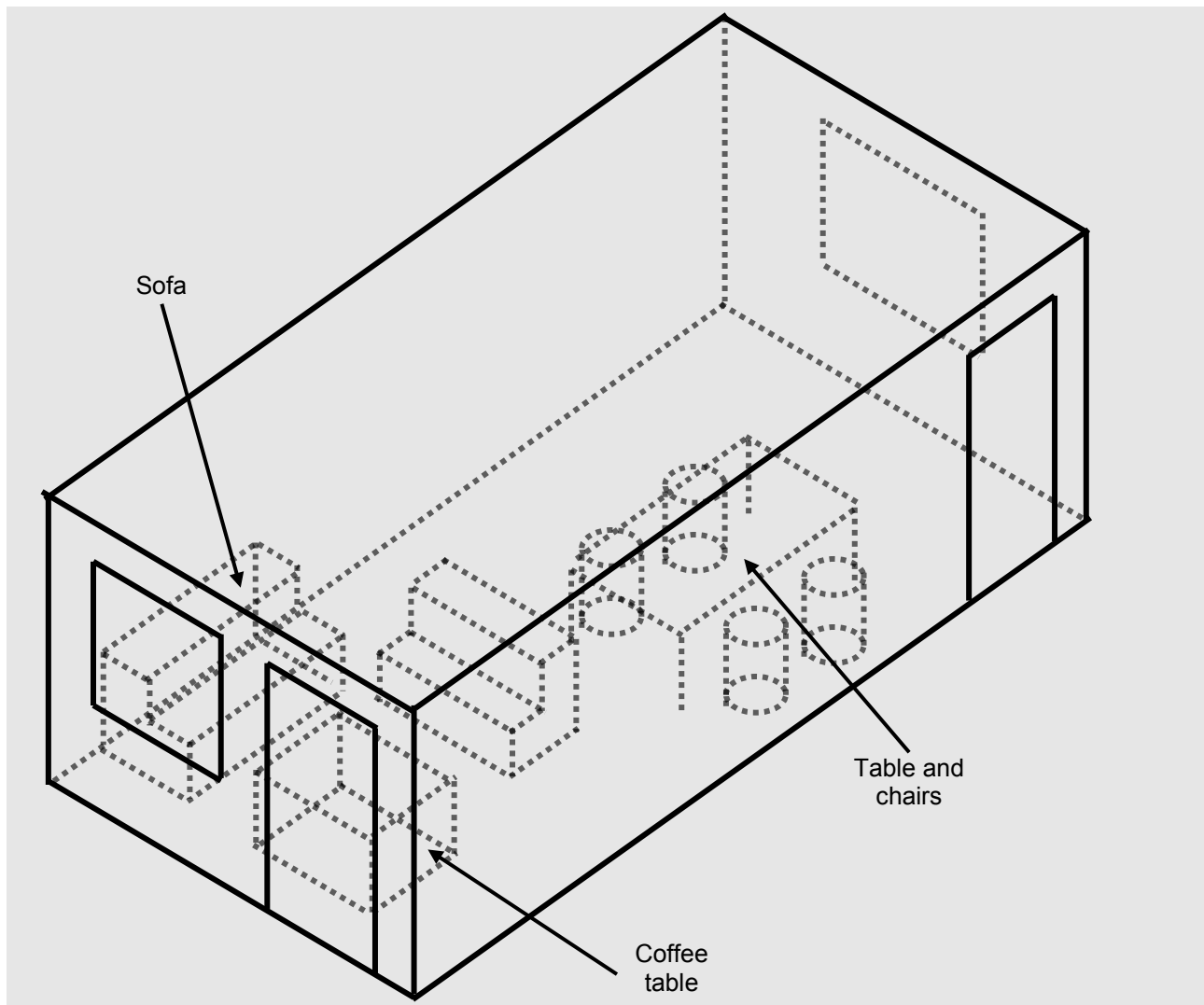


Figure 49: Furniture included in modelled downstairs of an open plan terraced house scenario

### 3.4.3 *Vent cover failure pressure and inertia*[18]

The "simplified" model [1] (described in Section 3.4.1) used to approximate overpressures and impulses from a vented explosion in an enclosure does not consider the *resistance* or the *inertial* behaviour of the vent cover or covers such as closed windows and doors.

Studies by Molkov in [36] show that if the enclosure where a vented flammable explosion occurs has a vent cover with a resistance and inertia greater than zero, then two (or sometimes three as indicated in Figure 9) distinct peaks can be identified in the internal overpressure time transient. The first overpressure peak is related to the vent opening time, vent cover resistance and vent cover inertia (this is referred to the 'transition' between a "closed vessel deflagration" and a fully vented explosion in Figure 9 and Figure 10). The second peak is associated with the "mixture burnout" [36]. Figures 2 and 3 in [36] show that increasing vent cover inertia (measured in $kg/m^2$) and vent cover resistance (measured in kPa) increases the size of the first peak in the overpressure time transient. Figures 2 and 3 in [36] also show that the vent cover inertia and vent cover resistance has negligible effect on the second peak in the internal overpressure time transient. 50 is an excerpt of Figure 3 from [36] showing the influence of vent cover resistance on the first overpressure peak, and Figure 51 is an excerpt of Figure 2 from [36] showing the influence of vent cover inertia on the first overpressure peak.
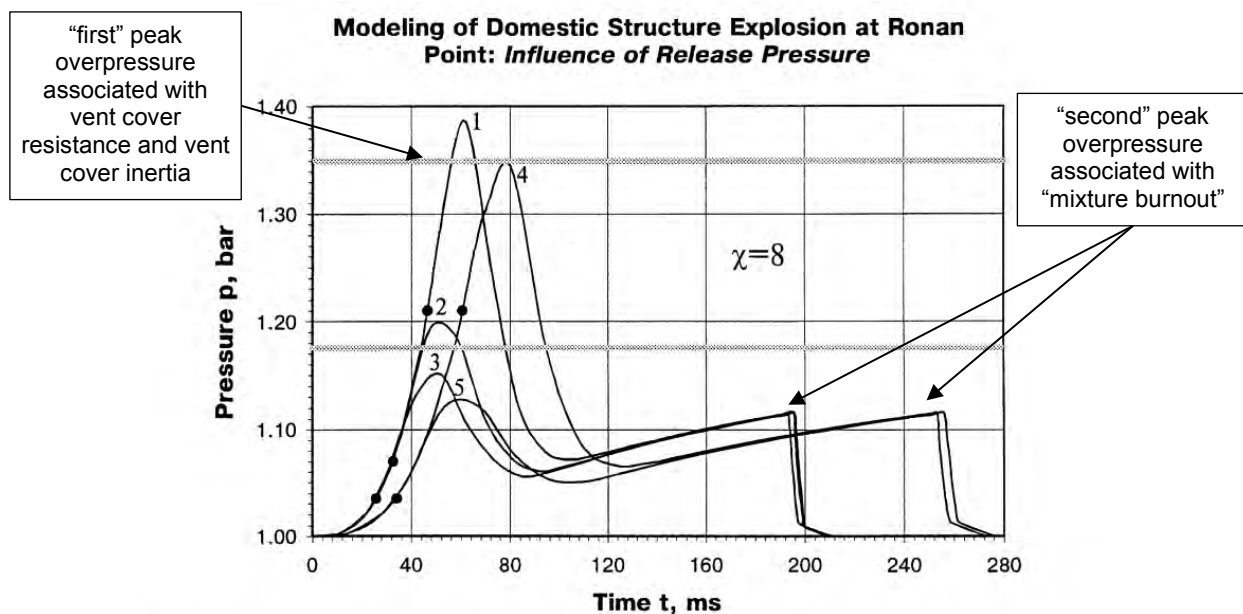


Fig. 3. Pressure-time history in 29.4 $m^3$ kitchen (curves 1, 2, 3) and in 65.3 $m^3$ living-room of domestic structure at Ronan Point with different release overpressure: 1,4–21 kPa; 2–7 kPa; 3,5–3.5 kPa. ● – beginning of vent opening. Turbulence factor before and after beginning of vent opening $\chi_o = \chi = 8$. Total venting space area is 4.25 $m^2$ in the kitchen and 7.02 $m^2$ in the living room. Total weight of vent cover is 63.6 kg for kitchen and 96 kg for living-room. Horizontal line at $p = 1.175$ bar – minimum estimated explosion pressure [1]. Horizontal line at $p = 1.35$ bar – nearby maximum estimated explosion pressure (and the pressure under which the maximum explosion pressure on external load-bearing walls might be reduced [1]).

Figure 50: Excerpt of Figure 3 from [36]

---

[18] This section has been added since the issue of the first draft of this report to the HSE
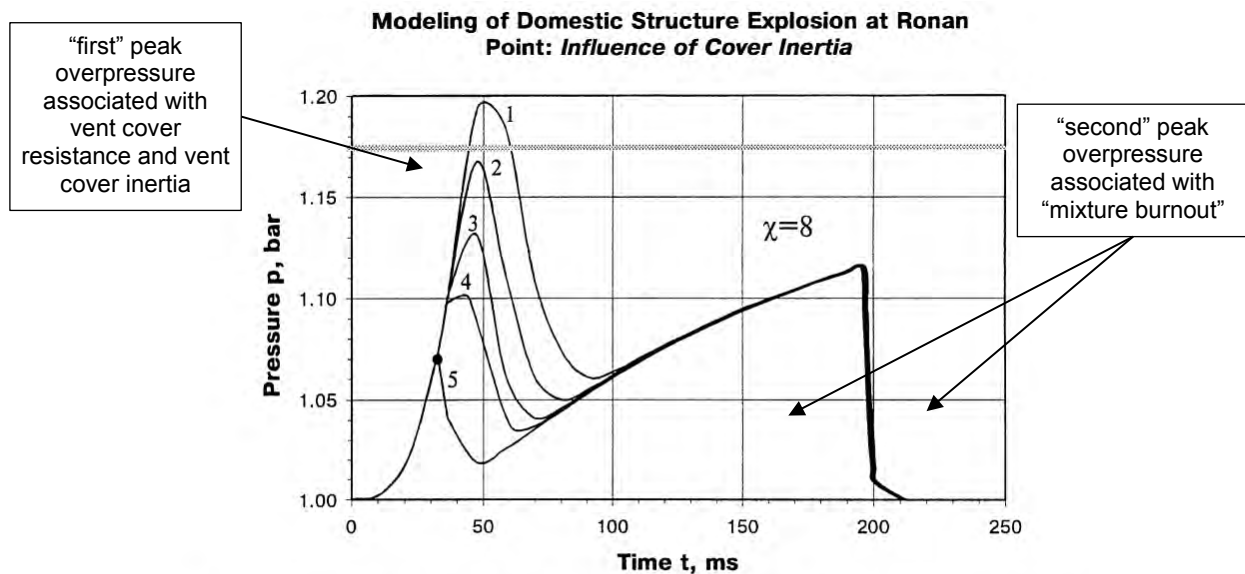
Fig. 2. Pressure-time history in 29.4 m³ kitchen of domestic structure at Ronan Point with different mass of vent cover: $1 - m = 63.6$ kg; $2 - m = 31.8$ kg; $3 - m = 15.9$ kg; $4 - m = 7.95$ kg; $5 - m = 0$ kg. ● – beginning of vent opening. Turbulence factor before and after beginning of vent opening $\chi_o = \chi = 8$. Total venting space area 4.25 m². Vent cover release overpressure 7 kPa. Horizontal line at $p = 1.175$ bar – minimum estimated explosion pressure [1].

Figure 51: Excerpt of Figure 2 from [36]

For all concentrations of methane and low concentrations of hydrogen (below a peak concentration of approximately 15%), it is non-conservative to assume that the vent cover resistance and inertia is zero (i.e. that there is no "first" overpressure peak as described on page 72). In practice, modern double-glazed windows and a well fitted strong door have a resistance and inertia that can influence the "first" peak overpressure.

To make an estimate of the influence of vent cover resistance and inertia in the modelling in this assessment, an estimate of the *ratio* of the "first" overpressure peak to the "second" overpressure peak is made using the peak vent cover resistance. For example, curve 2 in Figure 50 represents the overpressure profile from a vented methane explosion in an enclosure with similar dimensions and volume to the kitchen scenario modelled in this assessment, but with a vent cover resistance of 7kPa. In this instance, the ratio of the "first" overpressure peak to the "second" of curve 1 in Figure 50 is approximately 1.8, i.e. the "first" peak overpressure is approximately 1.8 times the "second" peak overpressure. The modelling in this assessment is based on a well fitted 1.6 x 1.0m single glazed window with a dynamic annealed glass breaking strength of 80N/mm². Using the methodology described in Section 2.8 and guidance from Chapter 6 of a vent cover resistance of 7kPa is estimated so the ratio of the "first" overpressure peak to the "second" can be approximated to 1.8 (see Appendix E for further detail).

To determine whether the enclosure boundaries of the enclosure where the initial leak, dispersion and ignition event occurs undergo structural collapse, an estimate of the peak overpressure and impulse is made using the "simplified" model in [10] *assuming a zero* vent cover resistance and inertia. If the peak vented explosion overpressure and impulse estimated using the "simplified" model (with a zero vent cover resistance and inertia) is enough to cause structural collapse, then it is reasonable to assume that structural collapse will occur when vent cover resistance and inertia *is* considered. However, if the peak overpressure and impulse estimated using the "simplified" model in [10] is not enough to fail the enclosure boundaries using the initial leak, dispersion and ignition event occurs, then the SDoF response of the enclosure boundaries is assessed using an estimated overpressure profile constructed as shown in Figure 52 to determine whether the initial enclosure boundaries fail. Figure 53 shows the steps involved in this process.
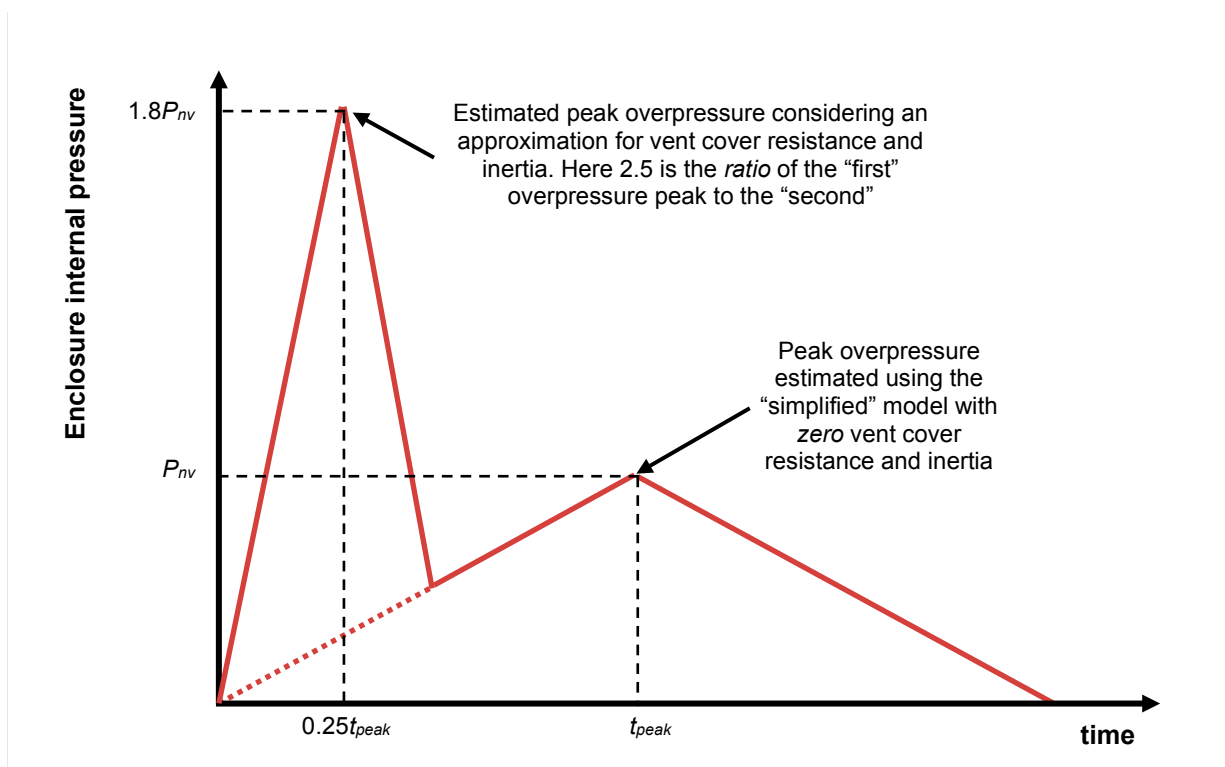


Figure 52: Constructing an estimated internal overpressure profile considering vent cover resistance and inertia (or vent failure pressure)
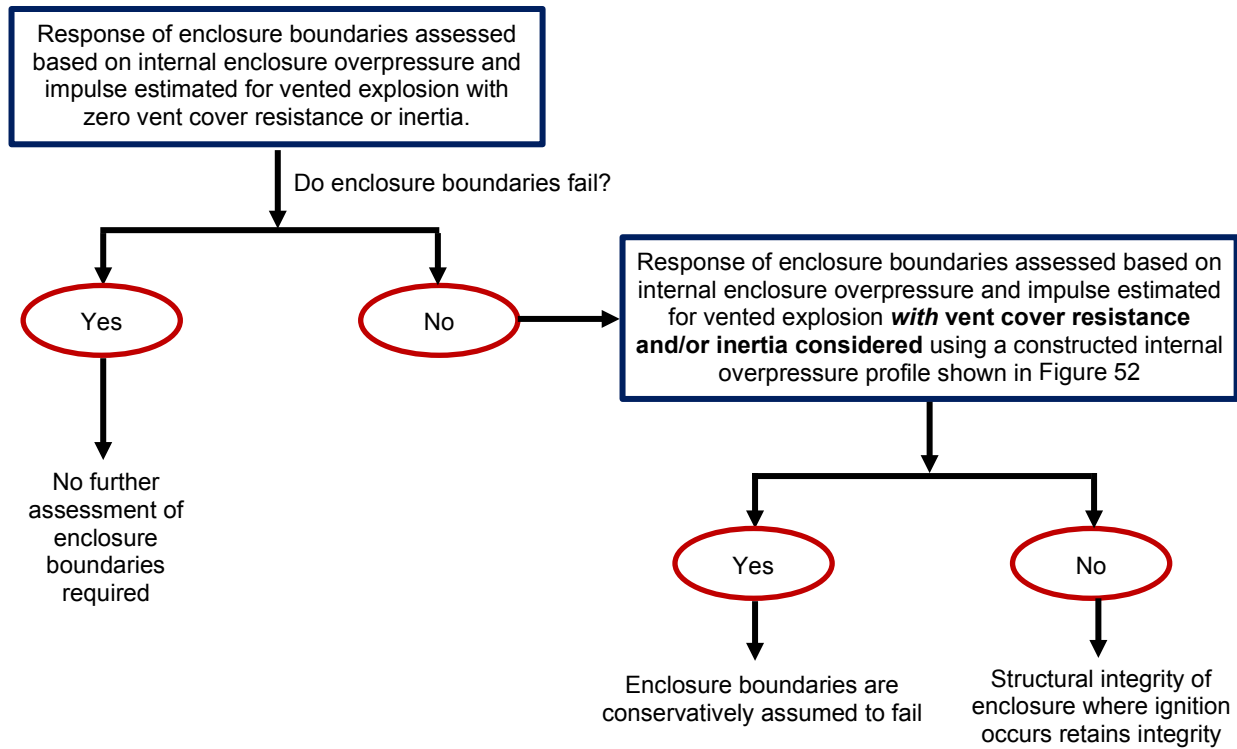
Figure 53: Flow chart for assessing structural collapse of enclosure where initial leak, dispersion and ignition event occurs. Vent cover resistance and inertia is considered.

### *3.4.4    Structural collapse and residual pulse*

Whilst the peak internal enclosure overpressures and impulses have been determined using the method in Sections 3.4.1 and 3.4.2, determining the response of the masonry walls forming the boundary of the enclosures is undertaken using the methodologies described in Section 2.7. A bespoke written Single Degree of Freedom (SDoF) script was written in Python and verified using the Oasys software Ergo [37] to model the masonry wall as a SDoF system.

An iso-damage diagram (Figure 54) has been constructed numerically (by trial and error) using the estimated resistance function based on a load bearing downstairs double leaf brick wall of a two-storey terrace, and a series of overpressure and impulse inputs. The iso-damage curves in Figure 54 represents the boundary between retainment of structural integrity, and collapse for both an isosceles triangular shaped pulse and a shock-fronted pulse. If the internal overpressure and impulse estimated using the method in Sections 3.4.1 and 3.4.2 is to the left and or below the lines in Figure 54, the load bearing wall retains its structural integrity and is assumed to continue supporting the vertical axial load from above. If the internal overpressure and impulse is to the right or above the curves, the load bearing wall is assumed to fail.
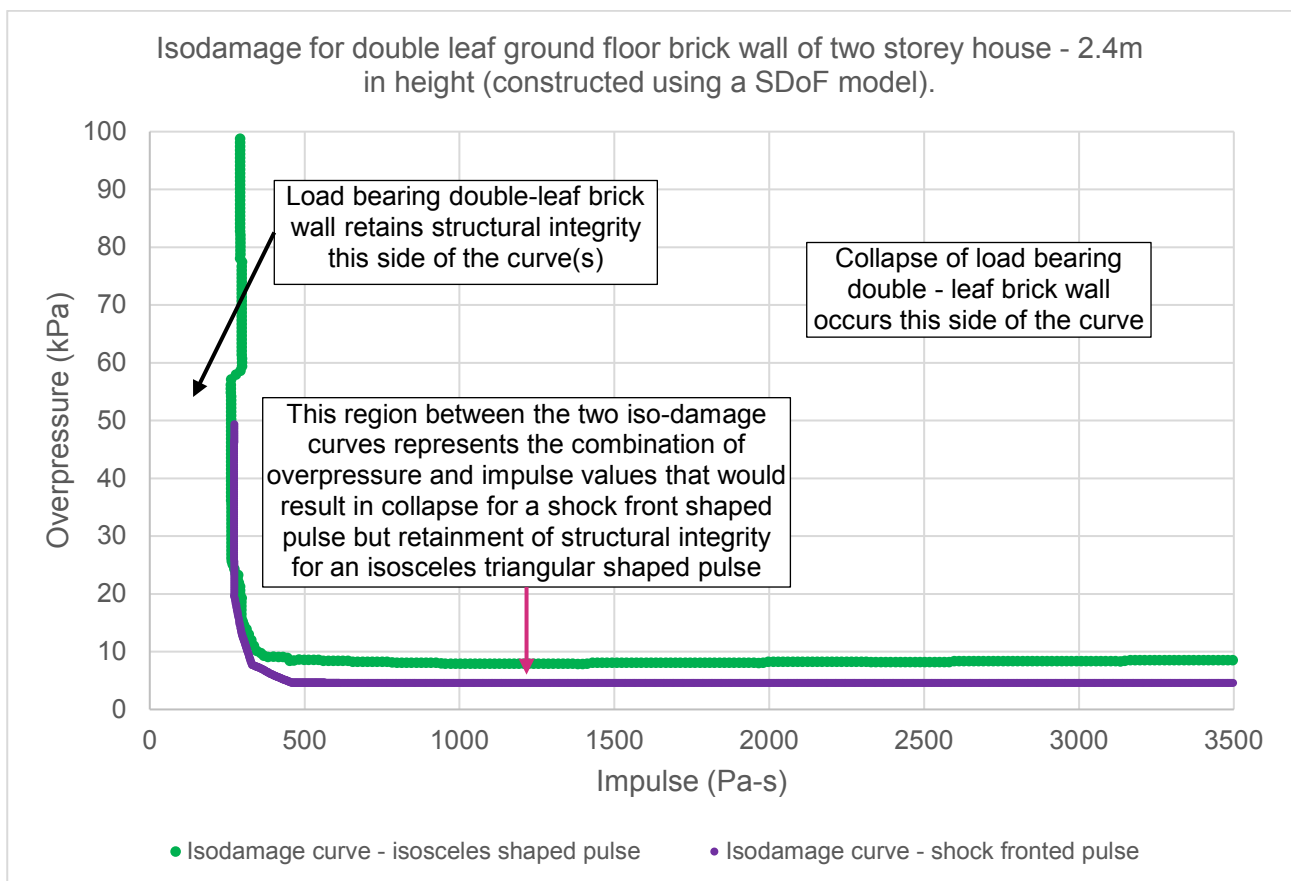


Figure 54: Iso-damage curve for double leaf brick wall (for a ground floor of a two-storey terraced house)

Department for Business, Energy & Industrial Strategy        Hy4Heat
ARP-WP7-GEN-REP-0003 | Issue 01 | 1 May 2021        Consequence Modelling Report

Page 76

Once the load-bearing walls of the enclosure initially confining the flammable vapour cloud fail, the high-pressure gases resulting from the vented explosion will expand into the neighbouring enclosures, which could be in neighbouring properties. To determine the internal overpressure and impulse exerted to the neighbouring enclosure boundaries (assumed to also be double leaf load bearing walls), a combination of the adiabatic gas behaviour theory (where pressure is inversely proportional to volume) and residual pulse analysis is used.

Adiabatic gas behaviour theory results in a cube-root decay of blast pressures with distance for a deflagrative event for non-congested areas [9]. The cube-root decay relationship being attributed to the rate of increase in volume that an expanding spherical pressure front bounds. A sensitivity study has been undertaken using the Wiekema piston-blast model [2] which is based upon the gas dynamics induced by a spherical expanding piston for different levels of fuel reactivity and shows the approach is sensible for the assessment undertaken here.

An estimation of the overpressure and impulse exerted on the neighbouring enclosure boundaries is based on the increased volume that the expanding flammable vapour cloud now occupies (Figure 55). It is assumed that the combustible blast wave at the boundaries of the failed initial enclosure (such as the kitchen or downstairs of a terraced house) will expand in five directions; forwards, backwards, sideways and upwards with a six-fold increase in volume leading to a six-fold decrease in the overpressure (Figure 55 and Figure 58).
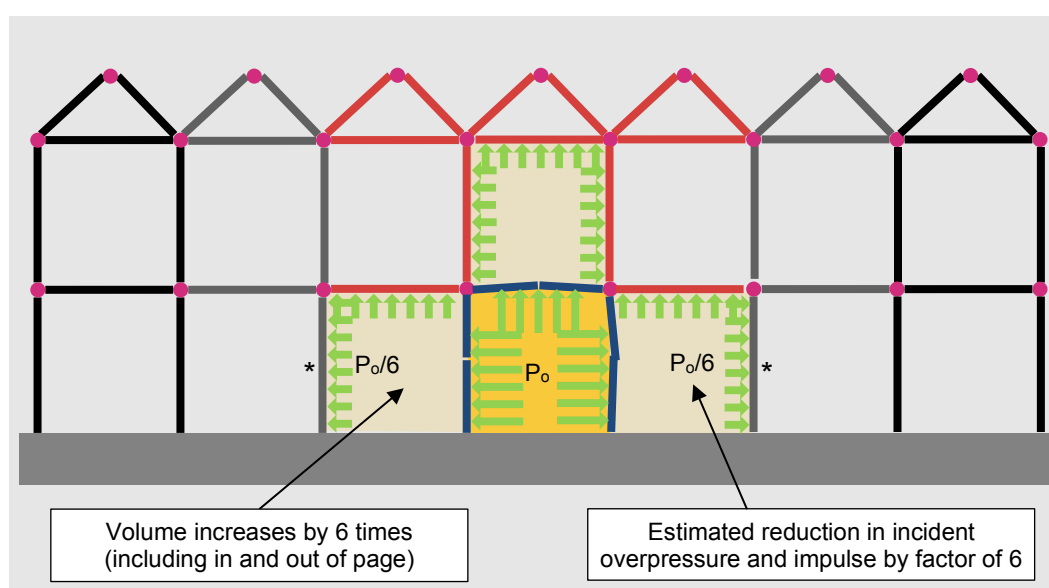


Figure 55: Estimating overpressure and impulse beyond enclosure where gas leak originates (in this instance where there is a possible collapse of 3-5 houses)

If the residual overpressure is high enough that the load bearing walls indicated by a * in Figure 55 also fail, then the overpressure at the load bearing walls indicated by ** in Figure 56 will also be subjected to a residual overpressure from the propagating blast wave. It is assumed that the combustible blast wave at the locations indicated by ** in Figure 56 experience an overpressure that

is a fourteen-fold decrease of the original overpressure that the boundary walls of the enclosure where the ignition event takes place, were subject to. This is concept is explained further in Figure 58.
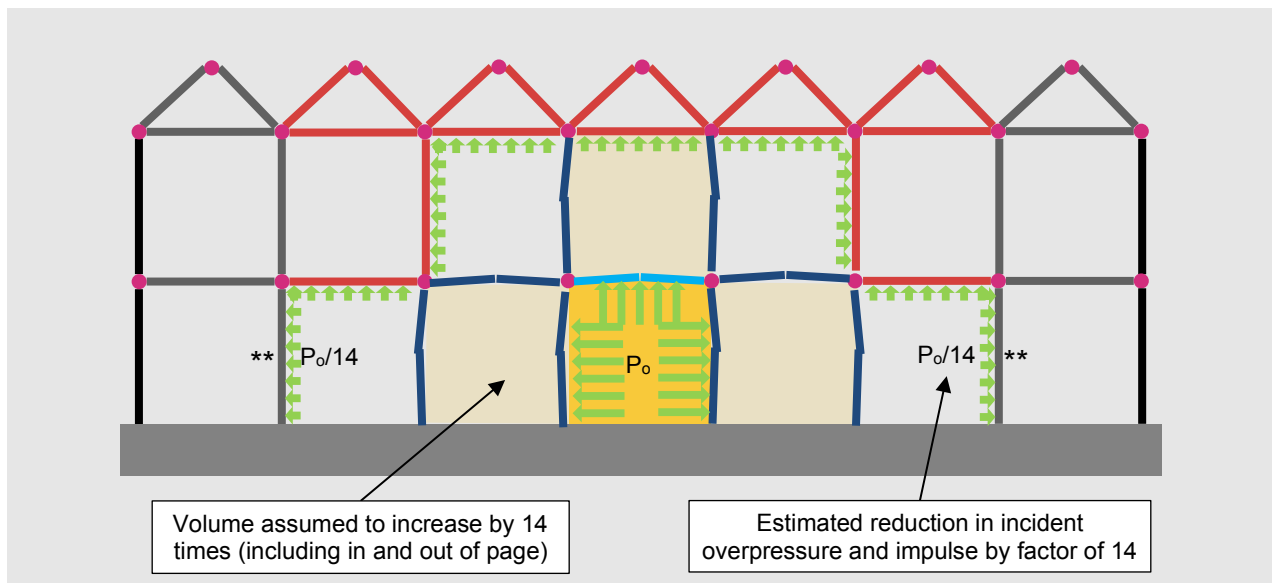


Figure 56: Estimating overpressure and impulse beyond enclosure where gas leak originates (in this instance where there is a possible collapse of 5-7 houses)

A residual pulse analysis is used to consider the portion of explosion energy converted to strain energy in the deformation of the double leaf load bearing walls. The residual blast load following failure of the initial enclosure load bearing walls is calculated based on time to failure of the wall (Figure 57 - time to reach maximum strain energy). For concentrations **above 18% hydrogen, the response of the double leaf load bearing walls is determined for both an isosceles shaped pulse representing a deflagration, and a shock fronted pulse shape representing a detonation following a possible DDT.**
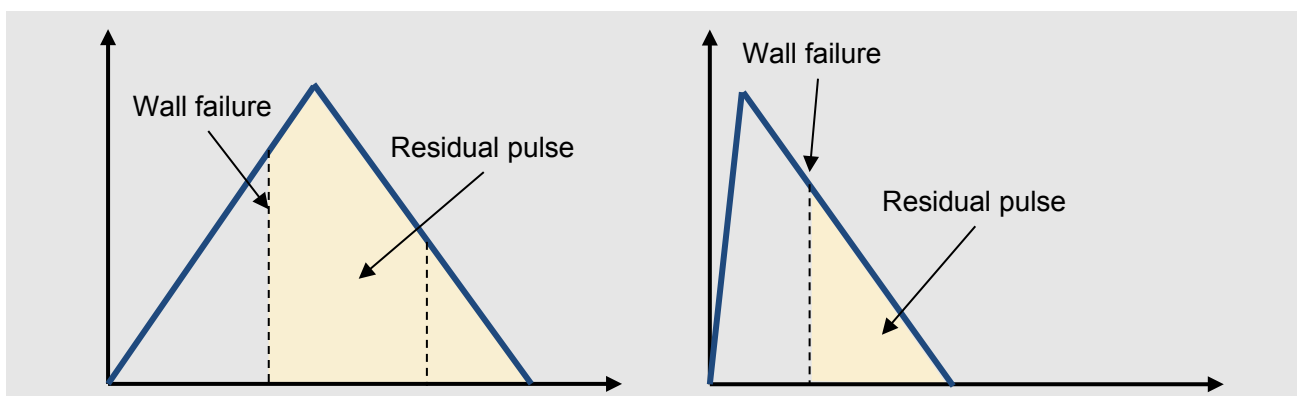


Figure 57: Residual pulse methodology for both an isosceles triangular shaped and shock fronted pulse shape
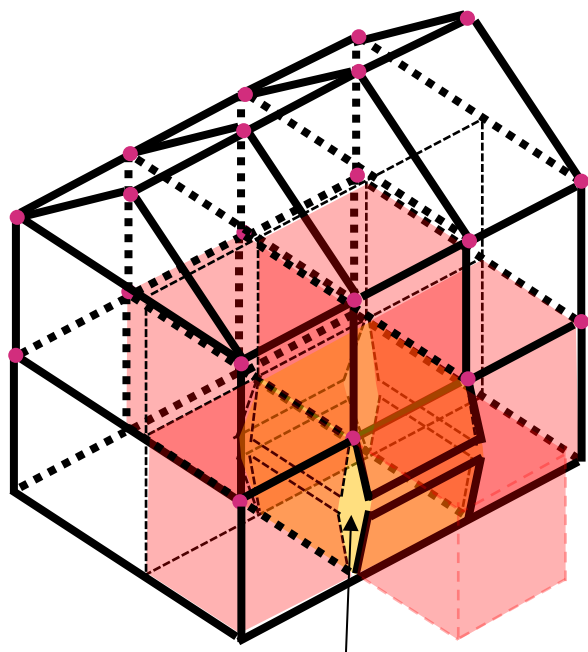
If the internal overpressure in the kitchen where the initial leak, dispersion and ignition event takes place (indicated in yellow) causes structural failure of the enclosure boundaries, then the expanding flammable vapour cloud is assumed to then occupy

- the volume directly above the kitchen on the first floor
- the kitchens in the next-door neighbouring properties
- the rest of the ground floor of the house in which the initial event occurs
- a volume equal to the kitchen outside the 'back' of the property

This approximated six fold increase in volume is the basis for assuming a six fold decrease in the peak internal overpressure at the boundaries indicated in Figure 55
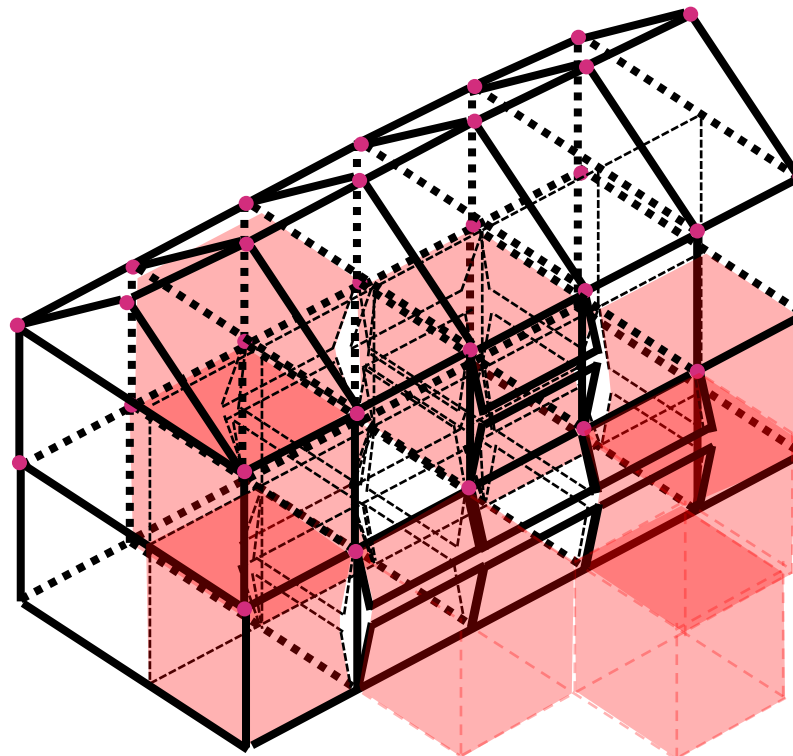
If the internal overpressure in the kitchen where the initial leak, dispersion and ignition event takes place causes structural failure of the enclosure boundaries AND failure of the boundaries of further enclosures shaded in red (excluding shaded volumes external to the dwelling on the diagram to the left), then the volume occupied by the expanding flammable vapour cloud is assumed to then occupy a further eight times the volume equal to the kitchen volume where the initial leak, dispersion and ignition event takes place. This would result in a total approximate 14 fold increase in volume and a fourteen fold decrease in the peak internal overpressure at the boundaries indicated in Figure 56.

Figure 58: Estimating overpressure in neighbouring 'enclosures' following failure of enclosure boundaries where initial leak, dispersion and ignition event takes place for kitchen scenario

# 4. Results

## 4.1 Overpressures and impulses

Except for determining injury due to burns, quantitatively measuring injury against all the categories of injury discussed in Section 3.3 requires an estimate of the internal overpressures and impulses developed following ignition of a confined flammable vapour cloud in the two scenarios (kitchen and downstairs of an open plan house - see Section 3.2) considered in this assessment.

Estimates of overpressure have been made using the "simplified" model from [1] (see Section 3.4.1 and 3.4.2). Consideration to the effects that vent cover resistance and inertia have on increasing internal overpressure have been made using the methodology described in Section 3.4.3. Both overpressure *with* and *without* vent cover resistance and inertia considered are included in Figure 59 through to Figure 64.

Figure 59 through to Figure 61 show the modelled peak overpressure following a leak, dispersion and ignition event of methane and hydrogen respectively for the kitchen scenario that are used to determine the number of people injured in this assessment. Figure 62 to Figure 64 show the modelled peak overpressure following a leak, dispersion and ignition event of methane and hydrogen respectively for the downstairs of a terraced house scenario.

**It is important to recognise that the peak overpressures estimated for hydrogen using the simplified model above assumes the enclosure retains structural integrity (i.e. the enclosure volume remains constant).** The modelling is therefore conservative for high concentrations of hydrogen because in practice the enclosure boundaries (the walls and ceiling) would fail before the vented explosion has fully developed and the peak overpressures in Figure 61 and Figure 64 would in practice not be realised. See Appendix B.1 for further discussion. Furthermore, both A.Sinha and J.Wen confirm that for high concentrations of hydrogen (+~24%) the "simplified" model is already highly conservative in the prediction of internal overpressure. Appendix F contains examples with further explanation of determining overpressure and impulse using the "simplified" method from [1].
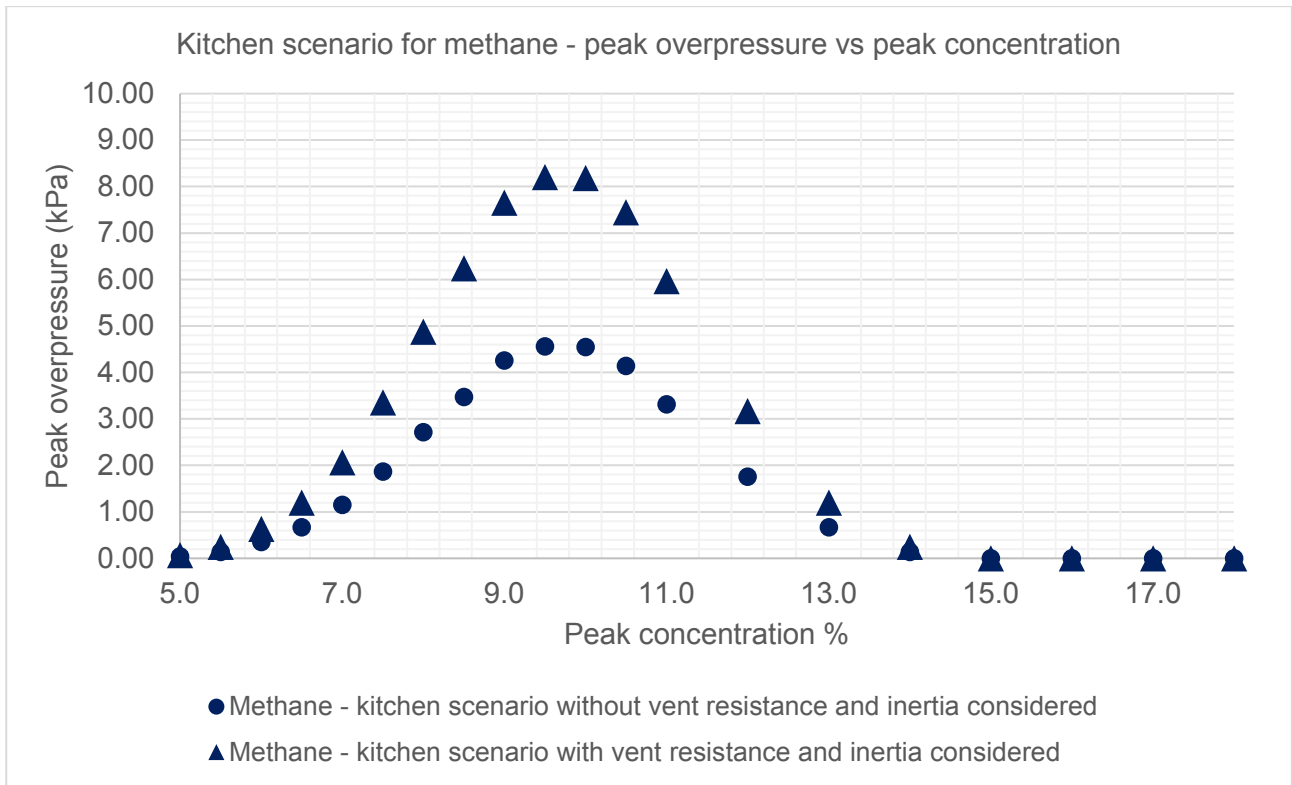
Figure 59: Modelled peak overpressure following a leak, dispersion and ignition event of methane for kitchen scenario
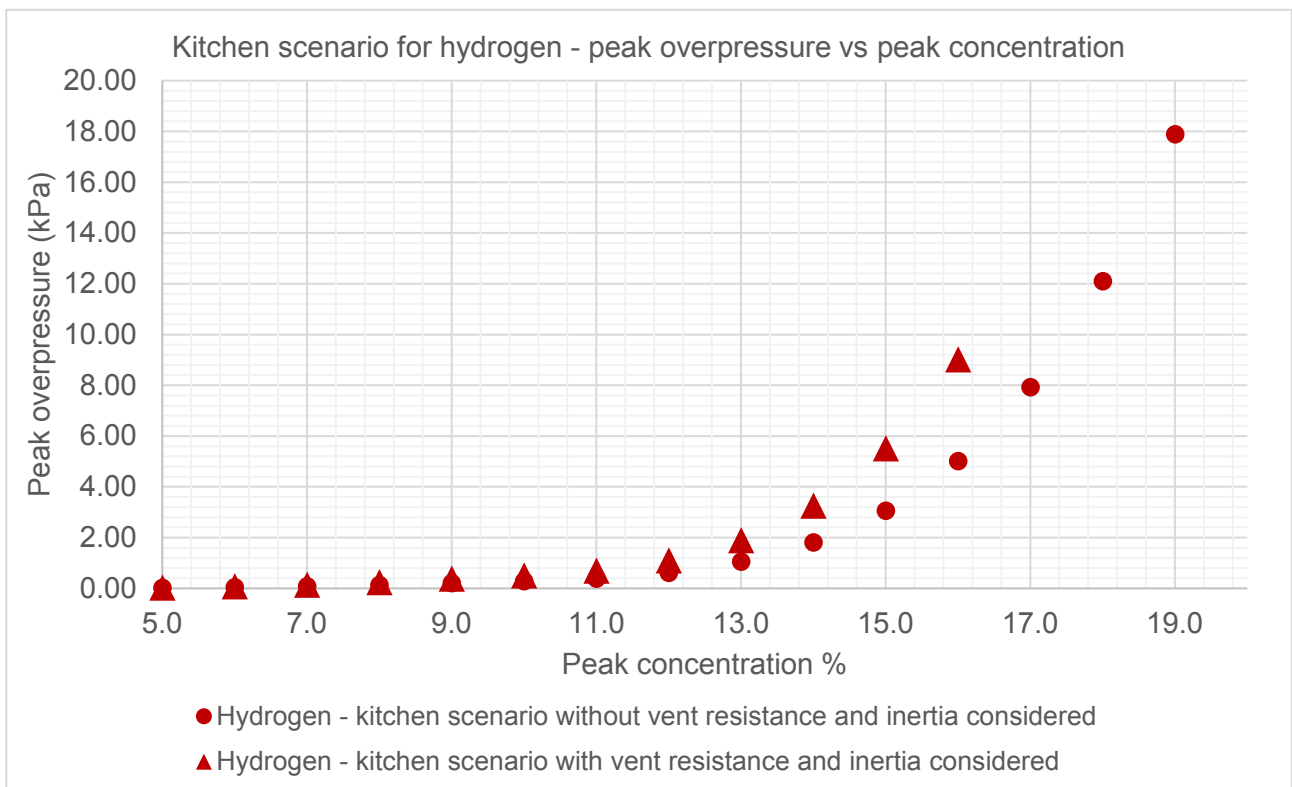


Figure 60: Modelled peak overpressure following a leak, dispersion and ignition event of hydrogen for kitchen scenario (5 to 19% peak concentration)
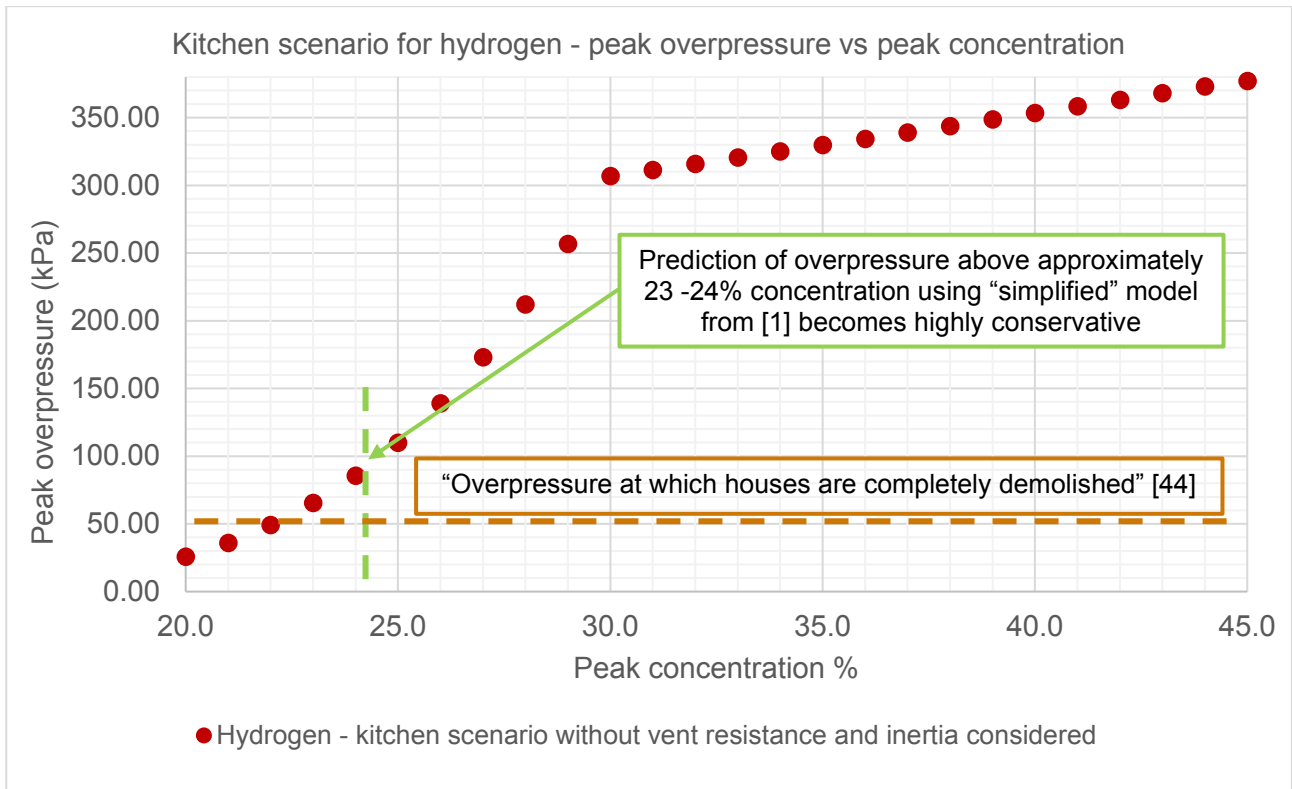
Figure 61: Modelled peak overpressure following a leak, dispersion and ignition event of hydrogen for kitchen scenario (20 to 45% peak concentration)
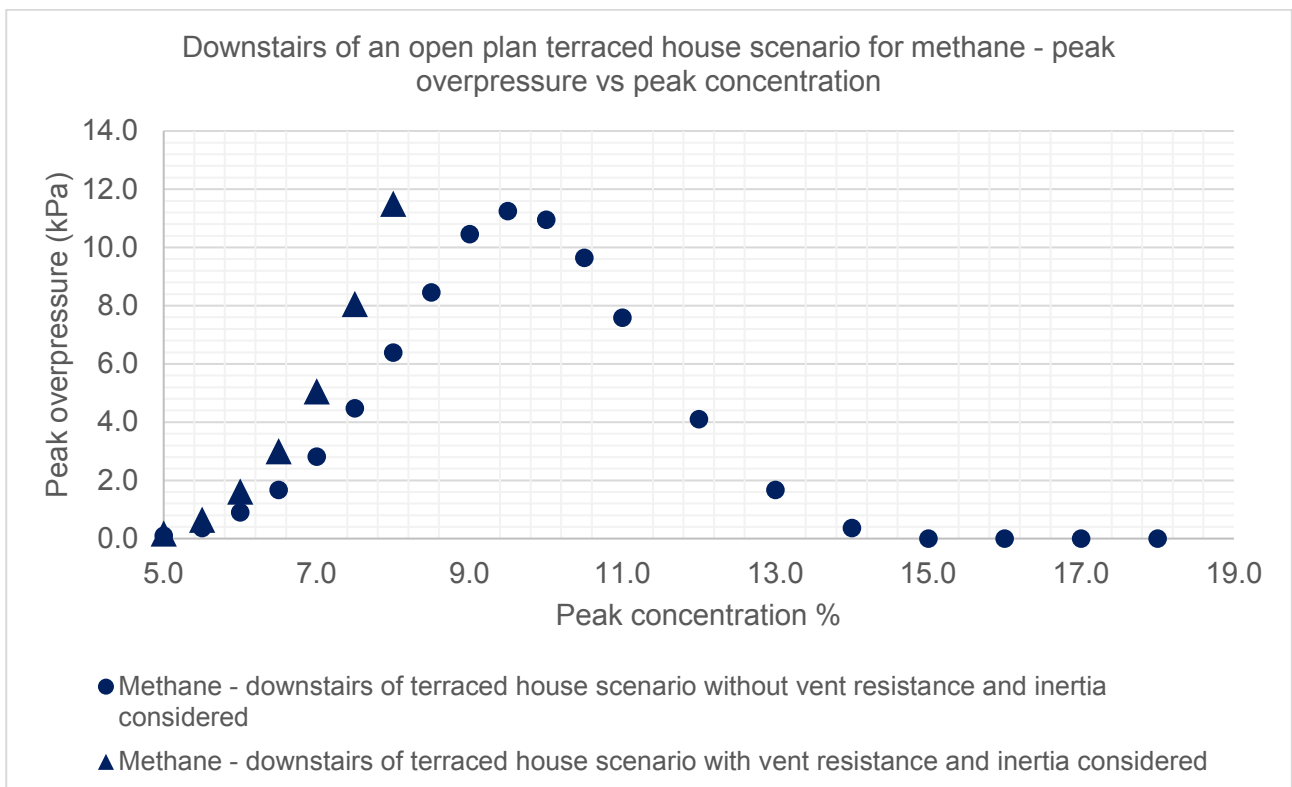


Figure 62: Modelled peak overpressure following a leak, dispersion and ignition event of methane for downstairs of an open plan terraced house scenario
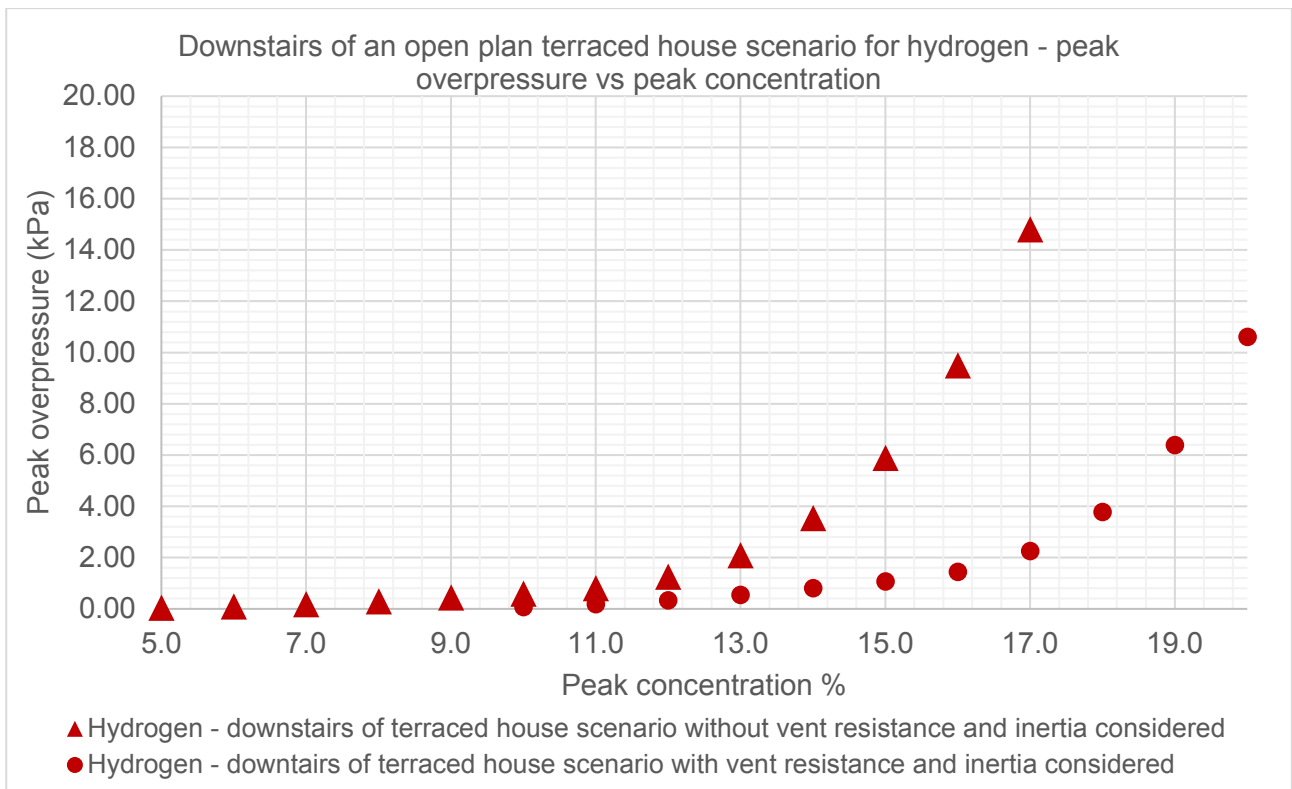
Figure 63: Peak overpressure following a leak, dispersion and ignition event of hydrogen for downstairs of an open plan terraced house scenario (5 to 19% peak concentration)
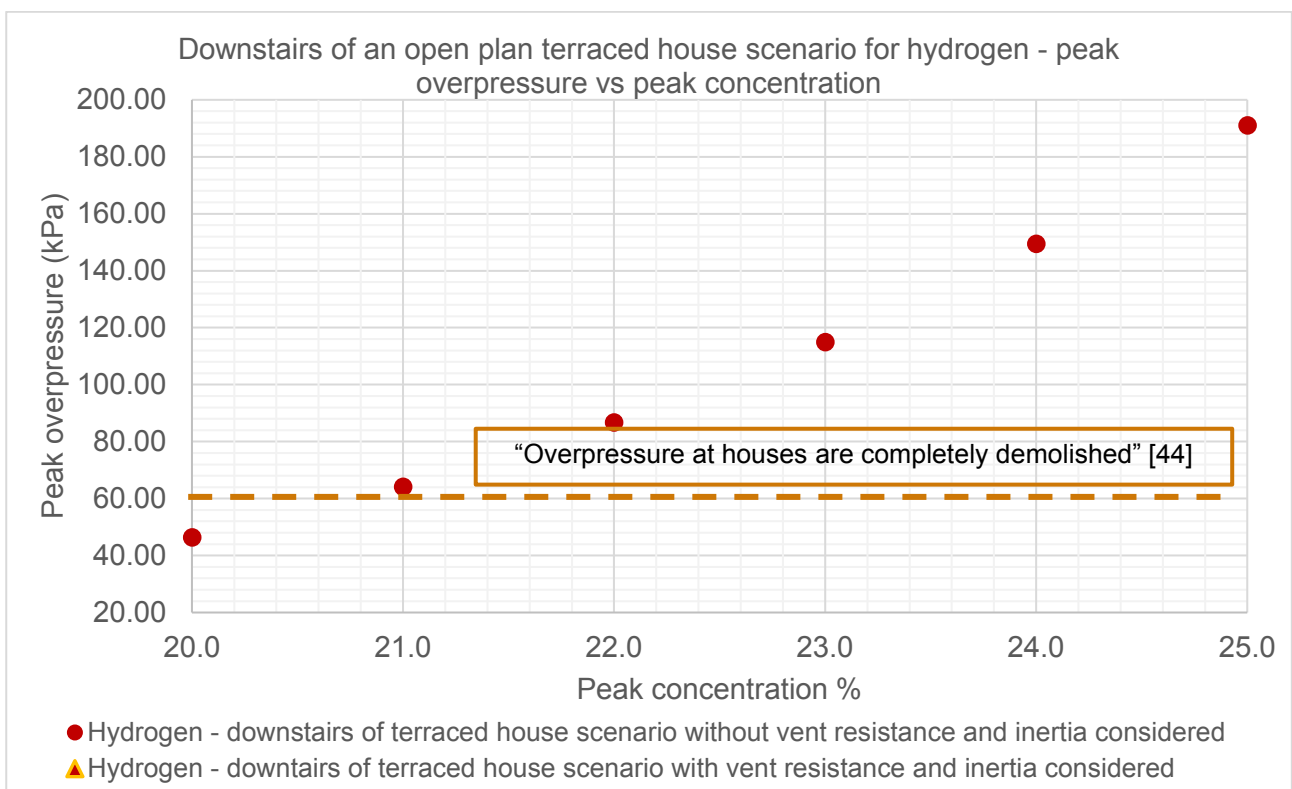


Figure 64: Peak overpressure following a leak, dispersion and ignition event of hydrogen for downstairs of an open plan terraced house scenario (20 to 25% peak concentration)

## 4.2 Structural collapse results

### 4.2.1 Kitchen scenario

For the kitchen scenario in Section 3.2, the number of injuries due to structural collapse is measured by determining the quantity of damage to the property where the initial explosion occurs and neighbouring properties.

The kitchen is assumed to be at the back or front of the terraced house. If the explosion is not enough to fail the kitchen walls where the ignition of the flammable vapour cloud takes place, the number of injuries *due to structural collapse* is measured as zero. If the explosion is large enough to fail the walls of the kitchen where the ignition of the flammable vapour cloud takes place, then the first floor area that collapses in both the property in the which the explosion occurs, and the neighbouring properties, is estimated as shown in Figure 65. The area of collapse on the first floor and the area of floor below the collapsed floor (on the ground floor) is divided by the total entire floor area in all three properties to produce a fraction. This fraction is then multiplied by **an occupancy of 1.79 people per dwelling** as described in Section 3.3.1 to quantitatively estimate the number of injuries:

$$\frac{\left[A_{1st\,floor\,Collapse-Origin} + 2 \times A_{1st\,floor\,Collapse-Neigbour}\right]}{A_{Total\,1st\,floor}} \times 1.79$$

Where $A_{1st\,floor\,Collapse-Origin}$ is the area of first floor collapsed in the dwelling where the explosion occurs, $A_{1st\,floor\,Collapse-Neigbour}$ is the area of first floor collapsed in *one* neighbouring dwelling, and $A_{Total\,1st\,floor}$ is the total floor area on the first floor in one terraced house. $A_{1st\,floor\,Collapse-Neigbour}$ in this assessment is assumed to be the same as $A_{1st\,floor\,Collapse-Origin}$ with each house having an identical floor plan. For this assessment, $A_{Total\,1st\,floor}$ is assumed to be the floor area indicted for the downstairs of a terraced house scenario in Figure 27 (i.e. the floor area of the ground floor is identical to the floor area of the first floor).

If the kitchen explosion is large enough to damage not only the neighbouring properties but also the properties "next door but one" then the number of injuries is measured by:

$$\frac{2 \times A_{1st\,floor\,Collapse-Neigbour} + 3 \times A_{Total\,1st\,floor}}{A_{Total\,1st\,floor}} \times 1.79$$

Here the, all the load bearing party walls of the dwelling where the gas explosion occurs are assumed to fail resulting in the collapse of the total first floor area in the neighbouring dwellings also, and partial collapse of the area in the dwellings "next door but one" (see Figure 66).

The results for methane are shown in Table 5 and for hydrogen in Table 6.

The results indicate that load bearing walls to the kitchen enclosure where the explosion occurs retain structural integrity below a peak methane concentration of 8.5%, and above a peak concentration of 10.5%. Between a peak methane concentration of 8.5% and 10.5%, partial collapse of three houses is expected due to failure of the kitchen load bearing walls where the explosion occurs.

The load bearing walls to the kitchen where the explosion occurs retain structural integrity below a peak hydrogen concentration of 15%. Between a peak hydrogen concentration of 15% and 23%, partial collapse of three houses is expected due to failure of the kitchen load bearing walls in the enclosure where the explosion occurs. Above a concentration of 23%, total collapse of three houses (one where the initial explosion occurs, and the two immediately adjoining houses), plus partial collapse of a further two houses is expected.

Table 5: Kitchen scenario structural collapse results for methane

| Peak concentration (in stratified mixture) | Failure of walls of kitchen in which explosion occurs? | Failure of walls of next-door neighbour kitchen? | Assumed extent of structural damage | Number of people injured due to structural collapse |
|---|---|---|---|---|
| < 5.0% | Below LFL so no ignition | | | |
| 5.0% to 8.5% | No | - | Structural integrity maintained in dwelling where ignition occurs | 0.0 |
| 8.5% to 10.5% | Yes | No | Partial collapse of 3 houses | 2.0 |
| >10.5% | No | - | Structural integrity maintained in dwelling where ignition occurs | 0.0 |

Table 6: Kitchen scenario structural collapse results for hydrogen

| Peak concentration (in stratified mixture) | Failure of walls of kitchen in which explosion occurs? | Failure of walls of next-door neighbour kitchen? | Assumed extent of structural damage | Number of people injured due to structural collapse |
|---|---|---|---|---|
| < 5.0% | Below LFL so no ignition | | | |
| 5.0% to 15.0% | No | - | Structural integrity maintained in dwelling where ignition occurs | 0.0 |
| 15.0% to 23.0% | Yes | No | Partial collapse of 3 houses | 2.0 |
| > 23.0% | Yes | Yes | Total collapse of 3 houses, partial collapse of a further 2 houses | 6.7 |
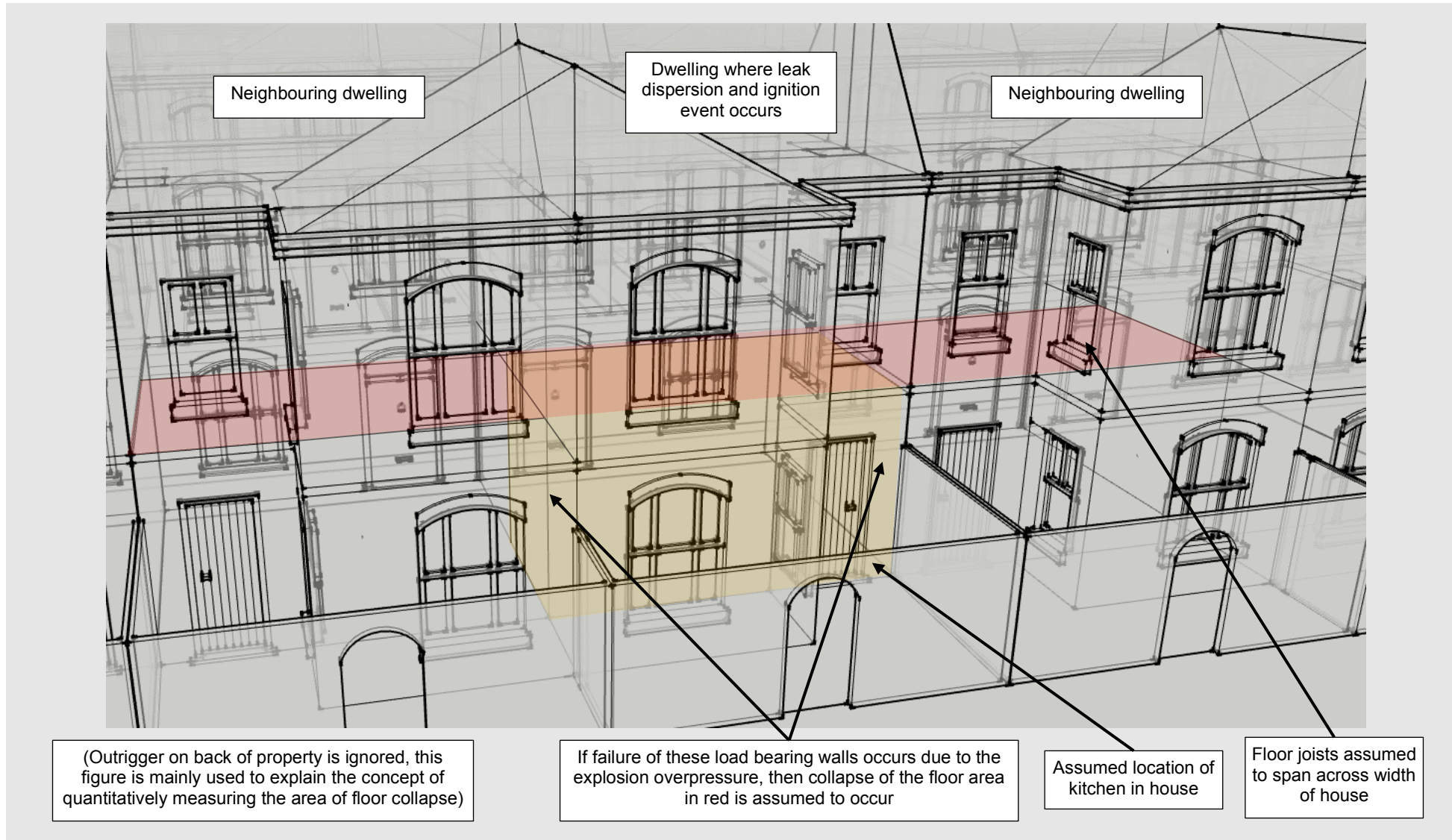
Figure 65: Quantitatively measuring the collapsed area of floor in immediate neighbouring dwellings following a gas explosion in kitchen scenario (extract taken from [20]).
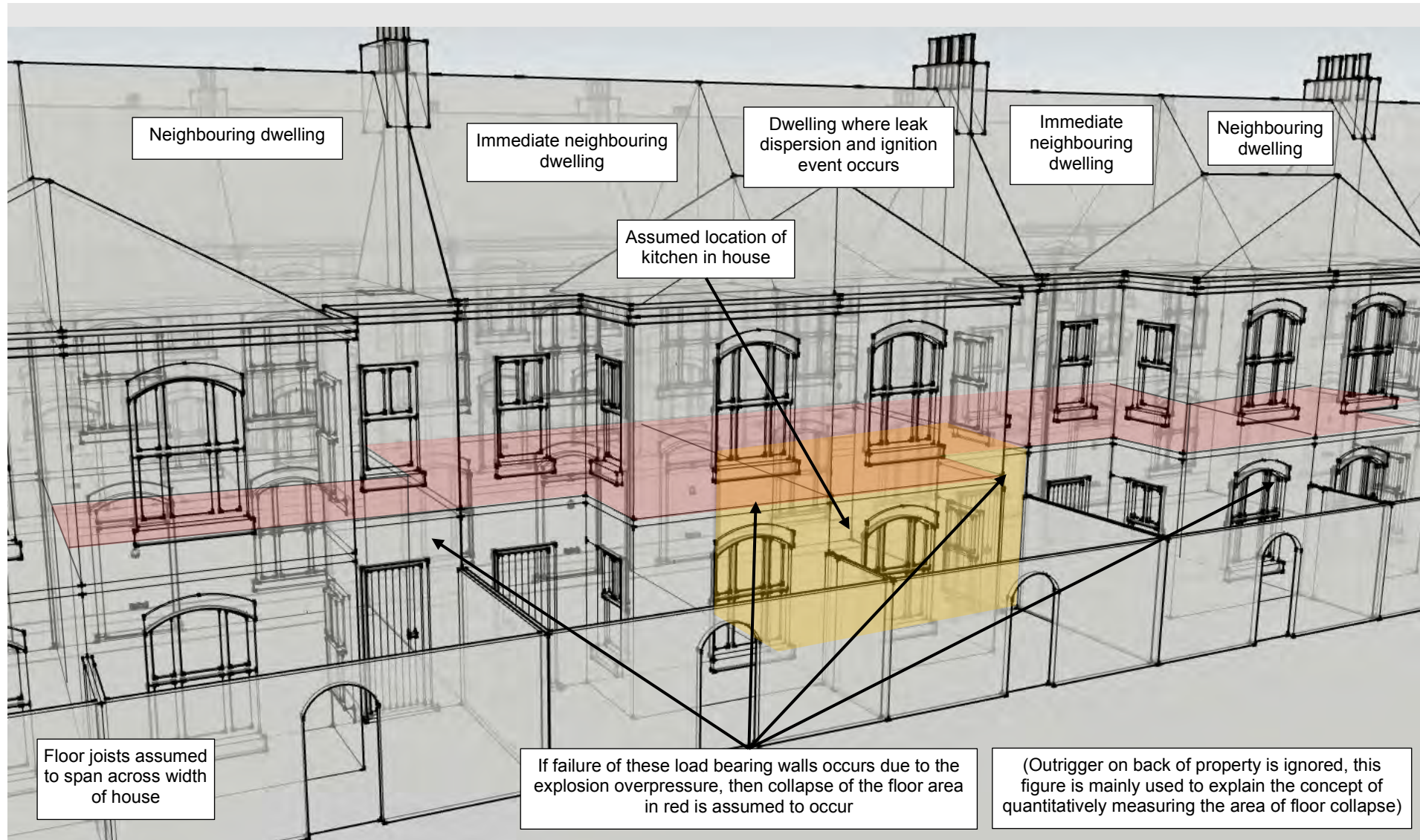
Figure 66: Quantitatively measuring the collapsed area of floor in neighbouring dwellings following gas explosion in kitchen scenario that causes failure of immediate neighbouring dwellings kitchen walls (extract taken from [20]).

Figure 67 shows a selection of the overpressure and impulse result from Section 4.1 for the kitchen scenario have been overlaid on the iso-damage curves from Figure 54 for both methane and hydrogen.

For comparison, Figure 68 shows selection of the hydrogen overpressure and impulse results from Section 4.1 for the kitchen scenario have been overlaid on the iso-damage curves from Figure 54 and the iso-damage curves from the "Damage graphs" in Section 5.1 of [28].

Figure 68 suggests that the iso-damage curves used in this assessment to determine the extent of structural collapse (and therefore the number of people injured due to structural collapse), are bounded between the "threshold for major structural damage" and the "threshold for minor structural damage" curves from the "Damage graphs" in Section 5.1 of [28]. It is difficult to make a direct comparison between the iso-damage curves generated from first principles in this assessment with the iso-damage curves in the "Damage graphs" in Section 5.1 of [28] because the curves in the latter require a degree of subjectivity into how they are interpreted and it is difficult to quantitively measure the extent of structural collapse using them (i.e. how is "threshold for major structural damage" translated into number of people injured?) It is also worth remembering that the "Damage graphs" in Section 5.1 of [28] are mostly constructed using observations (for example by comparing buildings damaged by dropped bombs in World War II with crater locations and sizes) with a large selection of observations being detonations that occur external to the buildings and imposing an overpressure and impulse onto the exterior.

However, overlaying both sets of curves is still useful because it provides some degree of a sensitivity check to the iso-damage curves in this assessment generated using the methodology described in Sections 2.7 and 3.4.4. Figure 68 suggests that whilst the iso-damage curves generated in this assessment from first principles trend well with the "Threshold for major structural damage" from the "Damage curves" in Section 5.1 of [28] in the *impulsive* region of the iso-damage curves (the vertical asymptotes to the left side of Figure 68), the *quasi-static* part of the iso-damage curves generated in this assessment (the horizontal asymptote to the bottom of Figure 68), are shown to be conservative by the same degree for both methane and hydrogen.
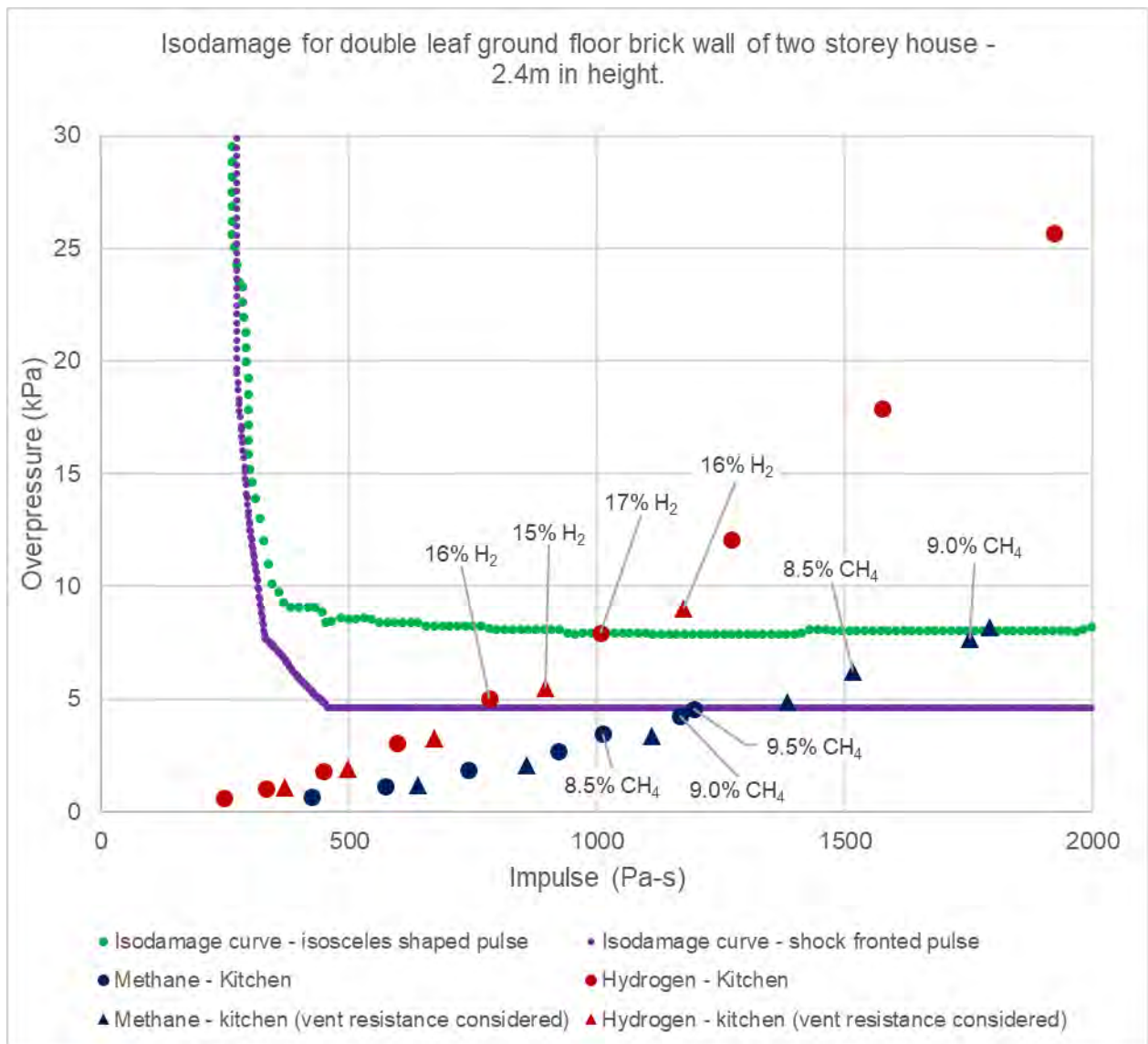
Figure 67: Selection of overpressure and impulse results from Section 4.1 for the kitchen scenario overlaid on Figure 54
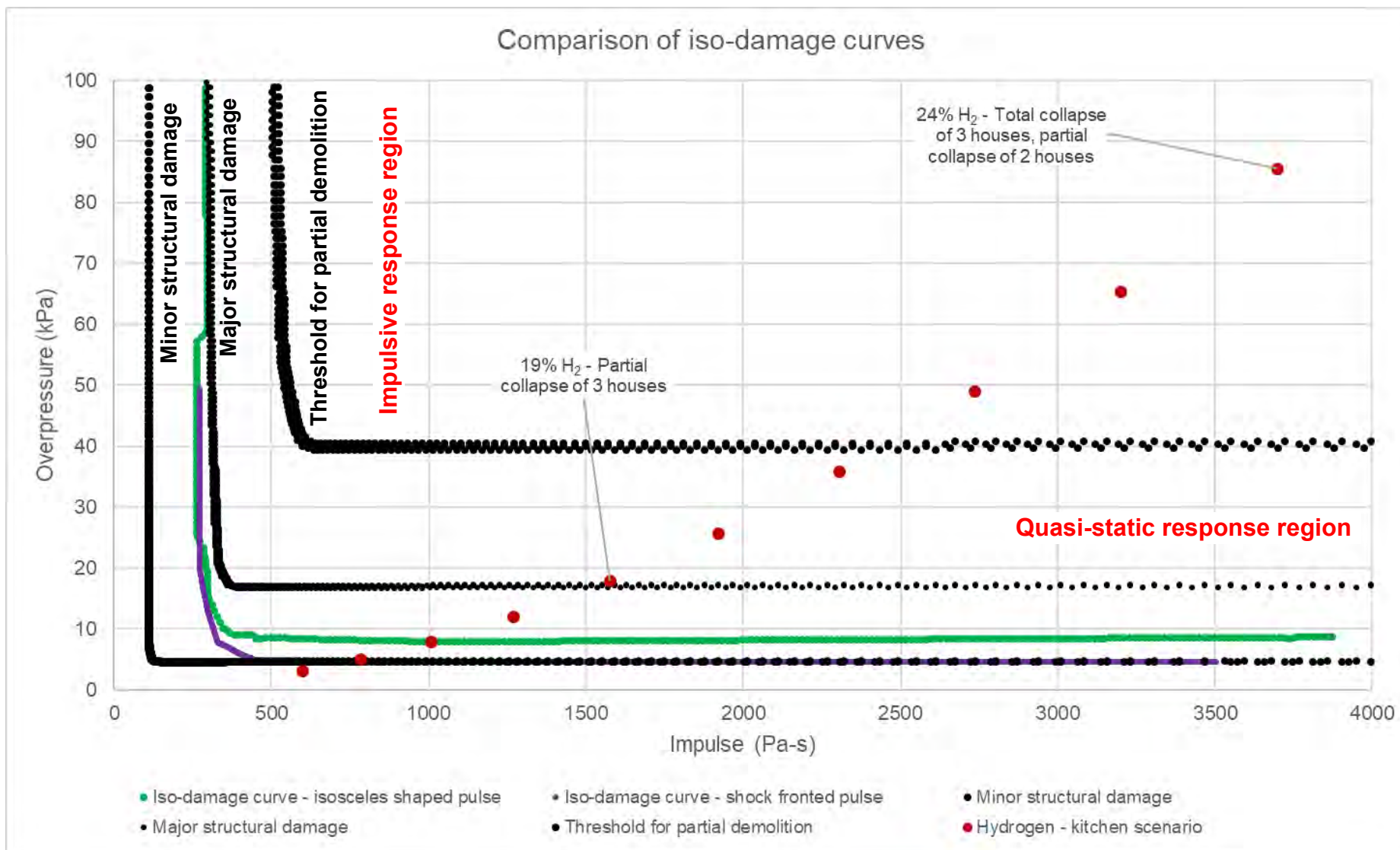
Figure 68: Selection of overpressure and impulse results for hydrogen from Section 4.1 for the kitchen scenario overlaid on Figure 54 and the "Damage graphs" in Section 5.1 of [28]

## 4.2.2 *Downstairs of an open plan terraced house scenario*

For the downstairs of an open plan terraced house scenario in Section 3.2, the number of injuries due to structural collapse is measured by determining the quantity of damage to the property where the initial explosion occurs and to neighbouring properties.

If the explosion is not strong enough to fail the downstairs enclosure walls, the number of injuries *due to structural collapse* is measured as zero. If the explosion is strong enough to fail downstairs enclosure walls (which are the party walls with neighbouring properties), then the total first-floor area in both the dwelling in which the explosion occurs, and the neighbouring properties, are assumed to collapse (i.e. floor area of three properties). This is multiplied by an occupancy of 1.79 people per dwelling as described in Section 3.3.1 to quantitatively estimate the number of injuries i.e. $3 \times 1.79$.

If the explosion is large enough to damage not only the neighbouring properties, but also the properties "next door but one" then the number of injuries is estimated by multiplying the number of properties where there is first floor collapse (i.e. five properties) by an occupancy of 1.79 people per dwelling.

The results for methane are shown in Table 7 and for hydrogen in Table 8.

The results indicate that load bearing walls to the enclosure (downstairs of an open plan terraced house) where the explosion occurs retain structural integrity below a peak methane concentration of 7.0% and above a peak concentration of 12.0%. Between a peak methane concentration of 7.0% and 12.0% methane, the load bearing walls to the downstairs of a terraced house enclosure where the explosion occurs fail and total collapse of three houses is expected.

The load bearing walls to the enclosure (downstairs of an open plan terraced house) where the explosion occurs retain structural integrity below a peak hydrogen concentration of 14%. Between a peak concentration of 14% and a peak concentration of 21% hydrogen, the load bearing walls to the downstairs of a terraced house enclosure where the explosion occurs fail, and total collapse of three houses is expected. Above a peak concentration of 21% hydrogen total collapse of 5 houses is expected.

**The downstairs of the open plan terraced house scenario has been modelled up to a 18% peak concentration of methane and a 25% peak concentration of hydrogen. This is the maximum peak concentration achieved in the Hy4Heat Dispersion modelling report** [23] **for the downstairs of an open plan terraced house scenario with a steady state full bore leak.**

Table 7: Downstairs of terraced house scenario structural collapse results for methane

| Peak concentration (in stratified mixture) | Failure of walls in house where explosion occurs? | Failure of walls of next-door neighbour's party walls? | Assumed extent of structural damage | Number of people injured due to structural collapse |
|---|---|---|---|---|
| < 5.0% | Below LFL so no ignition | | | |
| 5.0% to 7.0% | No | - | Structural integrity maintained in dwelling where ignition occurs | 0.0 |
| 7.0% to 12.0% | Yes | No | Total collapse of 3 houses | 5.4 |
| > 12.0% | No | - | Structural integrity maintained in dwelling where ignition occurs | 0.0 |

Table 8: Downstairs of terraced house scenario structural collapse results for hydrogen

| Peak concentration (in stratified mixture) | Failure of walls in house where explosion occurs? | Failure of walls of next-door neighbour's party walls? | Assumed extent of structural damage | Number of people injured due to structural collapse |
|---|---|---|---|---|
| 5.0% to 14.0% | No | - | Structural integrity maintained in dwelling where ignition occurs | 0.0 |
| 14.0% to 21.0% | Yes | No | Total collapse of 3 houses | 5.4 |
| 21.0% to 25.0% | Yes | Yes | Total collapse of 5 houses | 8.9 |

## 4.3    Primary injury results

A quantitative assessment of primary injury has been made using overpressure and impulse estimated using the methodology in Section 3.4.1. **The results show that the risk of primary injury is low.** Only above 19% peak hydrogen is there any risk of primary injury with no risk for methane. Compared to other types of injury, it easy to see that secondary and tertiary injury will be far more severe than primary injury and that anyone exposed to primary injury will also experience secondary and tertiary injury. The results in Figure 69 and Figure 70 are for primary injuries in the public realm outside the terraced house (such as the street) where the ignition of a leaked confined flammable vapour cloud occurs. It is assumed that injuries of occupants within the property are already injured due structural collapse or injury relating to fire and burns so are not included in the primary injury assessment.
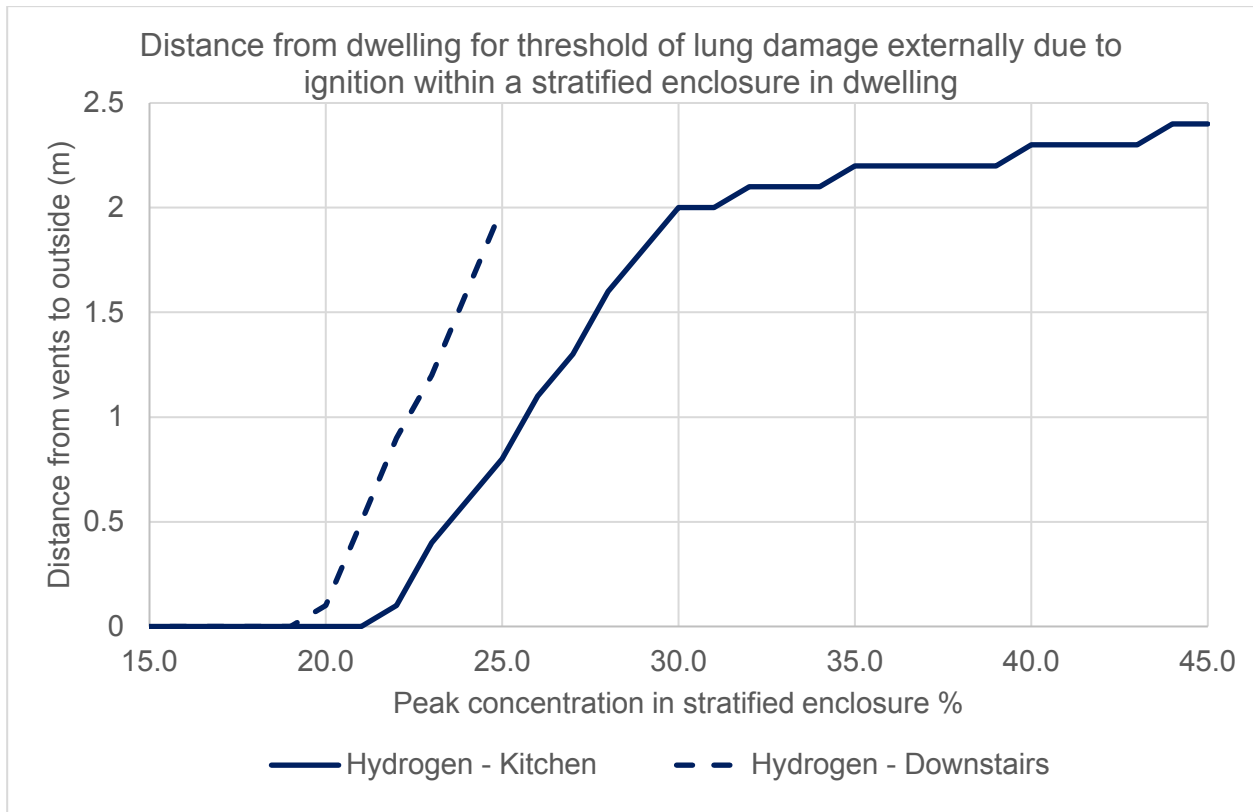
Figure 69: Peak concentration vs distance from dwelling for threshold of lung damage externally due to ignition within internal stratified enclosure in dwelling for hydrogen
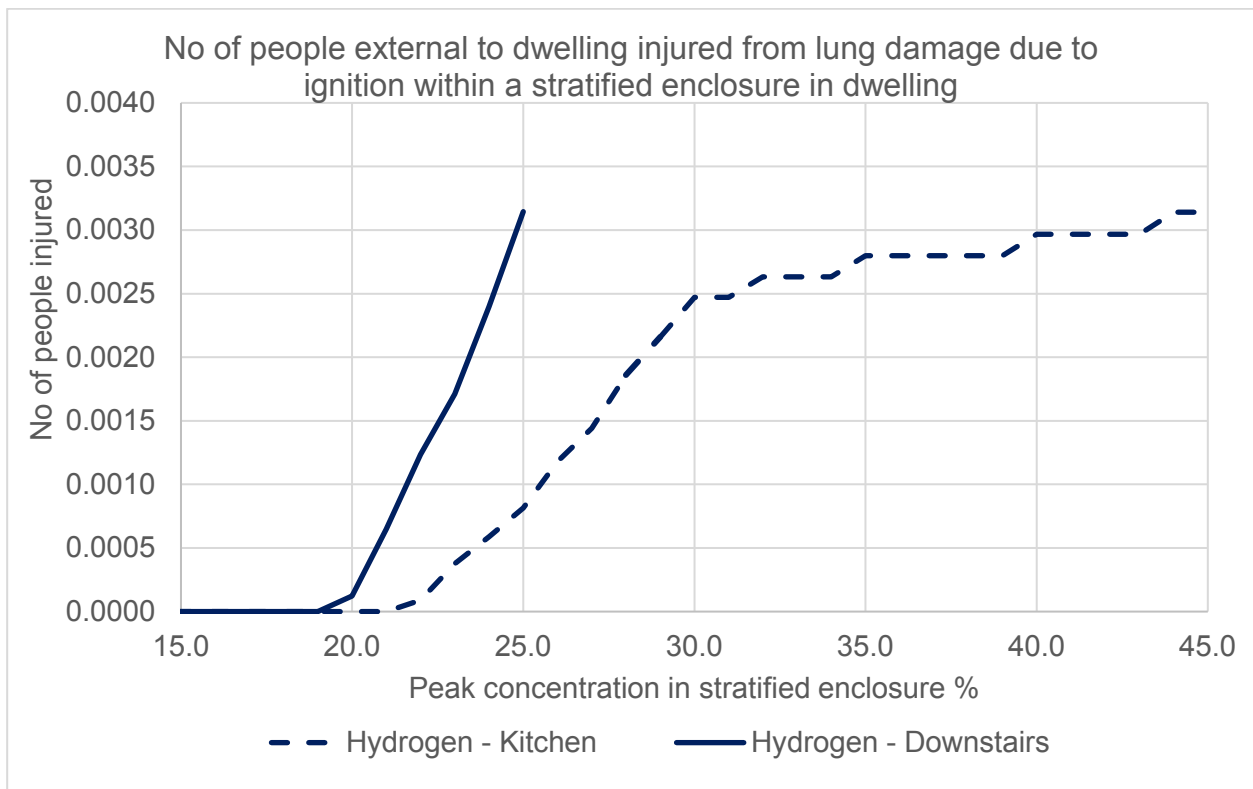


Figure 70: Primary injury results

## 4.4    Secondary injury results

A quantitative assessment of secondary injury has been made using overpressure and impulse estimated using the methodology in Section 3.4.1 (see Figure 71 and Figure 72) The results indicate a glass throw distance of approximately double for the peak concentration of hydrogen when compared to the peak concentration for methane. For low concentrations of methane and hydrogen it is possible that the glazing won't fail, or if it does it fail, it does so in a way that the entire glazing pane or glazing fragments only fall a very short difference from the window.

The results for glass throw here have been compared to experimental work undertaken by Kiwa using their Fire Investigation Box (FIB) [28]. The FIB is similar in dimensions to the dimensions of the kitchen used in this assessment. Comparison of results show that the modelling undertaken in this study compares well with experimental work. For example, in the FIB experimental work, an ignition of a peak hydrogen concentration of 29% in the FIB resulted in maximum glass throw distance of approximately 78m which is similar to the 72m distance for the scenario modelled in this study.

Further detail on the calculation of glass throw distance by way of example can be found in Appendix F.
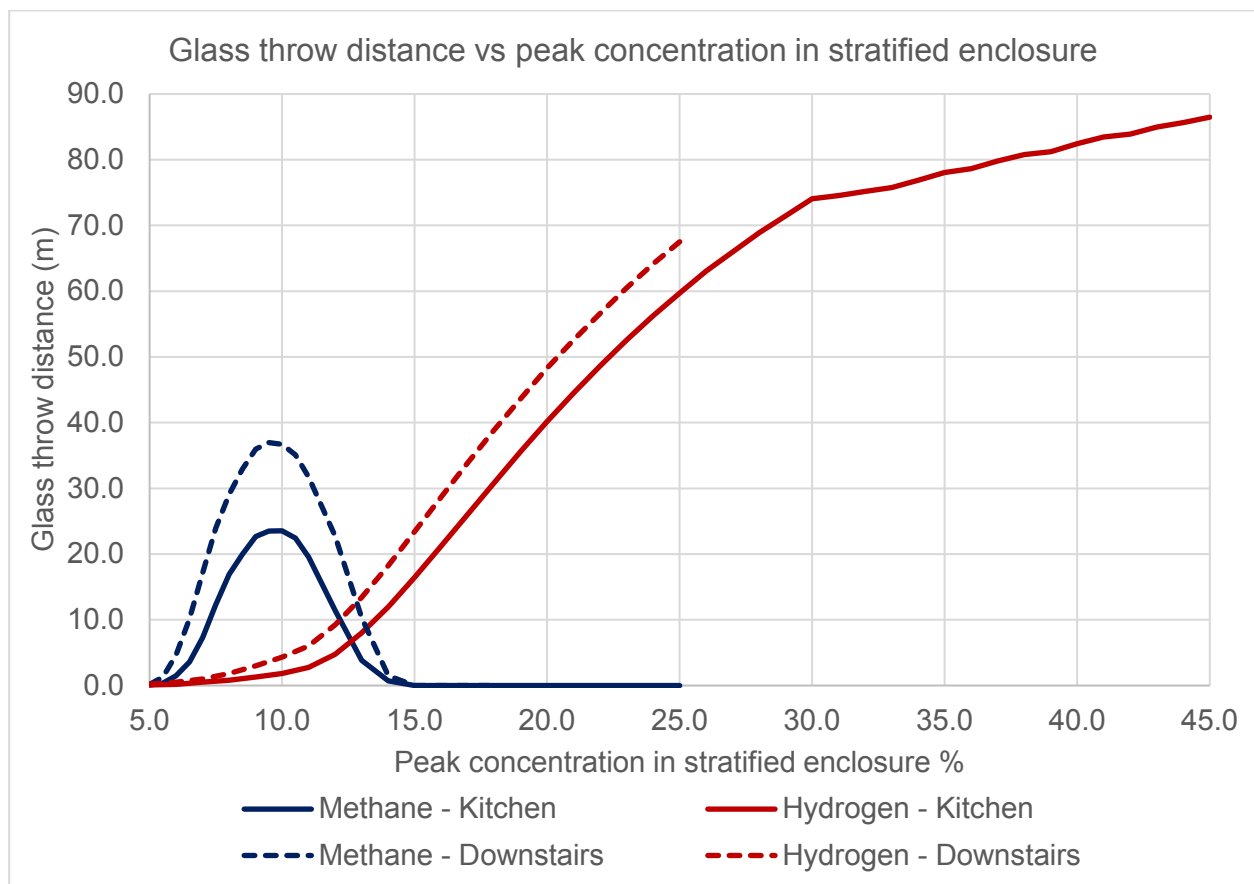


Figure 71: Glass throw distance for both kitchen and downstairs of terraced house scenario
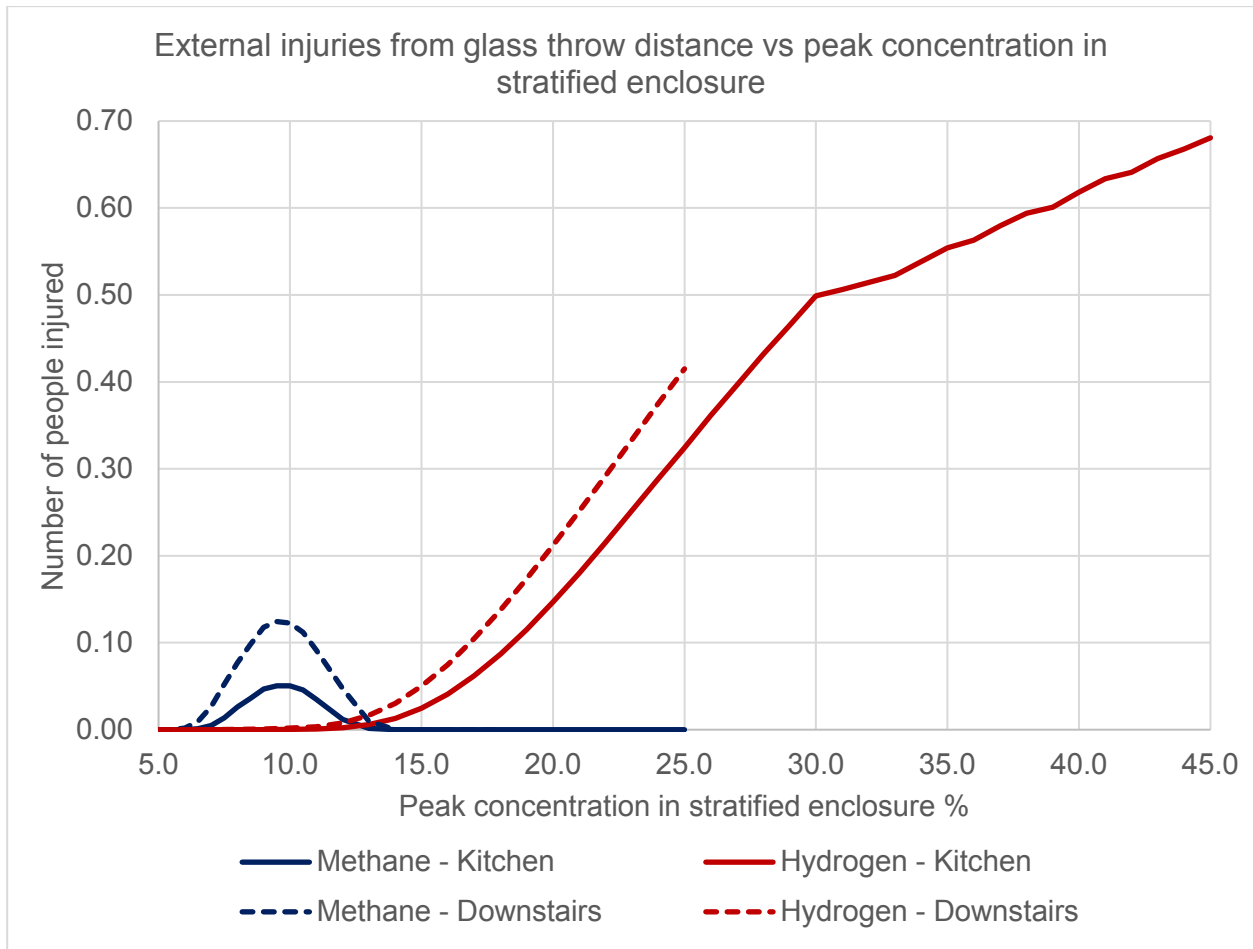
Figure 72: Number of people injured externally due to glass throw against concentration for both kitchen and downstairs of terraced house scenario

## 4.5    Tertiary injury results

A quantitative assessment of tertiary injury has been made using overpressure and impulse estimated using the methodology in Section 3.4.1. The distances from the property or dwelling where the explosion occurs for loss of balance leading to tertiary injury is larger than primary injury. For high concentrations of hydrogen in the kitchen and downstairs of an open plan terraced house scenario the quantity of tertiary injuries external to the property, although less than the estimated number of injuries from secondary injury (glass throw), it is not insignificant. The results in Figure 73 and Figure 74 are for tertiary injuries in the public realm outside the terraced house (such as the street) where the ignition of a leaked confined flammable vapour cloud occurs. It is assumed that injuries of occupants within the property are already injured due structural collapse or injury relating to fire and burns so are not included in the tertiary injury assessment.
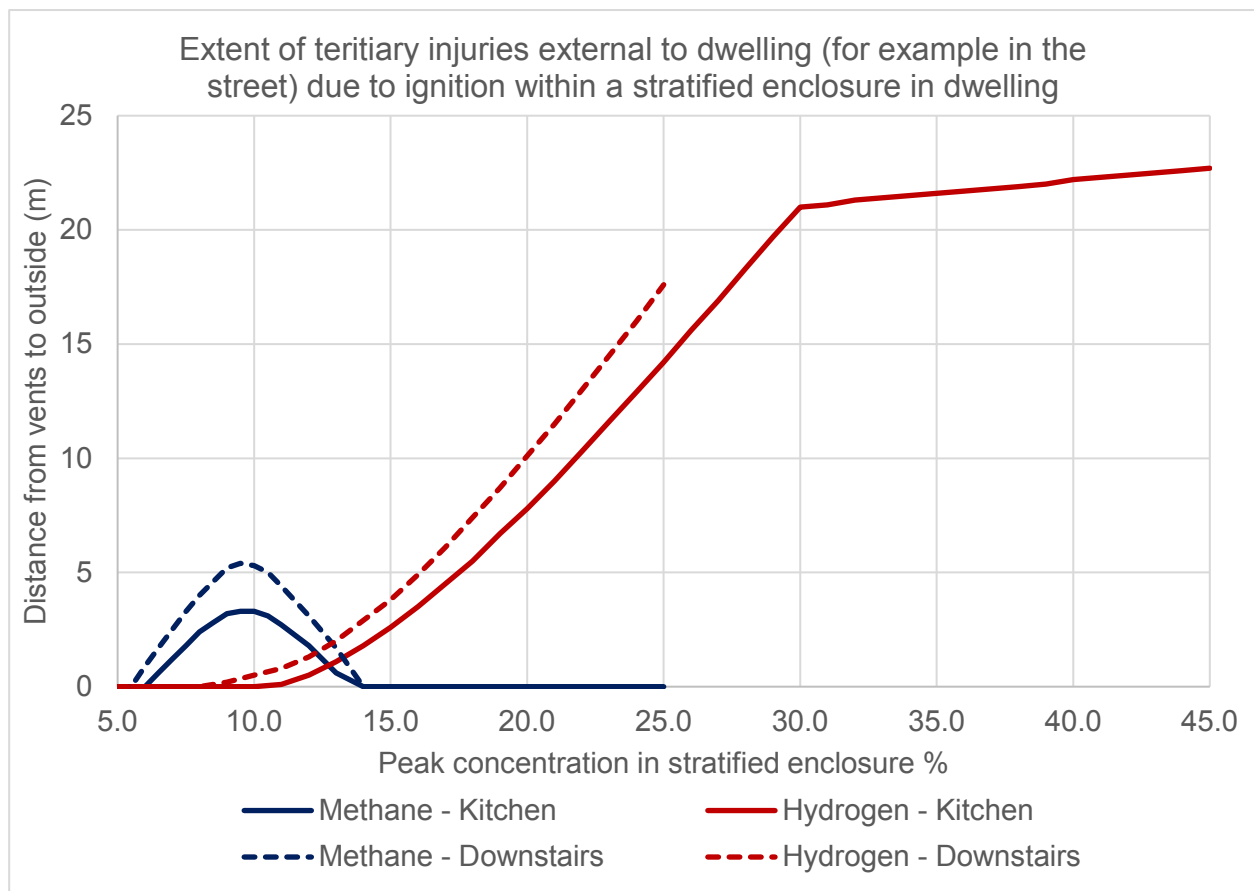


Figure 73: Extent of boundary from dwelling where tertiary injuries occur external to a dwelling
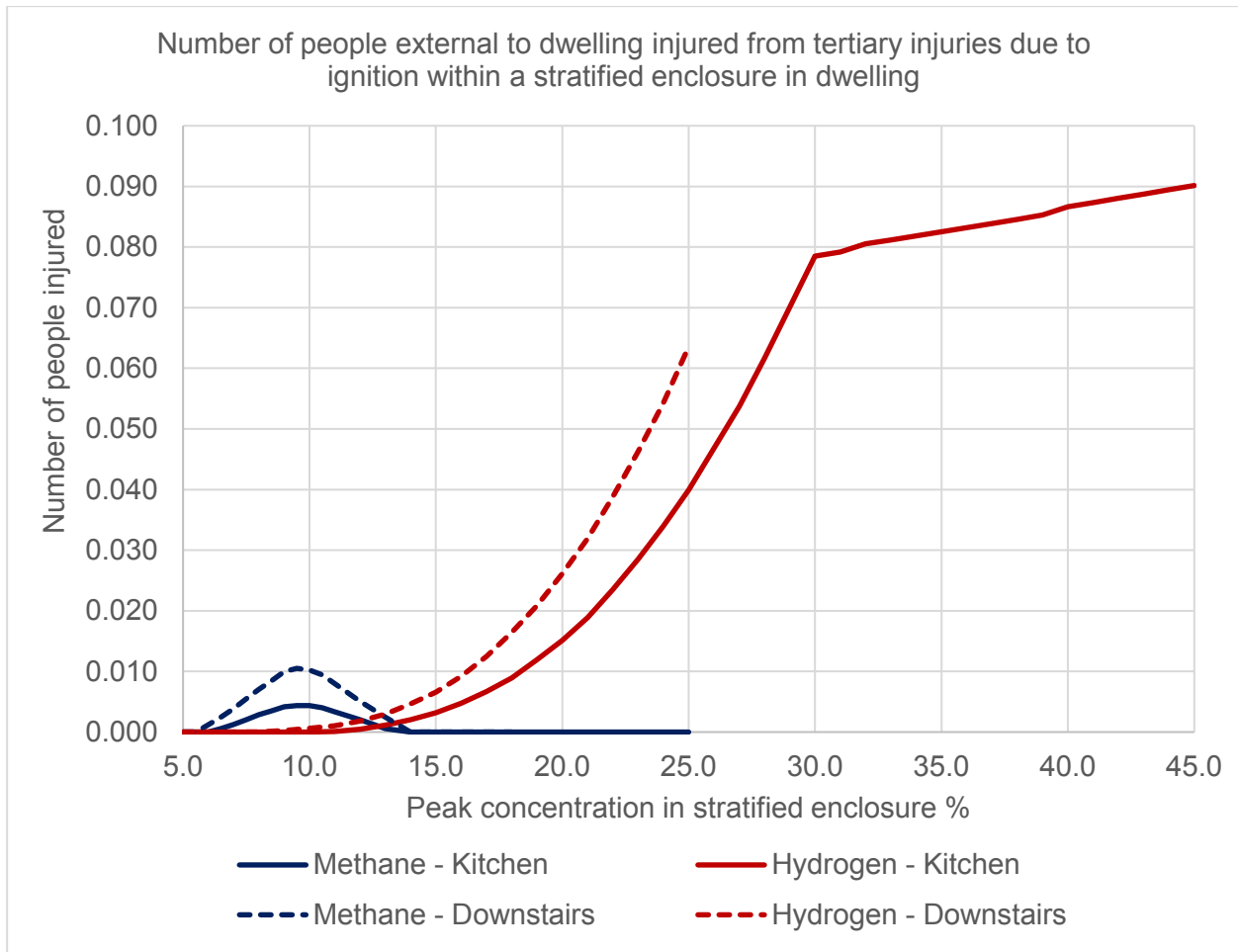
Figure 74: Number of people injured external to dwelling due to tertiary injuries

## 4.6 Injuries due to burns

The results for injuries incurred due to second degree burns from the modelling is presented in Figure 75 and Figure 76. Figure 75 indicates a comparison between methane and hydrogen of the number of people injured external to the property due to a deflagrative fireball being expelled through the external vents (windows and doors) of the dwelling. Although the number of injuries external to the dwelling are low, injuries due to burns from methane are higher than those for equivalent hydrogen concentrations. This is expected because the heat of combustion of methane in MJ (see Table 2) is approximately three times that of hydrogen increasing the duration of the flash fire and increasing the area over which second degree burns to the skin would occur external to the fireball. Additionally, the radiative fraction is lower for hydrogen also. The total number of injuries internally and externally is shown in Figure 76 for both the kitchen and downstairs of an open plan terraced house scenarios. It is evident from Figure 76 that injuries internal to the dwelling dominate the extent of injury from burns.

It is worth noting that for rich mixtures of methane above the stoichiometric concentration (approximately 9.5%), the number of injuries internal to the dwelling is conservatively underestimated. Although the combustion of a rich methane mixture in an enclosure will produce a low internal overpressure, the number of people injured due to burns inside a dwelling, such as a terraced house, would increase with concentration as the rich combusting methane flash fire would 'seek' out oxygen by spreading into other adjacent enclosures/rooms.
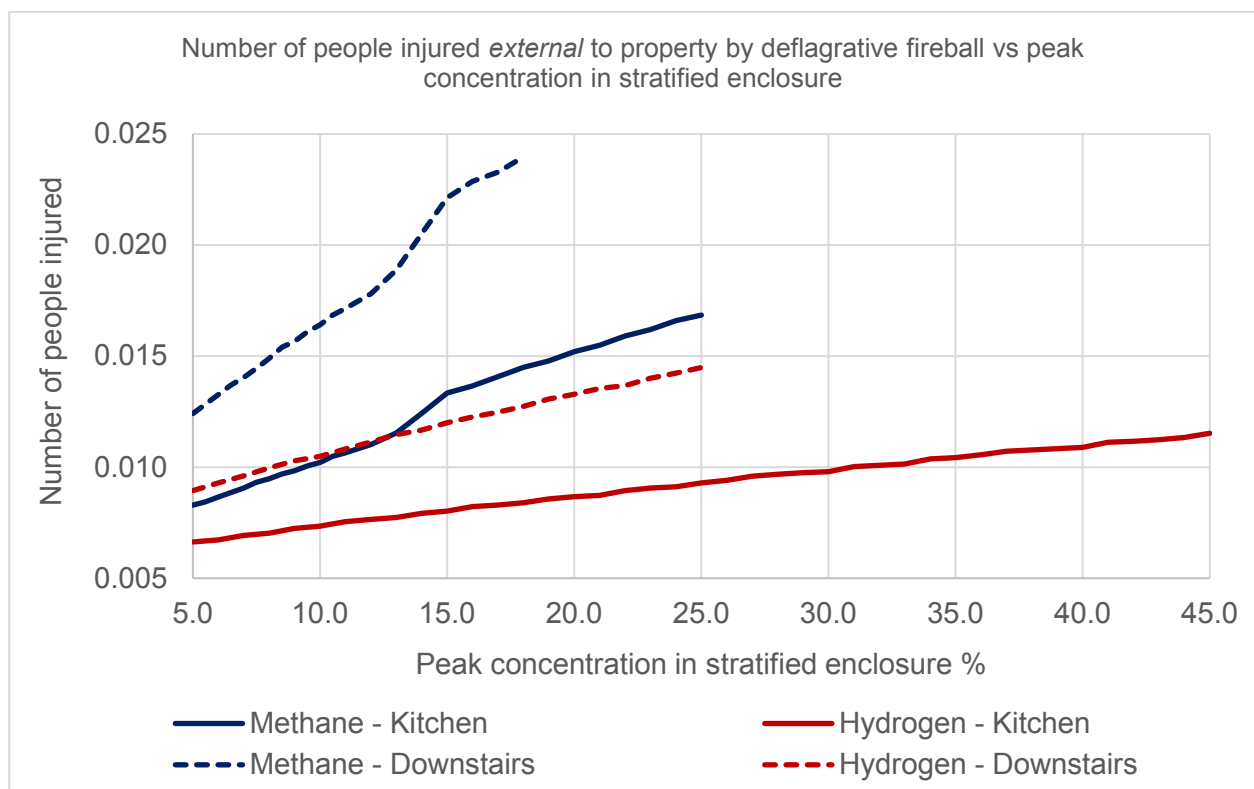


Figure 75: Number of people injured *external* to dwelling due to burns from fireball/flash fire
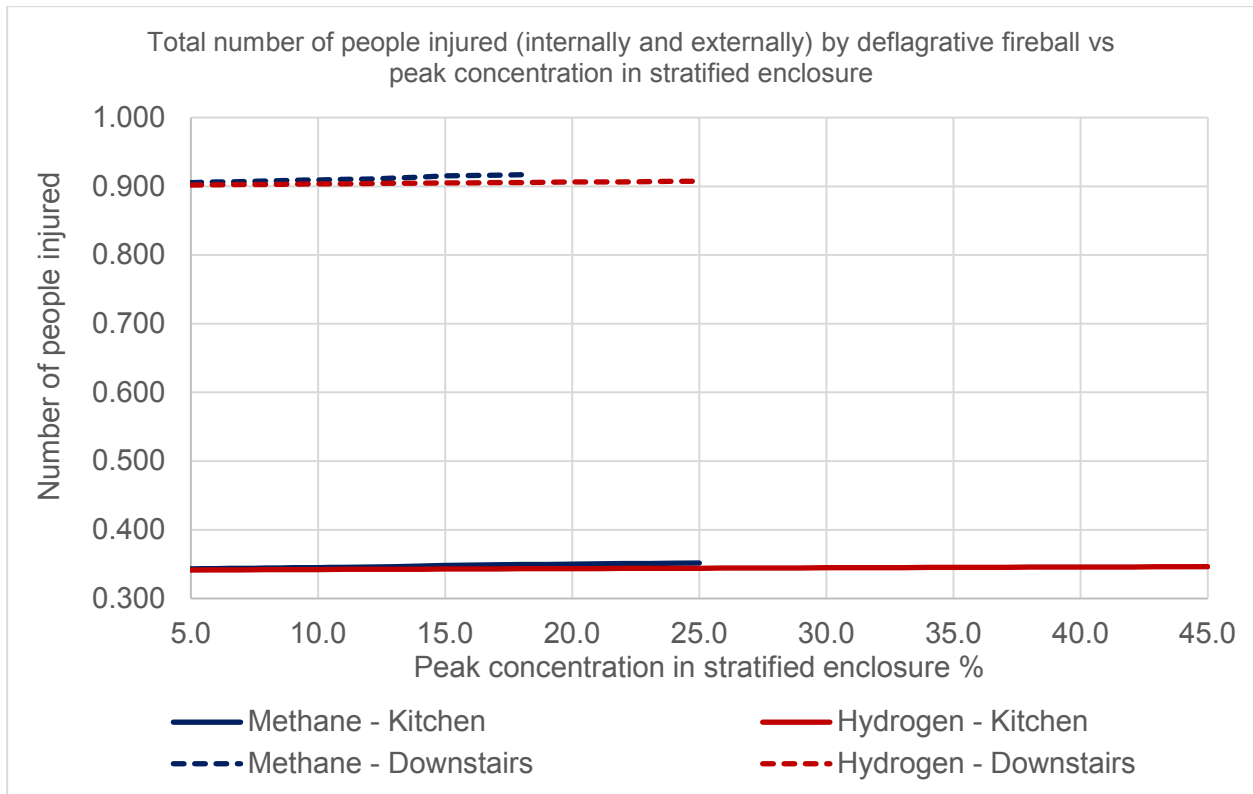
Figure 76: Total number of people injured external and *internal* to dwelling due to burns from fireball/flash fire

## 4.7    Total injury level

The results in the previous sub sections of Section 4 are combined to provide a total quantitative level of injury for the two different scenarios (kitchen and downstairs of an open plan terraced house scenario) considered in this assessment (see Section 3.2). Figure 77 give a representation of total injury level against peak concentration in a stratified confined methane or hydrogen cloud following ignition for both scenarios. Consideration as to the overlap of types of injuries using the methodology in Section 3.3.7 is included in these results.

Figure 77 shows that the total number of injuries is dominated by injuries to the dwelling occupants following structural collapse or impingement in a flash fire. The 'steps' in the curves in Figure 77 arise from the 'step-wise' increase in the number of load-bearing walls that have failed. This is expected because a load-bearing wall in the assessment either retains structural integrity or fails with no gradual transition between the two states. The level of external injuries (injuries in the street) increases more gradually with increasing peak concentration and this is dominated by secondary injuries arising from glass throw (see Figure 78).
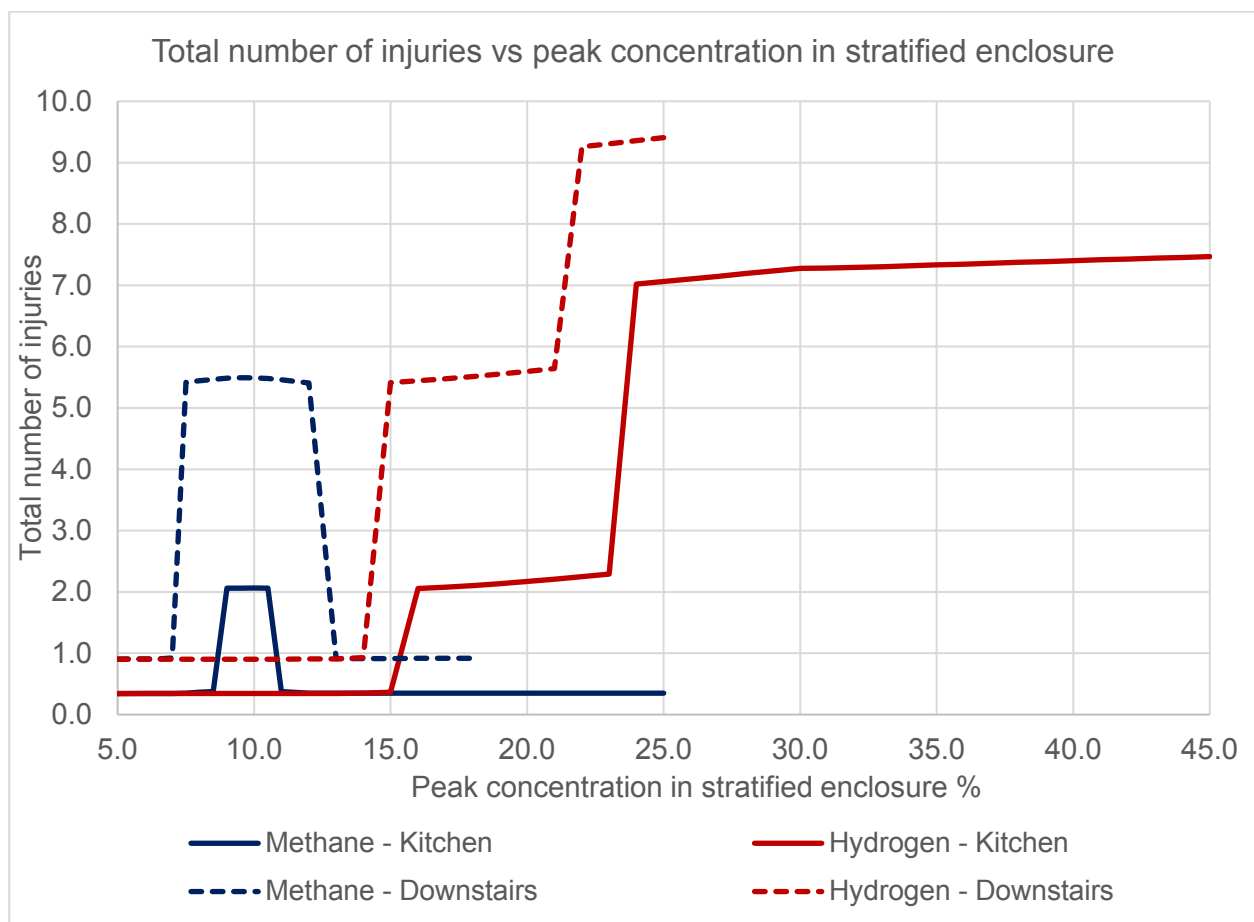


Figure 77: Quantitatively measuring total injury vs peak concentration
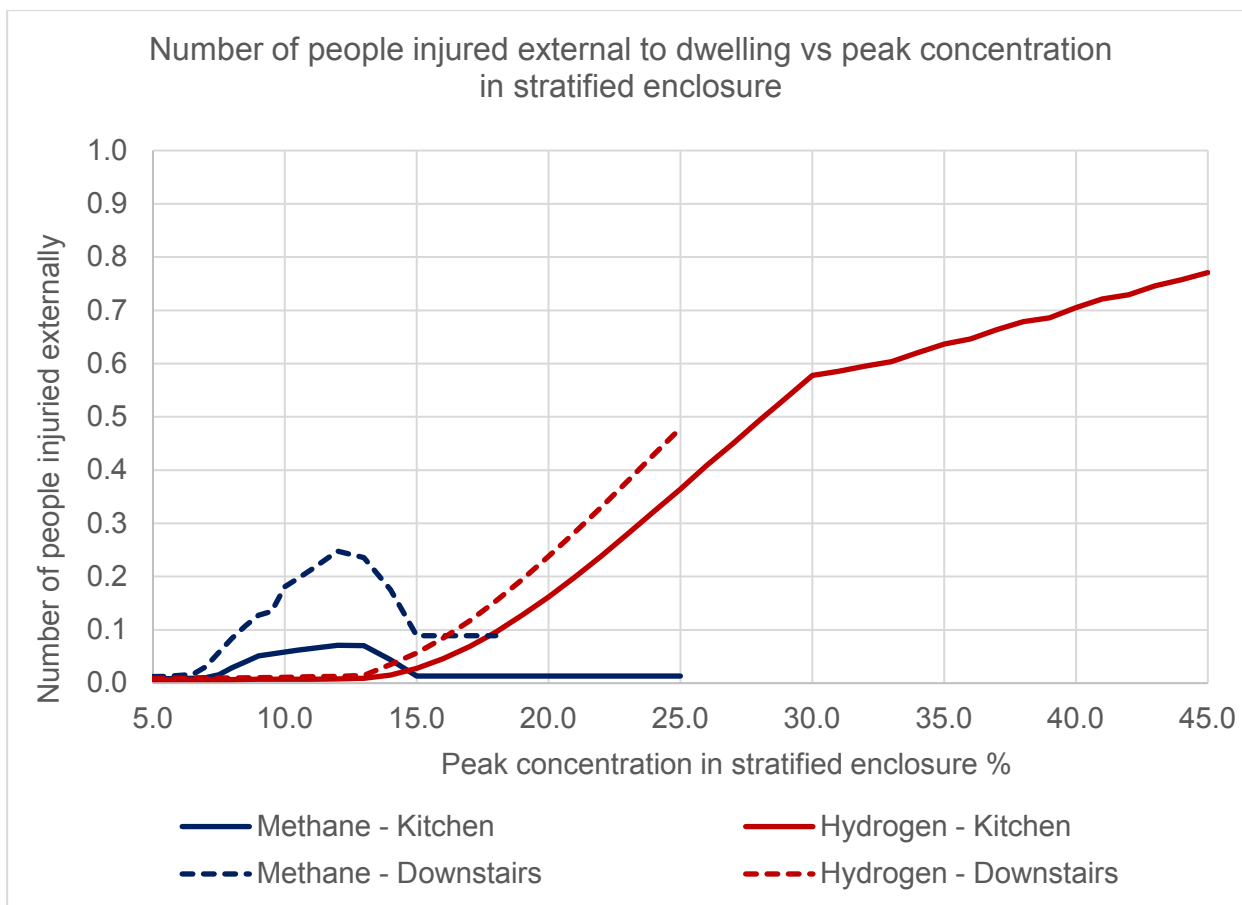
Figure 78: External injury vs peak concentration

# 5. Discussion and conclusions

The results indicate that the total quantity of people injured following a leak, dispersion and ignition event is dominated by internal dwelling occupants rather than people external to the dwelling in the public realm such as the street.

The results in Section 4 suggests that the level of injury and damage due to a leak dispersion, and ignition event in a domestic setting where the peak concentration of *hydrogen* up to approximately 15%, is similar to a leak dispersion, and ignition event in a domestic setting where the peak concentration of *methane* is up approximately 8.5%.

The results also suggest the level of injury and damage due to a leak dispersion, and ignition event in a domestic setting where the peak concentration range of *hydrogen* approximately between 15% and 22% is similar to a leak dispersion, and ignition event in a domestic setting where the peak concentration range of *methane* is between 8% to 12% for the downstairs of an open plan terraced house scenario, and between 9.0% and 10.5% *methane* for the kitchen case scenario.

Between a peak concentration range of 24% to 45% hydrogen in the kitchen scenario, the degree of structural damage and internal injuries is considerably greater than the worst case for methane. This is because the peak and average concentration of hydrogen in the enclosure is increasing towards the stoichiometric concentration for hydrogen. **It should be emphasised that above approximately 24% hydrogen concentration, the "simplified" model from [1] is highly conservative in predicting overpressure so prediction of consequences at these high concentrations of hydrogen is also conservative**

Above a peak concentration of 21% hydrogen in the downstairs of an open plan terraced house scenario, the degree of structural damage and internal injuries is considerably greater than the worst case for methane.

The external injuries dominated by glass throw continue to increase with increasing hydrogen concentration. Although only the level of injury from glass throw (based on glass throw distance) has been quantitatively estimated in this assessment for secondary injury, the results are an indicative comparison between the two gases of the expected radius of debris following a leak, dispersion and ignition event in a domestic dwelling.

The results in Section 4 will used in the Hy4Heat QRA and combined with probabilities to produce a quantitative assessment that considers both the risk (i.e. probability of a dispersion event at certain concentrations), and consequences of an ignition event to output a 'score' to make a comparison between the hydrogen and natural gas.

It is recognised that there are many limitations to the modelling undertaken here and that there are many simplifications of complex effects along with variation in input parameters that have a significant impact on the results. It is difficult to measure some input parameters and their variation without creating hundreds of iterations of models. For example, construction quality, dwelling floor plan, location of dwelling being assessed (quiet residential area or busy high street), levels of occupancy, behaviour of occupants and humans along with variation in their state of health, age etc. However, the assessment undertaken in this report does provide a means with which to compare hydrogen with methane when looking into the consequences of an ignition event following a leak in a domestic setting.

Department for Business, Energy & Industrial Strategy      Hy4Heat
ARP-WP7-GEN-REP-0003 | Issue 01 | 1 May 2021      Consequence Modelling Report

Page 103

# 6. Further work

Further work is recommended in the following areas:

- The dispersion experimental work undertaken at Spadeadam [24] was used to quantify how stratification could be conservatively considered in the consequence modelling. Only three measurements of concentration over the height of the enclosures in the dispersion experimental work were recorded [24]. Although useful, this is still a coarse picture of the extent to which methane and hydrogen stratifies. This experimental work is being repeated with a greater number of measurements for concentration being recorded over the height of enclosures to increase the resolution of understanding in stratification. It is also recognised that further work on modelling stratification is required and that there are several variations of the "equivalent volume" method that should be explored in further detail as per guidance in [25].

- The effect of vent cover resistance and inertia in a domestic setting when estimating overpressures and impulse. The "simplified" model [1] assumes that vent cover resistance and inertia is zero in the prediction of overpressures. Whilst the effect of vent cover resistance and inertia for high concentrations of hydrogen is less influential, for low to medium concentrations of hydrogen and all concentrations of methane, the effects can become significant. Work has already been undertaken to consider this in the modelling (see Section 3.4.3), but further refinement is recommended for quantitatively measuring consequences of ignition of confined flammable vapour clouds at lower concentrations for both hydrogen and methane in a domestic setting.

- At high concentrations of hydrogen (above approximately 24%) The "simplified" model from [1] is highly conservative in predicting overpressure. Additionally, the venting effects of any failing enclosure boundaries is neglected in the modelling when estimating internal enclosure overpressure and impulse. Although conservative, this overestimates the peak overpressures compared to what would be expected in practice, especially for high concentrations of hydrogen. Further work to incorporate this 'partial venting' effect is recommended to further refine the results in this assessment.

- The assessment has been undertaken for two scenarios following a leak, dispersion and ignition events in the downstairs of a terraced house. Further work should be undertaken to apply the assessment to other housing topologies such as blocks of flats and apartments. Additionally, further work could be undertaken to increase the granularity of the assessment, for example, by breaking up the binary threshold of "person injured"/"person not injured" into a graded criteria with differing thresholds.

- When considering injuries due to burns internal to a dwelling, the assessment not only assumes that level of injury due to impingement in a combusting methane or hydrogen cloud does not vary with concentration (see Sections 3.3.6 and 4.6), but it also assumes that only occupants of the enclosure (such as the kitchen) where the leak, dispersion and ignition event occurs are injured. In practice, a deflagration or flash fire that does not cause structural collapse, could injure occupants in adjacent enclosures or rooms in a dwelling as unburnt flammable gas spreads throughout the dwelling. This is particularly the case for rich mixtures of methane above the stoichiometric concentration (approximately 9.5%). It is suggested that further work is undertaken to better understand how injury due to impingement in combusting methane and hydrogen clouds increases with concentration, and understand the effects on an ignition event for multiple enclosures that are interconnected by doors.

# References

[1] A. Sinha, V. C. M. Rao and J. X. Wen, "A simple model for calculating peak pressure in vented explosions of hydrogen and hydrocarbons," *International Journal of Hydrogen Energy,* 25th February 2019.

[2] Center for Chemical Process Safety, *Guidelines for Evaluating the Characteristics of Vapor Cloud Explosions, Flash Fires, and BLEVEs,* American Institute of Chemical Engineers.

[3] Carbon Brief Ltd, "whats-the-difference-between-natural-gas-liquid-natural-gas-shale-gas-shale-oil-and-methane-an-oil-and-gas-glossary," 2015. [Online]. Available: https://www.carbonbrief.org/whats-the-difference-between-natural-gas-liquid-natural-gas-shale-gas-shale-oil-and-methane-an-oil-and-gas-glossary. [Accessed 10th July 2019].

[4] Society of Fire Protection Engineers, SFPE Handbook of Fire Protection Engineering, 3rd ed., National Fire Protection Association, 2002.

[5] B. Lewis and G. von Elbe, Combustion, Flames and Explosions of Gases, 3rd Edition ed., Harcourt Brace Jovanovich Publishers (United Kingdom Edition by Academic Press), 1987.

[6] L. G. Britton, Avoiding Static Ignition Hazards in Chemical Operations: A CCPS Concept Book, 1999 American Institute of Chemical Engineers, 1999.

[7] Society of Fire Protection Engineers, SFPE Handbook of Fire Protection Engineering - 5th Edition, 5th ed., Society of Fire Protection Engineers, 2016.

[8] M. J. Hurley, SFPE Handbook of Fire Protection Engineering, 5th ed., Springer, 2016.

[9] D. Cormie, Blast effects on buildings, 2nd ed., London: Thomas Telford, 2009.

[10] C. J. M. Van Wingerden and J. P. Zeeuwen, "Flame propagation in the presence of repeated obstacles: influence of gas reactivity and degree of confinement," 1983.

[11] A. J. Pierorazio, K. J. Thomas, Q. A. Baker and D. E. Ketchum, An update to the Baker-Strehlow-Tang vapor cloud explosion prediction methodology flame speed table, Wiley InterScience, 2005.

[12] A. Sinha, V. C. M. Rao and J. X. Wen, "Performance evaluation of empirical models for vented lean hydrogen explosions," *International Journal of Hydrogen Energy 44 (2019),* no. 44, p. 8711 to 8726, 11th September 2018.

[13] S. Zhang and Q. Zhang, "Effect of vent size on vented hydrogen-air explosion," *International Journal of Hydrogen Energy 43 (2018),* vol. 43, p. 17788 to 17799, 30th July 2018.

[14] Unified Facilities Criteria (UFC), *UFC 3-340-02 Structures to Resist the Effects of Accidental Explosions 2014 UPDATE,* United States of America Department of Defense, 2014.

[15] Department of Energy & Climate Change, "Statistical Release: Experimental Statistics - Estimates of Home Insulation Levels in Great Britain: April 2013," Department of Energy & Climate Change, London, 2013.

[16] Wiki, Designing Building, "Cavity Wall," Designing Buildings Wiki, 8th May 2019. [Online]. Available: https://www.designingbuildings.co.uk/wiki/Cavity_wall. [Accessed 9th July 2019].

[17] Publicatiereeks Gevaarlijke Stoffen 2, Methods for the calculation of physical effects 'Yellow Book', 3rd (revised print) ed., R. W. C.J.H. van den Bosch, Ed., The Hague: Publicatiereeks Gevaarlijke Stoffen 2, 2005.

[18] B. Lewis, Combustion, Flames and Explosions of Gases, Academic Press Inc;, 1961, p. 731.

[19] Unified Facilities Criteria (UFC), *UFC 3-340-02 Structures to Resist the Effects of Accidental Explosions,* United States of America Department of Defense, 2008.

[20] Trimble Inc., "Terraced house," Sketch up 3D warehouse, 9th July 2016. [Online]. Available: https://3dwarehouse.sketchup.com/model/79f2baf2-4f86-453f-9e76-290deada817b/Terraced-house?hl=en. [Accessed 10th July 2019].

[21] British Broadcasting Corporation (BBC), "Fifteen people injured in Salford gas explosion," British Broadcasting Corporation (BBC), 2nd November 2010. [Online]. Available: https://www.bbc.co.uk/news/uk-england-11671916. [Accessed 3rd April 2020].

[22] British Broadcasting Corporation (BBC), "Haxby house 'gas blast': Man, 63, dies," British Broadcasting Corporation (BBC), 19th February 2016. [Online]. Available: https://www.bbc.co.uk/news/uk-england-york-north-yorkshire-35610607. [Accessed 3rd April 2020].

[23] Arup, "Hy4heat dispersion modelling report," Arup+, London, 2020.

[24] DNV GL, "HY4HEAT WP7 LOT3 Property Level Leakage and Accumulation Data Report - Revision 1," GL Industrial Services UK Ltd, Brampton, 2020.

[25] J. Stewart and S. Gant, "A Review of the Q9 Equivalent Cloud Method for Explosion Modelling," *FABIG Technical Newsletter,* no. 75, p. 16 to 24, March 2019.

[26] Office for National Statistics, "Families and Households: 2017," Office for National Statistics, 8th November 2017. [Online]. Available: https://www.ons.gov.uk/peoplepopulationandcommunity/birthsdeathsandmarriages/families/bulletins/familiesandhouseholds/2017. [Accessed 15th August 2019].

[27] British Broadcasting Corporation (BBC), "Statistics reveal Britain's 'Mr and Mrs Average'," British Broadcasting Corporation (BBC), 13th October 2010. [Online]. Available: https://www.bbc.co.uk/news/uk-11534042. [Accessed 16th July 2019].

[28] Kiwa, "Gas Ignition and Explosion Assessment," Hy4heat, 2020.

[29] eglitis-media, "Average sizes of men and women," [Online]. Available: https://www.worlddata.info/average-bodyheight.php. [Accessed 10th August 2019].

[30] Reference.com, "What Is the Average Size of the Human Head?," Reference.com, [Online]. Available: https://www.reference.com/science/average-size-human-head-62364d028e431bf3. [Accessed 10th September 2019].

[31] British Standards Institute, *EN 14994: 2007 Gas explosion venting protective systems,* London: British Standards Institute, 2007.

[32] National Fire Protection Association, *NFPA 68. Standard on explosion protection by deflagration venting,* National Fire Protection Association, 2013.

[33] C. R. Bauwens, J. Chao and S. B. Dorofeev, "Effect of hydrogen concentration on vented explosion overpressures from lean hydrogen–air deflagrations," *International Journal of Hydrogen Energy Volume 37, Issue 22,* vol. 37, no. 22, p. 17599 to 17605, 2012.

[34] V. Molkov and M. Bragin, "Hydrogen–air deflagrations: Vent sizing correlation for low-strength equipment and buildings," *International Journal of Hydrogen Energy,* vol. 40, no. 2, p. 1256 to 1266, 2015.

[35] A. Sinha, V. C. M. Rao and J. X. Wen, "Modular phenomenological model for vented explosions and its validation with experimental and computational results," *Journal of Loss Prevention in the Process Industries,* vol. 61, p. 8 to 23, 2019.

[36] V. V. Molkov, "Explosions in buildings: modeling and interpretation of real accidents," *Fire Safety Journal 1999,* vol. 33, p. 45 to 56, 10th September 1998.

[37] Oasys Limited, *Oasys ERGO,* London, 2015.

[38] V. Molkov, R. Dobashi, M. Suzuki and T. Hirano, "Modeling of vented hydrogen-air deflagrations and correlations for vent sizing," *Journal of Loss Prevention in the Process Industries,* vol. 12, p. 147 to 156, 1999.

[39] T. Skjold, H. Hisken, S. Lakshmipathy, G. Atanga, L. Bernard, M. van Wingerden, K. L. Olsen, M. N. Holme, N. M. Turøy, M. Mykleby and K. van Wingerden, "Vented hydrogen deflagrations in containers: Effect of congestion for homogeneous and inhomogeneous mixtures," *International Journal of Hydrogen Energy,* vol. 44, no. 1st, p. 8819 to 8832, 1st October 2018.

[40] Daily Mail, "Terrifying moment that huge 'gas' explosion destroys house and leaves man, 55, injured, as witnesses describe 'whole street shaking'," Associated Newspapers Ltd, 31st March 2020. [Online]. Available: https://www.dailymail.co.uk/news/article-8172089/Huge-gas-explosion-destroys-house-leaves-man-injured-witnesses-street-shaking.html. [Accessed 6th May 2020].

[41] S. Anubhav, *Email corrospondence - Subject: "Overpressures at high concentrations - simplified model",* 2020.

[42] R. C. Bauwens, J. M. Bergthorson and S. B. Dorofeev, "Critical Peclet Numbers for the Onset of Darrieus-Landau Instability in Atmospheric-Pressure Methane-Air Flames," in *25th International Colloquium on the Dynamics of Explosions and Reactive Systems (ICDERS)*, Leeds, 2015.

[43] Engineering ToolBox, "Drag Coefficient," Engineering ToolBox, 2004. [Online]. Available: https://www.engineeringtoolbox.com/drag-coefficient-d_627.html. [Accessed 12th December 2019].

[44] Health and Safety Executive, "SAFETY REPORT ASSESSMENT GUIDE: HIGHLY FLAMMABLE LIQUIDS (HFL)," *Safety Report Assessment Guide: Highly flammable liquids - Criteria.*

# Appendices

## Appendix A – Modelling stratification

### *A.1 - Further detail on modelling stratification*

As discussed in Section 3.2.3, the experiments undertaken by DNV GL [24] at their "Hystreet" Spadedam testing site were analysed to gauge an understanding of the stratification that occurs within a confined flammable vapour cloud in an enclosure of a typical terraced house following a gas leak. A summary of the findings is already provided in Section 3.2.3.

The concept of the "equivalent volume" in providing a 'conservative best estimate' input to the "simplified" model, which in turn is used to estimate internal explosion overpressure, is based on the selected experimental work undertaken by DNV GL [24] shown in Table 9 for methane, and Table 10 for hydrogen. The aim is to get a 'conservative best estimate' by modelling an "equivalent volume" of an enclosure with a homogeneous confined methane or hydrogen cloud at the peak concentration (i.e. the concentration at the ceiling level)

With the exception of experimental lot DNVL2-021, Table 9 shows that the "ratio of concentrations at mid-height and floor height in relation to concentration at ceiling height" for a selection of *methane* dispersion experiments undertaken in the kitchen of the "Hystreet" test houses, are roughly similar. The "average of ratios" in the last column is an average of the three constituents of the ratio in the second to last column. For example, for DNVL2-022, the "average of ratios" is (1.0 + 0.84 + 0.53) / 3 = 0.79. This means that for an enclosure that has an inhomogeneous confined flammable vapour cloud with three different 'bands' over the enclosure height of $h$ representing the concentrations of 5.0% at floor, 8.0% at mid height, and 9.5% ceiling level, could be represented by an enclosure with an "equivalent" height of $0.79h$ with a homogeneous concentration of 9.5%. See Figure 79 for further clarity on this example. An overall constant "equivalent height factor" of 0.8 has been used throughout the modelling in this assessment for methane.

Table 10 shows that the "ratio of concentrations at mid-height and floor height in relation to concentration at ceiling height" for a selection of *hydrogen* dispersion experiments undertaken in the kitchen of the "Hystreet" test houses, are also roughly similar. An overall constant "equivalent height factor" of 0.67 has been used throughout the modelling in this assessment for hydrogen.

Table 9: Selected experimental data from DNV GL [24] used to estimate an 'equivalent volume' for methane

| Experimental lot from [24] (methane) | Measured % concentration at ceiling level | Measured % concentration at mid height in enclosure | Measured % concentration at floor level | Ratio of concentrations of mid-height and floor height in relation to concentration at ceiling height Ceiling : mid-height : floor | Average of the ratios (or "equivalent height factor") |
|---|---|---|---|---|---|
| DNVL2-020 | 2.6 | 2.2 | 1.2 | 1 : 0.85 : 0.46 | 0.77 |
| DNVL2-021 | 4.7 | 2.4 | 0.4 | 1 : 0.51 : 0.09 | 0.53 |
| DNVL2-022 | 9.5 | 8.0 | 5.0 | 1 : 0.84 :0.53 | 0.79 |
| DNVL2-023 | 17.7 | 14.4 | 10.3 | 1 : 0.81 :0.58 | 0.80 |
| DNVL2-024 | 25.6 | 21.4 | 14.8 | 1 : 0.84 :0.58 | 0.80 |

Table 10: Selected experimental data from DNV GL [24] used to estimate an 'equivalent volume' for hydrogen

| Experimental lot from [24] (hydrogen) | Measured % concentration at ceiling level | Measured % concentration at mid height in enclosure | Measured % concentration at floor level | Ratio of concentrations of mid-height and floor height in relation to concentration at ceiling height Ceiling : mid-height : floor | Average of the ratios (or "equivalent height factor") |
|---|---|---|---|---|---|
| DNVL2-062 | 10.8 | 9.5 | 1.8 | 1 : 0.88 : 0.17 | 0.68 |
| DNVL2-063 | 22.0 | 20.0 | 2.5 | 1 : 0.91 : 0.11 | 0.67 |
| DNVL2-064 | 32.2 | 30.1 | 2.6 | 1 : 0.94 : 0.08 | 0.67 |
| DNVL2-062A | 6.2 | 5.1 | 0.5 | 1 : 0.82 : 0.08 | 0.63 |
| DNVL2-063A | 14.3 | 12.0 | 1.4 | 1 : 0.84 : 0.10 | 0.65 |
| DNVL2-064A | 20.2 | 17.0 | 1.1 | 1 : 0.84 : 0.05 | 0.63 |
| DNVL2-064B | 19.9 | 18.5 | 2.5 | 1 : 0.93 : 0.13 | 0.69 |
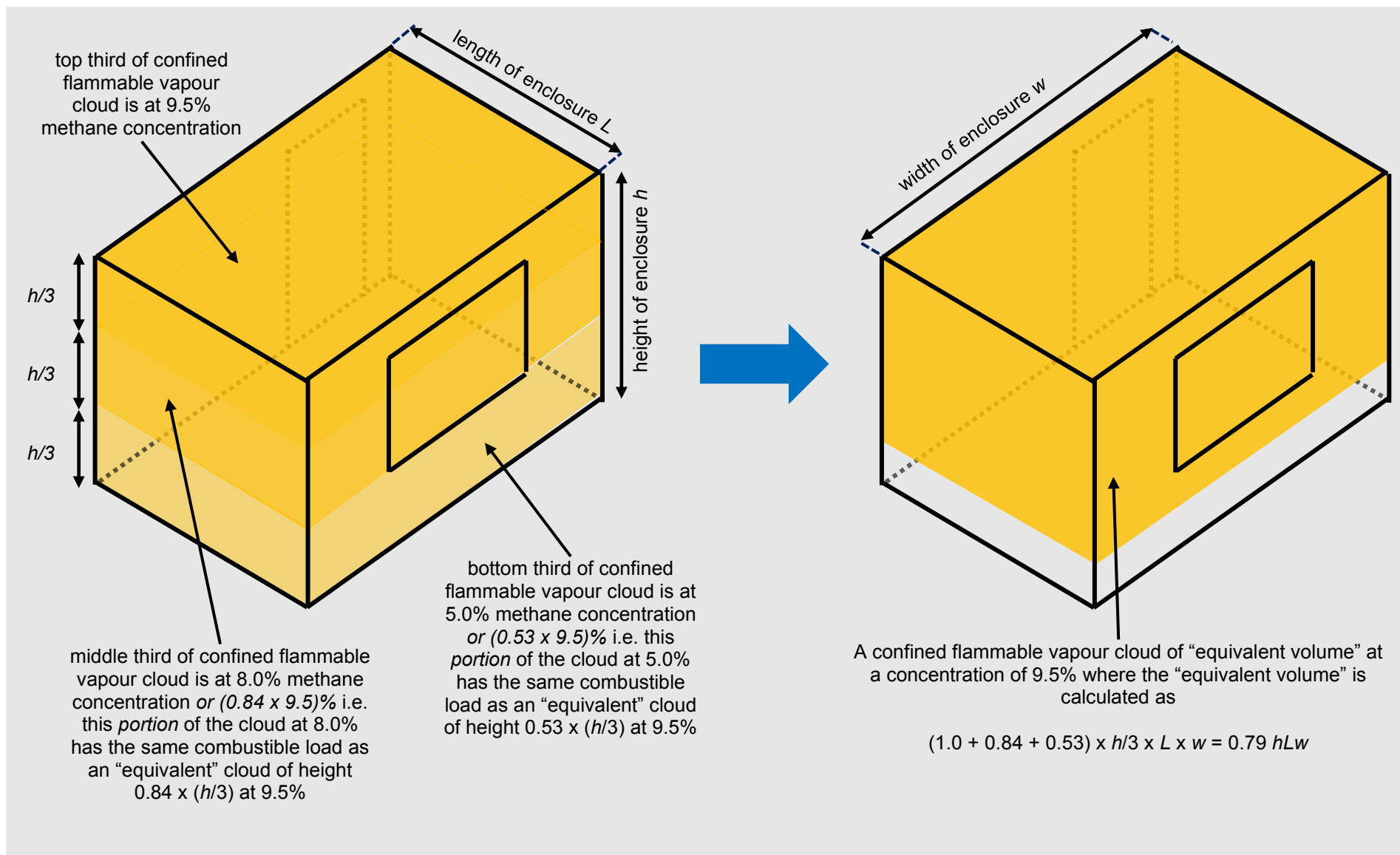
Figure 79: Worked example of estimating "equivalent volume" based on concentration levels over height for experimental lot DNVL2-022 from [24]

Using the same methodology as used in the example in Figure 77, the "equivalent volume" of the cloud at a homogeneous concentration of 32.2% hydrogen is $0.67hLw$

Although the concentration of this "equivalent" cloud is above the stoichiometric for hydrogen, there is enough oxygen in the enclosure for an efficient combustion to occur. To be conservative, the volume of the cloud should then be further equated to a confined cloud at stoichiometric concentration.

The *"Equivalent height factor" at stoichiometric concentration* is calculated as

$$(32.2 / 29.5) \times 0.67 = 0.73$$

Where 29.5 is the stoichiometric concentration of hydrogen.

Figure 80: Worked example of calculating *"Equivalent height factor" at stoichiometric concentration* for experimental lot DNVL2-064 from [24]

## A.2 – Comparison with the Q9 method

A sensitivity check on the approach used to estimate "equivalent volume" in Section 3.2.3 has been made by comparing the "equivalent volumes" used in this assessment with "equivalent volumes" estimated using the Q9 Equivalent Cloud metric method [25].

The Q9 Equivalent Cloud metric method is a means by which an inhomogeneous flammable vapour cloud can be estimated as an equivalent homogenous volume using the "burning velocity weighted volume" [25]:

$$V_{Q9} = \frac{1}{(SE)_{max}} \sum_{i=1}^{n} (fuel_{vol} \times S \times E)_i$$

Here, $V_{Q9}$ is the equivalent "burning velocity weighted volume" in m$^3$, $S$ is the laminar burning velocity that varies with concentration, $E$ is the expansion ratio that also varies with concentration, and $fuel_{vol}$ are the individual discretised volumes in the stratified or inhomogeneous cloud making up the total cloud volume for which the each has its own associated value of $S$ and $E$. The Q9 Equivalent Cloud metric method is usually used in Computational Fluid Dynamic (CFD) modelling of vapour cloud explosions where the "discretised volumes" represent the individual cells in the CFD model. In this sensitivity study, the total enclosure in this assessment is split into three discretised regions over the height of the enclosure in question (the kitchen or the downstairs of the downstairs of an open plan terraced house). The concentrations of these three discretised regions are based upon the concentration at ceiling, mid height and floor level in the enclosure (as indicated in Figure 28 and Figure 29 in Section 3.2.3).

Figure 81 shows a comparison between the "equivalent height" (which is directly proportional to the "equivalent volume") used for both gases to determine the results in Section 4, and the variation in "equivalent height with concentration for both gases using the Q9 Equivalent Cloud metric method from [25]. Although Figure 81 shows that the equivalent volume does vary with concentration, Figure 82 and Figure 83 indicate that the method used to model "equivalent height" and stratification in this assessment slightly overpredicts peak internal overpressure for both methane and hydrogen when compared to using the Q9 Equivalent Cloud metric method to model "equivalent height" and stratification.

As mentioned in [25], evidence that "equivalent stoichiometric cloud methods" such as the "Q9 method" are suitable and conservative is mixed but the results of this sensitivity study show that peak overpressure is more sensitive to the parameters of concentration and vent area to volume ratio ($K_v$) than "equivalent height" and volume.

Department for Business, Energy & Industrial Strategy                    Hy4Heat
ARP-WP7-GEN-REP-0003 | Issue 01 | 1 May 2021                    Consequence Modelling Report

Page 112
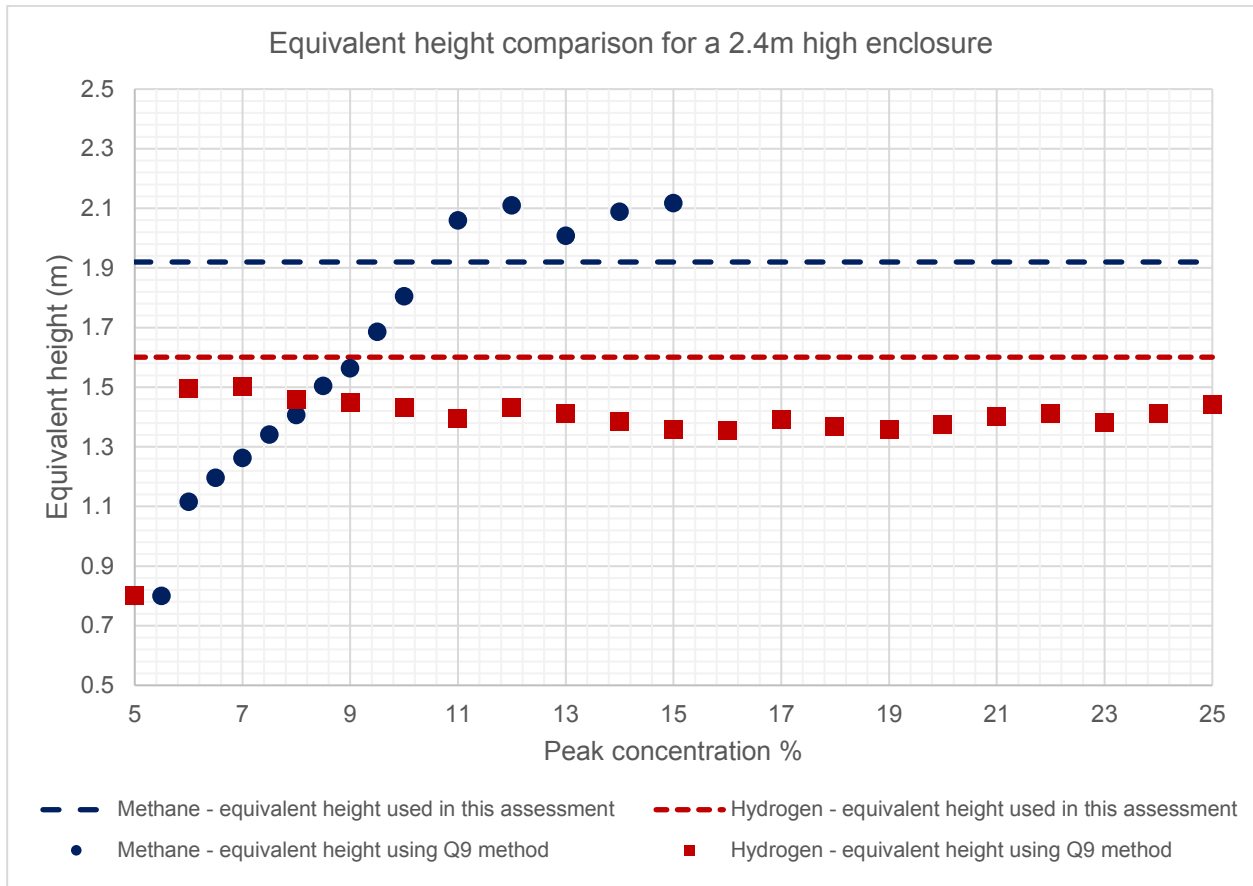
Figure 81: Comparison of equivalent height (or equivalent volume) using Q9 method
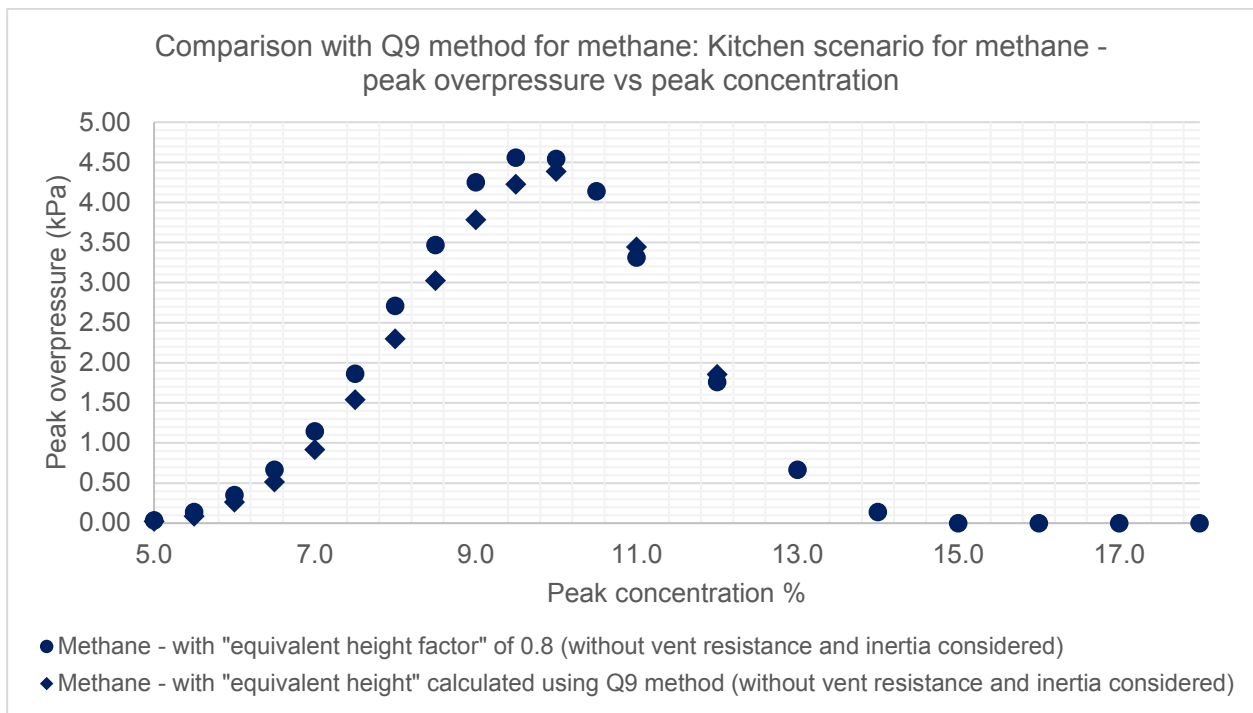


Figure 82: Comparison of equivalent height (or equivalent volume) using Q9 method for methane
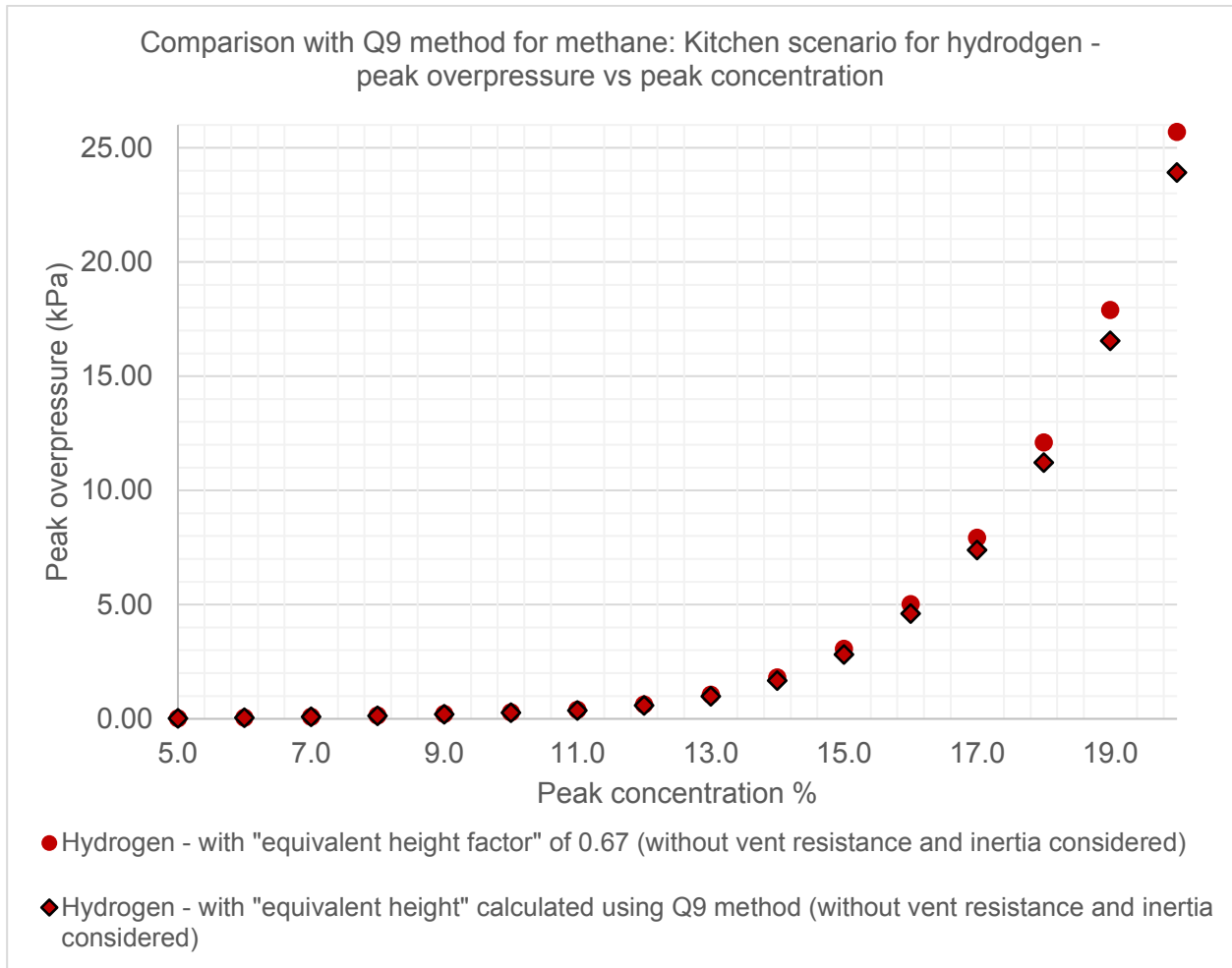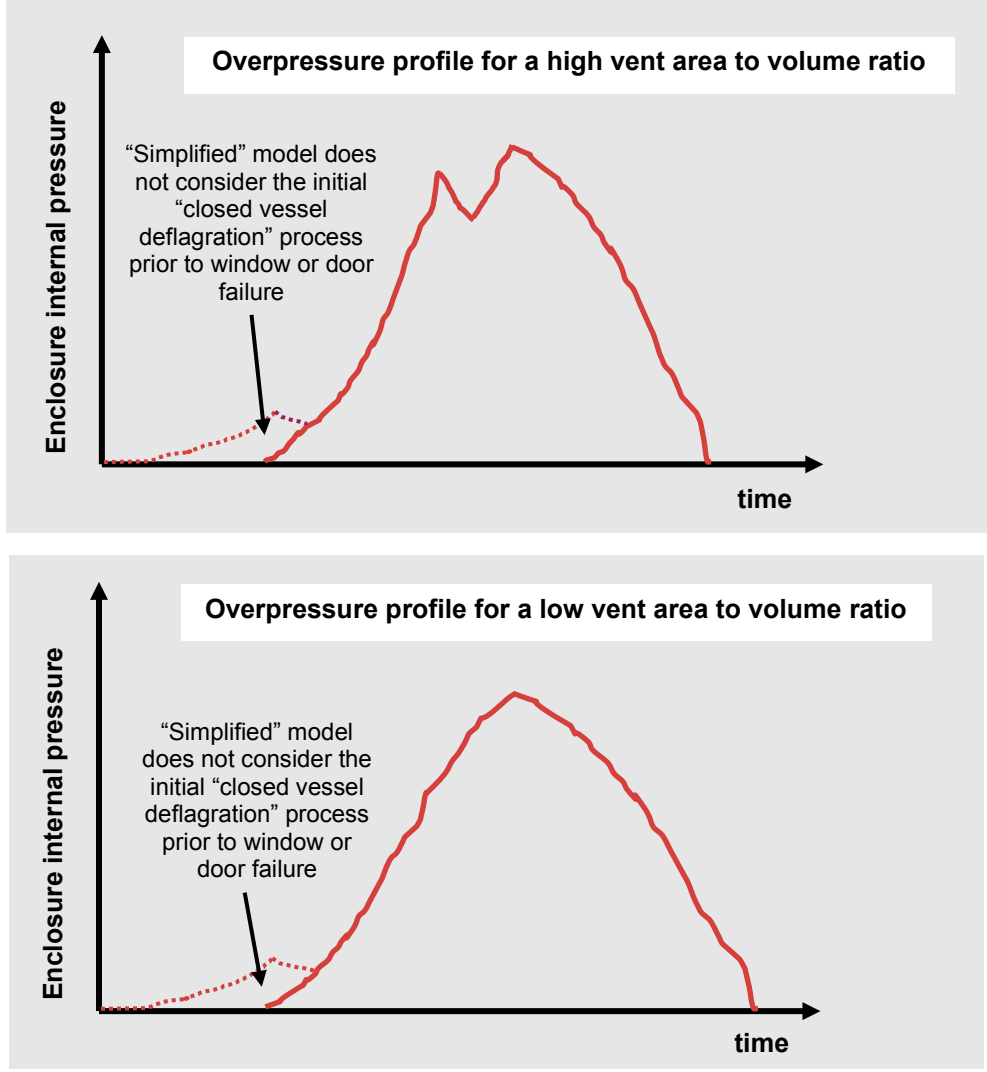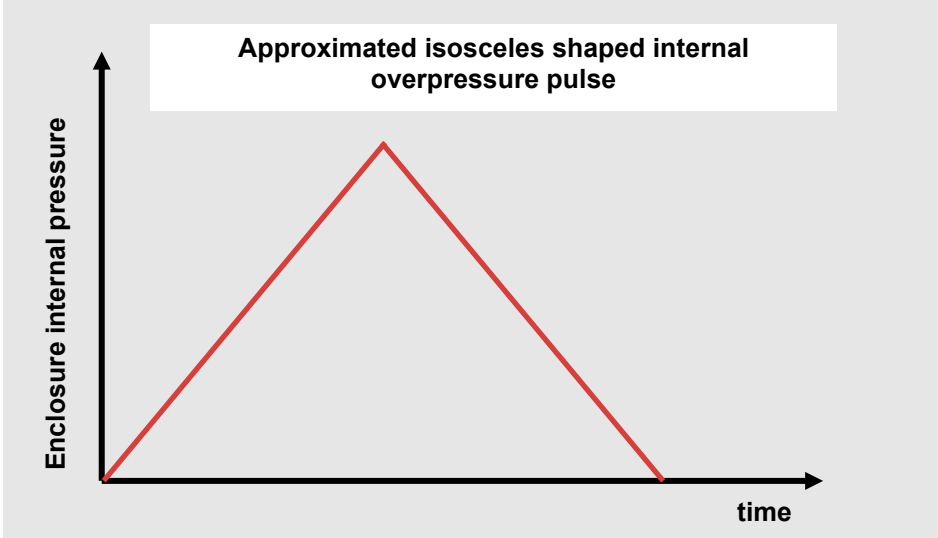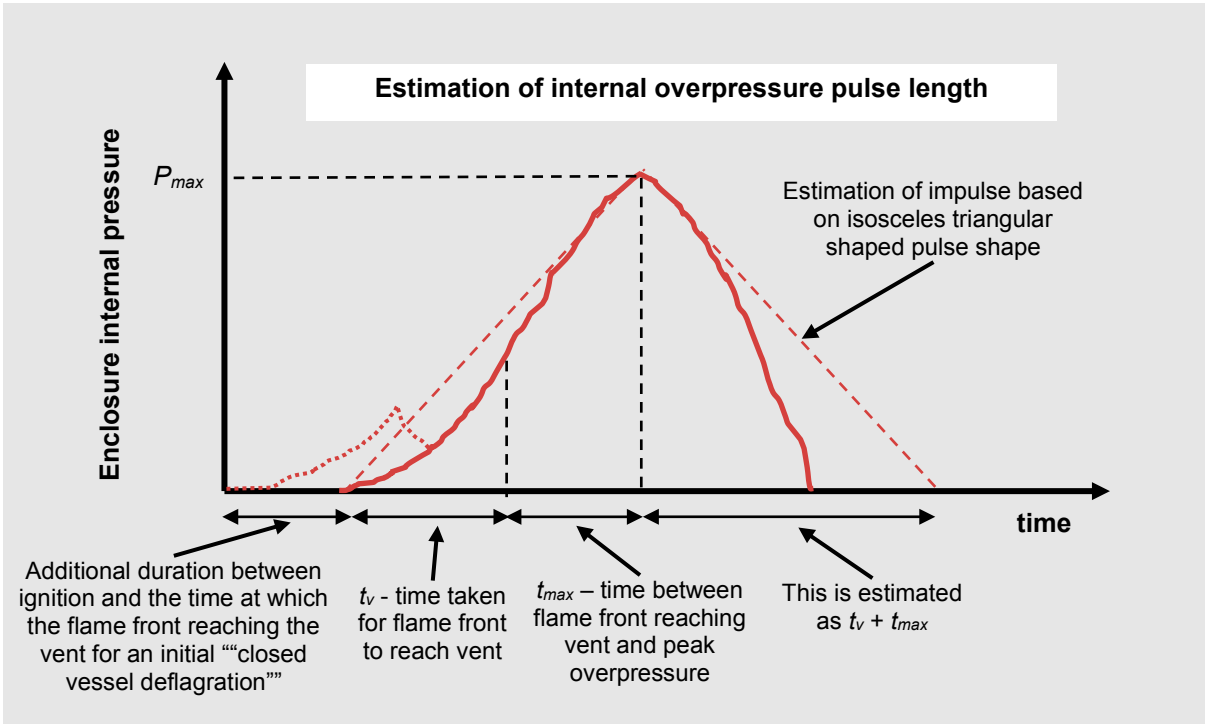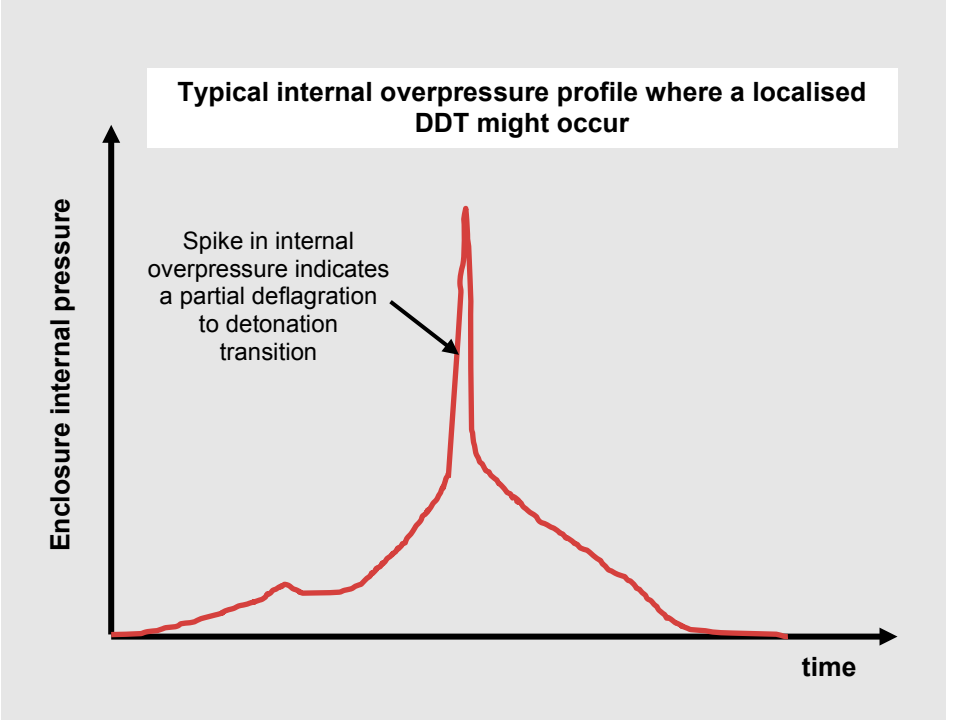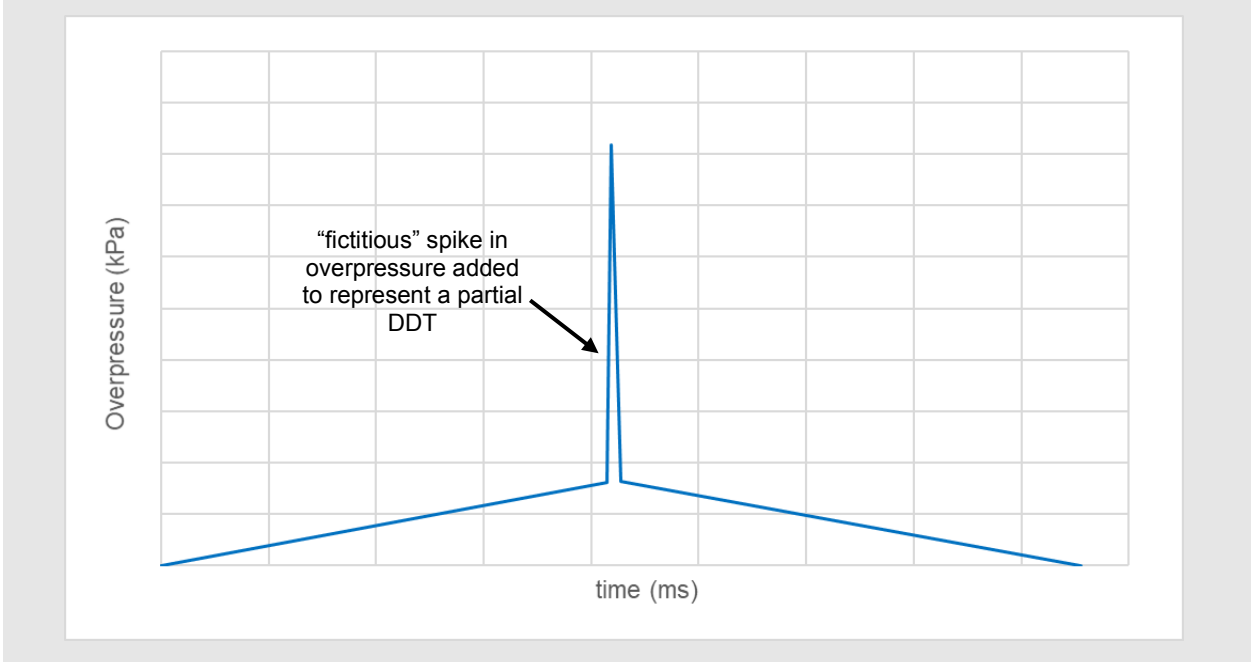
Figure 83: Comparison of equivalent height (or equivalent volume) using Q9 method for hydrogen
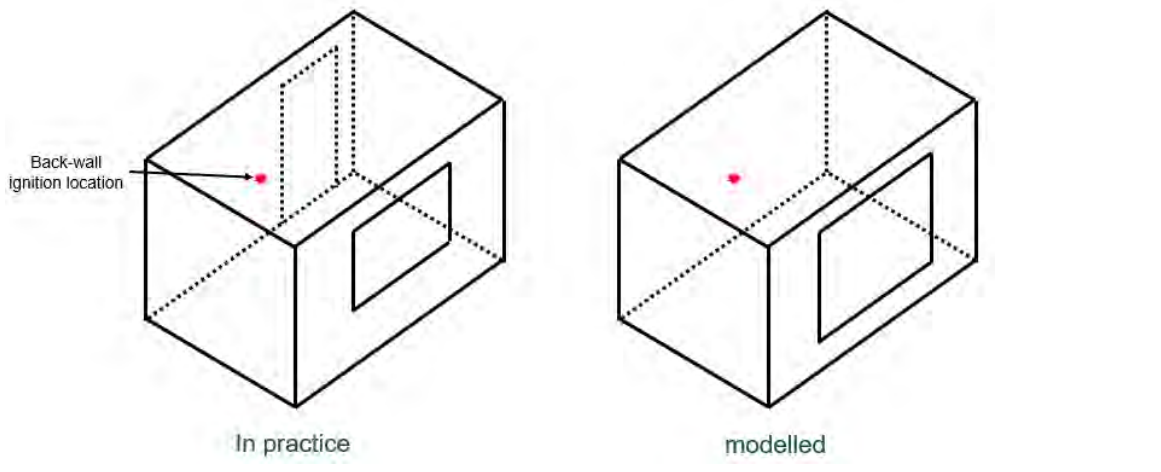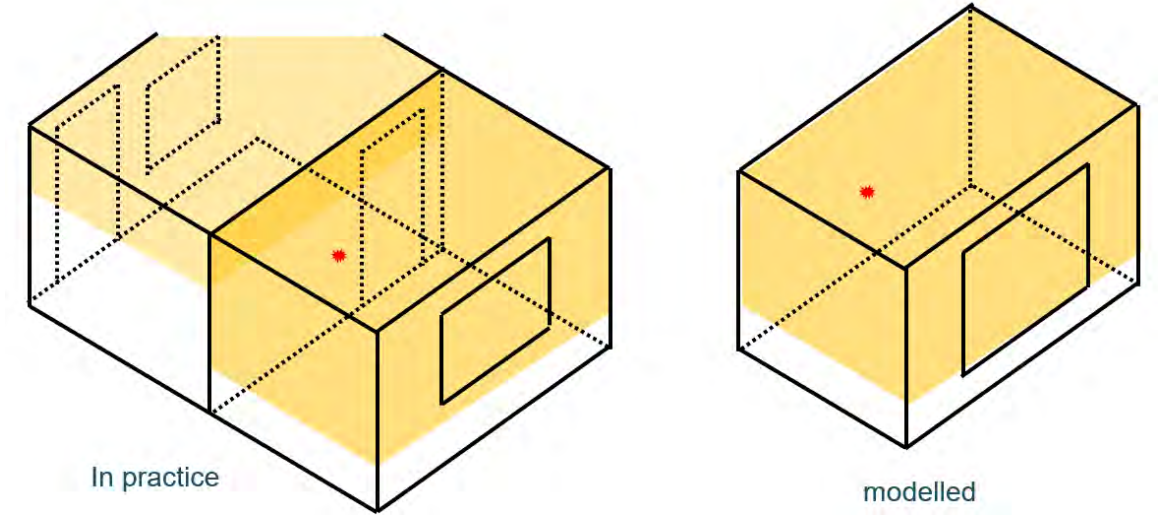
## Appendix B - Assumptions and Areas of conservatism

### B.1 - Assumptions and sensitivity studies
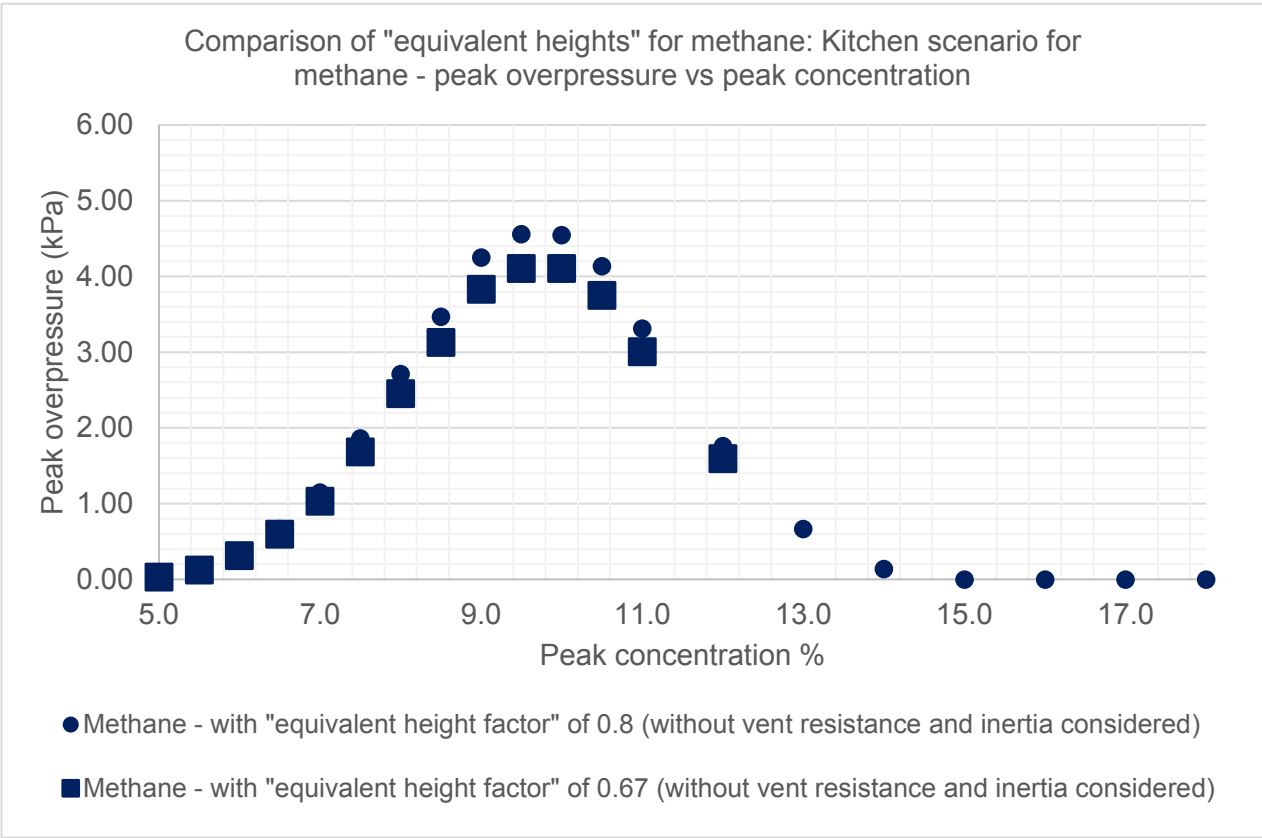
| Assumption | Description | Reason assumption is conservative |
|---|---|---|
| Development of vented explosion ignores resistance and mass of vent covers such as doors and windows for **high** peak concentrations of hydrogen | The "simplified" model [1] (described in Section 3.4.1) used to approximate overpressures and impulses from a vented explosion in an enclosure does not consider the *resistance* or the *inertial* behaviour of the vent cover. The *resistance* of the vent cover would increase the impulse induced upon the internal walls of the enclosure and the overpressure profile would resemble the curves shown in Figure 9 or Figure 10. The figures below represent the internal overpressure profile for an enclosure with no vent cover, or a vent cover with zero *resistance* and mass which is what is modelled using the "simplified" model in [1].<br><br>**Overpressure profile for a high vent area to volume ratio**<br><br>Enclosure internal pressure / time<br>"Simplified" model does not consider the initial "closed vessel deflagration" process prior to window or door failure<br><br>**Overpressure profile for a low vent area to volume ratio**<br><br>Enclosure internal pressure / time<br>"Simplified" model does not consider the initial "closed vessel deflagration" process prior to window or door failure<br><br>The inertia of the vent cover is not often accounted for in studies involving vented explosions [36]. However, studies by Molkov in [36] show that increasing the inertia of the vent increases the overpressure peak in the transition stage between the "closed vessel deflagration" and vented explosion. | The predictions of peak internal overpressure from a vented flammable vapour cloud explosion in the "simplified" model are based on the increase in flame speed as the flame front propagates through the unburnt confined flammable vapour cloud. The speed of the flame front is a combination of the spherical flame propagation (i.e. flame speed in relation to the unburnt flammable vapour cloud through which the flame front is burning), plus the bulk gas motion induced by the venting [35]. Studies by A.Sinha and J.Wen in [35] show that for low concentrations of hydrogen "the contribution from venting induced motion is dominant, whereas for higher fuel concentrations (where flame speed is higher), the contribution from spherical flame propagation and venting induced motion is comparable" [35]. During the "closed vessel deflagration" stage immediately following ignition within an enclosure with closed vent covers, the vent covers (closed windows and doors) prevent venting induced motion. The spherical flame propagation is the only contribution to the total flame speed in this stage. Only once the maximum *resistance* of the vent covers has been exceeded (i.e. point of window and door failure) does the venting induced motion make an additional contribution to the overall speed of the flame front in the enclosure. At this point the combustion process transitions to a fully vented flammable vapour cloud explosion.<br><br>For methane and low concentrations of hydrogen, the inertial effect of the vent covers (doors and windows) would increase the overpressure. The interaction effects between the resistance and inertial effects of the vent cover(s) (doors and windows in a domestic setting) and the combustion process following ignition are complex and very difficult to model. Comparisons with work undertaken by Kiwa on the H100 programme [28] show that the "simplified" model used here underpredicts internal peak overpressure but overestimates the impulse for concentrations of hydrogen up to approximately 12-13%. **A method for considering vent cover resistance and inertia is incorporated in the modelling as discussed in Section 3.4.3**. It is understood that further work as to the effects of vent cover *resistance* and *inertia* in a domestic setting is required to refine the modelling work in this assessment. |

| Assumption | Description | Reason assumption is conservative |
|---|---|---|
| Internal overpressure pulse is assumed to be isosceles shaped for a deflagration | The shape of the internal overpressure pulse in the modelling is assumed to be isosceles shaped for a vented deflagration.<br><br><br>**Approximated isosceles shaped internal overpressure pulse** | Modelling a deflagration as an isosceles pulse shape is in line with industry practice. Sensitivity studies have shown that modelling the internal overpressure pulse in this way conservatively over-estimates the impulse (area under the curve). The peak internal overpressure ($P_{max}$) is estimated using the "simplified" model from [1]. The duration between ignition and the time at which the flame front reaches the vent, $t_v$, is estimated using methods from [35]. It is noted that this assumption is based on zero vent cover *resistance* and *inertia*. The duration between the flame front reaching the vent and the time at which peak overpressure occurs, $t_{max}$, is estimated using the relationship between the volume to vent area ratio $K_v$ (see Section 2.6.2), and the time at which the peak internal overpressure occurs using data from [13]. The duration between the time at which the peak internal overpressure occurs and a return to atmospheric pressure (gauge pressure of zero) is simply estimated as $t_v + t_{max}$.<br><br><br>**Estimation of internal overpressure pulse length**<br><br>In practice, the internal overpressure in the vented enclosure increases exponentially or via a polynomial function with time as indicated by Fig. 2 in [35]. Modelling the pulse shape as an isosceles triangle shape with a linear increase in overpressure with time overestimates the impulse. Additionally, an isosceles triangle shaped pulse for the internal overpressure overestimates the duration between the peak overpressure and the time at which the overpressure in the enclosure returns to atmospheric pressure following a vented deflagration. Comparison with experimental work by Molkov et al in [38] indicates that it is smaller than the rise time.<br><br>Finally, for peak concentrations of hydrogen above 18.5%, the structural response of the load bearing walls (see Section 3.2) have been assessed for both an isosceles shaped pulse and a shock fronted pulse with the worst case structural response taken each time. In practice the pulse shape will resemble something between these two forms, so this approach is conservative. |
| Complete deflagration to detonation transition (DDT) does not occur | Even with a soft ignition source, DDT of hydrogen can occur for concentrations of hydrogen above 18.5% for certain configurations. For example, elongated enclosures such as pipes or tunnels, especially those with obstacles, can increase the risk of a DDT [1]. For non-elongated enclosures, like enclosures formed by rooms in a domestic property, repeated obstacles in the path of the flame front would be a requirement to initiate a | The presence of repeated obstacles such as congested repeated pipework found in a process facility is unlikely to be present in a domestic dwelling and so the risk of DDT is very low. However, it is recognised that some *local* form of DDT could occur, for example in a congested kitchen cupboard. There is evidence from some of the experimental work undertaken by Kiwa that *local* DDT during their Fire Investigation Box tests [28] did occur. As well as the structural response of the load bearing walls (see Section 3.2) being assessed for both an isosceles triangle shaped and a shock fronted pulse, a sensitivity study was |

| Assumption | Description | Reason assumption is conservative |
|---|---|---|
| for peak concentrations of hydrogen above the detonation concentration of 18.5% (see Section 2.9) | DDT. The overpressure profile below is a suggestion of the typical pulse shape observed following a partial or full DDT in an enclosure.  | undertaken to assess any change in quantitatively measured consequences following a partial DDT in an enclosure such as the kitchen. This was done by taking the original estimate for the pulse shape for a vented deflagration and adding a "fictitious" spike in overpressure near the time of the original peak overpressure to represent a partial DDT:  The sensitivity study was undertaken for the kitchen scenario at peak hydrogen concentrations of 45% and 23% where the peak overpressure of the fictitious "spike" was estimated at 5 times the peak overpressure had a DDT not occurred (using the estimated overpressure from the "simplified" model – see Section 3.4.1). The sensitivity study showed that the number of injuries from structural collapse was the same for a peak concentration of 45% under a partial DDT as for only a deflagration (i.e. no increase in the number of properties undergoing structural collapse). The sensitivity study also suggested that a partial DDT at a peak concentration of 20% hydrogen produces the same amount of 'damage' as a vented deflagration at a peak concentration of 20% hydrogen. As mentioned previously, above a peak concentration of 18% hydrogen, the response of the double leaf load bearing walls is determined for both an isosceles shaped pulse representing a deflagration, and a shock fronted pulse shape representing a DDT (see Section 3.4.3). |
| Individual vent areas (e.g. of windows and doors) are summed together to provide an overall vent area. | Almost all empirical or semi-empirical engineering models assume a vent area at the opposite end to the ignition location in a back-wall ignition scenario. For the modelling undertaken using the "simplified" model [1] here, the vent area of the individual vents is summed together to produce a total vent area for the modelling. For example, in the kitchen scenario (see Figure 26), the window and door are located on opposite walls to each other as would be expected in a kitchen located towards the back of a terraced house. The total vent area for both the window and door are summed together to give a total vent area which is modelled as being opposite the ignition location. | This simplification does negate some of the complex effects that would occur due to multiple vents with differing cover resistances, inertias and dimensions being on different walls of an enclosure. In practice, once the vent covers fail (probably at different times) – take for example the interior door and window in the kitchen scenario, the expanding flame front will be able to expand in two directions instead of one (albeit in differing proportions). This would mean that the spherical flame expansion and bulk gas movement would represent a total flame propagation behaviour between that of a central ignition and that of a back-wall ignition [12], with the later producing higher internal overpressures. The modelling in this study conservatively assumes a back-wall ignition for both gases. |

| Assumption | Description | Reason assumption is conservative |
|---|---|---|
| |  In practice      modelled | |
| Overpressures and impulses are estimated based on only the combustible load in the enclosure where the ignition event takes place | In practice, following a leak in one room of a dwelling, the gas would disperse quickly throughout the entire dwelling if all internal doors were left open, but the peak concentration in the room where the leak occurs would be less than if the door to that room or enclosure was closed. Conversely, if all the internal doors in a dwelling were kept closed, the enclosure or room where the leak occurs would have a considerably higher peak concentration than the other rooms in the dwelling with the dispersion of the gas hindered by the closed doors. In both cases, it is expected that some unburnt gas is present in neighbouring rooms or enclosures to the room or enclosure where an ignition event occurs. Following an ignition event, the vented deflagration would most likely "blow open" the internal doors entraining not only more oxygen but also unburnt gas from neighbouring rooms or enclosures.<br><br>The "simplified" model from [1] used to predict overpressures is based on experimental work using single vented enclosures and only considers the combustible load within the compartment where the ignition event takes place. | It is beyond the capability of empirical engineering models such as the simplified method [1] to capture the complex combustion processes involved in a vented deflagration involving multiple enclosures. However, it is the enclosure volume to vent area ratio or $K_v$ (see Section 2.6.2) that is most significant in predicting the peak overpressure in a vented deflagration for a single enclosure, assuming concentration remains constant with other variables changing. The enclosure volume to vent area ratio, or $K_v$, can be assumed to remain relatively constant if the total enclosure volume in the modelling is increased to include neighbouring enclosures (e.g. a living room) to the enclosure where the ignition event takes place (e.g. a kitchen). This is a reasonable assumption given that most rooms in a domestic dwelling will have similar window area to floor surface area ratios. Validation with experimental data for the "simplified" model in [12] shows that maximum overpressure is very much dependent on enclosure volume to vent area ratio for different sized enclosures with the same concentration and ignition location (e.g. back wall ignition) so increasing the combustible load and volume whilst maintaining the $K_v$ value is not expected to vary the peak internal overpressure significantly.<br><br>However, it is noted that impulse and duration of the overpressure pulse arising from a vented deflagration is affected by the enclosure volume and dimensions. The increased combustible load contributing to the vented explosions will increase the impulse. As mentioned previously in this section, the adapted "simplified" model used in this assessment overestimates impulse. |
| |  In practice      modelled | |

| Assumption | Description | Reason assumption is conservative |
|---|---|---|
| Only occupants of enclosures where the ignition event occurs are considered injured | This follows on from the assumption in the previous row. For deflagrations that do not initiate structural collapse, it is assumed that the only internal occupants in the enclosure where the ignition event occurs (i.e. the kitchen or the downstairs of an open plan terraced house) are impinged in the combusting flammable methane or hydrogen cloud. In practice, a flash fire will spread to other parts of the dwelling injuring occupants that are in enclosures or rooms beyond where the ignition event occurred. | It is difficult to model the spread of a flash fire associated with a flammable cloud mixture such as methane or hydrogen using empirical methods through different enclosures in a building. However, it is not necessary to quantitatively measure injury due to burns from a flash fire for other occupants in the dwelling beyond the enclosure where the ignition event occurs, *if structural collapse is initiated*. This is because the injury to occupants in the dwelling, but not in the enclosure where the ignition event occurs, will be assumed already injured due to structural collapse. Therefore, for all concentrations of hydrogen and concentrations of methane up to stoichiometric, the results in Section 4.7 will not change significantly. However, for rich concentrations of methane above stoichiometric, this approach underestimates the number of occupants injured due to burns from a flash fire. Whilst the overpressure and impulse following an ignition event is not high enough to initiate structural collapse, it is likely that most occupants in the dwelling will be injured due to burns. This approach makes the assessment bias towards methane. |
| Combustion of external cloud in vented explosion only uses oxygen initially within the enclosure (such as the kitchen) | The "simplified" model from [1] assumes that the volumetric concentration of the external cloud (stages 4 to 7 in Figure 8 on page 19) remains constant as it is expelled through the vent, during formation and when undergoing combustion. For example, if the concentration of the confined flammable vapour cloud within the enclosure is initially 20% hydrogen prior to ignition, it is assumed in the modelling that the unburnt gas being expelled through the vent forms a cloud of unburnt gas with a homogenous concentration of 20% also. In practice as the unburnt gas is expelled through the vent it will entrain air (and oxygen) from outside the enclosure which would decrease the concentration of the external cloud as it undergoes combustion. | If the concentration of the confined flammable vapour cloud in the enclosure prior to ignition is at or *less* than the stoichiometric concentration, then modelling the unburnt external cloud at the same concentration is conservative. This is because in practice, the concentration of the external cloud would decrease as air from outside is entrained and the external cloud explosion would be less severe.<br><br>If the concentration of the confined flammable vapour cloud in the enclosure prior to ignition is at or *greater* than the stoichiometric concentration, then modelling the unburnt external cloud at the same concentration could be non-conservative. This is because in practice, the concentration of the external cloud could become closer to the stoichiometric concentration as air from outside is entrained in the cloud and the external cloud explosion would increase in strength. For example, if the concentration of a confined methane cloud in the enclosure was 12% prior to ignition, the unburnt methane getting expelled through the vent would entrain air and the concentration of the external cloud could become closer to the stoichiometric concentration of 9.5% for methane.<br><br>However, the averaged concentration of the confined flammable vapour cloud in the modelling of vented hydrogen explosions in this assessment is not greater than stoichiometric concentration of approximately 30%. This means that the modelling of vented hydrogen explosions in this assessment is always conservative if the external cloud is assumed to be at the same concentration as the concentration in the enclosure prior to ignition.<br><br>Modelling the external cloud as having the same constant concentration as the mixture in the enclosure during a deflagration modelling of *rich* vented methane explosions could underpredict overpressures giving a bias towards methane if hydrogen and methane are being compared (because in practice, the rich external cloud would entrain air and become closer to stoichiometric concentration). |
| Degree of stratification over the height of the enclosure is the same for all levels of peak concentrations. | The approach to considering stratification in the enclosures of the domestic dwelling considered (kitchen and downstairs of an open plan terraced house scenarios) is outlined in Section 3.2.3. The ratio of the concentration at mid height to the concentration at the ceiling (peak concentration), and the ratio of the concentration at the floor to peak concentration at the ceiling is assumed to be constant for all peak concentrations. This is based on the "HyStreet" experimental work undertaken at Spadeadam [24] where the leak location in the house *was in the basement*. In this instance, a high degree of stratification was observed in the basement with very high concentrations occurring at the basement ceiling (underside of the ground floor) with 'seeping' of the gas (in both the methane and hydrogen experiments) through the ground floor into the ground floor rooms through multiple leak paths. There were also experiments undertaken with the leak location located within the boiler cupboard near ceiling level in the kitchen. In these instances, the observed concentration at ceiling level for hydrogen was very high (+45%) but the concentration at mid height and floor level was at or below the lower flammability limit. | Although Spadeadam experiments [24] where the leak location was within the closed kitchen boiler cupboard showed very high concentrations of hydrogen (and sometimes methane) at ceiling level and a highly stratified confined flammable vapour cloud, a sensitivity check on the results indicated that the overall combustible inventory for these cases was less than the cases from the Spadeadam data in [24] on which the modelling in this assessment is based, which is when the leak location is located in the basement (see Section 3.2.3). Appendix A provides further detail on the modelling of stratification in this assessment.<br><br>It is recognised that further work on modelling stratification is required, especially for cases that are highly stratified and that only one "release geometry" has been considered in the modelling. For example, there were experimental lots from the Spadeadam experiments [24] where the hydrogen concentration at the ceiling level in the kitchen was 53%, the concentration at mid height was 14%, and the concentration at floor level was 1% (experimental lot DNVL3-085). This occurred when the leak was in the closed boiler cupboard. In this example, the region of the stratified cloud near the ceiling is very rich, the region |

| Assumption | Description | Reason assumption is conservative |
|---|---|---|
| | | near mid height is approximately half the stoichiometric concentration for hydrogen, and the region near floor level is below LFL. The average concentration of this stratified cloud is approximately 22%. Equating this to an "equivalent volume" at stoichiometric concentration could be highly conservative because combustion of the rich part of the cloud would possible resemble more of a flash fire than a deflagration with significant overpressures, although the part of the cloud that is close to stoichiometric concentration would contribute significantly to the overpressure of a vented explosion. |
| Degree of stratification sometimes dependent on leak geometry rather than properties of the gas being leaked | For several sets of experimental results from the Spadeadam experiments where the leak location was within the closed kitchen boiler cupboard, the degree of stratification for both methane and hydrogen were very similar. For these scenarios, the leak geometry rather than gas properties (such as density) dominated the degree of stratification. | A sensitivity study has been undertaken using the same "equivalent height factor" (see Appendix A) of 0.67 used for hydrogen (instead of 0.8) to represent a scenario where leak geometry rather than gas properties dominate the degree of stratification. The results on the next page suggest that when using the same "equivalent height factor" for methane as hydrogen, the estimated peak overpressure using the "simplified" model reduces by approximately 10% and does not significantly change the results in Section 4. This sensitivity study demonstrates that the peak overpressure in a vented explosion is more sensitive to input parameters such as concentration and volume to vent area ratio ($K_V$), than "equivalent height factor".  |
| Overpressure pulse is assumed to be a positive pressure with any rarefaction (negative pressure) being ignored. | Significant negative pressures have been observed in vented flammable explosion experiments involving both methane and hydrogen. For example, Figure 16 from [39] shows peak negative pressures similar in magnitude to the peak positive pressures for deflagrations of confined hydrogen clouds above 18% concentration for some of the iso container experiments undertaken by Gexcon. | Below a concentration of 18% hydrogen, the rarefaction effects are considerably small (i.e. the negative phase of the pulse is much smaller in magnitude than the positive phase) for the experiments undertaken in an iso-container in [39]. For below hydrogen concentrations of 18%, it is reasonable to ignore rarefaction effects in this assessment. Above concentrations of 18% hydrogen, the significant rarefaction effects occurred in the iso-container experiments in [39] because the iso-container is made of steel and does not allow "partial venting" through the enclosure boundaries as the combustion occurs. Venting only occurs through the originally open vents. The significant rarefaction effect occurs in the iso-container experiments in [39] because the momentum of the expanding gas being pushed out the vent causes it to over-expand, resulting in the pressure at the tail of the deflagration to become negative, which "sucks" in the iso-container enclosure boundaries. However, for the domestic scenarios modelled in this assessment, the enclosure boundaries fail following a deflagration of a confined combustible peak concentration above 14% hydrogen for the kitchen scenario and above 13% for the downstairs of an open plan terraced house scenario. Masonry walls exhibit very little elastic behaviour and once failed due to the positive |

| Assumption | Description | Reason assumption is conservative |
|---|---|---|
| | | overpressure part of the deflagration pulse; the enclosure boundaries no longer have integrity meaning any negative pressure phase causes no further damage beyond the damage done by the positive phase of the pulse. |
| The comparison between of the behaviour of masonry structures forming the enclosure for vented explosions of methane and hydrogen is representative of the comparison between the vented deflagration of the two gases on the behaviour of other typical construction materials used in a domestic setting such as Structural insulated panels (SIPs). | When considering the behaviour of construction materials under dynamic loading, particularly from blast loading, engineers can categorise different methods of construction by the way they exhibit ductility and their capacity to absorb strain energy. For example, reinforced concrete, is dense and therefore can provide significant inertial resistance against blast loading compared to stud walling which is lightweight. The reinforcement in reinforced concrete provides significant ductility and reinforced concrete also redistributes stress well preventing the building up of stress concentrations in parts of a structure such as a slab to wall connection. Structural steel, although often less dense and considered lightweight when compared to concrete, also provides significant ductility, but it is recognised that structural steel in residential buildings is usually only used for the structural frame and not internal or external walls. Traditional brick-built structures and more modern cladding like building materials such as SIPs exhibit a poor response to blast loading, have very little resistance when compared to reinforced concrete or structural steel, and are brittle in nature. The methods of construction and the materials used in low rise residential and commercial structures are designed to provide nearly all their capacity for vertical downward dead and live load, not dynamic lateral and upward loading which would occur if such materials were used to form the enclosure boundaries of a vented flammable explosion. | The figure on the next page is Figure 67 with two additional iso-damage curves plotted; <br><br> • one for a single leaf brick wall (which can also represent a lighter in mass SIPS panel with equivalent stiffness as a brick wall), <br><br> • one for the same double leaf cavity wall used in this assessment but for a four storey instead of two storey house (i.e. three storeys above). This would increase the axial load in the wall forming part of the enclosure boundary where the leak, dispersion and ignition event occurs. <br><br> The graph indicates that the response of the brick wall enclosure boundaries modelled in this assessment are tending towards a quasi-static response in the region near the boundary between failure and retaining of structural integrity. It shows that if the assumptions are varied in the way described above then the boundary between failure and retaining of structural integrity would change by the same degree for both gases. <br><br> If the curves were all translated to the left, representing a reduction in mass of the enclosure boundaries (from replacement of a brick wall with a lightweight SIPs system), then the relative comparison in structural performance between methane and hydrogen would remain the same. <br><br>  |

## B.1 – Areas of conservatism

| Conservatism | Comment |
|---|---|
| Ignition location in the compartment is assumed to be an "end ignition" rather than a "central ignition" | From the experimental work discussed in [12], it is evident that a back-wall ignition produces higher overpressure than a central ignition for the same enclosure geometry and fuel composition (fuel medium and concentration). It is also considerably more likely for an ignition source, such as an electrical socket or appliance to be located, on or near a wall. |
| Peak overpressure is determined using the "simplified" model described in Section 3.4.1 assuming the enclosure dimension remain constant throughout combustion process for ignition events that eventually result in structural collapse (i.e. the venting effects of any failing enclosure boundaries is neglected in the modelling) | In practice, the natural period of the modelled load bearing enclosure walls in relation to the internal overpressure pulse duration from the vented explosion estimated in the modelling, puts it in the lower end of the "dynamic" category according to equations (5.8) and (5.9) from [9]. Analyses of the structural response using the SDoF method in the assessment shows that failure of the load bearing walls occurs at approximately $0.25t$, where $t$ is the total duration of the internal overpressure pulse This suggests that the wall has reached its deflection at failure before the peak overpressure from the vented deflagration occurs at $0.5t$. This would therefore mean that the dimensions of the enclosure are increasing as combustion of the flammable vapour cloud takes place, **which in turn would reduce the peak overpressure**. This effect is sometimes accounted for by modelling the flammable vapour cloud as "partially confined" [11]. However, for higher flame speeds such as seen for high concentrations of hydrogen, a degree confinement, that in turn increases the combustion rate, would still occur, following failure of the enclosure boundaries as the walls collapse (i.e. it is not reasonable to model the confining effect of the enclosure boundaries as immediately "non-existent" once they lose structural integrity). |
| Structural capacity of internal non-load bearing elements in a property are assumed to be negligible | Although non-load bearing elements (usually referred to as "non-structural" in Building Regulation documents) are not designed to be load bearing during normal operation, many do have some load bearing capacity when subjected to accidental or imposed and dead loading following an accident. An example is shown in Figure 84 where it appears that some internal walls not designed as load bearing, do withstand sudden dead and imposed loads following loss of structural integrity in other parts of the structure. Neglecting this is conservative in this assessment. |

Some structural integrity of likely non "load bearing" elements are evident following gas explosion. These are ignored in this assessment

Figure 84: Extract image from [40]. Gas explosion in Ravensthorpe, near Dewsbury, UK

## Appendix C – Dwelling Occupancy levels

An estimation on the occupancy level has been made for this assessment using an average dwelling occupancy level of 2.4 residents per dwelling from the Office for National Statistics 2017 household assessment [26] along with some assumptions regarding the amount of time occupants spend in and away from their dwelling.

These assumptions are:

- 50% of a dwelling's occupants spend 8 hours at work, 5 days a week, with 2 hours spent commuting on those days. i.e. an assumption that 50% of dwelling occupants spend 50 hours not in the dwelling over a working week (5 out of 7 days).

- If 50% of a dwelling's occupants are at work 5 days a week (a week being 7 days), this is 0.5 x 2.4 *occupants* = 1.1 *occupants* **not** in the dwelling 50 hours a week. 1.1 *occupants* x 50 hours = 60 'occupant hours' spent at or travelling to work a week. 'Occupant hours' is defined as the *number of occupants living in a dwelling* x *duration in hours*. For example, the total number of 'occupant hours' per dwelling, per week is 2.4 *occupants* x 7 *days* x 24 *hours* = 403.2 'occupant hours'. If the entire household of a dwelling spent 7 days in their home without leaving, then this would be a total of 403.2 'occupant hours' spent in the dwelling over 7 days

- With 50% of a dwelling's occupants assumed to be out the dwelling at work 50 hours a week, an assumption has been made that the other 50% of the occupants of the dwelling spend 4 hours in a working week out of the dwelling. This is a total of 50% x 2.4 *occupants* x 4 *hours* x 5 *days* = 24 'occupant hours'. So far, during the working week (5 out of 7 days), the total number of 'occupant hours' **not** spent in an average dwelling is 24 + 60 = 84 'occupant hours' out of a total of 403.2 'occupant hours'.

- It is assumed that at weekends, all occupants of an average dwelling spend 4 hours not in their dwelling on both weekend days. Over a weekend (2 days) this is 2.4 *occupants* x 4 *hours* x 2 *days* = 19.2 'occupant hours'.

Over a week (7 days), this is a total of 84 + 19.2 = 103.2 out of a total of 403.2 'occupant hours' not spent in the average dwelling. **This gives an average occupancy level of 74%** (from [403.2-103.2]/403.2). Multiplying this by 2.4 gives an average occupancy level of **1.79 persons per dwelling**.

These assumptions can vary significantly and do not consider factors such as

- Demographics (age, wealth, occupation of residents, geographical location etc)

- Mobility of the occupants

- Type of dwelling and the difference in occupancy levels for each type

- Number of visitors to a dwelling

- Holidays and extended periods of when properties may be empty

Department for Business, Energy & Industrial Strategy  Hy4Heat
ARP-WP7-GEN-REP-0003 | Issue 01 | 1 May 2021  Consequence Modelling Report

Page 124

–  Variation of occupancy levels throughout a year (such as going on vacations or working away from home)

However, the purpose of these assumptions is to make some consideration in the consequence assessment of the fact that occupants of residential dwellings are not occupying their dwellings twenty-four hours a day, seven days a week throughout the year. In summary, an overall assumption is that occupants of dwellings on average **spend 26%** of their time away from their dwelling a week, and **74%** in their dwelling. Finally, it is worth remembering that this assessment is a *comparative* consequence assessment between methane and hydrogen. Whilst increasing the resolution and understanding of *occupancy* levels may improve the relevance of the consequence results in this report to realistic scenarios, it will do so for both methane and hydrogen in equal measure.

For comparison to the assumptions in Appendix D, the average occupancy per $m^2$ in a dwelling with a floor area of 64 $m^2$ (8m x 4m x 2 storeys) is 0.028 persons per $m^2$

## Appendix D – Density of people in public realm

An estimation on the number of people in the public realm has been made using a similar approach as made to estimating an average occupancy level in Appendix C.

To help picture a scenario, the street in a residential area below has been considered:



To start, some assumptions are made regarding this setting:

- Length of street: 45m

- Width of street (front of one house to front of another house): 10m

- Number of houses in the street: 20 houses

- Average occupancy per house of 2.4 people [26].

- Average speed of a person walking is 3.1 mph (1.4 m/s)

The total area of the public realm in front of the terraced houses (i.e. in the street) is 450 m² (45m *street length* x 10m *street width*), and the total number of residents living in the street is 48 (2.4 *occupants per dwelling* x 20 *houses*).

Using the assumptions from Appendix C, it is assumed that 50% of the dwelling occupants in the street commute to work during the working week (5 days) making a return trip from their house to either end of the street each day (i.e. going to work and returning from work). The other 50% of the dwelling occupants in the street are assumed to leave the house twice a day to run errands etc and make two return trips from their house to either end of the street each day. This gives an average of 1.5 return trips from the house to either end of the street each working day (5 days out of 7), *per resident of the street*.

An assumption is then made that all residents in the street make two return trips from their house to either end of the street on *weekend* days.

It is also assumed that for every resident in the street, every other return trip they make from their house to the end of the street is to either end of the street. This means, on average, each resident in the street walks *half* the length of the street (22.5m) each time they go out, and *half* the length of the street each time they return home – **a total of a 45m walk every time a resident leaves their dwelling**. This average would be the same if one end of the street was a dead end or had a higher foot fall than the other.

If the average speed of a resident's walk is assumed to be 1.4 m/s, then on average, **each resident spends a total time of 32 seconds walking in the street** every time they leave their house to make a trip. If approximately 60 seconds is added on to each return trip time to consider time spent by each resident being stationary, for example, to load or unload a car, find keys etc, then the average time spent by each resident in the street, every time they leave their house, is approximately **92 seconds**.

Using all the above assumptions, an estimate of 553 seconds (approximately 9.2 minutes) per week (over 7 days) is spent by each resident in the residential public realm (the street in front of houses). If there are 48 occupants living in the street, this means that there is on average one resident in the public realm or street for 7.4 hours per week (over 7 days).

If it is further assumed that on average, a non-resident walks the length of the street every 15 minutes between the hours of 7am and 9pm on weekdays, and 9am and 10pm on weekends, this would mean that there is an additional 3.4 hours of the week where there is always one person in the public realm or street.

In summary, it is assumed that there is a one person in the public realm in the street for 10.7 hours every 7 days. There are 168hrs in a week (7 *days* x 24 *hours*) so on average there are 10.7 / 168 = 0.064 *people on average in the street or public realm*.

Furthermore, if 0.064 *people per street* is divided by the public realm area of 450 m$^2$ for the street, **an average *density of people in the public realm* of 1.43 x 10$^{-4}$ people per m$^2$** or 1 person every 7000m$^2$ can be assumed to quantitatively estimate the number of people in the public realm.

The above estimate of 1 person every $7000m^2$ is averaged with a quiet street that has no non-residents passing through it to provide a public realm density of **1 person per $8630m^2$** or **$1.16 \times 10^{-4}$ persons per $m^2$.**

As mentioned in Appendix C, although this assessment is a *comparison* of the consequences between the ignition following a methane/natural gas and a hydrogen leak, the purpose of the assumptions in Appendices C and D is to demonstrate that there has been some thought put into "number of people injured" in the results of Section 4.

Even if the number of people passing through a street is multiplied by say 10 (with one person walking through the street every 1.5 minutes), using the assumptions made in this appendix, the public realm density would be increased to 1 person per 6035 $m^2$ or $1.66 \times 10^{-4}$ persons per $m^2$.

When compared to the approximate internal occupant density of 0.028 occupants per $m^2$ for dwellings, the density of people in the public realm or street is smaller by a factor of approximately 100.

It should be noted that it is assumed that any person in the public realm or street in front of the dwellings is on foot (i.e. not in a vehicle)

## Appendix E – Estimating vent failure pressure

The vent failure pressure in this assessment is based upon a single glazed window with dimensions 1.6 x 1.0 m with a dynamic breaking strength of 80N/mm² (see Table 9.1 of [9]). Figure 9.8 from [9] is used to determine the resistance (vent failure pressure) where

- $a = 1.0\text{m}$ (the shortest dimension of the vent)

- $b = 1.6\text{m}$ (the width of the window)

- $t = 4\text{mm}$, the thickness of the annealed single glass pane

- $D = Et^3 / [12(1 - v^2)]$, the plate stiffness. In this instance $E$ is the Youngs modulus of glass at $6.9 \times 10^{10}$ N/m², and $v$ the Poisson's ratio of 0.22 [9]. So $D = 387\text{Nm}$

The failure pressure of the window $r$ can be estimated using Figure 9.8 from [9] (see Figure 85)
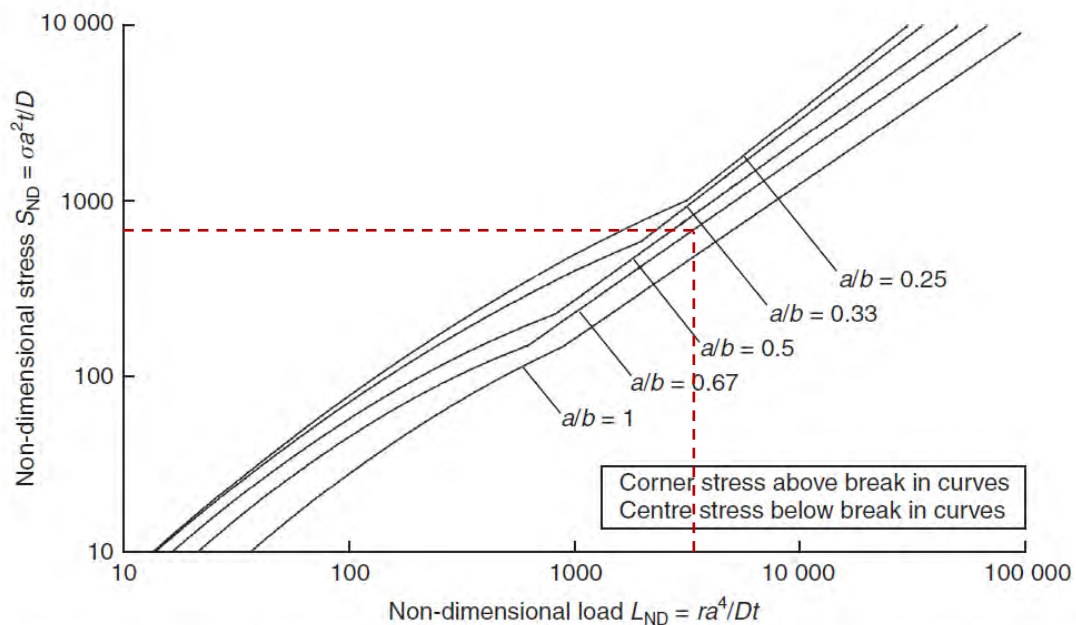


Figure 9.8. Non-dimensional static load–stress relationships for simply-supported elastic plates (after reference [6])

Figure 85: Estimation of Extract of Figure 9.8 from [9]

The non-dimensional stress $S_{ND} = [80\text{N/mm}^2 \text{ x } (1.0\text{m})^2 \text{ x } 4\text{mm}] / 387\text{Nm} = 827$

Aspect ratio of the glazing pane $a/b = 1.0\text{m} / 1.6\text{m} = 0.625$

Using Figure 85, the non-dimensional load $L_{ND} =\sim 4500$

Re-arranging for $r = L_{ND} Dt / a^2$ gives 7kPa, which is used as an estimate for the vent failure pressure in Section 3.4.3.

## Appendix F – Worked examples

This appendix will take the reader through examples of determining consequences following an ignition event that follows a leak and dispersion event which leads to:

– A confined methane cloud with a peak concentration of 9.5% developing in the kitchen

– A confined hydrogen cloud with a peak concentration of 30% developing in the kitchen

Each example will go into further detail on determining:

– Estimation of vented overpressure using the "simplified model from [1]

– Estimation of impulse using guidance from [1], [12] and [35]

– Consideration of vent cover resistance and inertia

– Determining the extent of structural collapse and the number of people incurring injury

– Determining the number of people incurring secondary injury

## F.1 – Peak concentration of 9.5% methane in kitchen scenario

Figure 86 is a screenshot of the tool used to estimate internal vented overpressure for the kitchen scenario containing an inhomogeneous confined combustible methane cloud with a peak concentration of 9.5%. Figure 87 is a screenshot of another part of the same tool but provides some commentary on how impulse is estimated. In both these figures, green boxes represent input parameters.

### Compute flame surface area

$$A_f = \begin{cases} 0.50\, A_{in} & \text{for ignition at the back} - \text{wall (BWI)} \\ 0.25\, A_{in} & \text{for ignition at the centre of the enclosure (CI)} \end{cases}$$ (E.1)

where $A_{in}$ is the total internal surface area of the enclosure:

$$A_{in} = 2 \cdot (L \cdot B + B \cdot H + H \cdot L)$$

| Length of enclosure | L | 3.0 | m |
| Breadth/width of enclosure | B | 4.0 | m |
| Height of enclosure | H | 1.9 | m |
| Internal area of enclosure | $A_{in}$ | 50.88 | m² |
| Centre or back wall ignition? | | Back-wall | |

*Check whether enclosure is elongated*

*Elongated enclosures*

These sets of experiments are undertaken in idealized conditions using an enclosure whose aspect ratio (L/D) is larger than 2.5. The studies that are considered for this section include the studies of Kumar [5] and Daubech et al. [6].

(iii) **For elongated enclosures** - For elongated enclosures, the flame area is computed as:

$$A_f = 0.25\, A_{in}$$ (E.7)

For longer pipes, especially with obstacles, there is additional risk of Deflagration to Detonation Transition (DDT) which is beyond the scope of this model. Hence, it is recommended to use this model for enclosures with L/D ≤ 4.

| Equivalent diameter | D | 3.127 | m |
| Aspect ratio | L/D | 0.959 | |
| Is L/D less than 2.5? | | Yes | |
| Is L/D less than or equal to 4? | | Yes | |
| | | | |
| Flame surface area | $A_f$ | 25.44 | m² |
| Add. obstacle flame area | | 0.00 | m² |

*Check to determine whether enclosure is categorised as elongated*

### Compute external cloud radius

*Estimation of external cloud radius*

$$R_{CI} = 0.5 V^{0.3}$$ (E.2)

where V is the volume of the enclosure.

| Volume of enclosure | V | 23.04 | m³ |
| External cloud radius | $R_{CI}$ | 1.28 | m |

$$G1 = \left[ \left( L_{eff}^{\beta1} \right)^2 \left\{ \left( \frac{A_f}{A_v} \right)^2 - 1 \right\} \right],$$ (E.3)

$$G2 = \left[ R_{CI}^{\beta2} \right]^2.$$ (E.4)

Where $L_{eff}$ can be defined as:

$$L_{eff} = \begin{cases} L & \text{for ignition at the back} - \text{wall (BWI)} \\ 0.5\, L & \text{for ignition at the centre of the enclosure (CI)} \end{cases}$$

| Medium | | Methane | |

*This is the "equivalent height" of the enclosure. To model this inhomogeneous confined methane cloud as a methane cloud with a homogeneous concentration of 9.5%, it is calculated as 0.8 x 2.4m (see Section 3.2.3 and Appendix A for further explanation of "equivalent height")*

*Dimensions of vent*

| Height of vent | | 1.0000 | m |
| Width of vent | | 3.1000 | m |
| Area of vent | $A_v$ | 3.1 | m² |

*Total summed vent area in kitchen (see Figure 26)*

*Distance from ignition to vent*

| Effective acceleration dist | $L_{eff}$ | 3 | m |

*β1 and β2 values used for configurations*

| Are obstacles present? | | No obstacles modelled | |
| Configuration | | Ideal | |
| Value β1 | β1 | 0.5 | |
| Value β2 | β2 | 0.5 | |

*Values G1 and G2*

| Value G1 | G1 | 199.0 | |
| Value G2 | G2 | 1.281 | |

*Beta values are based on obstacle configuration within enclosure – for this case there are no obstacles modelled (see Section 3.4.2)*

*Calculation of G1 and G2 values based on equation E.3 and E.4 from [1]. G1 and G2 are based on the geometry (dimensions and vent area) and are independent of combustible medium properties*

### Compute internal overpressure

| Concentration of medium | | 9.5 | % |
| Equivalence ratio $\phi$ | | 1.000 | |

*Lookup F1 and F2 values*

| Value F1 | F1 | 8.9585E-05 | |
| Value F2 | F2 | 2.1652E-02 | |

$$p = (F1 \cdot G1) + (F2 \cdot G2)$$ (17)

where

$$F1 = \left[ \frac{\rho_u}{2 \cdot 10^5} \left\{ \frac{U_0}{R_0^2} \left( \frac{\sigma - 1}{\sigma} \right) \right\}^2 \right],$$ (18)

$$F2 = \left[ \frac{2\, \gamma_u (\sigma^2 - \sigma)}{a_0^2} \left( \frac{U_0}{R_0^2} \right)^2 \right],$$ (19)

$$G1 = \left[ \left( L_{eff}^{\beta1} \right)^2 \left\{ \left( \frac{A_f}{A_v} \right)^2 - 1 \right\} \right],$$ (20)

$$G2 = \left[ R_{CI}^{\beta2} \right]^2.$$ (21)

| Overpressure | p max | 0.04558 | bar |
| | | | |
| Internal Overpressure | p | 4.56 | kPa |

*The peak concentration of methane is 9.5% for an equivalent homogenous confined cloud with an "equivalent height" of 0.8h (where h is the height of the enclosure).*

*F1 and F2 values are looked up from tables A1 and A2 from [1]. For methane concentrations other than stoichiometric, F1 and F2 have been calculated following equation 18 to 21 from [1]*

*Peak overpressure is estimated using equation 17 from [1], where F1*G1 represents the overpressure contribution from the internal flame propagation and F2*G2 the overpressure contribution from the combustion of the external cloud. They are conservatively superimposed upon each other*

### Ratio of vent area to compartment volume

The scaled vent size $K_v$ is given by the following relation: $K_v = A_v / V^{2/3}$, $A_v$ is the vent area, V is the volume of the room.

explosion of the cloud is related to vent size. For $K_v \le 0.3$, an external explosion occurs as the flame propagates outside the vent, causing the negative overpressure outside the vent and internal explosion overpressure to continue to rise.

| Check of K_v (ratio vent to volume) | | 0.383 | |

Kv value indicates internal pressure profile will have dual peak

*Check of the $K_v$ value. As this increases above 0.3, the model increases in conservatism because it continues to superimpose the overpressure due to internal flame propagation and overpressure due to external explosion*

Figure 86: Screenshot of calculation used to determine internal overpressure for a vented methane explosion in a kitchen with a peak concentration of 9.5%. This figure shows extracts from [1].

0.25

Impulse is measured in Pa-s and is the integral of a pressure-time transient i.e. the area under a pressure time graph. The "simplified" method from [1] contains a method to predict peak internal overpressure. To make an estimate of impulse, the **time element** of the pressure-time relationship needs to be estimated. This is done by firstly estimating the time taken for the reaction front to travel from the ignition point at the back wall, to the vent

*F1\*G1* from equation (17) in [1] is an estimate of the peak internal overpressure *due to internal flame propagation* and this occurs when the flame front reaches the vent.

The **total flame speed** is the *U* from equation (4.1) **plus** $U_1$ from equation (5) from [35]

The co-efficient *A* is iteratively increased until the distance travelled by the reaction front due to *spherical flame propagation* plus the *bulk gas motion*, is almost equal to the length of the kitchen enclosure (3m) **when** the trial values for *ΔP* and $U_1$ are close to the *F1\*G1* and $U_1$ originally calculated using equation (5). This is used to estimate the time taken for the flame front to reach the vent.

As stated in Appendix A, the overpressure pulse is assumed to be isosceles triangular shaped, so the total duration is double the rise time. i.e. 2 x 0.263s in this instance. This time is then used to estimate impulse

### Internal flame propagation (before external explosion)

*Spherical flame propagation*

The most critical parameter which affects the internal overpressure is the internal flame propagation. The flame propagation from source of ignition to the vent is a complex phenomenon which is challenging to model. However, flame propagation can broadly be attributed to a combination of two processes – spherical flame propagation, and bulk gas motion induced by venting.

The flame propagation velocity with radius can be written as:

$$\frac{U}{U_0} = \left(\frac{R}{R_0}\right)^\beta \qquad (4.1)$$

where U is the flame propagation velocity at radius R, $U_0$ is the flame propagation velocity at $R_0$, which is the critical radius for the onset of cellular instabilities, and β is fractal excess, experimentally observed to be constant at 0.243 for all hydrogen concentrations [26]. The values of $U_0$ and $R_0$ can be calculated using curve-fits to the experimental data [11,26].

$$U_0 = 0.0537\ x^2 - 1.008\ x + 5.5716 \quad (m/s)$$

$$R_0 = (1.4273\ x - 0.1942)/1000 \quad (m)$$

where x is the hydrogen concentration in percentage. Since,

| | | | |
|---|---|---|---|
| Spherical flame velocity at $R_0$ | $U_0$ | 2.613 | m/s |
| Critical radius | $R_0$ | 0.225 | m |

Estimations of $U_0$ and $R_0$ are made using these equations for hydrogen. For methane, values for $U_0$ are taken from [42] and $R_0$ is calculated using information from [7]

position R. This equation can be used to calculate the time for the flame-front to reach the vent. The distance from the ignition source to the vent (R) can be estimated as:

$$R = \begin{cases} L & \text{for } Back-wall\ ignition \\ \frac{L}{2} & \text{for } Central-ignition \end{cases}$$

where L is the length of the enclosure. So, for a known L, time taken can be calculated as:

$$\tau = \left(\frac{R^{(1-\beta)}}{1-\beta}\right)\left(\frac{R_0^\beta}{U_0}\right) \qquad (4.3)$$

| | | | |
|---|---|---|---|
| Fractal excess | β | 0.23 | |
| Maximum value of R | R | 3 | m |

*Bulk gas motion induced by venting*

As pressure rises inside the enclosure, vent opens, and unburnt gases escape out. Venting induces a bulk gas motion towards the vent. This bulk gas motion is also responsible to move the flame towards the vent. Gas venting can be modelled using Bernoulli's equation across the vent. Considering two points in the unburnt gases, just inside and outside the vent:

$$\frac{P_1}{\rho_u} + \frac{U_1^2}{2} = \frac{P_2}{\rho_u} + \frac{U_2^2}{2} \qquad (2)$$

where subscript 1 is for the internal point and 2 is for the point outside the vent. $P_1$ denotes the internal pressure and $P_2$ is for the external ambient pressure, $U_1$ and $U_2$ are velocities and $\rho_u$ is the unburnt gas density. $U_1$ is the bulk velocity induced inside the enclosure due to venting. Also, the velocities can be related to each other using equation of continuity and assuming density changes to be negligible. Hence,

$$A_1 U_1 = A_2 U_2 \qquad (3)$$

where $A_1$ is the cross-sectional area of the enclosure and $A_2$ is the vent area. Eq. (3) can be expressed in terms of enclosure dimensions as:

$$B. H. U_1 = A_v U_2 \qquad (4)$$

Where B and H are the enclosure breadth and height, respectively, and $A_v$ is the vent area. Eliminating $U_2$ from equations (2)–(4):

$$U_1 = \sqrt{\frac{2\ \Delta P}{\rho_u\left[\left(\frac{B\ H}{A_v}\right)^2 - 1\right]}} \qquad (5)$$

| | | |
|---|---|---|
| Maximum value of Δ P i.e. F1\*G1 | 1.78 | kPa |
| Maximum value of $U_1$ | 24.05 | m/s |

*TOTAL internal flame propagation*

To estimate the time for the internal flame propagation to reach the vent, the increase in ΔP is approximated to a function of the cubic of the time t . i.e. $\Delta P = At^3$ where A is a co-efficient to iteratively find. The maximum value of ΔP is assumed to be F1\*G1 (the maximum internal pressure due to internal flame propagation, external explosion excluded).

| | |
|---|---|
| Iteration step to determine A | 0.1 |

Calculate time for internal flame propagation to reach vent

**Start with a large iteration step and reduce it**

| | | |
|---|---|---|
| Co-efficient *A* in approximation $\Delta P = At^3$ | 114.300 | kPa s$^{-3}$ |

*TOTAL internal flame propagation continued*

| | | |
|---|---|---|
| Time for flame front to reach vent | 0.250 | sec |

*Check of guess*

| | | |
|---|---|---|
| Final *ΔP* value using approx relationship | 1.78 | kPa |
| Guess of $U_1$ using approx relationship | 23.65 | m/s |



### Estimation of pulse duration

The time taken for the internal flame to reach the vent, and the value of $K_V$ is used to make an estimate of the total internal pulse duration and therefore of the impulse.

| | | |
|---|---|---|
| Factor from $K_V$ for calculating pulse length | 1.05 | |

| | | |
|---|---|---|
| Total approx duration of pulse | 0.525 | sec |


Estimated internal pressure
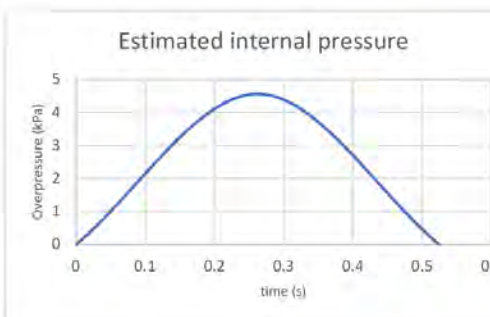
| | | |
|---|---|---|
| **Estimation of impulse** | 1195 | Pa s |

### Estimation of window failure time

Prior to the failure of the vent, the expansion of the vapour cloud is effectively a closed vessel deflagration where the internal pressure rise occurs due to the expansion ratio. In practice a room is rarely "fully closed" but some idea of the time that the maximum vent pressure is reached can be estimated

| | | |
|---|---|---|
| Maximum resistance of window | 9 | kPa |
| Time at which vent failure occurs | 0.193 | sec |
| % cloud consumed at failure | 1.17 | % |

Estimation of the distance travelled by the reaction front within the enclosure due to **spherical flame propagation** can be estimated using this equation

The relationship between $U_1$ (the bulk velocity of the unburnt gas in the enclosure) and the pressure rise can be estimated using equation (5) from [35]. However, although the peak internal overpressure due to *internal flame propagation* (F1\*G1) is known, how pressure rises as a function of time is not. It has been assumed that the internal pressure rises cubically with time.

With an estimate for the time taken for the flame/reaction front to reach the vent, the time at which the external explosion occurs is estimated based on Figure 7 in [13]. Here, the relationship between the duration from the flame arriving at the vent to the peak internal overpressure time, and the $K_V$ value is used to estimate this factor. In this case, the factor is 1.05 so the time between ignition and peak internal overpressure (the rise time) is estimated as 1.05 x 0.250s = 0.263s for this example

Figure 87: Screenshot of calculation used to estimate impulse for a vented methane explosion in a kitchen with a peak concentration of 9.5%. This figure shows extracts from [1] and [35].

The estimation of the overpressure and impulse in Figure 86 and Figure 87 assumes that the vent cover resistance and inertia are zero. Although in practice, this would not be the case, the response of the enclosure boundaries i.e. the kitchen walls, are firstly assessed using the overpressure and impulse of 4.56kPa and 1195Pa-s respectively. Figure 88 shows the input force function to the SDoF model used to estimate response for a strip of wall, 2.4m high and 1m wide for an overpressure of 4.56kPa and impulse of 1195Pa-s.
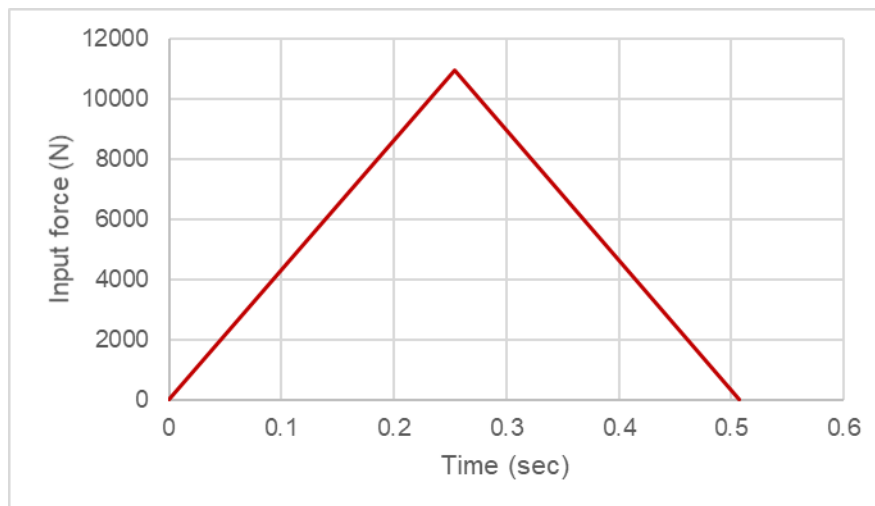


Figure 88: Input force function for a vented 9.5% peak concentration methane explosion on a 1m strip of 2.4m spanning double cavity brick wall (zero vent cover resistance and inertia)

Figure 89 shows the resistance function used to model the response of the ground floor double cavity brick enclosure walls. This is constructed using the methodology described in Section 2.7 and Chapter 6 of UFC-3-340-02 [14]. A displacement greater than 102mm indicates structural collapse for the scenarios in this assessment.
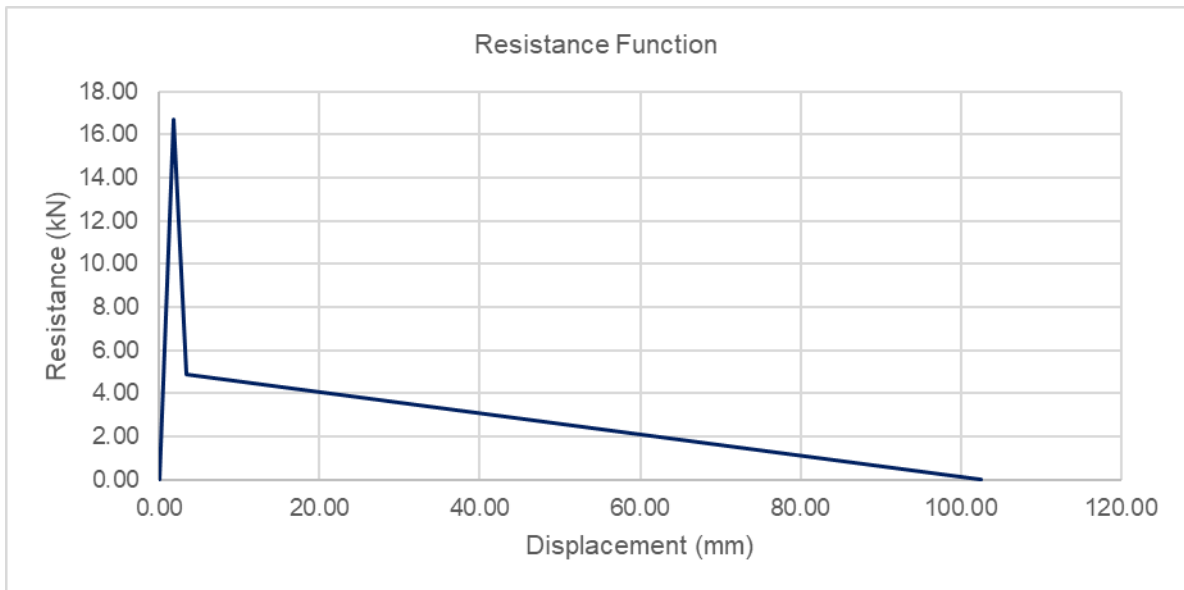
Figure 89: Resistance-deflection function for the modelled ground floor cavity brick wall in this assessment

Based on the input function in Figure 88, Figure 90 shows the response (deflection at mid height) of the kitchen walls. A peak deflection is 1.3mm means the enclosure boundaries maintain integrity because the response does not exceed 102mm
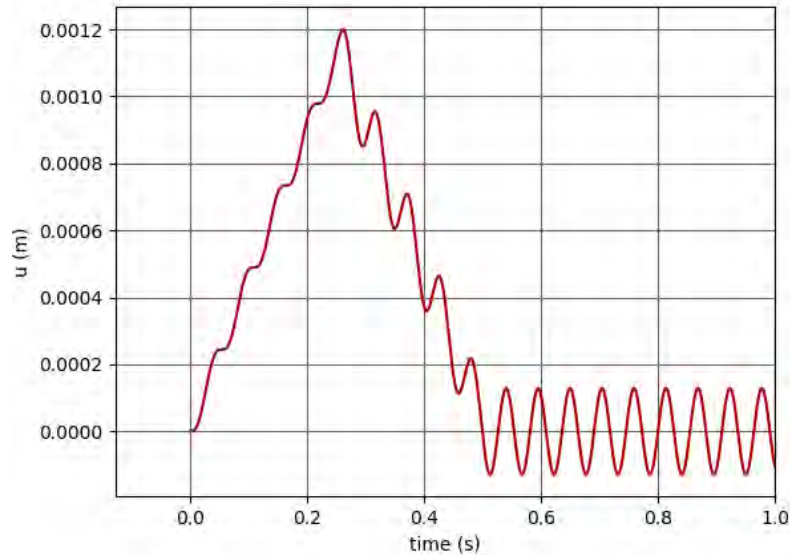


Figure 90: Response of cavity brick wall for a vented 9.5% peak concentration methane explosion in the kitchen (zero vent cover resistance and inertia)

The response of the kitchen enclosure boundaries are then assessed with vent cover resistance and inertia considered. The input force function in Figure 91 is constructed using the approach described in Section 3.4.3 to make some consideration of vent cover resistance and inertia.
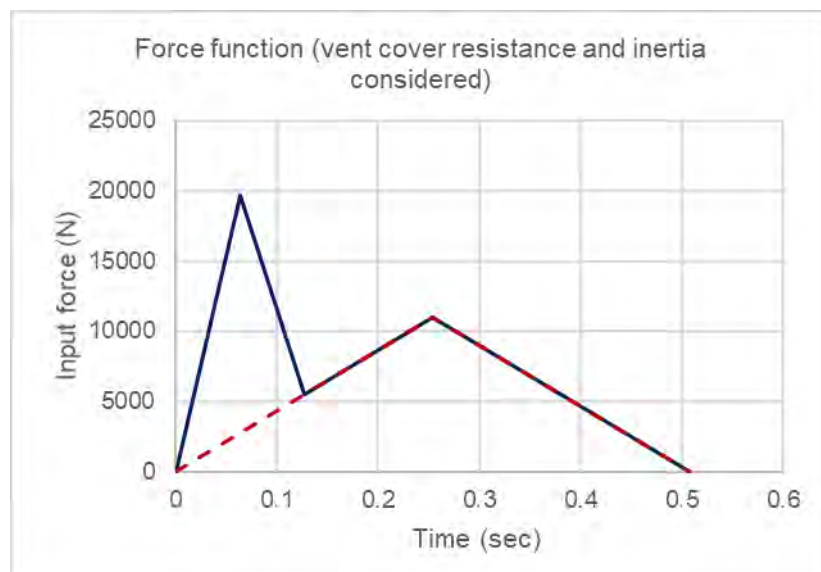


Figure 91: Input force function for a vented 9.5% peak concentration methane explosion on a 1m strip of 2.4m spanning double cavity brick wall *with vent cover resistance and inertia*

Figure 92 shows the response of the kitchen walls for the input force function in Figure 91. The deflection exceeds 102mm indicating failure of the kitchen enclosure boundaries. The number of people injured due to structural collapse is estimated as 2.0 using the equations and methodology in Section 4.2.1 and Figure 65.
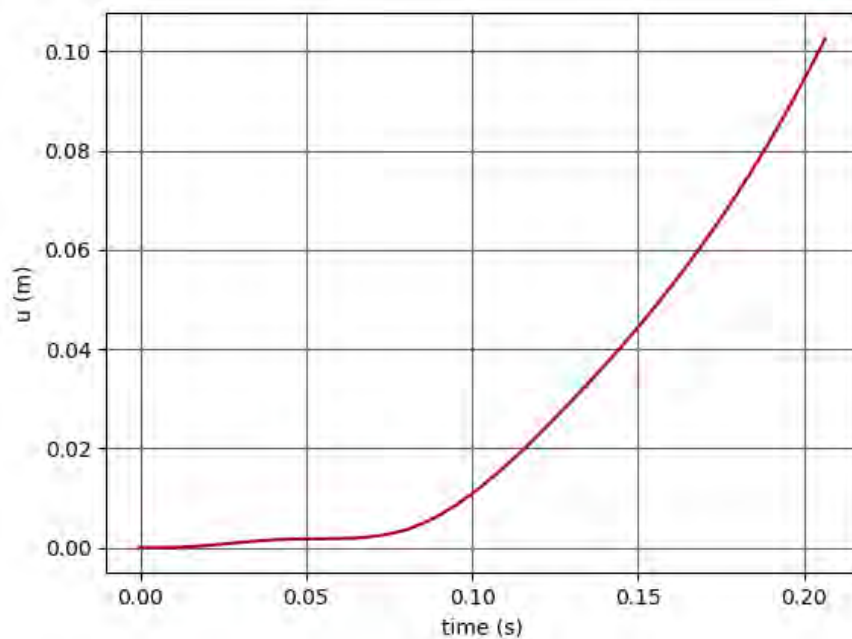


Figure 92: Response of cavity brick wall for a vented 9.5% peak concentration methane explosion in the kitchen *with vent cover resistance and inertia* considered

To estimate the overpressure that the enclosure boundaries of the neighbouring kitchens are subjected to following failure of the initial kitchen enclosure, the peak overpressure of 4.56 kPa is divided by six (see Figure 55 in Section 3.4.4). This gives an estimated internal overpressure of 0.8kPa for the neighbouring enclosures (next door kitchens and rest of dwelling in which the leak, dispersion and ignition event initially occurred) which is not high enough to initiate further structural collapse. Using the equations in Section 4.2.1, the total number of people injured would be 2.0.

To estimate the glass throw distance, firstly, the time taken for the glass to vertical fall to the ground is estimated using $\sqrt{[2h / g]}$ where $h$ is the distance from the centre of a ground floor window pane to the ground (assumed to be 1.8m) and $g$ is the acceleration due to gravity of 9.8m/s$^2$, i.e. if the pane of glass in the window simply fell to the ground, it would take 0.61 seconds.

A Microsoft Excel VBA script is then used to estimate the glass throw distance based on the estimated peak overpressure and impulse determined in Figure 86 and Figure 87. An annotated screenshot of the tool used to estimate glass throw distance is shown in Figure 93

Input of window dimensions, height of unit from the ground and thickness

Peak overpressure and impulse calculated earlier. This is used to construct a pressure time transient that is assumed to accelerate the glass. The calculation conservatively assumes that the glazing has no initial resistance to breaking.

It this example, the glazing hits the floor before the internal overpressure pulse has finished acting

| | |
|---|---|
| Unit height | 1.6 m |
| Unit width | 1 m |
| Cill height | 1 m |
| Centre of pane | 1.8 m |
| Glass thickness | 0.004 m |
| Element is projected | **23.5 m** |
| Mass of glass | 16 kg |
| | |
| Load area | 1.6 m2 |
| Peak Pressure | 4.56 kPa |
| Impulse | 1195 kPa-ms |
| Load duration | 0.52412 s |
| Half load duration | 0.26206 s |
| Gravity acc | 9.81 m/s$^2$ |

| Distance travelled (m) | Vertical Velocity (m/s) | time (s) |
|---|---|---|
| 0.00 | 0 | 0 |
| 0.18 | 1.88 | 0.192 |
| 0.36 | 2.66 | 0.271 |
| 0.54 | 3.25 | 0.332 |
| 0.72 | 3.76 | 0.383 |
| 0.90 | 4.20 | 0.428 |
| 1.08 | 4.60 | 0.469 |
| 1.26 | 4.97 | 0.507 |
| 1.44 | 5.32 | 0.542 |
| 1.62 | 5.64 | 0.575 |
| 1.80 | 5.94 | 0.606 |

Total time for glazing to vertically fall to the ground

Determine glass throw distance
ISOSCELES

| time (s) | P (kPa) | Fragment Drag Coefficient | Accel force (N) | Drag force (N) | Total force (N) | Velocity (m) | Distance glass throw (m) |
|---|---|---|---|---|---|---|---|
| 0 | 0.00 | 1.170 | 0.00 | 0.00 | 0.000 | 0.00000 | 0.0 |
| 0.00061 | 0.01 | 1.170 | 16.87 | 0 | 16.865 | 0.00064 | 0.0 |
| 0.00121 | 0.02 | 1.170 | 33.73 | 4.5798E-07 | 33.73 | 0.00192 | 0.0 |
| 0.00182 | 0.03 | 1.170 | 50.60 | 4.1218E-06 | 50.60 | 0.00383 | 0.0 |
| 0.00242 | 0.04 | 1.170 | 67.46 | 1.6487E-05 | 67.46 | 0.00639 | 0.0 |
| 0.00303 | 0.05 | 1.170 | 84.33 | 4.5798E-05 | 84.33 | 0.00958 | 0.0 |
| 0.00363 | 0.06 | 1.170 | 101.19 | 0.00010305 | 101.19 | 0.01341 | 0.0 |
| 0.00424 | 0.07 | 1.170 | 118.06 | 0.00020197 | 118.06 | 0.01788 | 0.0 |
| 0.00485 | 0.08 | 1.170 | 134.92 | 0.00035906 | 134.92 | 0.02299 | 0.0 |
| 0.00545 | 0.09 | 1.170 | 151.79 | 0.00059354 | 151.79 | 0.02873 | 0.0 |
| 0.00606 | 0.11 | 1.170 | 168.65 | 0.00092741 | 168.65 | 0.03512 | 0.0 |
| 0.00666 | 0.12 | 1.170 | 185.52 | 0.00138539 | 185.52 | 0.04214 | 0.0 |
| 0.00727 | 0.13 | 1.170 | 202.39 | 0.00199495 | 202.38 | 0.04981 | 0.0 |
| 0.00788 | 0.14 | 1.170 | 219.25 | 0.00278633 | 219.25 | 0.05811 | 0.0 |
| 0.00848 | 0.15 | 1.170 | 236.12 | 0.0037925 | 236.11 | 0.06705 | 0.0 |
| 0.00909 | 0.16 | 1.170 | 252.98 | 0.00504917 | 252.98 | 0.07663 | 0.0 |
| 0.00969 | 0.17 | 1.170 | 269.85 | 0.00659482 | 269.84 | 0.08684 | 0.0 |
| 0.01030 | 0.18 | 1.170 | 286.71 | 0.00847064 | 286.70 | 0.09770 | 0.0 |

1.17 is the "Fragment Drag Coefficient" representing a "flat plate perpendicular to the direction of travel". 1.17 is used for the duration of the initial internal overpressure pulse accelerating the glass. If the glass is still travelling through the air after the initial pulse has stopped accelerating it (like in the example in Appendix F.2, the "Fragment Drag Coefficient" alternates between 0.001 and 1.17 every other timestep to represent a fragment of glazing spinning about an axis perpendicular to its direction of travel. Drag coefficients are taken from [43]

Charts: Pressure accelerating glass; Accelerating force; Drag force; Total accelerating force; Velocity (with drag)

At each timestep, the following steps are undertaken:

- Interpolation of the internal overpressure-time transient to determine accelerating force on glazing pane
- Estimation of the drag force on the glazing pane based on the velocity and drag co-efficient
- Calculation of the *total* accelerating force on the pane. This is the accelerating force due to the internal overpressure pulse **minus** the drag force. When the *total* accelerating force becomes negative the drag force is exceeding the accelerating force.
- Integration to estimate average velocity between the previous timestep and current timestep (explicit approach). This is then integrated again to find the increase in *horizontal* distance the glazing pane has travelled during the timestep and added to the cumulative total distance.

Once the sum of the timesteps exceeds the time taken for the glazing pane to vertically fall to the ground, the loop is broken, and the total distance is recorded as the glass throw distance. In this example it is 23.5m.

The number of people injured is then estimated using the glass throw distance and area subtended by an arc that as described in Section 3.3.4 and Figure 39 on page 58.
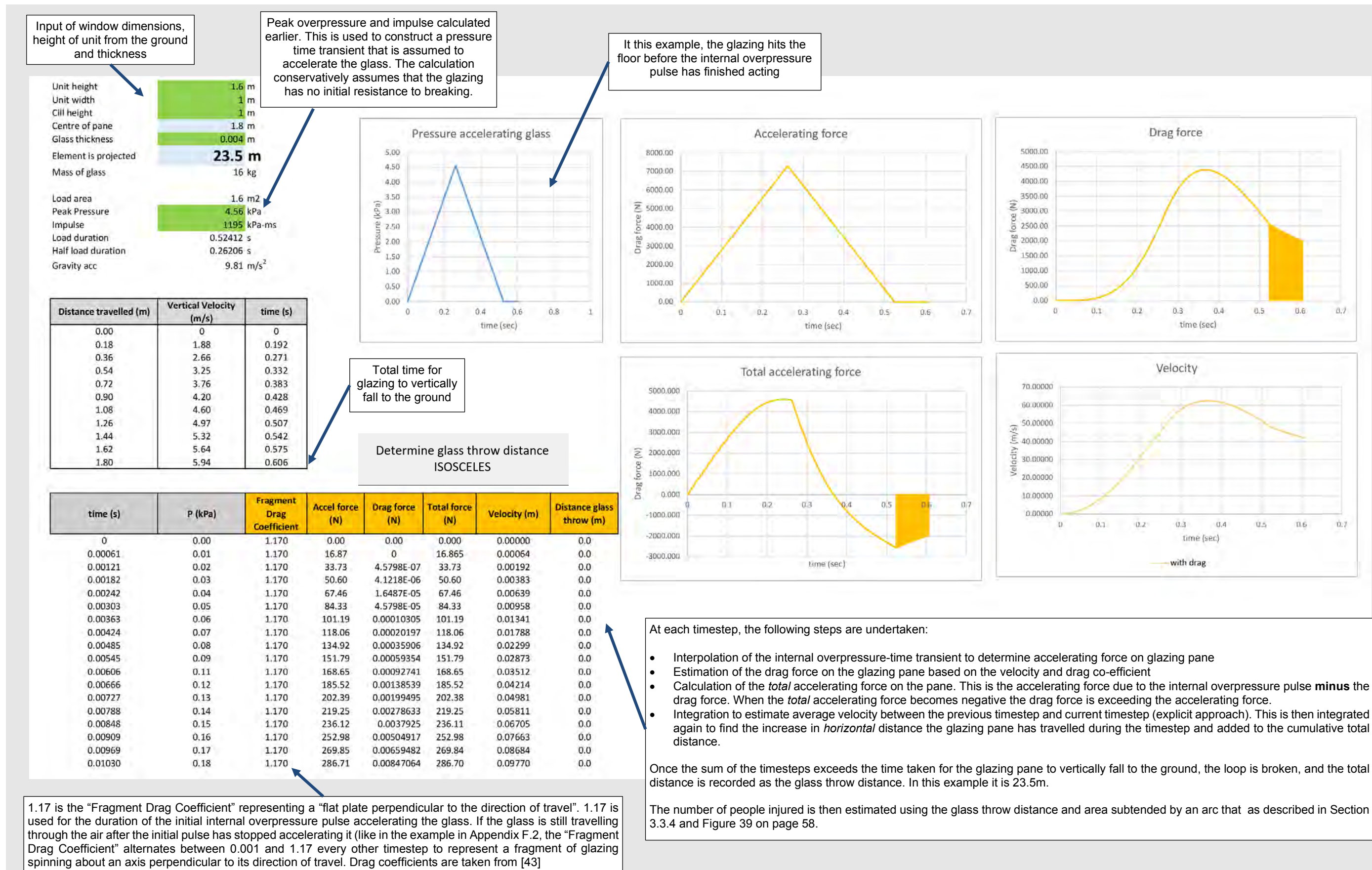
Figure 93: Screenshot of calculation used to estimate glass throw distance for a vented methane explosion in a kitchen with a peak concentration of 9.5%.

## F.2 – Peak concentration of 30% hydrogen in kitchen scenario

Figure 94 is a screenshot of the tool used to estimate internal vented overpressure for the kitchen scenario containing an inhomogeneous confined combustible hydrogen cloud with a peak concentration of 30%. Figure 95 is a screenshot of the same tool but provides some commentary on how impulse is estimated. Annotations that would duplicate the annotations in Figure 86 and Figure 87 from Appendix F.1 have been omitted from Figure 94 and Figure 95.

**Compute flame surface area**

$$A_f = \begin{cases} 0.50\ A_{in} & \text{for ignition at the back} - \text{wall (BWI)} \\ 0.25\ A_{in} & \text{for ignition at the centre of the enclosure (CI)} \end{cases} \quad (E.1)$$

where $A_{in}$ is the total internal surface area of the enclosure:

$$A_{in} = 2 \cdot (L \cdot B + B \cdot H + H \cdot L)$$

| | | | |
|---|---|---|---|
| Length of enclosure | L | 3.0 | m |
| Breadth/width of enclosure | B | 4.0 | m |
| Height of enclosure | H | 1.6 | m |
| Internal area of enclosure | $A_{in}$ | 46.51 | m² |
| Centre or back wall ignition? | | Back-wall | |

*Check whether enclosure is elongated*

*Elongated enclosures*

These sets of experiments are undertaken in idealized conditions using an enclosure whose aspect ratio (L/D) is larger than 2.5. The studies that are considered for this section include the studies of Kumar [5] and Daubech et al. [6].

(iii) For elongated enclosures- For elongated enclosures, the flame area is computed as:

$$A_f = 0.25\ A_{in} \quad (E.7)$$

For longer pipes, especially with obstacles, there is additional risk of Deflagration to Detonation Transition (DDT) which is beyond the scope of this model. Hence, it is recommended to use this model for enclosures with L/D ≤ 4.

| | | | |
|---|---|---|---|
| Equivalent diameter | D | 2.862 | m |
| Aspect ratio | L/D | 1.048 | |
| Is L/D less than 2.5? | | Yes | |
| Is L/D less than or equal to 4? | | Yes | |
| Flame surface area | $A_f$ | 23.26 | m² |
| Add. obstacle flame area | | 0.00 | m² |

> This is the "equivalent height" of the enclosure. To model this inhomogeneous confined hydrogen cloud as a hydrogen cloud with a homogeneous concentration of 30%, it is calculated as 0.67 x 2.4m (see Section 3.2.3 and Appendix A for further explanation of "equivalent height")

**Compute external cloud radius**

$$R_{CI} = 0.5 V^{0.3} \quad (E.2)$$

where V is the volume of the enclosure.

| | | | |
|---|---|---|---|
| Volume of enclosure | V | 19.296 | m³ |
| External cloud radius | $R_{CI}$ | 1.22 | m |

$$G1 = \left[ (L_{eff}^{\beta 1})^2 \left\{ \left( \frac{A_f}{A_v} \right)^2 - 1 \right\} \right]. \quad (E.3)$$

$$G2 = [R_{CI}^{\beta 2}]^2. \quad (E.4)$$

Where $L_{eff}$ is can be defined as:

$$L_{eff} = \begin{cases} L & \text{for ignition at the back} - \text{wall (BWI)} \\ 0.5\ L & \text{for ignition at the centre of the enclosure (CI)} \end{cases}$$

| | | |
|---|---|---|
| Medium | | Hydrogen |

*Dimensions of vent*

| | | | |
|---|---|---|---|
| Height of vent | | 1.0000 | m |
| Width of vent | | 3.1000 | m |
| Area of vent | $A_V$ | 3.1 | m² |

*Distance from ignition to vent*

| | | | |
|---|---|---|---|
| Effective acceleration dist | $L_{eff}$ | 3 | m |

*β1 and β2 values used for configurations*

| | | |
|---|---|---|
| Are obstacles present? | | No obstacles modelled |
| Configuration | | Ideal |
| Value β1 | β1 | 0.243 |
| Value β2 | β2 | 0.243 |

*Values G1 and G2*

| | | |
|---|---|---|
| Value G1 | G1 | 94.3 |
| Value G2 | G2 | 1.099 |

**Compute internal overpressure**

| | | | |
|---|---|---|---|
| Concentration of medium | | 30 | % |
| Equivalence ratio $\phi$ | | 1.017 | |

*Lookup F1 and F2 values*

| | | |
|---|---|---|
| Value F1 | F1 | 1.1353E-02 |
| Value F2 | F2 | 1.8169E+00 |

$$p = (F1 \cdot G1) + (F2 \cdot G2) \quad (17)$$

where

$$F1 = \left[ \frac{\rho_u}{2 \cdot 10^5} \left\{ \frac{U_0}{R_0^{\beta}} \left( \frac{\sigma - 1}{\sigma} \right) \right\}^2 \right], \quad (18)$$

$$F2 = \left[ \frac{2\ \gamma_u (\sigma^2 - \sigma)}{a_0^2} \left( \frac{U_0}{R_0^{\beta}} \right)^2 \right], \quad (19)$$

$$G1 = \left[ (L_{eff}^{\beta 1})^2 \left\{ \left( \frac{A_f}{A_v} \right)^2 - 1 \right\} \right]. \quad (20)$$

$$G2 = [R_{CI}^{\beta 2}]^2. \quad (21)$$

| | | | |
|---|---|---|---|
| **Overpressure** | p max | 3.06775 | bar |
| **Internal Overpressure** | p | 306.78 | kPa |

> It is recognised that above hydrogen concentrations of approximately 24%, the estimate of peak overpressure using this model is highly conservative using this model.

**Ratio of vent area to compartment volume**

The scaled vent size $K_v$ is given by the following relation: $K_v = A_v/V^{2/3}$, $A_v$ is the vent area, V is the volume of the room.

explosion of the cloud is related to vent size. For $K_v \leq 0.3$, an external explosion occurs as the flame propagates outside the vent, causing the negative overpressure outside the vent and internal explosion overpressure to continue to rise.

| | |
|---|---|
| Check of $K_V$ (ratio vent to volume) | 0.431 |

Kv value indicates internal pressure profile will have dual peak

Figure 94: Screenshot of calculation used to determine internal overpressure for a vented hydrogen explosion in a hydrogen with a peak concentration of 30%. This figure shows extracts from [1]. Duplicated annotations from Figure 86 have been omitted)

# Internal flame propagation (before external explosion)

## Spherical flame propagation

> The most critical parameter which affects the internal overpressure is the internal flame propagation. The flame propagation from source of ignition to the vent is a complex phenomenon which is challenging to model. However, flame propagation can broadly be attributed to a combination of two processes – spherical flame propagation, and bulk gas motion induced by venting.

The flame propagation velocity with radius can be written as:

$$\frac{U}{U_0} = \left(\frac{R}{R_0}\right)^\beta \tag{4.1}$$

where $U$ is the flame propagation velocity at radius $R$, $U_0$ is the flame propagation velocity at $R_0$, which is the critical radius for the onset of cellular instabilities, and $\beta$ is fractal excess, experimentally observed to be constant at 0.243 for all hydrogen concentrations [26]. The values of $U_0$ and $R_0$ can be calculated using curve-fits to the experimental data [11,26].

$$U_0 = 0.0537\,x^2 - 1.008\,x + 5.5716 \quad (m/s)$$

$$R_0 = (1.4273\,x - 0.1942)/1000 \quad (m)$$

where x is the hydrogen concentration in percentage. Since:

| | | | |
|---|---|---|---|
| Spherical flame velocity at $R_0$ | $U_0$ | 23.662 | m/s |
| Critical radius | $R_0$ | 0.043 | m |

position R. This equation can be used to calculate the time for the flame-front to reach the vent. The distance from the ignition source to the vent (R) can be estimated as:

$$R = \begin{cases} L & for\ Back-wall\ ignition \\ \dfrac{L}{2} & for\ Central-ignition \end{cases}$$

where L is the length of the enclosure. So, for a known L, time taken can be calculated as:

$$\tau = \left(\frac{R^{(1-\beta)}}{1-\beta}\right)\left(\frac{R_0^{\beta}}{U_0}\right) \tag{4.3}$$

| | | | |
|---|---|---|---|
| Fractal excess | $\beta$ | 0.243 | |
| Maximum value of R | R | 3 | m |

## Bulk gas motion induced by venting

As pressure rises inside the enclosure, vent opens, and unburnt gases escape out. Venting induces a bulk gas motion towards the vent. This bulk gas motion is also responsible to move the flame towards the vent. Gas venting can be modelled using Bernoulli's equation across the vent. Considering two points in the unburnt gases, just inside and outside the vent:

$$\frac{P_1}{\rho_u} + \frac{U_1^2}{2} = \frac{P_2}{\rho_u} + \frac{U_2^2}{2} \tag{2}$$

where subscript 1 is for the internal point and 2 is for the point outside the vent. $P_1$ denotes the internal pressure and $P_2$ is for the external ambient pressure, $U_1$ and $U_2$ are velocities and $\rho_u$ is the unburnt gas density. $U_1$ is the bulk velocity induced inside the enclosure due to venting. Also, the velocities can be related to each other using equation of continuity and assuming density changes to be negligible. Hence,

$$A_1 U_1 = A_2 U_2 \tag{3}$$

where $A_1$ is the cross-sectional area of the enclosure and $A_2$ is the vent area. Eq. (3) can be expressed in terms of enclosure dimensions as:

$$B.\,H.\,U_1 = A_v\,U_2 \tag{4}$$

Where $B$ and $H$ are the enclosure breadth and height, respectively, and $A_v$ is the vent area. Eliminating $U_2$ from equations (2)–(4):

$$U_1 = \sqrt{\frac{2\,\Delta P}{\rho_u\left[\left(\frac{B.H}{A_v}\right)^2 - 1\right]}} \tag{5}$$

| | | |
|---|---|---|
| Maximum value of $\Delta P$ i.e. F1*G1 | 107.04 | kPa |
| Maximum value of $U_1$ | 232.34 | m/s |

## TOTAL internal flame propagation

To estimate the time for the internal flame propagation to reach the vent, the increase in ΔP is approximated to a function of the cubic of the time t. i.e. $\Delta P = At^3$ where A is a co-efficient to iteratively find. The maximum value of ΔP is assumed to be F1*G1 (the maximum internal pressure due to internal flame propagation, external explosion excluded).

| | | |
|---|---|---|
| Iteration step to determine A | | 1000 |

> Calculate time for internal flame propagation to reach vent

**Start with a large iteration step and reduce it**

| | | |
|---|---|---|
| Co-efficient A in approximation $\Delta P = At^3$ | 8129000.000 | kPa s⁻³ |

**TOTAL internal flame propagation continued**

| | | |
|---|---|---|
| Time for flame front to reach vent | 0.024 | sec |

**Check of guess**

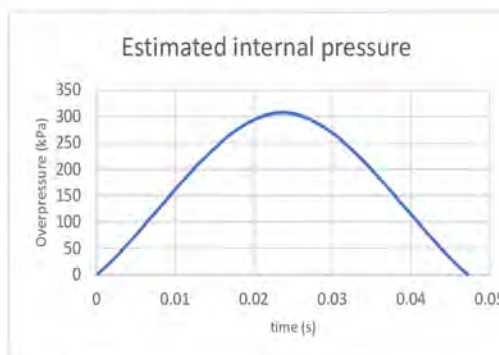| | | |
|---|---|---|
| Final ΔP value using approx relationship | 106.84 | kPa |
| Guess of $U_1$ using approx relationship | 226.47 | m/s |
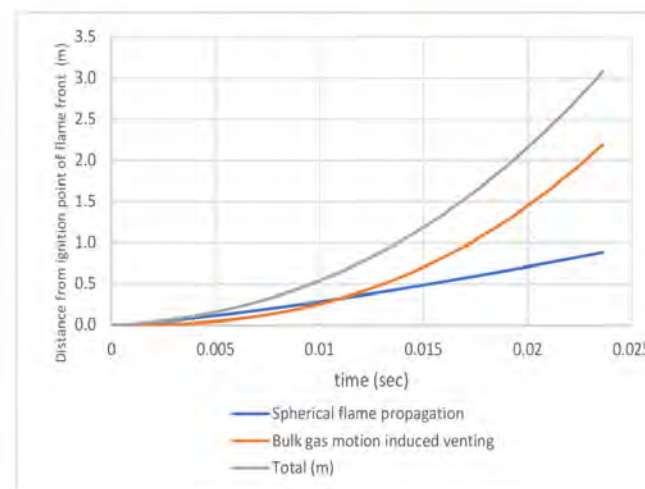


## Estimation of pulse duration

The time taken for the internal flame to reach the vent, and the value of $K_v$ is used to make an estimate of the total internal pulse duration and therefore of the impulse.

| | | |
|---|---|---|
| Factor from $K_v$ for calculating pulse length | 1.00 | |

| | | |
|---|---|---|
| Total approx duration of pulse | 0.047 | sec |



| | | |
|---|---|---|
| Estimation of impulse | 7240 | Pa s |

## Estimation of window failure time

Prior to the failure of the vent, the expansion of the vapour cloud is effectively a closed vessel deflagration where the internal pressure rise occurs due to the expansion ratio. In practice a room is rarely "fully closed" but some idea of the time that the maximum vent pressure is reached can be estimated

| | | |
|---|---|---|
| Maximum resistance of window | 9 | kPa |
| Time at which vent failure occurs | 0.022 | sec |
| % cloud consumed at failure | 1.52 | % |

Figure 95: Screenshot of calculation used to estimate impulse for a vented hydrogen explosion in a kitchen with a peak concentration of 30%. This figure shows extracts from [1] and [35]. Duplicated annotations from Figure 87 have been omitted.

The estimation of the overpressure and impulse in Figure 94 and Figure 95 assumes that the vent cover resistance and inertia are zero. Firstly, the kitchen walls, are assessed using the overpressure and impulse of 307kPa and 7240Pa-s respectively. Figure 96 shows the input force function to the SDoF model used to estimate response for a strip of wall, 2.4m high and 1m wide for an overpressure of 307kPa and impulse of 7240Pa-s
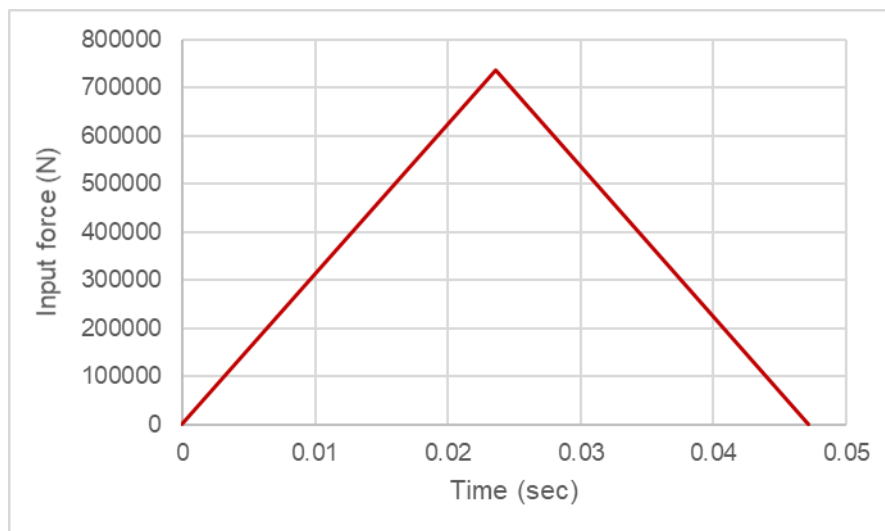


Figure 96: Input force function for a vented 30% peak concentration hydrogen explosion on a 1m strip of 2.4m spanning double cavity brick wall

The resistance function used to model the response of the ground floor double cavity brick enclosure walls is shown in Figure 89. Based on the input function in Figure 96, Figure 97 shows that the response (deflection at mid height) of the kitchen enclosure walls exceeds 102mm, indicating failure of the enclosure boundaries with failure occurring at approximately 0.023 seconds after ignition.
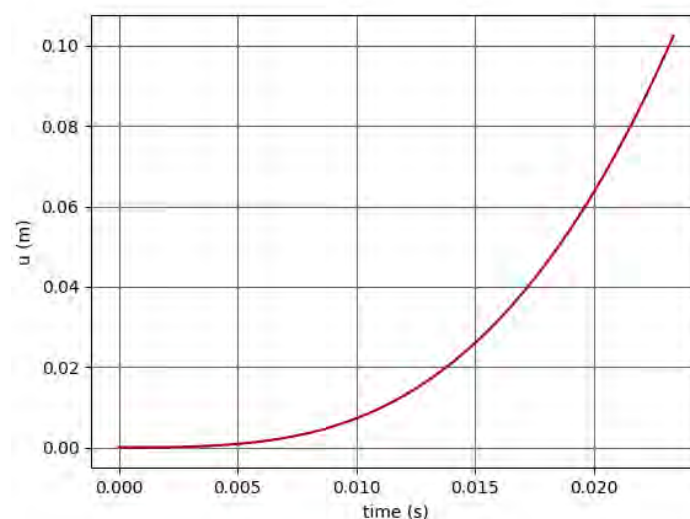


Figure 97: Response of cavity brick wall for a vented 30% peak concentration hydrogen explosion in the kitchen

As per the flow chart in Figure 53 from Section 3.4.3, the effect of vent cover resistance and inertia is not considered given that the enclosure boundaries already loose structural integrity when both these input parameters are zero.

For concentrations above 18% hydrogen, the response of the double leaf load bearing walls is determined for both an isosceles shaped pulse representing a deflagration, and a shock fronted pulse shape representing a detonation following a DDT or a partial DDT. An assessment of the SDoF response of the kitchen double leaf brick wall enclosures are also undertaken using a shock fronted profile in Figure 96 with the same peak overpressure and impulse of 307kPa and 7240Pa-s respectively.
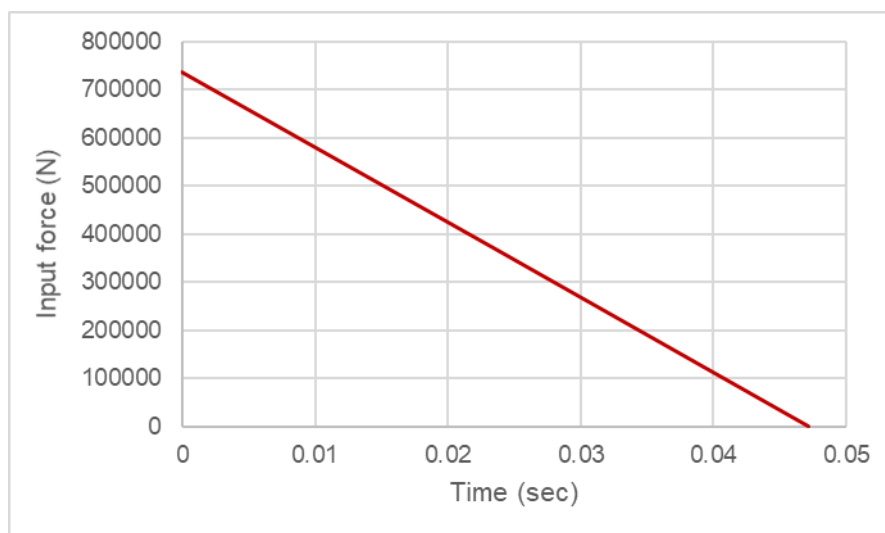


Figure 98: Input force function as a shock front for a vented 30% peak concentration hydrogen explosion on a 1m strip of 2.4m spanning double cavity brick wall

Next the peak overpressure and impulse that the *neighbouring* enclosures boundaries would be subject to is estimated using a combination of residual pulse and adiabatic gas behaviour theory for both the isosceles and shock-front shaped pulse shapes.

Table 11 shows that the residual impulse for the isosceles shaped internal overpressure pulse following the failure of the *initial* enclosure boundaries is slightly larger than the residual impulse for a shock-front shaped internal overpressure pulse.

The residual impulse of 3808Pa-s is divided by six as per the methodology in Section 3.3.2 to give a residual impulse of 635 Pa-s. This is the impulse that the boundaries of the *neighbouring* enclosures (next door kitchens and other parts of the house where the leak, dispersion and ignition event initially occurs) would be subject to. The initial peak overpressure of 307kPa is divided by six to give a *residual* peak overpressure of 51 kPa.

Table 11: Residual pulse for a vented 30% peak concentration hydrogen in the kitchen scenario

| Assumed shape of input pulse | Failure time of initial enclosure boundaries (t = 0 is time of ignition) | Wall fails before or after peak overpressure at time t = 0.024 sec) for isosceles shaped pulse? | Residual impulse following boundary failure of initial kitchen enclosure (before reduction by factor of six) |
|---|---|---|---|
| Isosceles | 0.023 sec | Before (just) | 3808 Pa-s |
| Shock fronted | 0.014 sec | N/A | 3586 Pa-s |

The boundaries of the *neighbouring* enclosures are then assessed in the same manner as the *initial* enclosure boundaries using the *residual* impulse and overpressure to construct input force functions for the same SDoF model (Figure 99 and Figure 100)
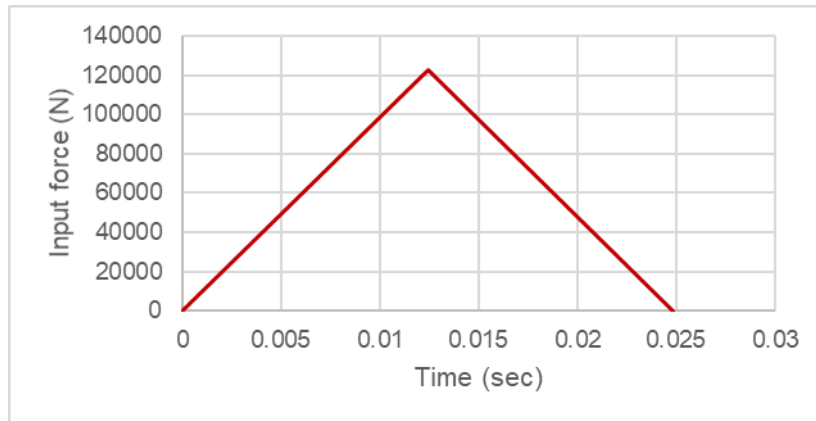


Figure 99: Residual internal overpressure pulse exerted on *neighbouring* enclosure boundaries for a vented 30% peak concentration hydrogen in the kitchen scenario
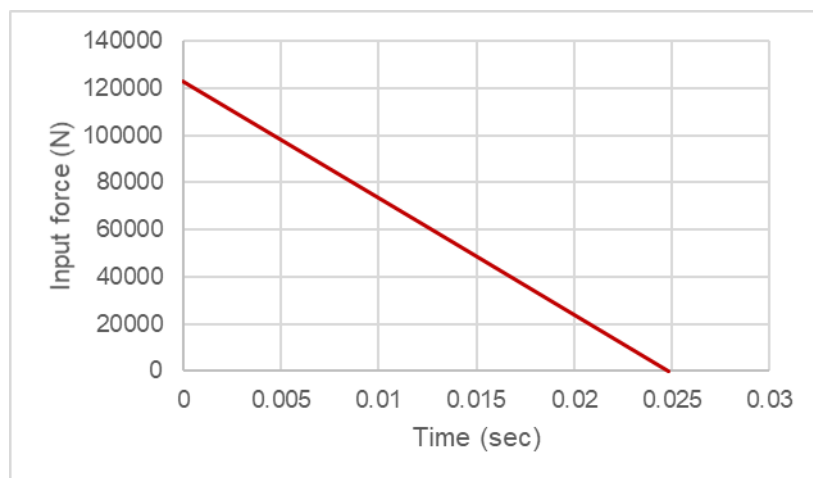


Figure 100: Residual internal overpressure shock fronted pulse exerted on *neighbouring* enclosure boundaries for a vented 30% peak concentration hydrogen in the kitchen scenario

The response of the *neighbouring* enclosure boundaries following failure of the initial boundaries where the leak, dispersion and ignition event takes place are shown in Figure 101 for an isosceles shaped pulse and show that the *neighbouring* enclosure boundaries fail after 0.061 seconds from when they are subjected to the *residual* pulse (the shock fronted shape response has been omitted from this example calculation but is used).
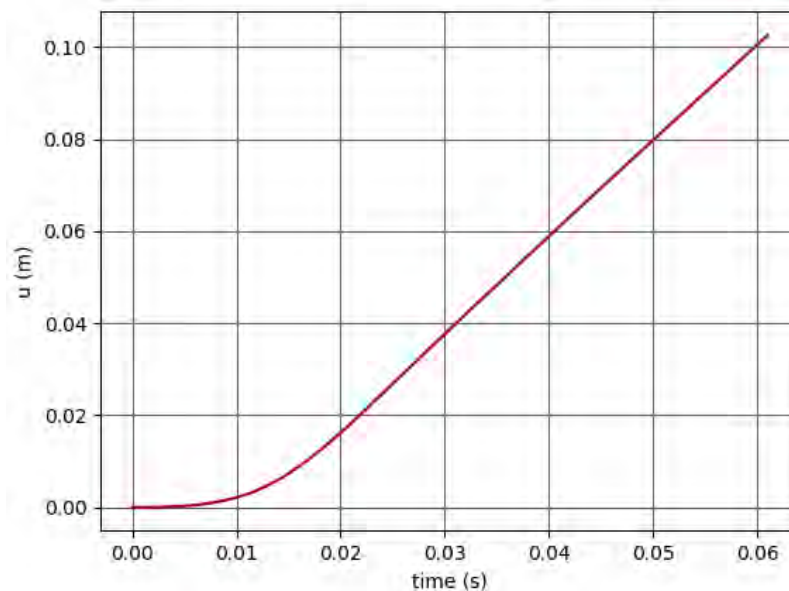


Figure 101: Response of *neighbouring* enclosure cavity brick walls for a vented 30% peak concentration hydrogen explosion occurring in kitchen scenario (isosceles shaped pulse)

The results in Table 12 show that the duration until failure of the *neighbouring* enclosure boundaries *plus* the duration till failure of the *initial* enclosure boundaries is greater than the initial pulse duration of 0.047 seconds (see Figure 96 and Figure 98). This indicates that the overpressure pulse has been and gone before an overpressure can be exerted on the boundary walls of the "next door but one". neighbour. The maximum number of dwellings that undergo collapse is therefore total collapse of three houses and partial collapse of a further two houses for this kitchen scenario case as per the equations in Section 4.2.1.

An annotated screenshot of the calculation of glass throw for this example of 30% peak hydrogen concentration in the kitchen scenario is shown in Figure 102.

Table 12: Residual pulse following boundary failure of *neighbouring* enclosures for a vented 30% peak concentration hydrogen in the kitchen scenario

| Assumed shape of input pulse | Failure time of initial enclosure boundaries (t = 0 is ignition) | Failure time of *neighbouring* enclosure boundaries (t = 0 is when residual overpressure pulse is exerted on *neighbouring* enclosure boundaries) | Failure time of initial enclosure boundary + Failure time of *neighbouring* enclosure boundaries |
|---|---|---|---|
| Isosceles | 0.023 sec | 0.061 seconds | 0.083 seconds > 0.047 seconds so maximum of total collapse of 3 houses, partial collapse of a further 2 houses |
| Shock fronted | 0.014 sec | 0.057 seconds | 0.071 seconds > 0.047 seconds so maximum of total collapse of 3 houses, partial collapse of a further 2 houses |
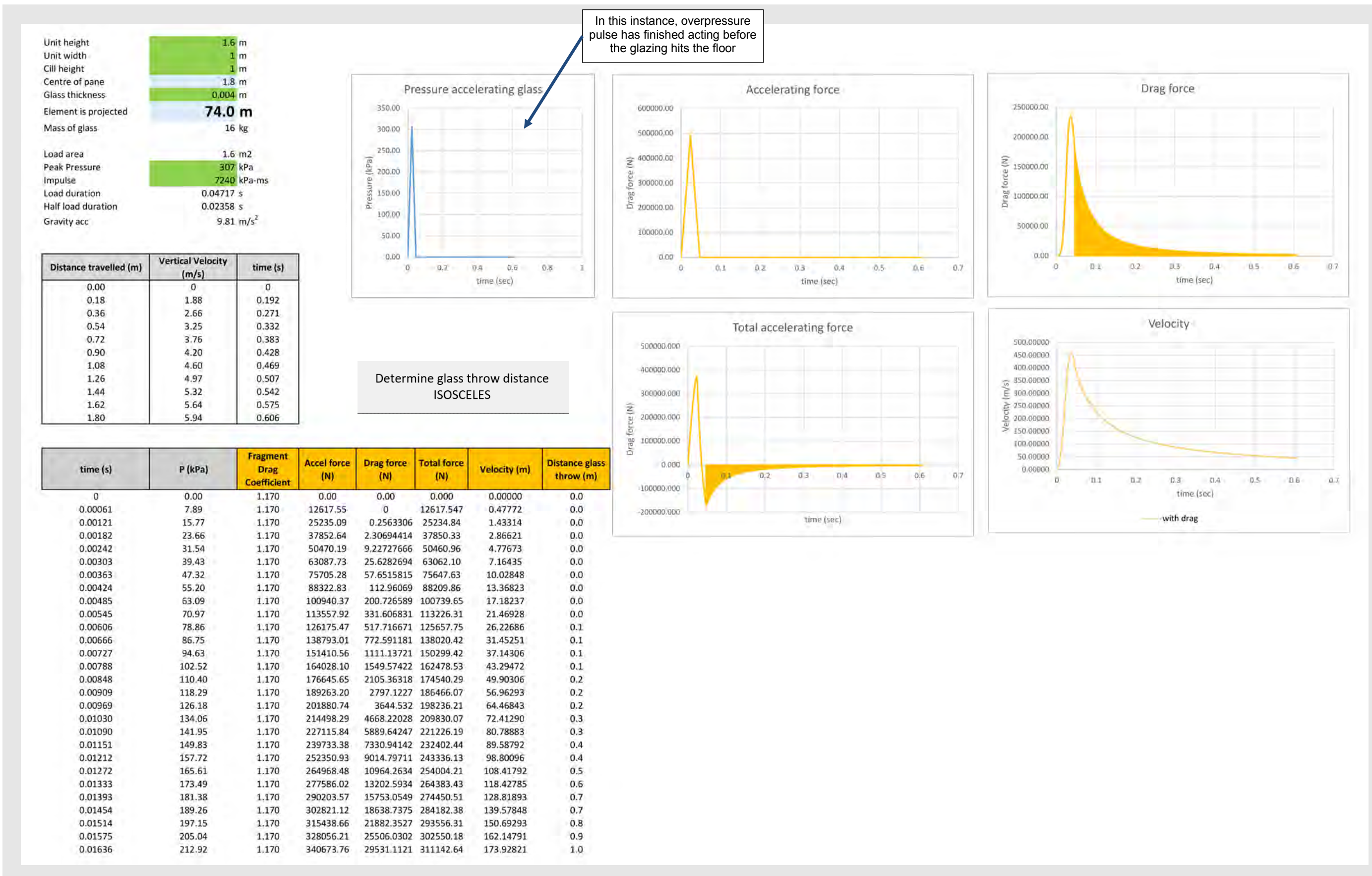
Figure 102: Screenshot of calculation used to estimate glass throw distance for a vented hydrogen explosion in a kitchen with a peak concentration of 30%. Duplicated annotations from Figure 93 have been omitted